

Verena Butzen

Vom Fachbereich VI Raum- und Umweltwissenschaften der Universität Trier
zur Erlangung des akademischen Grades
Doktor der Naturwissenschaften (Dr. rer. nat.)
genehmigte Dissertation

Räumliche Verteilung und zeitliche Variabilität von Oberflächenprozessen

**Quantifizierung von Oberflächenabflussbildung
und Bodenerosion mittels experimenteller
Geländemethoden**



Betreuer
Prof. Dr. Johannes B. Ries

Berichterstattende
Prof. Dr. Ing. Markus C. Casper
Prof. Dr. Helge Bormann

Datum der wissenschaftlichen Aussprache
02. Februar 2015

Überall geht ein früheres Ahnen dem späteren Wissen voraus.

Alexander von Humboldt (1769-1859) *Kosmos – Entwurf einer physischen Weltbeschreibung*

Danksagung

Diese Dissertationsschrift wäre ohne die Hilfe und Unterstützung von vielen fleißigen Helfern in Gelände, Labor und Artikelreview in dieser Form nicht möglich gewesen. Aus diesem Grund möchte ich mich an dieser Stelle bei allen bedanken, die zum Vorankommen und zum Abschluss dieser Arbeit beigetragen haben.

Zunächst möchte ich gerne Herrn Prof. Dr. Johannes B. Ries danken, der nicht nur die Betreuung dieser Arbeit übernommen hat, sondern mir auch schon während des Studiums der Physischen Geographie als Hiwi die Teilnahme an vielen interessanten Forschungsaufenthalten in Untersuchungsgebieten vor allem in Nord- und Südspanien ermöglichte. Damit wurde bereits der Grundstein gelegt und mein Interesse für die Erforschung von Oberflächenabflussbildung- und Bodenerosionsprozessen geweckt. Auch im gesamten Verlauf meiner Promotionszeit war er stets offen für Fragen und Diskussionen.

Als zweites möchte ich Herrn Prof. Dr. Markus Casper dafür danken, dass er die Zweitbetreuung dieser Arbeit übernahm und mir stets mit Rat und Tat zur Seite stand. Ohne die Diskussionen, sowie Fragen und Denkanstöße seinerseits, insbesondere bei der Entstehung und Verbesserung der Artikel, wären einige Teile dieser Arbeit sicher nicht in der Form entstanden.

Herrn Prof. Dr. Helge Bormann möchte ich sehr herzlich dafür danken, dass er dazu bereit war, diese Arbeit als externer Gutachter zu betreuen.

Herrn Dr. Manuel Seeger möchte ich an dieser Stelle ganz besonders danken für alles was er zum Gelingen dieser Arbeit beigetragen hat. Da ich dies unmöglich alles auflisten kann, hier nur ein kleiner Einblick: angefangen mit dem legendären Lehrforschungsprojekt Arnas 2005, über die Diplomandengeländephase Arnas 2007 mit der „Gamaschengang“, bis hin zu zahlreichen Geländephasen in die drei Untersuchungsgebiete in Deutschland und Luxemburg, die wesentliche Teile der Datengrundlage dieser Arbeit lieferten. Vielen Dank vor allem aber auch dafür, dass er immer diskussionsbereit war und immer wieder mit den richtigen Impulsen die Weichen für meine Arbeit gestellt hat.

Danken möchte ich an dieser Stelle auch Stefan Wirtz, René Wengel, Alexander Remke, Sabrina Plegnière, Britta Schäfer, Bastienne Engels, Thomas Iserloh und Miriam Marzen dafür, dass sie bei einer oder mehreren der elf Geländephasen in den fünf Testgebieten dabei waren, und viel Zeit und Geld investiert haben, um die

Forschung ein Stück voran zu treiben. Ohne euch wäre diese Datenbasis definitiv so nicht zustande gekommen.

Mein besonderer Dank gilt Lianne De Jonge und Amaia Marruedo-Arricibita, den beiden Masterstudentinnen der 'Land Degradation and Development Group' an der Universität Wageningen, die jeweils die Daten zu ihren Masterarbeiten zum Thema 'water repellency' in einem unserer Testgebiete hier in der Nähe von Trier sammelten und damit ebenfalls zu dieser Arbeit beitrugen.

Vielen Dank auch an die Studentinnen und Studenten der sieben Lehrforschungsprojekte, ohne die eine solche Anzahl an Niederschlagssimulationen und Rinnenerosionsversuchen nicht möglich gewesen wäre.

Den Mitarbeitern der Physischen Geographie sei ebenfalls gedankt, für nette Gespräche, technische Unterstützung, Tipps bei verwaltungstechnischen Problemen, sowie gute Ratschläge und Ideen. Grüße an Harry Willger.

Danke auch an alle Korrekturleser und Reviewer, die durch zielsichere Kommentare und konstruktive Kritik diese Arbeit in ihrer Qualität deutlich verbessert haben. Außer den oben bereits erwähnten Personen sind hier noch Rita Ley und Oliver Gronz zu nennen.

Mein ganz besonderer Dank gilt meinen Eltern, die mich während des Studiums und auch vor allem gegen Ende der Promotionsphase immer wieder unterstützt und aufgemuntert haben.

Trier, April 2015

Verena Butzen

Kurzfassung

Gerade in der heutigen Zeit im Spannungsfeld zwischen der globalen Klimaveränderung und einer stetig wachsenden Weltbevölkerung wird es immer wichtiger, die aktuell ablaufenden Oberflächenprozesse quantifizieren zu können. Infolge von häufiger auftretenden Starkregenereignissen wird es in Zukunft tendenziell auch verstärkt zu Oberflächenabflussbildung und damit zu mehr Bodenerosion kommen (IPCC 2013). Dies führt langfristig zu geringeren Ernteerträgen auf den zunehmend degradierten Ackerflächen und somit zu einer Verschlechterung der Ernährungssituation einer wachsenden Weltbevölkerung.

In fünf Testgebieten in Deutschland, Luxemburg und Spanien wurden experimentelle Geländemessmethoden eingesetzt, um Oberflächenabflussbildung und Bodenerosion zu quantifizieren. Je nach geographischer Lage der Testgebiete sind unterschiedliche Einflussgrößen wichtig für die Abflussreaktion und den Bodenabtrag. Jahreszeit und Vorfeuchte des Bodens beispielsweise, können zu verschiedenen Systemzuständen führen und damit die Oberflächenabflussbildung- und Bodenerosionsraten stark beeinflussen. Die Verwendung von experimentellen Messmethoden wie den im Gelände durchführbaren Niederschlagssimulationen ermöglicht es uns, die Reaktion derselben Flächen bei unterschiedlichen Ausgangsbedingungen auf ein und dasselbe (simulierte) Niederschlagsereignis zu messen.

Insgesamt konnte durch die Anwendung der experimentellen Geländemessmethoden immer eine Verbesserung der Prozesskenntnis für das jeweilige Untersuchungsgebiet erreicht werden. Die Kombination der experimentellen Messungen mit Geländekartierungen und GIS-Auswertungen ermöglichen zumindest eine qualitative Übertragung der punktuellen Messergebnisse auf die Fläche. Die Identifikation dominierender Abflussprozesse mittels eines gewichteten topographischen Indexes ist in diesem Zusammenhang eine geeignete Methode zur Untersuchung der räumlichen Verteilung von SOF-generierenden Flächen (SOF: *saturation overland flow*).

In den beiden Untersuchungsgebieten in Deutschland wurden häufig hydrophobe Bedingungen in den Humushorizonten und im Oberboden festgestellt, vor allem auf Nadelwaldstandorten in Trockenphasen im Sommer. Durch die Hydrophobizität dringt ein Teil des Niederschlagswassers gar nicht bis zum Mineralboden durch, sondern wird in der Streuschicht gehalten oder fließt

innerhalb der Streuschicht quasi oberflächlich ab. Dies führt zu einer Erhöhung der Oberflächenabflusskoeffizienten, bzw. dadurch kommt es überhaupt erst zur Bildung von Oberflächenabfluss.

Auch der Einfluss der Landnutzung auf die Intensität der Oberflächenprozesse konnte für die Testgebiete in Deutschland und Luxemburg klar nachgewiesen werden: Auf Wegen und Fahrspuren, sowie auf Ackerflächen wurden die höchsten Oberflächenabflusskoeffizienten und Bodenabtragsraten gemessen. Hydrophobe Waldstandorte zeigten ebenfalls relativ hohe Oberflächenabflussraten, allerdings keinen nennenswerten Bodenabtrag, weil die Humusauflage die Bodenoberfläche vor Erosion schützt.

Die im Rahmen dieser Arbeit verwendeten Rinnenerosionsversuche ermöglichen es, die Effizienz natürlicher Erosionsrinnen zu messen und zu vergleichen. Durch die Verwendung von beiden Methoden, Berechnung und Rinnenerosionsversuch, können die im Rinneneinzugsgebiet gemessenen Abtragsraten und -mengen mit den Abtragswerten der Erosionsrinne selbst verglichen werden. Der Vergleich zwischen flächenhafter und linienhafter Erosion zeigt, dass die Rinnenerosion um mehr als eine Größenordnung höhere Abtragsraten aufweist als die flächenhafte Erosion.

Insgesamt kann festgestellt werden, dass die Ergebnisse der experimentellen Messungen in Kombination mit einer Kartierung der aktuellen Geomorphodynamik sowie der Auswertung großmaßstäbiger Luftbilder, eine Quantifizierung der aktuellen Prozessdynamik ermöglichen. Allerdings ist eine Anpassung des Messkonzeptes an die Gegebenheiten des jeweiligen Untersuchungsgebietes absolut unerlässlich, um die wichtigsten Einflussfaktoren und Prozesse zu erfassen und treffende Aussagen zur rezenten Prozessdynamik treffen zu können.

Inhaltsverzeichnis

Kurzfassung	vi
1 Einleitung	1
1.1 Fragestellung und Ziele	3
1.2 Untersuchungsgebiete.....	4
1.3 Aufbau und Struktur der Arbeit	5
1.4 Zusammenhänge zwischen den Artikeln	6
2 Stand der Forschung.....	11
2.1 Abflussprozesse und deren flächenhafte Ausweisung	11
2.2 Hydrophobizität (<i>Soil Water Repellency</i>).....	12
2.3 Bodenerosion durch Wasser	14
3 Auswahl der wichtigsten experimentellen Geländemethoden	16
3.1 <i>Water Drop Penetration Time</i> (WDPT) Tests	16
3.2 Niederschlagssimulationen	17
3.3 Rinnenspülversuche	17
4 Iserloh et al. (2013): European small portable rainfall simulators: A comparison of rainfall characteristics. Catena, Vol. 110, pp. 100-112.	18
5 Butzen et al. (2011): Spatial pattern and temporal variability of runoff processes in Mediterranean Mountain environments - a case study of the Central Spanish Pyrenees. Zeitschrift für Geomorphologie, Vol. 55, Suppl. 3, pp. 025-048, Stuttgart, doi: 10.1127/0372-8854/2011/0055S3-0050.	43
6 Butzen et al. (2014): Quantification of Hortonian overland low generation and soil erosion in a Central European Low Mountain range using rainfall experiments. Catena, Vol. 113, pp. 202-212.	69

7	Butzen et al. (re-submitted in March 2015): Water repellency under coniferous and deciduous forest - Experimental assessment and impact on overland flow. <i>Catena</i>	101
8	Wirtz et al. (2012): Soil erosion on abandoned land in Andalusia - a comparison of interrill- and rill erosion rates. <i>ISRN Soil Science</i> , doi: 10.5402/2012/730870.	128
9	Synthese	145
9.1	Methodische Aspekte	145
9.2	Prozessdifferenzierung	147
10	Schlussfolgerungen und Ausblick	151
	Literaturverzeichnis	154

Abbildungsverzeichnis

1.1	Untersuchungsgebiete	4
1.2	Gliederungsgraphik	7
2.1	hydrophober Waldboden.....	13
9.1	Foto: Erosion Frankelbach	148

1

Einleitung

Oberflächenabfluss und die daraus resultierende Bodenerosion sind gerade unter dem Aspekt des Klimawandels und des stetigen Wachstums der Weltbevölkerung, große und wichtige Probleme der Menschheit (BREVIK 2013; MORGAN 2005; PIMENTEL 2006; PIMENTEL u. BURGESS 2013). Infolge von häufiger auftretenden Starkregenereignissen wird es zukünftig tendenziell auch verstärkt zu Oberflächenabflussbildung und damit zu mehr Bodenerosion kommen (IPCC 2013). Dies führt langfristig zu geringeren Ernteerträgen auf den zunehmend degradierten Ackerflächen und somit zu einer Verschlechterung der Ernährungssituation einer wachsenden Weltbevölkerung.

Starkregenereignisse und lang anhaltende Dauerregen können zu starker Oberflächenabflussbildung führen. In kleinen Bacheinzugsgebieten kommt es in der Folge von Starkregenereignissen zu einem schnellen, starken Anstieg der Pegel und damit zu Überflutungen (MÜLLER u. BISTRY 2008). Auch in den großen Flusseinzugsgebieten führt dies zu steigenden Pegelständen und zu Überflutungen, dabei können in dicht besiedelten Gebieten sehr hohe Schadenssummen entstehen (GRÜNEWALD u. MERZ 2011; KRON 2013; MERZ 2006). Durch die Auswirkungen des Klimawandels werden solche Extremereignisse in Zukunft tendenziell häufiger auftreten und auch intensiver sein (IPCC 2007, 2013).

Das häufigere Auftreten von Starkregenereignissen führt auch zu mehr Oberflächenabfluss, wodurch sich die Bodenerosion voraussichtlich infolge des Klimawandels ebenfalls verstärken wird (BREVIK 2013; IPCC 2013; PIMENTEL u. BURGESS 2013). Durch den verstärkten Bodenabtrag werden zudem Nährstoffe ausgetragen; dies führt wiederum langfristig zu geringeren Ernteerträgen der betroffenen Ackerflächen (*On-site-Schäden*) (PIMENTEL 2006; PIMENTEL u. BURGESS 2013). Das abgetragene Bodenmaterial wird in Flussauen, Seen und Stauseen abgelagert (*Off-site-Schäden*) und führt so zu einer Verschlechterung

der Wasserqualität (MARZOLFF u. a. 2003; MULLAN 2013; SIMONIT u. PERRINGS 2011; YOO u. a. 2014). Die verstärkte Belastung der Ressource Boden bedeutet auch gleichzeitig eine Verschlechterung der Lebensgrundlage (z. B. Nahrungsmittelproduktion) der Menschen (HUANG u. a. 2012). Dies wird angesichts der steigenden Weltbevölkerungszahlen zunehmend zu Problemen führen. Eine detaillierte Erforschung der Prozesse und Einflussfaktoren zu Oberflächenabflussbildung und Bodenerosion durch Wasser ist wichtig, um die Nachhaltigkeit der heutigen Landnutzung zu bewerten und ggf. Schutzmaßnahmen für die Zukunft ergreifen zu können.

Im Folgenden werden die Wirkungszusammenhänge zwischen Hydrophobizität, Oberflächenabfluss und Bodenerosion durch Wasser kurz dargestellt und die Begriffe definiert. Zur Bildung von Oberflächenabfluss kommt es dann, wenn die Niederschlagsintensität die Infiltrationsrate des Bodens, bzw. der Bodenoberfläche, übersteigt (*Hortonian Overland Flow (HOF)*), oder wenn der Boden bereits wassergesättigt ist (*Saturation Overland Flow (SOF)*) (BUSCHE u. a. 2005; MORGAN 2005; RICHTER 1998; ZEPP 2011). Zunächst entscheiden die Eigenschaften der Bodenoberfläche darüber, ob das Wasser infiltrieren kann oder nicht. Ist die Bodenoberfläche z. B. verkrustet oder hydrophob, so kann entweder kein Wasser infiltrieren oder es infiltriert deutlich langsamer (DOERR u. a. 2000; KIDRON 2014; SCHERRER u. NAEF 2003). Dadurch kommt es bei einem Starkregenereignis, bereits bei sehr geringem Gefälle zu Oberflächenabfluss. Die räumliche Verteilung von Flächen mit unterschiedlichem Abflussverhalten hängt im Wesentlichen von der Landnutzung ab, sowie von den damit einhergehenden Oberflächeneigenschaften (GARCÍA-RUIZ 2010; MAETENS u. a. 2012). Landnutzung und Bodenbearbeitung beeinflussen maßgeblich die Oberflächenstruktur und die Porosität des Bodens, diese Faktoren sind bestimmt für die Infiltrationsrate und die Wasserspeicherkapazität des Bodens (NERIS u. a. 2012; ZUCCO u. a. 2014).

Die Oberflächenabflussbildung als Reaktion auf Starkregenereignisse unterliegt einer zeitlichen Variabilität, die häufig mit einer zeitlichen Veränderung der Bodenfeuchte zusammenhängt. Dabei kommt es bei Starkregenereignissen zum einen dann zu Oberflächenabflussbildung, wenn der Boden mit Wasser gesättigt oder gefroren ist (SCHERRER u. NAEF 2003; SYMADER 2004), zum anderen kann es bei relativ trockenen Bedingungen durch das Auftreten von Hydrophobizität der Bodenoberfläche, oder durch Verkrustung oder Versiegelung, ebenfalls zu Oberflächenabflussbildung kommen (DOERR u. a. 2000; KIDRON 2014; SCHERRER

u. NAEF 2003). Tendenziell ist eine Wassersättigung der Böden in den gemäßigten Breiten eher im Winter (wenn der Boden nicht gefroren ist) und im Frühjahr festzustellen, während Hydrophobizität eher in Trockenphasen im Sommer auftritt. In diesem Zusammenhang spielen natürlich auch die Veränderungen durch den Klimawandel eine entscheidende Rolle, da es im Sommer in Zukunft auch in den gemäßigten Breiten häufiger zu Trockenphasen kommen kann (IPCC 2013).

Sobald das Wasser beginnt an der Bodenoberfläche abzufließen, kommt es auch zu flächenhafter Bodenerosion (*Interrill-Erosion*), sofern die Bodenoberfläche nicht von einer dichten, bodennahen Vegetationsbedeckung oder von einer Streuauflage (z. B. im Wald) geschützt wird (LI u. a. 2014). Durch eine Konzentration des Oberflächenabflusses kann es sogar zur Ausbildung von Rillen- und Rinnenerosion kommen (MORGAN 2005; RICHTER 1998). Dieser gesamte Themenkomplex wird in der vorliegenden Arbeit mit verschiedenen experimentellen Geländemessmethoden in Testgebieten in Deutschland, Luxemburg und Spanien untersucht.

1.1 Fragestellung und Ziele

Die im Rahmen dieser Arbeit behandelten Forschungsfragen lauten wie folgt:

1. Wie können die Ergebnisse unterschiedlicher Beregnungsanlagen vergleichbar gemacht werden?
2. Welches sind die wichtigsten Faktoren, die Oberflächenabflussbildung und Bodenerosion beeinflussen?
3. Wie und warum verändern sich Oberflächenabflussbildung und Bodenerosion mit der Zeit in Abhängigkeit von der Bodenfeuchte?
4. Wie beeinflusst die Hydrophobizität die Oberflächenabflussbildung unter Wald?
5. Wie beeinflussen Landnutzung und -bedeckung die Oberflächenabflussbildung und die Bodenerosion?
6. Wie effizient ist Rinnenerosion im Vergleich zu flächenhafter Erosion?

Die Zielsetzung dieser Arbeit besteht darin, die in den jeweiligen Untersuchungsgebieten wichtigsten Einflussfaktoren auf Oberflächenabflussbildung und Bodenerosion zu erkennen und die Intensität der Oberflächenprozesse mittels experimenteller Geländemethoden quantitativ zu erfassen. Einen besonderen Schwerpunkt bildet dabei die Untersuchung der zeitlichen und räumlichen Variabilität der Oberflächenprozesse, sowie

die Quantifizierung von Oberflächenabfluss und Bodenerosion. Bezuglich der zeitlichen Variabilität sind vor allem deutliche „Umschaltprozesse“ wichtig, etwa das „Umschalten“ zwischen hydrophilen und hydrophoben Bedingungen, oder die Änderung des Abflussverhaltens einer Fläche aufgrund sich ändernder Bodenfeuchtebedingungen. Im Hinblick auf die räumliche Variabilität der Oberflächenprozesse wird hauptsächlich auf den Einfluss der Landnutzung eingegangen.

1.2 Untersuchungsgebiete

Abbildung 1.1 zeigt eine Karte mit allen Untersuchungsgebieten, die im Rahmen dieser Arbeit beprobt und kartiert wurden. Die Untersuchungsgebiete liegen zwischen $49^{\circ}43'$ Nord und $37^{\circ}32'$ Nord sowie zwischen $2^{\circ}53'$ West und $7^{\circ}38'$ Ost.

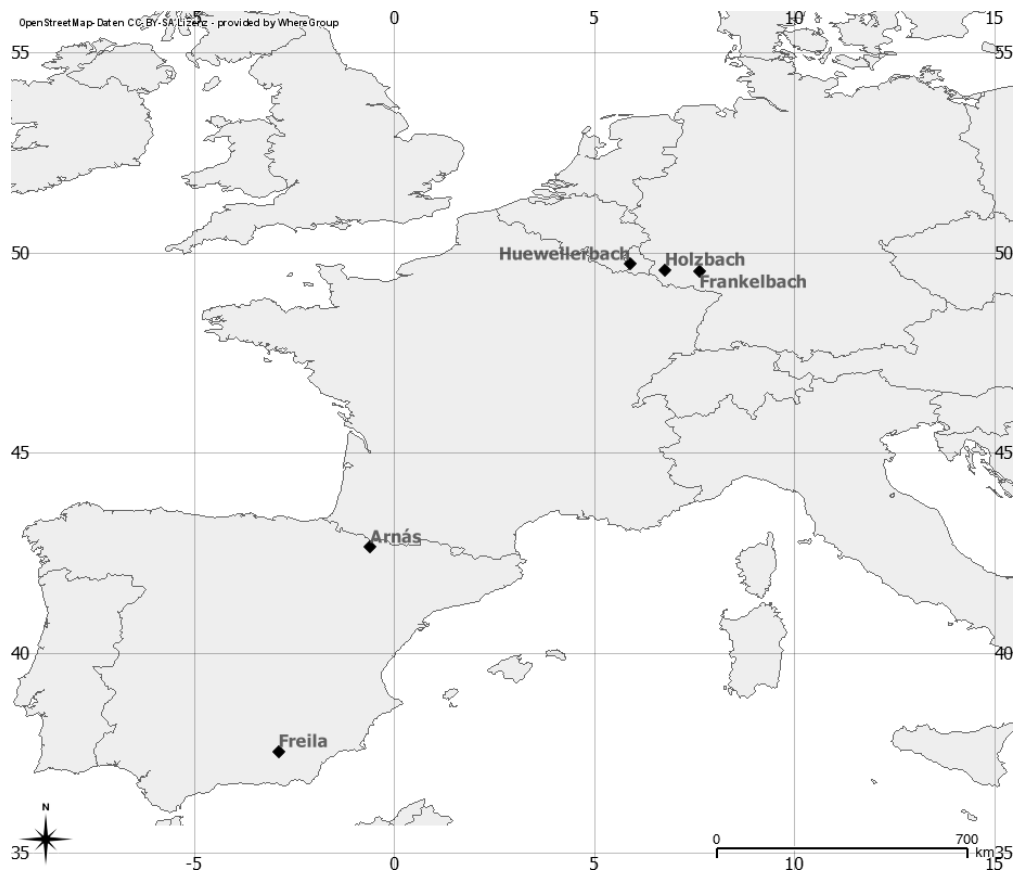


Abb. 1.1: Karte zur Lage der Untersuchungsgebiete

Die Untersuchungsgebiete wurden gezielt so ausgewählt, dass sie repräsentativ für eine größere Fläche sind, für die bestimmte Einflussfaktoren wichtig

sind, die die Oberflächenprozesse maßgeblich steuern. Die drei Testgebiete in Deutschland und Luxemburg sind in Landnutzung und Lage sehr unterschiedlich. Das Untersuchungsgebiet Holzbach (BUTZEN u. a. (2014, subm), Kapitel 6 und 7) ist fast ausschließlich mit Wald bedeckt, und zwar hauptsächlich mit Buchen- oder Fichtenwald; dies ist repräsentativ für große Flächen im Hunsrück. Im Einzugsgebiet des Frankelbachs (BUTZEN u. a. (2014), Kapitel 6), im Nordpfälzer Bergland, werden die Hochflächen ackerbaulich genutzt, während die steilen Hänge der tief eingeschnittenen Täler bewaldet sind und einige Flächen im Bereich der Flussaue als Grünland und Weidefläche genutzt werden. Das Huewelerbach-Einzugsgebiet (BUTZEN u. a. (2014), Kapitel 6) ist hauptsächlich mit Buchenwald bedeckt und befindet sich im Eich-Marmer-Gutland in Luxemburg. Die beiden Untersuchungsgebiete in Spanien unterscheiden sich, vor allem klimatisch, deutlich von den Untersuchungsgebieten in Deutschland und Luxemburg. Das in den Pyrenäen im Norden Spaniens gelegene Untersuchungsgebiet Arnás (BUTZEN u. a. (2011), Kapitel 5) wird bereits seit ca. 70 Jahren nicht mehr ackerbaulich genutzt. Die Flächen liegen größtenteils brach und werden noch von Schafen und Ziegen sowie gelegentlich von Kühen beweidet. Das Untersuchungsgebiet Freila (WIRTZ u. a. (2012a), Kapitel 8) befindet sich in der Hoya de Baza im südost-spanischen Andalusien und besteht hauptsächlich aus Brachland. Die ehemaligen Ackerflächen werden heute nur noch als Weideland für Ziegen und Schafe genutzt. Genauere Informationen zu den Untersuchungsgebieten sind in den jeweiligen Artikeln zu finden.

1.3 Aufbau und Struktur der Arbeit

Im Folgenden werden zunächst die Struktur dieser Arbeit (Kapitel 1.3) und die Zusammenhänge zwischen den im Rahmen dieser Arbeit in wissenschaftlichen Fachzeitschriften veröffentlichten Artikeln vorgestellt (Kapitel 1.4). Im Anschluss folgt Kapitel 2, das den Stand der Forschung zu Abflussprozessen und deren flächenhafter Ausweisung (Kapitel 2.1), Hydrophobizität (Kapitel 2.2) sowie Bodenerosion durch Wasser (Kapitel 2.3) erklärt. In Kapitel 3 werden die verwendeten Geländemessmethoden *water drop penetration time* (WDPT) Tests (Kapitel 3.1), Niederschlagssimulationen (Kapitel 3.2) und Rinnenspülversuche (Kapitel 3.3) vorgestellt.

Von Kapitel 4 bis 8 sind die veröffentlichten, bzw. eingereichten Artikel aufgeführt. Der erste Artikel ISERLOH u. a. (2013) (Kapitel 4) beantwortet die

erste Forschungsfrage, wie die Ergebnisse unterschiedlicher Berechnungsanlagen vergleichbar gemacht werden können. Die zweite Forschungsfrage wird in den Artikeln BUTZEN u. a. (2011), BUTZEN u. a. (2014), BUTZEN u. a. (subm) und WIRTZ u. a. (2012a) jeweils für die entsprechenden Untersuchungsgebiete beantwortet (Kapitel 5-8). Forschungsfrage 3, wie sich Oberflächenabflussbildung und Bodenerosion in Abhängigkeit von der Bodenfeuchte verändern, wird in den Artikeln BUTZEN u. a. (2011), BUTZEN u. a. (2014) und BUTZEN u. a. (subm) ebenfalls jeweils für die beprobteten Untersuchungsgebiete beantwortet (Kapitel 5-7). Die vierte Forschungsfrage, nämlich die Frage, wie die Hydrophobizität die Oberflächenabflussbildung beeinflusst, wird in den Artikeln BUTZEN u. a. (2014) und BUTZEN u. a. (subm) behandelt (Kapitel 6 und 7). Forschungsfrage 5 beschäftigt sich mit dem Einfluss der Landnutzung bzw. Landbedeckung auf die Oberflächenabflussbildung und die Bodenerosion. Diese Frage wird ebenfalls in allen anwendungsbezogenen Artikeln (Kapitel 5-8) für die jeweils untersuchte Region beantwortet. Die letzte Forschungsfrage nach der Effizienz der Rinnenerosion im Vergleich zur flächenhaften Erosion, wird in WIRTZ u. a. (2012a) für das Untersuchungsgebiet in Andalusien beantwortet (Kapitel 8).

Nach den Artikeln selbst, werden in der Synthese (Kapitel 9) die Kernaussagen der Artikel zusammengefasst, um so weiterführende Aussagen zu ermöglichen. Den Abschluss bildet Kapitel 10: Hier werden die wichtigsten Schlussfolgerungen, die sich aus dieser Arbeit ergeben noch einmal kurz zusammengestellt. Außerdem wird ein Ausblick gegeben auf zukünftig noch zu bearbeitende Forschungsaufgaben.

Abbildung 1.2 veranschaulicht die Struktur der Arbeit. Es sind die für diese Arbeit wichtigen Abfluss- und Bodenerosionsprozesse dargestellt, dazu wird jeweils die verwendete Mess- oder Untersuchungsmethode genannt. Die Zahlen 1-5 stehen für die Artikel, die in derselben Reihenfolge in den Kapiteln 4-8 aufgeführt sind (siehe Legende in Abbildung 1.2). Zu jedem der untersuchten Prozesse sind jeweils die Artikel angegeben, in denen der Prozess oder Einflussfaktor untersucht wird. Die wichtigsten Zusammenhänge zwischen den Prozessen sind durch die blauen (Oberflächenprozesse) und braunen (Prozesse im Untergrund) Pfeile angedeutet.

1.4 Zusammenhänge zwischen den Artikeln

Der erste Artikel, ISERLOH u. a. (2013) (Kapitel 4), ist ein methodischer Artikel, der sich mit einem Vergleich der wichtigsten in Europa verwendeten Berechnungsanlagen beschäftigt. Durch eine einheitliche Kalibrierung und

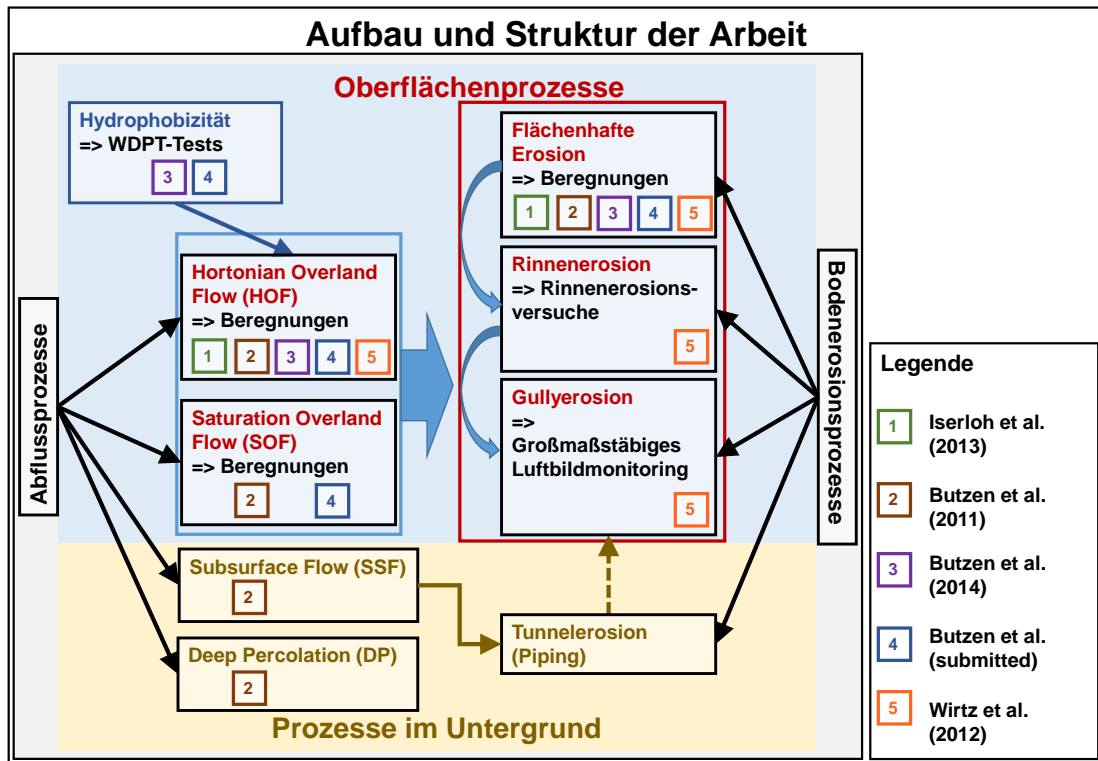


Abb. 1.2: Gliederungsgraphik mit der Zuordnung der Artikel zu den jeweiligen Prozessen und den verwendeten Messmethoden

Vermessung der simulierten Niederschläge der untersuchten Beregnungsanlagen, werden Vergleiche zwischen den Ergebnissen dieser Anlagen ermöglicht. Dies ist allerdings nur möglich, wenn identische Messmethoden verwendet werden, um die Eigenschaften der simulierten Niederschläge zu messen. Das Laserdistrometer (laser precipitation monitor (LPM)) wird weltweit genutzt, um die Eigenschaften natürlicher Niederschläge zu messen und sollte auch zur Niederschlagscharakterisierung der simulierten Niederschläge einheitlich verwendet werden. Alle getesteten Beregnungsanlagen sind dazu geeignet, Niederschlagssimulationen im Gelände durchzuführen, wenn die Randbedingungen und Niederschlagsparameter bekannt sind und genau kontrolliert werden. Verbesserungen an einzelnen Anlagen könnten in den Bereichen Minimierung des Wasserverbrauchs, Tropfengrößenverteilung, räumliche Verteilung des Niederschlages, sowie Reproduzierbarkeit, Anwendbarkeit und Kontrolle der Testbedingungen liegen. Generell werden Beregnungsanlagen verwendet, um in Gelände oder Labor Oberflächenabflussbildung und Bodenerosion für ein definiertes und reproduzierbares Niederschlagsereignis zu messen. Für alle weiteren Artikel in dieser Arbeit (Kapitel 5-8) wurden baugleiche Kleinberegnungsanlagen

nach ISERLOH u.a. (2012) genutzt, um vergleichbare Geländedaten zu Oberflächenabflussbildung und flächenhafter Bodenerosion zu generieren.

Die Artikel zwei bis fünf (Kapitel 5-8) sind Anwendungsartikel der Beregnungsanlagen und weiterer experimenteller Geländeforschungen. Diese Methoden wurden verwendet, um Oberflächenabflussbildung, flächenhafte Erosion und Rinnenerosion (Rinnenerosionsversuche) in räumlicher und zeitlicher Differenzierung zu messen (BUTZEN u.a. 2011, 2014, subm). Ziel der Untersuchungen ist es außerdem, die im jeweiligen Untersuchungsgebiet wichtigsten Einflussfaktoren auf Oberflächenabflussbildung und Bodenerosion zu bestimmen.

Die Ergebnisse der Niederschlagssimulationen in den Spanischen Pyrenäen zeigen zum Beispiel, dass es in Abhängigkeit von der Vorfeuchte ein Umschalten der Abflussreaktion auf größeren Flächen gibt (BUTZEN u.a. 2011) (Kapitel 5). Unter trockenen Bedingungen im Sommer produzieren diese Flächen keinerlei Oberflächenabfluss, aber unter feuchten Bedingungen neigen dieselben Flächen zu Sättigungsüberflächenabfluss (SOF). Die Identifikation dominierender Abflussprozesse mittels eines gewichteten topographischen Indexes ist ein geeignetes Werkzeug, um die räumliche Verteilung von SOF-generierenden Flächen zu untersuchen. Besonders das Einbeziehen von qualitativen Bodendaten in Form von Bodenkarten verbessert die Ergebnisse der Prozessidentifikation deutlich. Dennoch bleiben experimentelle Geländedaten unverzichtbar, um die tatsächlich im Gelände auftretenden Oberflächenabflussprozesse und deren Intensitäten sicher bestimmen zu können.

In BUTZEN u.a. (2014) (Kapitel 6) werden die Ergebnisse von Niederschlagssimulationen vorgestellt, die in den drei Testgebieten in Deutschland und Luxemburg durchgeführt wurden. Im Wesentlichen wird hier der Einfluss der Landnutzung und damit einhergehend der Hydrophobizität auf Oberflächenabflussbildung und Bodenerosion untersucht. Für die untersuchten Flächen wurde eine klare Abhängigkeit der Oberflächenabfluss- und Bodenerosionsraten von der Landnutzung festgestellt. Auf Ackerflächen, Harvester-Fahrspuren und ungeteerten Wegen wurden hohe Oberflächenabfluss- und Bodenerosionsraten gemessen. Auf Wiesen, Aufforstungsflächen und auf hydrophoben Nadelwaldstandorten wurden ebenfalls noch beachtliche Oberflächenabflussraten gemessen. Vom Menschen geschaffene lineare Strukturen wie Harvester-Fahrspuren und unbefestigte Wege sind die wichtigsten Sedimentquellen (neben dem Bachbett) in den Untersuchungsgebieten, zumindest

unter Wald. Die Hydrophobizität ist ein wichtiger Faktor, der die hydrologische Reaktion von Waldstandorten auf ein Starkregenereignis maßgeblich beeinflussen kann.

Der vierte Artikel BUTZEN u. a. (subm) (Kapitel 7) beschäftigt sich mit Persistenz und zeitlicher Variabilität der Hydrophobizität. Hier steht vor allem der Einfluss der Hydrophobizität auf die Oberflächenabflussbildung im Fokus. Es werden Niederschlagssimulationen verwendet, um festzustellen, ob die Hydrophobizität einen messbaren Einfluss auf die Oberflächenabflussbildung hat. Die Ergebnisse der Laubwald- und Nadelwaldstandorte werden miteinander verglichen, um festzustellen, ob sich die unterschiedlichen Waldtypen hinsichtlich Oberflächenabflussmengen und Hydrophobizität signifikant unterscheiden. Anhand des vorliegenden Datensatzes kann klar festgehalten werden, dass Hydrophobizität in Mitteleuropäischen Waldgebieten vorkommt. In den untersuchten Böden tritt Hydrophobizität vorwiegend in den Humushorizonten auf, während im Mineralboden (Ah) kaum Hydrophobizität festgestellt wurde. Die häufig stark von Pilzhyphen durchzogenen Of-Horizonte weisen unter trockenen Bedingungen mit Abstand die stärkste Hydrophobizität auf. Außerdem zeigen die Ergebnisse klar, dass die Nadelwaldstandorte (hauptsächlich Fichte) viel stärker von Hydrophobizität betroffen sind als die Laubwaldstandorte (hauptsächlich Buche).

Unter Laubwald tritt Hydrophobizität praktisch nur im Of-Horizont auf. Der Zusammenhang zwischen der WDPT (*water drop penetration time*) in Sekunden und der Oberflächenabflussbildung auf der entsprechenden Fläche ist nicht direkt ableitbar, weil hier noch viele andere Faktoren (z.B. Bodenfeuchte und Vorregenindex) eine Rolle spielen. Auf vielen der untersuchten Flächen unter Wald, vor allem wenn sie eine Streuauflage aufweisen und vorher relativ trockene Bedingungen herrschten, wurden beachtliche Oberflächenabflussraten mit den Kleinberegnungsanlagen gemessen.

Das Auftreten von Hydrophobizität verstärkt maßgeblich die Oberflächenabflussraten auf Nadelwaldstandorten, die bei Starkregenereignissen auf trockenem Boden auftreten. Insgesamt zeigen die Ergebnisse der Niederschlagssimulationen aber auch, dass die Waldflächen unter hydrophilen Bedingungen kaum Oberflächenabfluss liefern und kaum Bodenerosion stattfindet. Durch den klimatischen Wandel ist es allerdings sehr wahrscheinlich, dass Trockenperioden in den Sommermonaten in Zukunft auch im humiden

Mitteleuropa häufiger auftreten, und so auch häufiger Hydrophobizität auftreten kann.

Auf brachliegenden ehemaligen Ackerflächen in einem Testgebiet in Andalusien (WIRTZ u. a. (2012a), Kapitel 8) wurden die Ergebnisse von Rinnenspülversuchen, Niederschlagssimulationen, Geländekartierung und großmaßstäbigen Luftbildern ausgewertet, um einen quantitativen Eindruck der Dimension der Bodenerosion auf der Fläche im Vergleich zur Rinnenerosion zu bekommen. Hier wird besonders auf den Vergleich zwischen flächenhafter und linienhafter Erosion eingegangen, die mit Niederschlagssimulationen bzw. Rinnenspülversuchen im Gelände gemessen wurden.

Für dieses Testgebiet in Andalusien wurden in den Rinnen ca. 20 bis 60 mal höhere Erosionsraten gemessen als auf den umliegenden Flächen. Aufgrund der größeren Ausdehnung der Flächen waren allerdings die absoluten Erosionsraten der Flächen ca. 5 bis 15 mal höher als die der Rinnenfläche. Die Ergebnisse dieser Untersuchung verdeutlichen die Wichtigkeit der Rinnen als Abflusssammler und Sedimentlieferant.

2

Stand der Forschung

Im Folgenden wird der aktuelle Stand der Forschung zu den Themenbereichen „Abflussprozesse und deren flächenhafte Ausweisung“ (2.1), „Hydrophobizität“ (2.2) und „Bodenerosion durch Wasser“ (2.3) kurz vorgestellt. Im Zusammenhang mit der Oberflächenabflussbildung wird die Hydrophobizität als Einflussgröße besonders differenziert beschrieben und erklärt, weil hier eines der Schwerpunktthemen dieser Arbeit liegt.

2.1 Abflussprozesse und deren flächenhafte Ausweisung

Zunächst einmal bestimmt die Niederschlagsintensität, wie viel Regen pro Zeit an der Bodenoberfläche ankommt. Dann hängt es von den Eigenschaften der Bodenoberfläche ab, ob und mit welcher Rate, Wasser in den Boden infiltrieren kann. Die Bodenoberfläche als Bindeglied zwischen Atmosphäre und Bodenmatrix kann die Infiltration stark verringern, wenn z. B. Oberflächenversiegelung, Bodenkrusten oder Hydrophobizität das Wasser an der Infiltration hindern (DOERR u. a. 2000; SCHERRER u. NAEF 2003). Als drittes wird die Infiltrationsrate durch die Eigenschaften und den Wassergehalt des Oberbodens bestimmt sowie durch die Versickerungsrate im tieferen Bodenprofil.

Es können zwei Typen von Oberflächenabfluss unterschieden werden, zum einen der Horton'sche Oberflächenabfluss (HOF), und zum anderen der Sättigungsüberflächenabfluss (SOF) (BEVEN 2004). Horton'scher Oberflächenabfluss tritt dann auf, wenn die Niederschlagsintensität die Infiltrationsrate übersteigt, während der Sättigungsüberflächenabfluss nur dann auftritt, wenn das Porenvolumen des Bodens bereits mit Wasser gesättigt ist (SCHERRER u. NAEF 2003; SYMADER 2004). Die Intensität des Sättigungsüberflächenabflusses wird durch die gesättigte Leitfähigkeit der Bodenmatrix und durch die Niederschlagsintensität bestimmt.

Sobald das Wasser in den Boden infiltriert ist können auch die unterirdischen Abflussprozesse auftreten. Hier wird unterschieden in den lateralen Bodenwasserabfluss (*subsurface flow*: SSF) und die Tiefensickerung (*deep percolation*: DP) (SCHERRER u. NAEF 2003).

Nach SCHERRER u. NAEF (2003) und SCHMOCKER-FACKEL u. a. (2007) kann mit entsprechend guter Geländekenntnis und den notwendigen Bodendaten, für Flächen mit gleichen Eigenschaften (Bodenoberfläche, Bodentyp, geologischer Untergrund, usw.) ein dominierender Abflussprozess bestimmt werden (siehe auch HÜMANN u. a. (2011); MÜLLER (2010)). Die Ausweisung von Flächen mit den gleichen dominierenden Abflussprozessen ermöglicht es, die punktuell mit der Kleinberegnungsanlage gemessenen Daten zumindest qualitativ auf größere Flächen zu übertragen. Dies wurde für das Untersuchungsgebiet in den spanischen Pyrenäen in BUTZEN u. a. (2011) (Kapitel 5) durchgeführt.

2.2 Hydrophobizität (*Soil Water Repellency*)

Nach DOERR u. a. (2000) ist eine Oberfläche dann hydrophob, wenn die Oberflächenspannung des Wassertropfens (Kohäsion) größer ist als die adhäsiven Kräfte der Oberfläche. Abbildung 2.1 zeigt ein Photo von Wassertropfen auf dem Of-Horizont eines hydrophoben Buchenwaldstandortes.

Wasser hat eine Oberflächenspannung von $72,75 * 10^{-3} \text{ Nm}$ (DOERR u. SHAKESBY 2012; PARKER 1987). Mineralböden können Oberflächenspannungen zwischen 500 und $5000 * 10^{-3} \text{ Nm}$ haben (DOERR u. SHAKESBY 2012; ZISMAN 1964). Damit das Wasser eine Bodenoberfläche benetzen kann, muss die Oberflächenspannung der Oberfläche größer sein als der Schwellenwert von $72,75 * 10^{-3} \text{ Nm}$ (DOERR u. a. 2000; DOERR u. SHAKESBY 2012). Bodenminerale haben normalerweise eine höhere Oberflächenspannung als Wasser und sind deswegen hydrophil (TSCHAPEK 1984). Allerdings können organische Polymere und Wachse deutlich geringere adhäsive Kräfte aufweisen. Oberflächen mit diesen Substanzen zeigen verstärkt hydrophobe Eigenschaften (DOERR u. SHAKESBY 2012; ZISMAN 1964). Wenn die adhäsiven Kräfte der Oberfläche zu gering sind, nehmen die Wassermoleküle in den Tropfen eine sphärische Anordnung ein und die Bodenoberfläche wird folglich nicht benetzt, dadurch kann zunächst kein Wasser infiltrieren (DOERR u. SHAKESBY 2012).

Um die Oberfläche des Tropfens zu vergrößern, ist Arbeit nötig, nämlich durch höhere adhäsive Kräfte der Oberfläche. Aus diesem Grund ist der



Abb. 2.1: Wassertropfen auf dem hydrophoben Boden eines Buchenwaldstandortes (Holzbach, 27.08.2010).

Kontaktwinkel zwischen Wassertropfen und Oberfläche auch ein Maß für die Intensität (*severity*) der Hydrophobizität (DOERR u. SHAKESBY 2012). Die hydrophoben Substanzen bestehen aus lebendem oder totem Pflanzenmaterial in unterschiedlichen Abbaustadien oder aus Pilzen und Mikroorganismen, die sich in den Humushorizonten oder im Mineralboden befinden (CHAU u. a. 2012; DOERR u. a. 2000; MORLEY u. a. 2005; ATANASSOVA u. DOERR 2010).

Ein weiterer wichtiger Faktor, der die Hydrophobizität beeinflusst, ist die Bodenfeuchte. Nach DOERR u. a. (2000) wird ein hydrophober Boden wieder hydrophil, sobald ein bestimmter kritischer Wassergehalt überschritten wird. Auch laut ZEHE u. a. (2007) und ZEHE u. SIVAPALAN (2009) kann die Hydrophobizität als ein Schwellenwertprozess angesehen werden, der nur dann auftreten kann, wenn die Bodenfeuchte unter einen bestimmten Wert abfällt und gleichzeitig bestimmte organische Verbindungen an der Oberfläche vorhanden sind (ATANASSOVA u. DOERR 2010; MORLEY u. a. 2005; NERIS u. a. 2013). Die hydrophoben Enden der organischen Moleküle sind unter trockenen Bedingungen in Richtung der Bodenporen bzw. der Bodenoberfläche ausgerichtet und führen so zu den hydrophoben Eigenschaften der Bodenoberfläche. Eine längere Durchfeuchtung des Bodens führt zu einer „Auffaltung“ dieser hydrophoben Molekül-Enden,

dadurch werden hydrophile Bereiche der Bodenoberfläche frei. Dies kann unter anderem zum „Umschalten“ der Oberflächeneigenschaften zwischen hydrophob und hydrophil führen (TSCHAPEK 1984; MORLEY u. a. 2005; DOERR u. SHAKESBY 2012).

In den letzten 20 Jahren wurden auf dem Forschungsgebiet der Hydrophobizität bereits deutliche Fortschritte erzielt, besonders im Bezug auf die Erforschung der Faktoren, die das Auftreten und die Intensität der Hydrophobizität kontrollieren (DOERR u. a. 2000, 2009). Dennoch sind diese Einflussfaktoren und die ablaufenden Prozesse auch bisher noch nicht komplett verstanden und erforscht (ATANASSOVA u. DOERR 2010; DOERR u. a. 2000; MORLEY u. a. 2005; WITTER u. a. 1991) und besonders die spezifischen Substanzen, die zur hydrophoben Reaktion einer Oberfläche führen, sind noch nicht gänzlich bekannt. Die meisten wissenschaftlichen Untersuchungen zur Hydrophobizität von Waldböden beschäftigen sich mit mediterranen oder tropischen Wäldern und stehen im Kontext mit Waldbränden als auslösendem Faktor, der zu Hydrophobizität führt (ARCENEGUI u. a. 2007; ATANASSOVA u. DOERR 2011; BODÍ u. a. 2012; CERDÀ u. DOERR 2008; DOERR u. a. 2009; KAJIURA u. a. 2012; RAVI u. a. 2009; RODRÍGUEZ-ALLERES u. a. 2012; SHAKESBY 2011; SHAKESBY u. a. 2003; ZAVALA u. a. 2009).

In den letzten 10-15 Jahren wurden allerdings auch einige Studien zur Hydrophobizität in Mitteleuropäischen Wäldern veröffentlicht (BENS u. a. 2007; BUCZKO u. a. 2002, 2005, 2006, 2007; DOERR u. a. 2006; GREIFFENHAGEN u. a. 2006; HARTMANN u. a. 2009; ORFÁNUS u. a. 2008; WAHL u. a. 2003, 2005; WESSOLEK u. a. 2008).

Die untersuchten Flächen liegen im südlichen Großbritannien (DOERR u. a. 2006), in der südwestlichen Slowakei (ORFÁNUS u. a. 2008), im östlichen Deutschland (WESSOLEK u. a. 2008) und in Nordost-Deutschland (BENS u. a. 2007; BUCZKO u. a. 2005, 2007; HARTMANN u. a. 2009; WAHL u. a. 2003, 2005). Alle diese auf Mitteleuropa bezogenen Untersuchungen zeigen, dass die Hydrophobizität ein wichtiger Faktor ist, der den Infiltrationsprozess stark beeinflussen kann, sogar in einem gemäßigten, humiden Klima.

2.3 Bodenerosion durch Wasser

Der Bodenabtragsprozess wird eingeleitet durch den Tropfeneinschlag und durch den Oberflächenabfluss als solches. Der Bodenabtrag durch Regentropfen wird

im englischsprachigen Raum als *Splash* bezeichnet und wird kontrolliert durch die kinetische Energie der Regentropfen (BRODIE u. ROSEWELL 2007; BRYAN 2000), sowie durch die Eigenschaften der Bodenoberfläche und des Bodens (KUHN u. BRYAN 2004; LE BISSONNAIS u. a. 2005). Durch den *Splash-Effekt* werden kleine Bodenpartikel bereit gestellt, die vom aufkommenden Oberflächenabfluss leicht abgetragen werden können (ROTH 1996; MORGAN 1986; KRETZSCHMAR 1992). Den Bodenabtrag durch flächenhaft auf der Bodenoberfläche fließendes Wasser bezeichnet man als flächenhafte Erosion (interrill erosion). Sobald es zu einer Konzentration des Oberflächenabflusses kommt, kann es zu Rillen- und Rinnenerosion (rill erosion) kommen (GOVERS u. a. 2007; RICHTER 1998; RIES 2012). Innerhalb der Rinnen sind Tiefe und Geschwindigkeit des fließenden Wassers wesentlich höher als auf der Fläche und somit sind auch höhere Erosionsraten zu erwarten (GOVERS u. a. 2007).

3

Auswahl der wichtigsten experimentellen Geländemethoden

In den folgenden drei Abschnitten werden die im Rahmen dieser Arbeit verwendeten experimentellen Geländemethoden kurz vorgestellt und es wird begründet, warum die jeweilige Methode ausgewählt wurde.

3.1 Water Drop Penetration Time (WDPT) -Tests zur Messung der Hydrophobizität

Bei den *Water Drop Penetration Time (WDPT)* -Tests werden Wassertropfen mittels einer Pipette auf eine Bodenoberfläche gesetzt (DOERR u. a. 2000, 2006). Dann wird die Zeit gestoppt, die bis zum vollständigen Infiltrieren des Tropfens vergeht. Die WDPT in Sekunden ist ein Maß für die Persistenz der Hydrophobizität einer Oberfläche. Die Persistenz der Hydrophobizität beschreibt, wie lange es dauert, bis die Oberfläche den Wassertropfen aufnehmen kann. Dies ist eine Eigenschaft, die für die Bestimmung der hydrologischen Reaktion eines Bodens auf ein Starkregenereignis sehr entscheidend sein kann. Je länger ein Boden wasserabweisend bleibt, desto mehr Oberflächenabfluss kann entstehen. Die Methode der WDPT Tests wurde vor allem deswegen ausgewählt, weil sie die im Gelände am einfachsten einzusetzende Methode ist; sie ist wenig fehleranfällig sowie Zeit und Ressourcen sparend. Im Gegensatz dazu ist die sonst häufig verwendete Methode, bei der die Kontaktwinkel zwischen Tropfen und Bodenoberfläche gemessen werden, im Gelände deutlich schwieriger umsetzbar und auch fehleranfälliger. Die Methode der WDPT Tests wurde in den beiden Artikeln BUTZEN u. a. (2014, subm) (Kapitel 6 und 7) verwendet.

3.2 Niederschlagssimulationen zur Messung der Oberflächenabflussbildung und flächenhaften Bodenerosion durch Wasser

Die Niederschlagssimulationen nach RIES (2000) und ISERLOH u. a. (2012) werden durchgeführt, um die Reaktion der jeweiligen Testfläche auf ein definiertes und reproduzierbares Niederschlagsereignis von $40 \text{ mm } h^{-1}$ im Hinblick auf Oberflächenabflussbildung und Bodenerosion (vor allem den Ablösungsprozess) zu testen.

Diese Methode wurde ausgewählt, weil sie im Vergleich zu Langzeitmessplots oder Erosionmessstäben mit deutlich geringerem Aufwand durchgeführt werden kann. Außerdem lassen nur die experimentellen Messungen unter Verwendung eines einheitlichen, reproduzierbaren Niederschlages auch Vergleiche zwischen den verschiedenen Testgebieten zu, weil sowohl Messfläche als auch Niederschlag gleich sind. Ebenfalls ist es nur mit den künstlichen, reproduzierbaren Niederschlägen möglich, im selben Testgebiet gleiche Flächen zu unterschiedlichen Jahreszeiten zu untersuchen und so unterschiedliche Systemzustände erfassen und vergleichen zu können. All dies ist auf Langzeitmessplots mit natürlichen Niederschlägen so nicht möglich. Die Niederschlagssimulationen wurden in ISERLOH u. a. (2013) (Kapitel 4), BUTZEN u. a. (2011) (Kapitel 5), BUTZEN u. a. (2014) (Kapitel 6), BUTZEN u. a. (subm) (Kapitel 7) und WIRTZ u. a. (2012a) (Kapitel 8) angewendet.

3.3 Rinnenspülversuche zur Messung der Effektivität der Rinnenerosion im Gelände

Die Rinnenspülversuche nach WIRTZ u. a. (2010, 2012b) werden durchgeführt, um die Effizienz der Rinnenerosion in natürlich im Gelände vorkommenden Rinnen unter experimentellen, und damit reproduzierbaren Bedingungen, zu bestimmen.

Die Rinnenspülversuche wurden ausgewählt, weil es bisher noch keine wirklich etablierte und standardisierte Methode zur Messung der Erosion in bereits existierender Rinnen im Gelände gibt. Die hier verwendete Methode wurde eigens entwickelt, um die vorhandene Lücke der Messmethoden zu schließen. Mit Hilfe der Ergebnisse der Rinnenspülversuche ist es nun auch möglich, die Effektivität der Rinnenerosion mit der Effektivität der flächenhaften Erosion im selben Gebiet zu vergleichen, bzw. die Ergebnisse zueinander in Beziehung zu setzen. Die Rinnenspülversuche wurden in WIRTZ u. a. (2012a) angewendet (Kapitel 8).

Iserloh et al. (2013): European small portable rainfall simulators: A comparison of rainfall characteristics. *Catena*, Vol. 110, pp. 100-112.

European small portable rainfall simulators: a comparison of rainfall characteristics.

T. Iserloh^{a*}, J.B. Ries^a, J. Arnaez^b, C. Boix Fayos^c, V. Butzen^a, A. Cerdà^d, M.T. Echeverría^e, J. Fernández-Gálvez^f, W. Fister^g, C. Geißler^h, J.A. Gómezⁱ, H. Gómez-Macphersonⁱ, N.J. Kuhn^g, R. Lázaro^j, F.J. León^e, M. Martínez-Mena^c, J.F. Martínez-Murillo^k, M. Marzen^a, M.D. Mingorance^f, L. Ortigosa^b, P. Peters^l, D. Regués^m, J.D. Ruiz-Sinoga^k, T. Scholten^h, M. Seeger^{a,l}, A. Solé-Benet^j, R. Wengel^a, S. Wirtz^a

^aPhysical Geography, Trier University, 54286 Trier, Germany

^bPhysical Geography, University of La Rioja, 26004 Logroño, Spain

^cSoil and Water Conservation Department (CEBAS-CSIC), University of Murcia, 30100 Murcia, Spain

^dDepartment of Geography, University of Valencia, 46010 Valencia, Spain

^eDepartment of Geography and Spatial Management, University of Zaragoza, 50009 Zaragoza, Spain

^fAndalusian Institute for Earth Sciences (UGR-CSIC), 18100 Granada, Spain

^gPhysical Geography and Environmental Change, University of Basel, 4056 Basel, Switzerland

^hPhysical Geography and Soil Science, Eberhard Karls University Tübingen, 72070 Tübingen, Germany

ⁱInstitute for Sustainable Agriculture (IAS-CSIC), Apartado 4084, 14080 Córdoba, Spain

^jArid Zones Experimental Station (EEZA-CSIC), 04120 Almería, Spain

^kDepartment of Geography, University of Málaga, 29079 Málaga, Spain

^lLand Degradation and Development, Wageningen University, 6700 Wageningen, the Netherlands

^mPyrenean Institute of Ecology (IPE-CSIC), 50059 Zaragoza, Spain

*Corresponding author: Tel.: +49-651-2013390, e-mail: iserloh@uni-trier.de, Fax: +49-651-2013976.

Abstract

Small scale portable rainfall simulators are an essential research tool for investigating the process dynamics of recent soil erosion and surface hydrology. Such rainfall simulators differ in design, applied rainfall intensities, rain spectra, research questions, etc. therefore this impedes drawing comparisons between results. A standardization of rainfall simulators or simulation characteristics is not in sight. Nevertheless, these data become progressively important for soil erosion assessment and therefore, the basis for decision-makers in application-oriented erosion protection.

The artificially generated rainfall of the simulators used at the Universities Basel, La Rioja, Malaga, Trier, Tübingen, Valencia, Wageningen, Zaragoza, and at different CSIC (Spanish Scientific Research Council) institutes (Almeria, Cordoba, Granada, Murcia and Zaragoza) were measured with the same methods (Laser Precipitation Monitor for drop spectra and rain collectors for spatial distribution). Data are very beneficial for improvements of simulators and comparison of simulators and results. Furthermore, they can be used for comparative studies, e.g. with measured natural rainfall spectra. A broad range of rainfall data was measured (e.g. intensity: 37 – 360 mm h⁻¹; Christiansen Coefficient for spatial rainfall distribution: 61 – 98 %; median volumetric drop diameter: 0.375 – 6.5 mm; mean

kinetic energy expenditure: $25 - 1322 \text{ J m}^{-2} \text{ h}^{-1}$; mean kinetic energy per unit area and unit depth of rainfall: $0.77 - 50 \text{ J m}^{-2} \text{ mm}^{-1}$). Similarities among the simulators could be found e.g. concerning drop size distributions (maximum drop numbers are reached within the smallest drop classes $< 1 \text{ mm}$) and low fall velocities of bigger drops due to a general physical restriction. The comparison represents a good data-base for improvements and provides a consistent picture of the different parameters of the simulators that were tested.

Keywords:

Rainfall simulator comparison; Runoff; Drop size; Drop velocity; Kinetic energy; Spatial rainfall distribution; Water erosion

1. Introduction

Rainfall simulation has become an important method for assessing the subjects of soil erosion and soil hydrological processes. It is an essential tool for investigating the different erosion processes in situ and in the laboratory, particularly for quantifying rates of detachment and transportation of material (e.g. Cerdà, 1999). Its application allows a quick, specific and reproducible assessment of the meaning and impact of several factors, such as slope, soil type (infiltration, permeability), soil moisture, splash effect of raindrops (aggregate stability), surface structure, vegetation cover and vegetation structure (Bowyer-Bower and Burt, 1989; Schmidt, 1998). The possibility of high repetition rate offers a systematic approach to address the different factors that influence soil erosion even in remote areas and in regions where highly erosive rainfall events are rare or irregular. A compilation of different rainfall simulator systems is given by Meyer (1988) and Hudson (1995). Cerdà (1999) reports on the history of rainfall simulation over the past 62 years and lists 229 different simulators by author, year of construction, application by country, nozzle type, capillary material, drop diameter, precipitation intensity, plot size and by research question.

The need to distinguish the different partial processes of runoff generation and erosion led to the development of rainfall simulations on small plots (Calvo et al., 1988). The advantages of small portable rainfall simulators are, among others, the low costs, the easy transport in inaccessible areas and the low water consumption. Small portable rainfall simulators also enable data to be obtained under controlled conditions and over relatively short time periods. They have been used worldwide by different research groups for many years. Since 1938 more than 100 rainfall simulators with plot dimensions $< 5 \text{ m}^2$ (most of them $< 1 \text{ m}^2$) were developed (e.g. Abudi et al., im Druck; Adams et al., 1957; Alves Sobrinho et al., 2008; Battany and Grismer, 2000; Birt et al., 2007; Blanquies et al., 2003; Bork, 1981; Bryan, 1974; Calvo et al., 1988; Cerdà et al., 1997; Clarke and Walsh, 2007; Farres, 1987; Hudson, 1965; Humphry et al., 2002; Imeson, 1977; Kamphorst, 1987; Loch et al., 2001; Luk,

1985; Martínez-Mena et al., 2001a; Medalus, 1993; Nadal-Romero and Regués, 2009; Neal, 1937; Norton, 1987; De Ploey, 1981; Poesen et al., 1990; Regmi and Thompson, 2000; Regués and Gallart, 2004; Roth et al., 1985; Torri et al., 1999; Wilm, 1943). There is no standardization of rainfall simulation and these rainfall simulators differ in design, rainfall intensities, rain spectra, etc. which impede drawing a meaningful comparison between results. Nevertheless, the data have become progressively important for soil erosion assessment and decision-making in application-oriented erosion protection. Therefore, the accurate knowledge of test conditions is a fundamental requirement and is essential to interpret, combine and classify results (Boulal et al., 2011; Clarke and Walsh, 2007; Lascelles et al., 2000; Ries et al. 2013).

A summary of major requirements for small portable rainfall simulators is given in Iserloh et al. (2012). The most substantial and critical properties of a simulated rainfall are the drop-size distribution (DSD), the fall velocities of the drops and the spatial distribution of the rainfall on the plot-area. Since the 1970s, published studies have shown variations in these properties generated by respective simulators (e.g. Cerdà et al., 1997; Fister et al., 2011, 2012; Hall, 1970; Hassel and Richter, 1988; Humphry et al., 2002; Iserloh et al., 2012; Kincaid et al., 1996; King et al., 2010; Lascelles et al., 2000; Ries et al., 2009; Salles et al., 1999; Zhao et al., 1996). Many techniques were used to characterise simulated rainfall, such as the flour pellet method, laser particle measuring system, plaster micro plot, indication paper, Joss-Waldvogel Disdrometer and the oil method among others. It was shown that the results of the characterisation of simulated rainfall were extremely dependent on the particular method that was applied (Ries et al., 2009). Against this backdrop, a standardized method for verifying and calibrating the characteristics of simulated rainfall is paramount, and the Thies Laser Precipitation Monitor (LPM) represents the most up-to-date and accurate measurement technique for obtaining information on drop-spectra and drop fall velocities (King et al., 2010; Ries et al., 2009), along with an optimal price-performance ratio. Quantity and spatial distribution of the simulated rain can be easily measured with rain-collectors (covering the complete testplot) at low cost and good performance.

In this study, artificial rainfall generated by 13 rainfall simulators based in various European research institutions from Germany, the Netherlands, Spain and Switzerland was characterized using LPM and rain collectors in all simulations in order to ensure comparability of the results. The studied rainfall simulators represent most of the devices that have been used in Europe over the last decade and they present a wide range of designs, plot dimensions (0.06 m^2 up to 1 m^2), numbers and types of nozzles and rainfall intensities. The main research question to be answered is: What are the most important differences/similarities in the suite of simulated rainfall characteristics investigated?

2. Material & methods

2.1. Rainfall simulators

The 13 small portable field rainfall simulators that were tested are shown in Fig. 1 and their main characteristics are listed in Table 1. The simulators are three new developed prototype nozzle-type simulators based at Tübingen (TU), Cordoba (CO) and Basel (BA) as well as two capillary-type simulators from Granada (GR) and Wageningen (WA). The eight other simulators are round plot nozzle-type simulators based at Almeria (AL), Malaga (MA), Murcia (MU), Trier (TR), Zaragoza-CSIC (ZAC), Valencia (VA), Zaragoza-University (ZAU) and La Rioja (LR), and their design follows Calvo et al. (1988). This round plot type of rainfall simulator is the most common device used in semi-arid areas in Europe, especially in Spain, and major differences typically occur in pumps, nozzles and applied intensities. Duration of all simulators is adjustable, only the WA-simulator is limited to 3 min, due to its compact design.

Table 1: The main characteristics of small scale portable rainfall simulators tested (ranked in order of plot size).

ID	Plot size [m ²]	Plot design	Falling height [m]	Nozzle/drop formers	Water source	Details
TU	1.000	1 m × 1 m, rectangular	3.43	Lechler 460.788.30	Electric pressure pump (driven by power generator)	Iserloh et al. (2013)
CO	0.700	1 m × 0.7 m, rectangular	2.30	Veejet 80.150	Electric pressure pump (driven by power generator)	Alves Sobrinho et al. (2008)
BA	0.700	1.34 m × 1.0 m × 0.3 m, trapezoid	1.10	Spraying Systems 3/8 HH 20 W SQ	Electric pressure pump (driven by power generator)	Hikel et al. (2013); Iserloh et al. (2013)
GR	0.250	0.5 m × 0.5 m, rectangular	1.50	4900 capillaries per m ²	Electric peristaltic pump (driven by power generator) + Mariotte's bottle	Fernández-Gálvez et al. (2008)
AL	0.283	Round	2.00	Hardi 4680-10E	Gasoline engine driven pressure pump	e.g. Li et al. (2011)
MA	0.283	Round	2.00	Hardi 1553-20	Electric pressure pump (driven by power generator)	e.g. Martínez-Murillo and Ruiz-Sinoga (2007)
MU	0.283	Round	2.00	Lechler 402.608.30	Gasoline engine driven pressure pump	Martínez-Mena et al. (2001b)
TR	0.283	Round	2.00	Lechler 460.608.30	Gasoline engine driven pump or electrical pump (driven by battery)	Iserloh et al. (2012), (2013)
ZAC	0.283	Round	2.22	Lechler 460.688.30	Gasoline engine driven pressure pump	Nadal-Romero and Regués (2009); Nadal-Romero et al. (2011)
VA	0.246	Round	2.00	Hardi 1553 12	Gasoline engine driven pump or electrical pump (driven by battery)	Cerdà et al. (1997); Iserloh et al. (2013)
ZAU	0.212	Round	2.18	Lechler 460.688.30	Gasoline engine driven pressure pump	Iserloh et al. (2013); León et al. (2013)
LR	0.160	Round	2.50	Lechler 460.608.17	Gasoline engine driven pressure pump	Arnaez et al. (2007)
WA	0.159	0.24 m × 0.24 m, rectangular	0.40	49 capillaries	Cylindrical reservoir over capillaries	Iserloh et al. (2013); Kamphorst (1987)

2.2. Methods for evaluating rainfall characteristics

2.2.1. Drop size distribution and drop fall velocities

The Thies Laser Precipitation Monitor (LPM) was used for analyzing the DSD and drop fall velocities. LPM measures the amount and intensity of rainfall and determines rain-drop size and velocity as the drops fall through a laser beam (area of 48 cm²). It registers individual drops with diameters ranging from 0.16 mm to 8 mm, and fall velocities ranging from 0.2 m s⁻¹ to 20⁻¹, up to a maximum intensity of 250 mm h⁻¹ (Thies, 2004). A more detailed description of the LPM is given in Angulo-Martínez et al. (in press), Fister et al. (2012), King et al. (2010) and Scholten et al. (2011). Because the LPM records only drop size and drop velocity classes, we used the mean value of each class to calculate kinetic energy, momentum and median volumetric drop diameter (d₅₀).

2.2.2. *Spatial rainfall distribution*

In order to generate quantitative information about the homogeneity and the reproducibility of rainfall, small rainfall collectors were used to measure the spatial rainfall distribution. The entire test plot was covered by collectors: square ones (7.5 cm^2 ; in case of Basel: 10 cm^2) for square plots and round collectors (5 cm^2) for round plots (Fig. 2).

2.3. *Test procedure*

A standardized test procedure was developed and performed with the simulators. Prior to each test sequence, rainfall intensity was calibrated using the method generally applied by each group to maintain the customary rainfall conditions of their experimental work. TR and VA used a calibration plate covering the whole plot, TU used the LPM technique, and the remaining groups used rain collectors.

Water flow and discharge of nozzles were measured by positioning a 10 L bucket directly underneath the nozzle of each simulator. The volume of water collected over a one minute interval was then quantified by weighing the bucket. The total water consumption and water efficiency of each rainfall simulator (dividing total water consumption and water amount across the entire plot) was then calculated.

In order to analyze drop spectra with the LPM, five representative positions within the total plot area were chosen (Fig. 2). At each position, five replications at one minute measurement intervals were performed (except the WA-simulator whose design allows only a maximum duration of three minutes). Due to the bodywork of the LPM, the measurement height is 15 cm above ground.

Exposure time of collectors to rainfall during each replicate experiment was 5 min, and a total of three repetitions were undertaken. The individual collectors were weighed to determine spatial variations in the mass, and hence the volume of water at each location within the plot. The results were calculated as equivalent intensity values (mm h^{-1}) and spatially displayed. The measurement of rainfall distribution of the WA-simulator was not possible due to the compact construction of the simulator.



Fig. 1. The small scale portable rainfall simulators from a) Tübingen (TU), b) Cordoba (CO), c) Basel (BA), d) Granada (GR), e) Almeria (AL), f) Malaga (MA), g) Murcia (MU), h) Trier (TR), i) Zaragoza-CSIC (ZAC), j) Valencia (VA), k) Zaragoza-University (ZAU), l) La Rioja (LR) and m) Wageningen (WA).

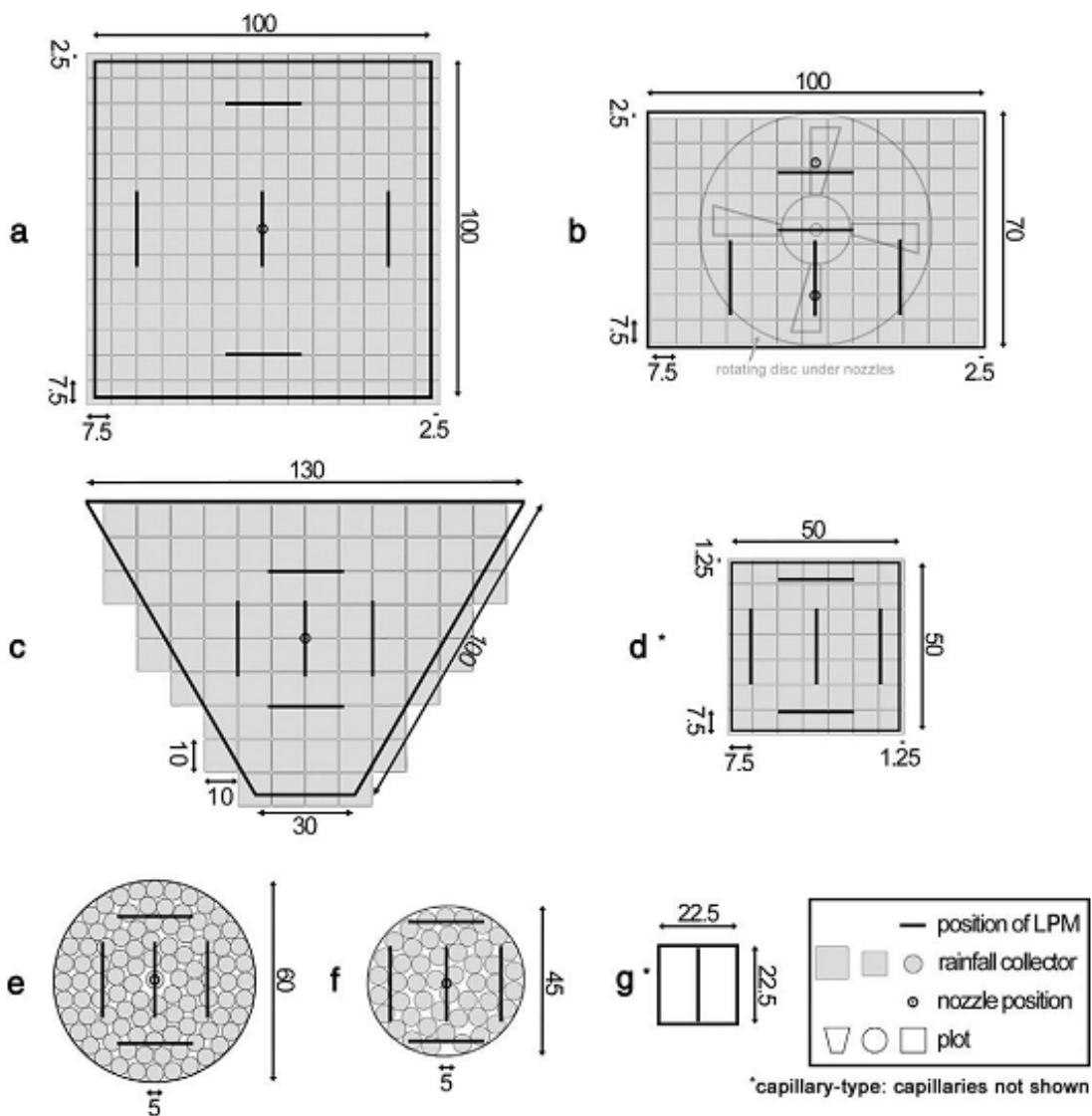


Fig. 2. Test set-up: a) Tübingen (TU), b) Cordoba (CO), c) Basel (BA), d) Granada (GR), e) Almeria (AL), Malaga (MA), Murcia (MU), Trier (TR), Zaragoza-CSIC (ZAC), Valencia (VA) and Zaragoza-University (ZAU), f) La Rioja (LR) and g) Wageningen (WA).

2.4. Further calculations

2.4.1. Rainfall kinetic energy and momentum

Rainfall kinetic energy was calculated using equations from Fornis et al. (2005). These equations were provided relating to the development of the Disdrometer RD-80 (Disdromet Ltd, Basel, Switzerland, 2001) and are optimally applicable for the LPM by Thies. In order to compute the rate of kinetic energy expenditure (KE_R , $J m^{-2} h^{-1}$) for every 1-min period, the following equation was used:

$$KE_R = \left(\frac{\pi}{12}\right) \left(\frac{1}{10^6}\right) \left(\frac{3600}{t}\right) \left(\frac{1}{A}\right) \sum_{i=1}^{20} n_i D_i^3 (v_{D_i})^2 \quad (1)$$

where $A = 0.0048 \text{ m}^2$ is the sampling area of the LPM, n_i the number of drops of diameter D_i ; v_{Di} the measured fall velocity of drop with diameter D_i and $t = 60 \text{ s}$.

The kinetic energy per unit area and unit depth of rainfall, $KE (\text{J m}^{-2} \text{ mm}^{-1})$ was calculated using equation (2):

$$KE = \left(\frac{KE_R}{I} \right) \quad (2)$$

where I is the rainfall intensity (mm h^{-1}) measured with the LPM.

Brodie and Rosewell (2007) concluded that key processes of particle wash off due to rainfall are slightly more dependant on momentum (M) than on KE , therefore momentum was calculated following their approach. The calculations in equation (3) were made on the basis that the momentum $M (\text{kg m s}^{-1})$ of an individual raindrop of diameter D_n is:

$$M_n = 10^{-3} \times m_n v_{Fn} \quad (3)$$

where m_n is mass (g) of D_n raindrop, v_{Fn} is terminal fall velocity (m s^{-1}) of D_n raindrop in still air.

v_{Fn} is measured by the LPM, the mass, m_n , must be calculated (Eq. 4), and the drop volume $V_n (\text{mm}^3)$ is to be determined (Eq. 5), while it is calculated from the measured drop diameters D_n .

$$m_n = 10^{-3} V_n \quad (4)$$

$$V_n = \frac{\pi}{6} D_n^3 \quad (5)$$

2.4.2. Median volumetric drop diameter

The median volumetric drop diameter (d_{50}) was calculated from the percentage total mass of raindrops in each size class according to Hudson (1995) and Clarke and Walsh (2007). For the calculation, the volumes of spherical drops have been assumed.

2.4.3. Uniform Coefficient and spatial rainfall variability

In order to compare results between different simulators, the mean Christiansen Uniformity (CU) coefficient (Christiansen, 1942) was calculated using equation (6).

$$CU = \left(1 - \frac{\sum_{i=1}^n |x_i - \bar{x}|}{\bar{x} * n} \right) \quad (6)$$

where $\sum_{i=1}^n |x_i - \bar{x}|$ is the sum of the absolute deviations from mean water amount of all rain collectors [ml], x_i is individual water amount per rain collector [ml], x is the arithmetic mean of applied water

amount per rain collector [ml] and n is the total number of rain collectors.

For the characterization of spatial rainfall variability, the deviation from the mean was calculated for each collector based on the three replicate tests performed for each rainfall simulator. The deviation was then normalized by the mean rainfall intensity of the respective cell to compute a quantitative measure for the spatial reproducibility of simulated rainfall.

3. Results and discussion

The main rainfall characteristics for each simulator are presented in Table 2. The rainfall simulators of the participating institutes produced a broad range of intensities, from 37 mm h⁻¹ (MA) to 360 mm h⁻¹ (WA). Total water consumption per min depends on the applied intensity, the plot size and the size of nozzle used (e.g. due to different spray angles and applied water pressure). The results ranged from 0.49 L min⁻¹ for AL and VA, to 3.24 L min⁻¹ for TU. Water efficiency showed a broad data range from 4.2 % (LR: large spray angle, high water pressure) to 49.3 % (AL: small spray angle, low water pressure). Particularly for those in situ rainfall simulator studies in (semi-) arid areas with limited water availability, water consumption should be as low and used as efficiently as possible. On the other hand, most scientists deliberately irrigate the adjacent soil surrounding the plot for several reasons: soil characteristics concerning the water content are adapted to the test plot and therefore disturbance by e.g. compensation fluctuations are avoided and surface disturbing tests can take place in the adjacent area without destroying the test plot.

Table 2: Main results of simulated rainfall characteristics for each rainfall simulator: water consumption, water efficiency, mean Intensity [I], Christiansen Uniformity [CU], mean spatial variability (average deviation from mean) of rainfall distribution, mean drop number [n], median volumetric drop diameter [d₅₀], mean kinetic energy expenditure [KER], mean kinetic energy per unit area per unit depth of rainfall [KE] and mean momentum [M].

ID	Water consumption [L min ⁻¹]	Water efficiency [%]	I [mm h ⁻¹]	CU [%]	Spatial variability [%]	n [min ⁻¹]	d ₅₀ [mm]	KER [J m ⁻² h ⁻¹]	KE [J m ⁻² mm ⁻¹]	M [kg m s ⁻¹]
TU	3.24	28.4	55	88.4	3.4	19,956	1.25–1.75	475	9.88	0.0265
CO	a	a	67	81.4	4.4	19,073	2.00–3.00	1322	13.76	0.0459
BA	a	a	43	87.0	8.9	18,217	1.25–1.75	172	7.52	0.0132
GR	a	a	94	76.4	10.6	5640	4.00–5.00	1149	8.40	0.0518
AL	0.49	49.3	51	60.6	12.8	5094	2.00–3.00	638	11.51	0.0327
MA	0.48	36.7	37	89.3	5.1	16,671	1.25–1.75	252	7.56	0.0170
MU	1.36	26.0	75	66.9	13.2	12,823	2.00–3.00	355	7.78	0.0176
TR	0.80	27.0	40	90.6	3.8	19,695	1.00–1.50	214	5.81	0.0157
ZAC	2.60	8.8	48	97.6	1.2	26,797	0.50–1.00	77	3.86	0.0085
VA	0.49	42.9	51	86.2	3.5	8393	1.75–2.50	423	10.84	0.0244
ZAU	2.90	5.9	48	97.8	2.1	24,494	0.50–1.00	54	4.16	0.0071
LR	2.85	4.2	45	96.5	7.9	20,725	0.375–0.750	25	0.77	0.0042
WA	a	a	360	a	a	1190	5.50–6.50	1296	50.32	0.0917

^aNot measured.

3.1. Drop spectra

The mean drop size and fall velocity measurements with the LPM are listed in Fig. 3. The major similarity is that maximum drop numbers are attained within the two smallest drop size classes <1 mm (Fig. 3 and Fig. 4): in all cases, except TU and WA, >1000 drops per min were only measured in those

classes <1 mm. TU also reached 1059 drops in the drop size class 1.0-1.49 mm; the drop amounts of WA are lower than 1000 drops per min for all drop size classes. Amounts of drops >1 mm were generally much lower than that of <1 mm: max. 833 drops per min (ZAU) were measured in the drops size class 1.0-1.49 mm and a max. of 554 drops per min (AL) was detected for sizes >1.5 mm. The highest number of drops per min >2.0 mm was measured for WA (320 drops per minute). More than 100 drops per min >3.0 mm were only produced by the two capillary-type simulators GR (166 drops per minute) and WA (153 drops per minute).

The data also show that the fall velocity of bigger drops is lower due to the general physical restriction of low drop fall heights (Fig. 3). During all simulations, 90% or more of the measured drops were slower than 3.4 m s^{-1} . Only TU (237 drops), CO (321 drops) and GR (158 drops) generated more than 100 drops per minute with fall velocities $>5 \text{ m s}^{-1}$. Drops $>5.8 \text{ m s}^{-1}$ were rarely measured. A few drops with velocities around 9 m s^{-1} were measured during simulations of CO, because the special water application unit in the simulator is able to accelerate bigger drops to higher fall velocities. The velocities of smaller drops (<1 mm) generated by the simulators were often similar to that expected for natural drops, as indicated by Atlas et al. (1973) and Mätzler (2002), for vertical rainfall in calm conditions. In two cases (TU and TR), more than 100 larger drops (1.0-1.49 mm) per min were accelerated to expected natural velocities.

By examining single rainfall simulators, four groups can be distinguished. During the runs of BA, ZAC, ZAU and LR, hardly any big drops ($>2.5 \text{ mm}$) were measured. The simulators from TU, MA, MU, TR and VA produced drops $>2.5 \text{ mm}$, but this was much less than the capillary-type simulators from GR and ZAU. The simulators from CO and AL also generated drops $>2.5 \text{ mm}$ but reached higher velocities than GR and ZAU.

Unfortunately, determining exact d_{50} values for volumetric drop diameter were not possible with the LPM for two reasons. As mentioned above, the device records only size classes and not actual drop sizes, besides the fact that only drop diameters are registered. We assumed a circular form of the falling drops for our calculations (Fister et al., 2011). Nevertheless, calculation of d_{50} values represents the best possible option for comparison with other rainfall simulators (Fister et al., 2012; Hudson, 1995). Hence, the lowest d_{50} value of the 13 simulators was 0.375-0.750 mm (LR), and the highest 5.5-6.5 mm (WA) (Table 2).

Most studies lack this accuracy about calculated kinetic energy of simulated rainfall (Clarke and Walsh, 2007): the values are predominantly calculated from intensities only, based on the assumption that diameters and/or velocities from natural rainfall apply for simulated rainfall, too. Considering the general physical restrictions of simulated rainfall (e.g. fall height), we therefore assume, that most of the published data overestimate real values of kinetic energy. The KE values calculated in this study were maximal 56 % (minimal 3 %) of the KE calculated with the three of the most commonly

used equations for determining natural rainfall of equal intensities (van Dijk et al., 2002; Morgan et al., 1998; Wischmeier and Smith, 1978). Only the WA produced rainfall with a KE that was greater than that calculated for natural rainfall (up to 77 % more than calculated with each of the three mentioned equations). The high KE of the WA-simulator was caused by the specific characteristics (very short test duration with large, high-energy drops as described in Iserloh et al. (in press) and Kamphorst (1987)).

The calculated momentums of simulated rainfalls ranged from $0.0042 \text{ kg m}^2 \text{ s}^{-1}$ for LR up to $0.0917 \text{ kg m}^2 \text{ s}^{-1}$ for WA. As mentioned above, some researchers concluded that key processes of particle wash off due to rainfall are slightly more dependant on momentum than on KE (Brodie and Rosewell, 2007). Rose (1960) found that this was the case for the rate of soil detachment per unit area, and Park et al. (1980) used a momentum power relationship to predict splash erosion (Brodie and Rosewell, 2007).

In Fig. 4 the results of the LPM measurements were plotted in relation to the drop size distribution for a hypothetical Marshall & Palmer distribution (Marshall and Palmer, 1948) of equal intensities. The box plots in Fig. 4 give additional information about the scattering of drop amounts over the 25 1-min measurement intervals on five positions. A broad scattering, reflects the heterogeneity of the spatial distribution of rainfall on the respective plot, described below.

The simulators from CO, ZAC, ZAU and LR showed little scattering in all classes, the measured values were close to the Marshall & Palmer distribution. However, in most cases there were too many drops in the 0.5-0.99 mm drop size class and too little in the 1.0-1.49 mm and 1.5-1.99 mm drop size class. The simulators from TU, GR, MA, MU, TR and VA showed higher scattering, especially in the small drop classes. The values were still close to the Marshall-Palmer distribution. The results from the GR simulator were remarkable because of the higher amount of drops $>3 \text{ mm}$ diameter. The simulators from AL and WA showed deviations from the Marshall-Palmer distribution. The AL simulator produces much too less drops smaller than 0.50 mm, whereas the WA simulator produces a relatively regular drop size distribution over all classes.

3.2. Spatial rainfall distribution

The mean intensities based on three replicate measurements for each rain collector are presented in Fig 5. Only the two simulators from Zaragoza (ZAC and ZAU) showed evenly distributed intensities, caused by large spraying angles of the full cone nozzles used. All other simulators showed variations over the total plot area, caused by number of applied nozzles (CO) or nozzle-types as well as applied water pressure.

TU showed an almost uniform rainfall distribution across the whole plot ($>55 \text{ mm h}^{-1}$, max. 68 mm h^{-1}) with only small patches of lower intensity values in the left upper corner and at the outlet

(35-55 mm h⁻¹). The average spatial rainfall variability over the three repetitions was low (\varnothing 3.4 %, Table 2), in most cases between 0 and 5 %, only in few cases between 5 % and 10 % (Fig. 6).

For CO, lower rainfall intensities (50-70 mm h⁻¹) were measured at the right and the left edges of the plot, and at one strip in the middle. Higher intensities (70-97 mm h⁻¹) occurred on the upper and the lower area of the plot. Average deviations from the mean were low (\varnothing 4.4 %), and almost all collectors showed values between 0 and 10 %. In one case, the value was between 10 % and 15 %.

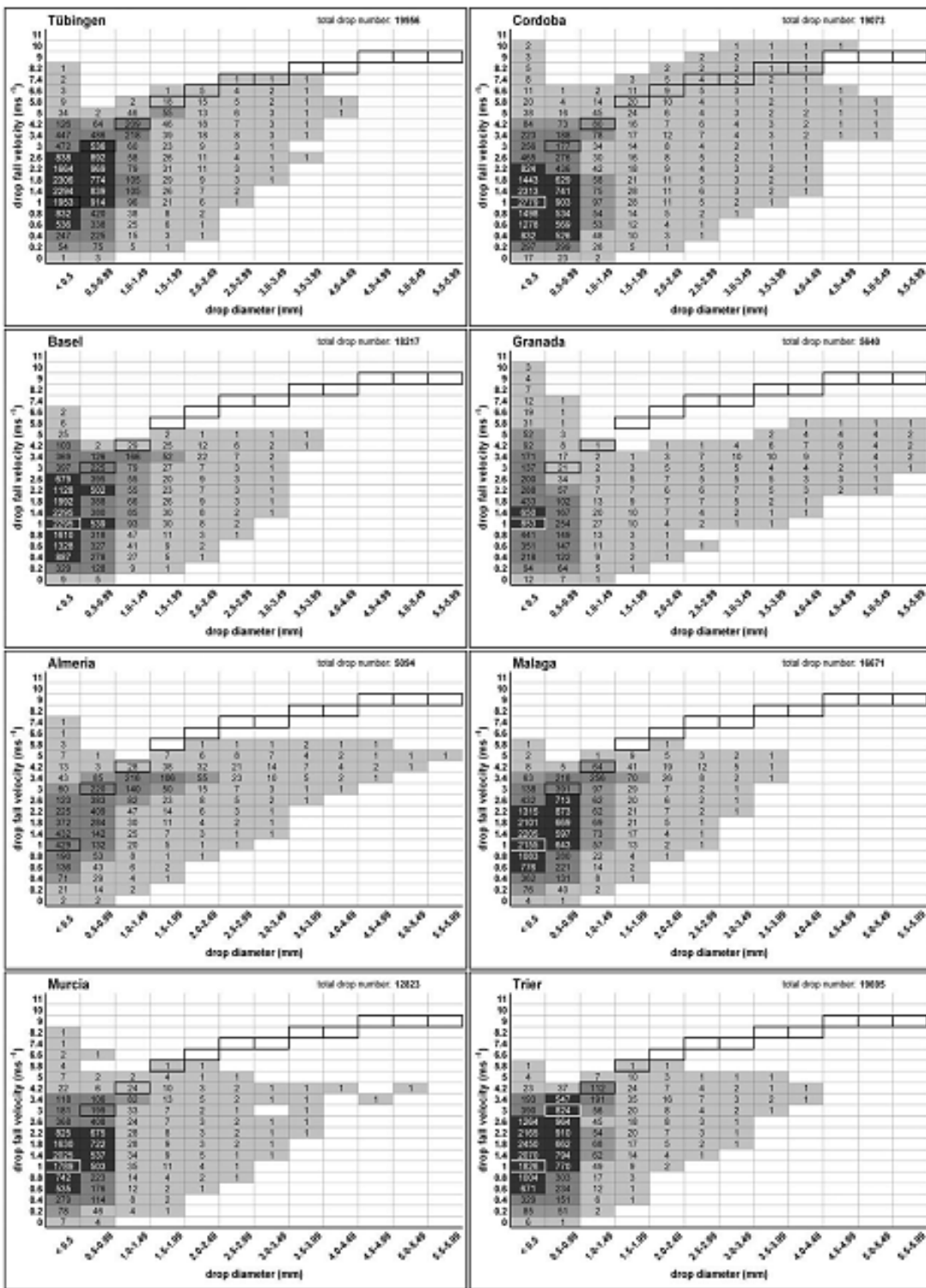


Fig. 3. Average drop size distribution and drop fall velocity for each rainfall simulator. Shown are mean values representing 1 minute simulated rainfall (n: 25 on five positions [WA; n: 3 on one position]). Each box gives counted total number of drops, fall velocity and drop size class. Calculated drop diameter ranges and corresponding fall velocities for natural rain (Atlas et al., 1973; Mätzler, 2002) are marked with a bold frame.

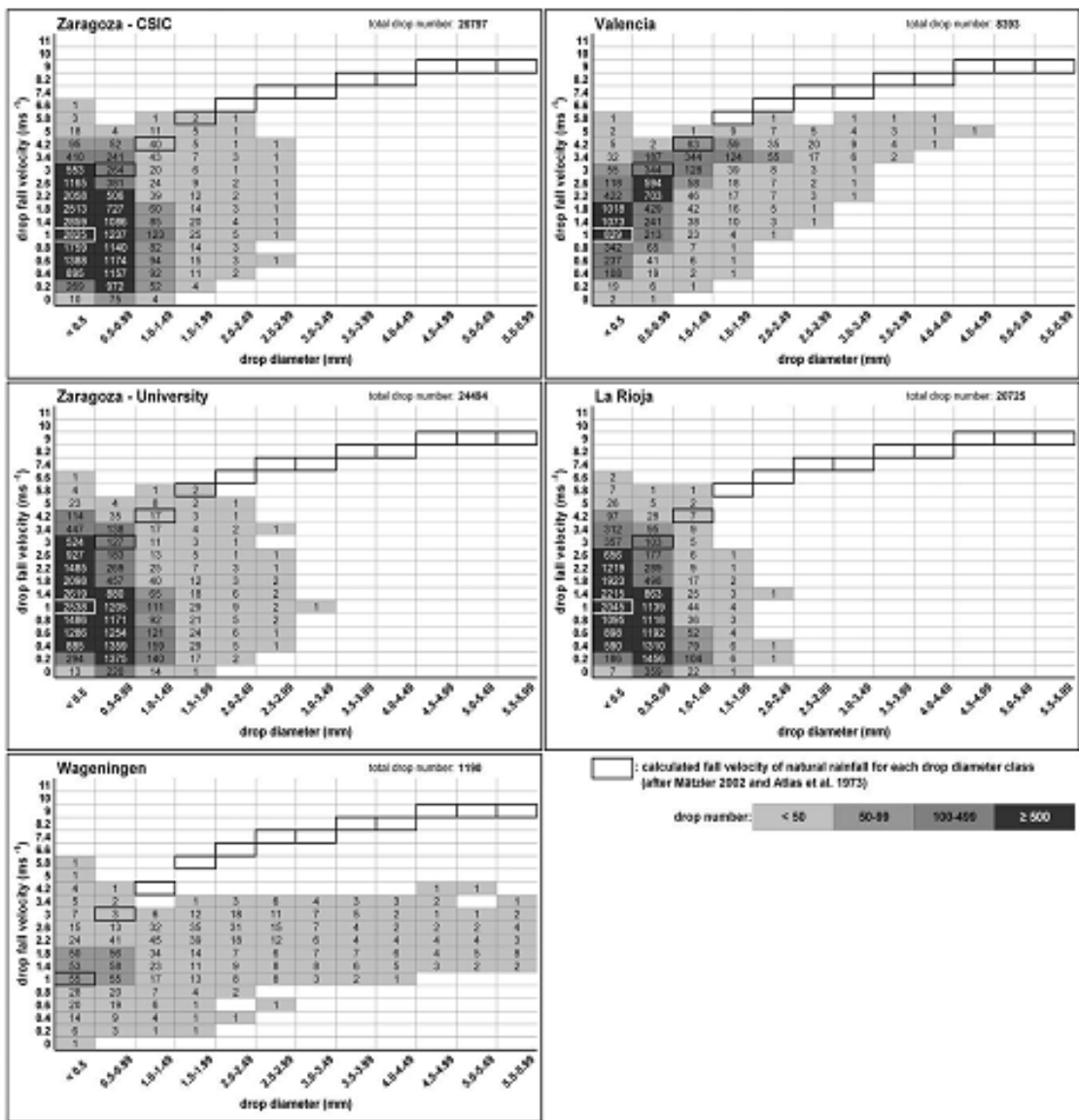


Fig. 3 continued.

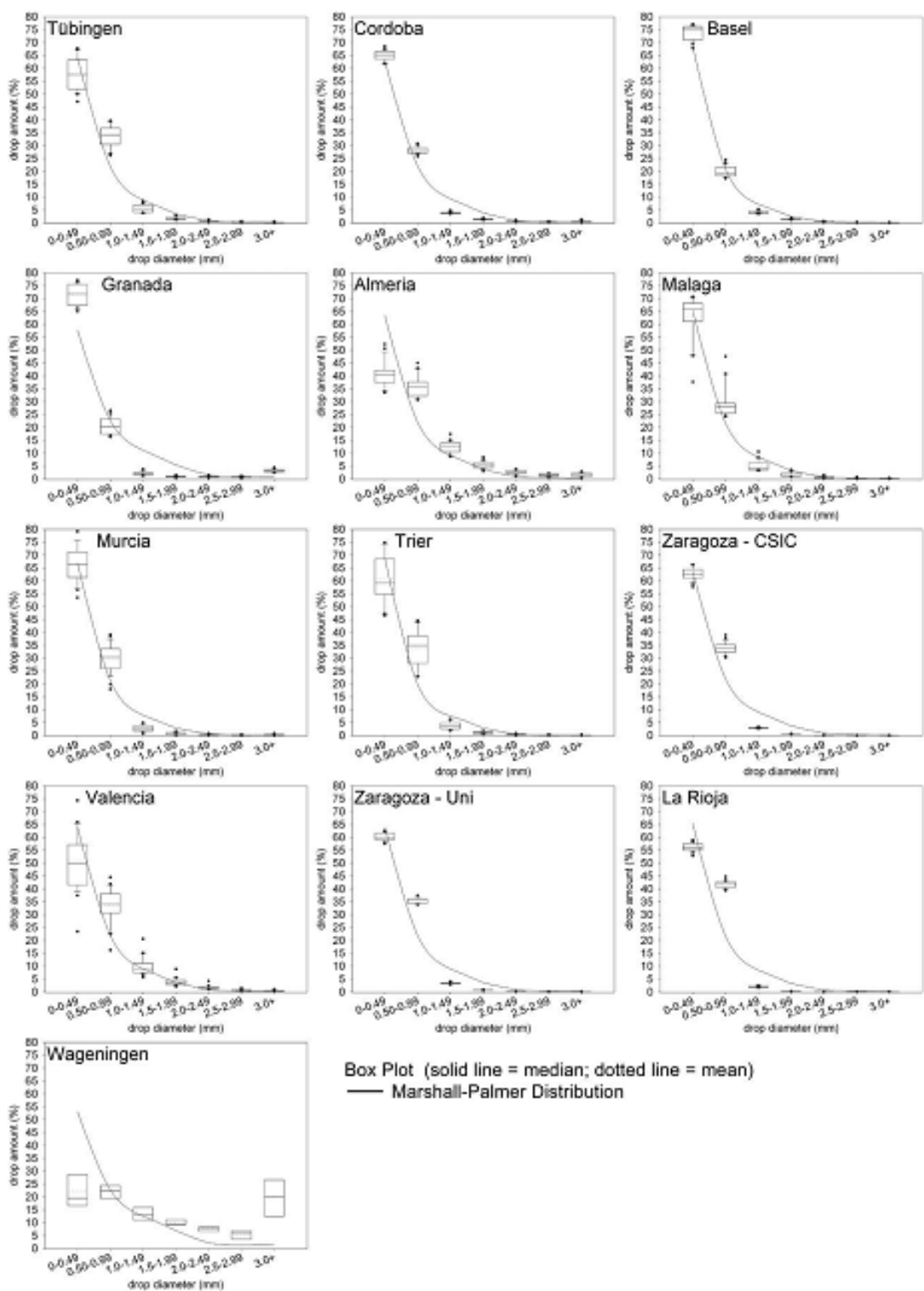


Fig. 4. Measured drop size distributions and calculated Marshall & Palmer distributions of equal intensities expressed as box plots for total plot (n: 25 on 5 positions [WA: n: 3 on one position]). The lower and upper boundaries of each box represent the 25th and 75th percentiles, respectively, and the lower and upper error bars represent the 10th and 90th percentiles, respectively.

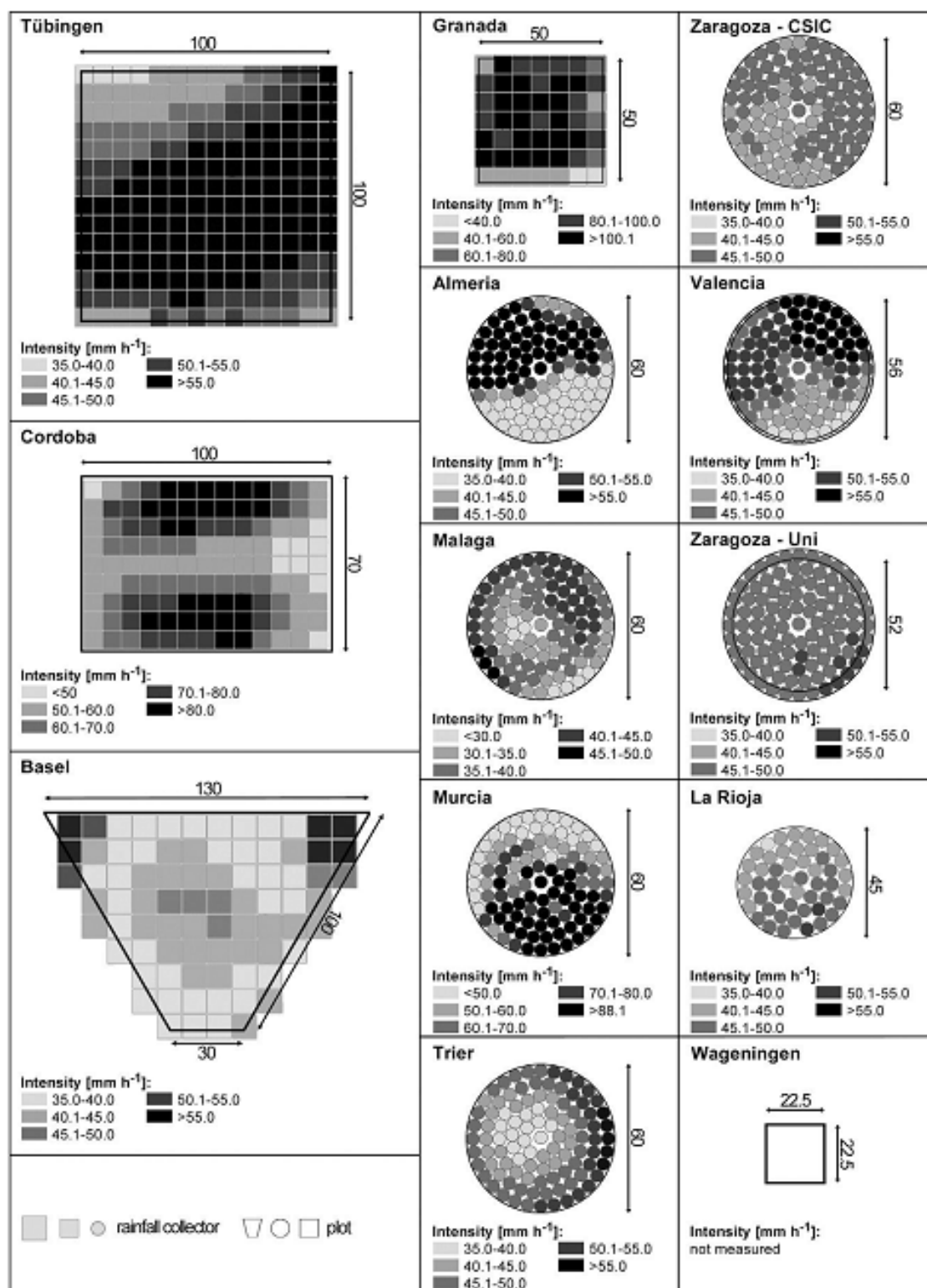


Fig. 5. Average spatial rainfall distributions for the rainfall simulators (mm h⁻¹; n=3 replicates per simulator).

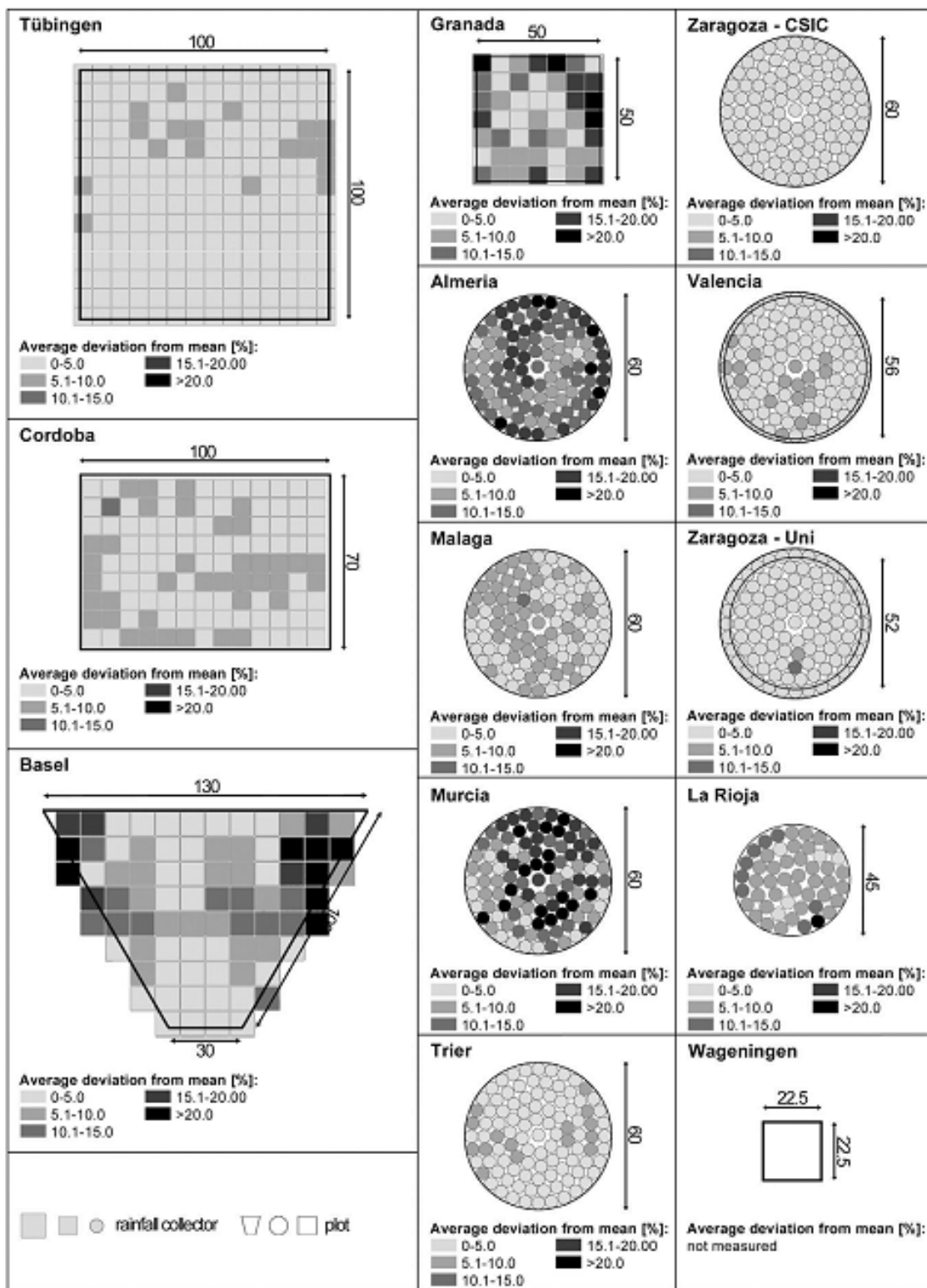


Fig. 6. Average spatial rainfall variability (%) calculated from 3 replicate measurements for each simulator.

The rainfall simulator from BA produced the highest intensities at the upper left and right corners ($51\text{-}100 \text{ mm h}^{-1}$) and in the middle ($45\text{-}50 \text{ mm h}^{-1}$). The other collectors on the plot showed values between 35 mm h^{-1} and 45 mm h^{-1} . The average deviation from the mean ($\varnothing 8.9 \%$) was highest at the upper left and right corners, with deviations up to $>20 \%$.

The intensities for GR were lowest in the first row directly at the outlet ($39\text{-}60 \text{ mm h}^{-1}$). In contrast, in most of the other collectors across the plot more than twice the amounts (up to 136 mm h^{-1}) were measured. The average deviation from the mean ($\varnothing 10.6 \%$) showed an almost concentric pattern of rainfall distribution. Central values ranged from 0 to 5 % and increased outwards, with values higher than 20 % recorded around the edges.

The rainfall simulator from AL produced a spatial rainfall distribution with intensities below 40 mm h^{-1} on the front half of the plot. In contrast, the upper half was characterized by high intensities, most of them $>55 \text{ mm h}^{-1}$. The average deviation from the mean was $\varnothing 12.8 \%$; many collectors showed deviations $>10 \%$, some of them $>20 \%$.

The rainfall simulator from MA produced a near concentric pattern of rainfall intensity, with highest intensities ($40.1\text{-}50 \text{ mm h}^{-1}$) recorded on the right upper area and near the left rim of the plot. The other collectors showed values ranging from 28 mm h^{-1} to 40 mm h^{-1} . The plot was evenly covered by collectors with average deviation from the mean values $<5 \%$ and 5 % to 10 %.

The intensities generated by MU were higher on the front half ($>70 \text{ mm h}^{-1}$) of the plot than on the upper half ($50\text{-}60 \text{ mm h}^{-1}$). The average deviation from the mean ($\varnothing 13.2 \%$) was similar to the AL plot. Many deviations higher than 15% were recorded across the plot.

The TR-simulator produced a concentric pattern. Lower intensities were measured in the middle ($37\text{-}45 \text{ mm h}^{-1}$); the values increase outwards up to 57 mm h^{-1} . Most of the collectors showed an average deviation from the mean ($\varnothing 3.8 \%$) of less than 5 %, and only a few collectors showed values between 5 % and 10 %.

The spatial rainfall distribution of the ZAC-simulator can be separated into two parts. In the lower left quarter of the plot, intensities between 40 mm h^{-1} and 45 mm h^{-1} were measured, whereas the other three quarters of the plot recorded intensities of between 45 mm h^{-1} and 50 mm h^{-1} . The average deviation from the mean ($\varnothing 1.2 \%$) for all collectors was less than 5 %.

The intensities on the plot of the VA-simulator can be separated into three distinct areas. The front area (seen from outlet) was characterized by relatively low intensities that ranged between 35 mm h^{-1} and 45 mm h^{-1} . The upper right area recorded intensities up to 55 mm h^{-1} , and the upper left area recorded values $>55 \text{ mm h}^{-1}$. The average spatial variability over the three replicates was low $\varnothing 3.5 \%$; and most of the collectors showed values lower than 5 %, with only a few collectors showing values between 5 % and 10 %.

The rainfall simulator from ZAU produced a very uniform intensity distribution. Almost in all of the

collectors, intensities between 45 mm h^{-1} and 50 mm h^{-1} were measured. Only in nine collectors, the intensity increased to values ranging between 50.1 mm h^{-1} and 55 mm h^{-1} . With the exception of two collectors, the average deviations from the mean ($\bar{\sigma} 2.1\%$) were less than 5 %.

The simulator used in LR produced a uniform intensity distribution. For almost all of the collectors, intensities between 40 mm h^{-1} and 50 mm h^{-1} were measured. The spatial variability ($\bar{\sigma} 7.9\%$) is very heterogeneous across the plot: One collector showed an average deviation from mean higher than 20 %, eight collectors recorded values of between 10 % and 15 %, five collectors between 0 and 5 %, all other collectors on the plot showed values between 5 % and 10 %.

Researchers argue (e.g. Esteves et al., 2000; Neff, 1979) that Christiansen Coefficients over 80 % are essential for rainfall simulation experiments. Most of the simulators meet this requirement, with measured CUs ranging from 60.6 % (AL) to 97.8 % (ZAU). Additionally, the good reproducibility of the spatial rainfall distribution (max. average deviation from mean over total plot of 13.2 %) demonstrates the reproducibility of artificial rainfall of most of the simulators tested.

4. Conclusions

The comparison of rainfall characteristics provides a good data base for improvements and a consistent picture of the parameters and performance of the simulators can be quantified:

- The use of uniform measurement methods provides a means of comparing simulated rainfall characteristics of different simulators.
- The detailed database of artificial rainfall characteristics and the exact knowledge of test conditions represent a prerequisite when assessing erosion, infiltration and runoff results generated during field experiments.
- The LPM is used worldwide for measurements of natural rainfall. This allows detailed comparisons between natural and simulated characteristics in further investigations to be made.
- Kinetic energy values of the simulators are low when compared against calculated values of natural rainfall. Due to the low fall height, it is not possible to reach terminal velocity of large, natural raindrops. This must be taken into account when field results are evaluated.
- All devices investigated are adequate to perform simulations in the field. Nevertheless, an accurate handling and control of test conditions is essential.
- Further improvements of individual simulators should concentrate on water efficiency and spatial rainfall distribution, as well as reproducibility, handling and control of test conditions.

Finally, it can be concluded, that a general understanding about relevant features of simulators as well as calibration and test procedure strategies will help to focus global results and knowledge, for the purpose of creating a reliable and convincing source of information for researchers and decision-

makers alike. Nevertheless, for practical uses, further characteristics of the simulators should be considered e.g. plot size (Iserloh et al., in press).

Acknowledgements

The research for this study was funded by the Deutsche Forschungsgemeinschaft (DFG) project number Ri-835/6-1.

References

- Abudi, I., Carmi, G., Berliner, P., Rainfall simulator for field runoff studies. *J. Hydrol.* in press.
- Adams, J.E., Kirkham, D., Nielsen, D.R., 1957. A portable rainfall-simulator infiltrometer and physical measurements of soil in place. *Soil Sci. Soc. Amer. Proc.* 21, 473–477.
- Alves Sobrinho, T., Gómez-Macpherson, H., Gómez, J.A., 2008. A portable integrated rainfall and overland flow simulator. *Soil Use Manage.* 24, 163–170.
- Angulo-Martínez, M., Beguería, S., Navas, A., Machín, J., Splash erosion under natural rainfall on three soil types in NE Spain. *Geomorphology* in press.
- Arnaez, J., Lasanta, T., Ruiz-Flaño, P., Ortigosa, L., 2007. Factors affecting runoff and erosion under simulated rainfall in Mediterranean vineyards. *Soil Till. Res.* 93, 324–334.
- Atlas, D., Srivastava, R.C., Sekhon, R.S., 1973. Doppler radar characteristics of precipitation at vertical incidence. *Rev. Geophys.* 11, 1–35.
- Battany, M.C., Grismer, M.E., 2000. Development of a portable field rainfall simulator for use in hillside vineyard runoff and erosion studies. *Hydrol. Process.* 14, 1119–1129.
- Birt, L., Persyn, R., Smith, P., 2007. Technical Note: Evaluation of an Indoor Nozzle-TypeRainfall Simulator. *Appl. Eng. Agric.* 23, 283–287.
- Blanquies, J., Scharff, M., Hallock, B., 2003. The design and construction of a rainfall simulator. In: A gathering of global solutions, proceedings of the 34th annual conference (9pp.). International Erosion Control Association, 24–28 February, Las Vegas, Nevada. Available on-line at: <http://www.owp.csus.edu/research/papers/papers/PP044.pdf>, accessed 07.08.2012.
- Bork, H.R., 1981. Oberflächenabfluss und Infiltration. Ergebnisse von Starkregensimulationen in der Südheide, Ostniedersachsen und in Südost- Spanien. *Deutscher Geographentag* 43, 159–163.
- Boulal, H., Gómez-Macpherson, H., Gómez, J.A., Mateos, L., 2011. Effect of soil management and traffic on soil erosion in irrigated annual crops. *Soil Till. Res.* 115–116, 62–70.
- Bowyer-Bower, T.A.S., Burt, T.P., 1989. Rainfall simulators for investigating soil response to rainfall. *Soil Technol.* 2, 1–16.
- Brodie, I., Rosewell, C., 2007. Theoretical relationships between rainfall intensity and kinetic energy variants associated with stormwater particle washoff. *J. Hydrol.* 340, 40–47.
- Bryan, R., 1974. A simulated rainfall test for the prediction of soil erodibility. *Z. Geomorphol.* 21, 138–150.

- Calvo, A., Gisbert, B., Palau, E., Romero, M., 1988. Un simulador de lluvia portátil de fácil construcción. In: M. Sala and F. Gallart (Eds.), *Métodos y técnicas para la medición de procesos geomorfológicos*, Sociedad Espanola de Geomorfología, Monografía 1, Zaragoza, pp. 6–15.
- Cerdà, A., 1999. Simuladores de lluvia y su aplicación a la Geomorfología. Estado de la cuestión. *Cuadernos de I. Geográfica* 25, 45-84.
- Cerdà, A., Ibàñez, S., Calvo, A., 1997. Design and operation of a small and portable rainfall Simulator for rugged terrain. *Soil Tech.* 11 (2), 161-168.
- Christiansen, J.E., 1942. Irrigation by Sprinkling. California Agricultural Experiment Station Bulletin 670.
- Clarke, M.A., Walsh, R.P.D., 2007. A portable rainfall simulator for field assessment of splash and slopewash in remote locations. *Earth Surf. Proc. Land.* 32, 2052–2069.
- De Ploey, J., 1981. Crusting and time-dependent rainwash mechanisms on loamy soil. In: Morgan, R.P.C. (Ed.), *Soil Conservation, Problems and Prospects*. Wiley, pp. 139–154.
- Disdromet Ltd, Basel, Switzerland, 2001. User Guide for Disdrodata V.1.22.
- Esteves, M., Planchon, O., Lapetite, J.M., Silvera, N., Cadet, P., 2000. The “EMIRE” large rainfall simulator: design and field testing. *Earth Surf. Proc. Land.* 25 (7), 681–690.
- Farres, P., 1987. The dynamics of rainsplash erosion and the role of soil aggregate stability. *Catena* 14, 119–130.
- Fernández-Gálvez, J., Barahona, E., Mingorance, M.D., 2008. Measurement of Infiltration in Small Field Plots by a Portable Rainfall Simulator: Application to Trace-Element Mobility. *Water Air Soil Poll.* 191, 257–264.
- Fister, W., Iserloh, T., Ries, J.B., Schmidt, R.G., 2011. Comparison of rainfall characteristics of a small portable rainfall simulator and a portable wind and rainfall simulator. *Z. Geomorphol.* 55, 109–126.
- Fister, W., Iserloh, T., Ries, J.B., Schmidt, R.-G., 2012. A portable wind and rainfall simulator for in situ soil erosion measurements. *Catena* 91, 72–84.
- Fornis, R.L., Vermeulen, H.R., Nieuwenhuis, J.D., 2005. Kinetic energy-rainfall intensity relationship for Central Cebu, Philippines for soil erosion studies. *J. Hydrol.* 300, 20–32.
- Hall, M., 1970. Use of the stain method in determining the drop size distribution of coarse liquid sprays. *Trans. ASAE* 13, 33–37.
- Hassel, J., Richter, G., 1988. Die Niederschlagsstruktur des Trierer Regensimulators. *Mitteilungen der Deutschen Bodenkundlichen Gesellschaft* 56, 93–96.
- Hikel, H., Yair, A., Schwanghart, W., Hoffmann, U., Straehl, S., Kuhn, N.J., Experimental investigation of soil ecohydrology on rocky desert slopes in the Negev Highlands, Israel. *Z. Geomorphol.* in press.
- Hudson, N., 1965. The influence of rainfall on the mechanics of soil erosion. M. Sc. Thesis,

University of Cape Town, Cape Town, South Africa.

Hudson, N., 1995. Soil Conservation. Batsford Ltd, London, 391 pp.

Humphry, J.B., Daniel, T.C., Edwards, D.R., Sharpley, A.N., 2002. A portable rainfall simulator for plot-scale runoff studies. *Appl. Eng. Agric.* 18, 199–204.

Imeson, A.C., 1977. A simple field-portable rainfall simulator for difficult terrain. *Earth Surf. Processes* 2, 431–436.

Iserloh, T., Fister, W., Seeger, M., Willger, H., Ries, J.B., 2012. A small portable rainfall simulator for reproducible experiments on soil erosion. *Soil Till. Res.* 124, 131–137.

Iserloh, T., Ries, J.B., Cerdà, A., Echeverría, M.T., Fister, W., Geißler, C., Kuhn, N.J., León, F.J., Peters, P., Schindewolf, M., Schmidt, J., Scholten, T., Seeger, M., Comparative measurements with seven rainfall simulators on uniform bare fallow land. *Z. Geomorphol.* in press.

Kamphorst, A., 1987. A small rainfall simulator for the determination of soil erodibility. *Netherlands Journal of Agricultural Science* 35, 407–415.

Kincaid, D.C., Solomon, K.H., Oliphant, J.C., 1996. Drop size distributions for irrigation sprinklers. *T. ASAE* 39, 839–845.

King, B.A., Winward, T.W., Bjorneberg, D.L., 2010. Laser Precipitation Monitor for Measurement of Drop Size and Velocity of Moving Spray-Plate Sprinklers. *Appl. Eng. Agric.* 26 (2), 263–271.

Lascelles, B., Favis-Mortlock, D.T., Parsons, A.J., Guerra, A.J.T., 2000. Spatial and temporal variation in two rainfall simulators: implications for spatially explicit rainfall simulation experiments. *Earth Surf. Proc. Land.* 25, 709–721.

León, F.J., Echeverría, M.T., Badía, D., Martí, C., Álvarez, C., Effectiveness of wood chips cover at reducing erosion in two contrasted burnt soils. *Z. Geomorphol.* in press.

Li, X.-Y., Contreras, S., Solé-Benet, A., Cantón, Y., Domingo, F., Lázaro, R., Lin, H., Van Wesemael, B., Puigdefábregas, J., 2011. Controls of infiltration–runoff processes in Mediterranean karst rangelands in SE Spain. *Catena* 86, 98–109.

Loch, R.J., Robotham, B.G., Zeller, L., Masterman, N., Orange, D.N., Bridge, B.J., Sheridan, G., Bourke, J.J., 2001. A multi-purpose rainfall simulator for field infiltration and erosion studies. *Soil Res.* 39, 599–610.

Luk, S., 1985. Effect of antecedent soil moisture content on rainwash erosion. *Catena* 12, 129–139.

Marshall, J.S., Palmer, W.M., 1948. Relation of drop size to intensity. *Journal of Meteorol.* 5, 165–166.

Martínez Mena, M., Abadía, R., Castillo, V., Albaladejo Montoro, J., 2001a. Diseño experimental con lluvia simulada para el estudio de los cambios en la erosión del suelo durante la tormenta. *Cuaternario y Geomorfología* 15, 31–43.

Martínez-Mena, M., Castillo, V., Albaladejo, J., 2001b. Hydrological and erosional response to natural rainfall in a semi-arid area of south-east Spain. *Hydrol. Process.* 15, 557–571.

- Martínez-Murillo, J.F., Ruiz-Sinoga, J.D., 2007. Seasonal changes in the hydrological and erosional response of a hillslope under dry-Mediterranean climatic conditions (Montes de Málaga, South of Spain). *Geomorphology* 88, 69–83.
- Mätzler, C., 2002. Drop-Size Distributions and Mie Computations for Rain. Research Report No. 2002-16. Institut für Angewandte Physik, Uni Bernensis.
- Medalus, 1993. Medalus II report. Silsoe College, Cranfield University, Silsoe.
- Meyer, L.D., 1988. Rainfall simulators for soil conservation research. In: Lal, R., (Ed.), *Soil Erosion Research Methods*. Soil and Water Conservation Society, Ankeny, IO, U.S.A., 75–95.
- Morgan, R.P.C., Quinton, J.N., Smith, R.E., Govers, G., Poesen, J.W.A., Auerswald, K., Chisci, G., Torri, D., Styczen, M.E., Folley, A.J.V., 1998. The European Soil Erosion Model (EUROSEM): Documentation and User Guide. Silsoe College, Cranfield University, Silsoe, Bedford.
- Nadal-Romero, E., Lasanta, T., Regüés, D., Lana-Renault, N., Cerdà, A., 2011. Hydrological response and sediment production under different land cover in abandoned farmland fields in a mediterranean mountain environment. *Boletín de la Asociación de Geógrafos Espanoles* 55, 303–323.
- Nadal-Romero, E., Regüés, D., 2009. Detachment and infiltration variations as consequence of regolith development in a Pyrenean badland system. *Earth Surf. Proc. Land.* 34 (6), 824–838.
- Neal, J.H., 1937. The effect of the degree of slope and rainfall characteristics on runoff and soil erosion. Research Bulletin, Agricultural Experiments Station University of Missouri, Columbia, USA.
- Neff, E.L., 1979. Why rainfall simulation? Proceedings of Rainfall Simulator Workshop, Tucson, Az. USDA-SEA ARM-W-10, 3–7.
- Norton, L.D., 1987. Micromorphological study of surface seals developed under simulated rainfall. *Geoderma* 40, 127–140.
- Park, S.W., Mitchell, J.K., Bubenzer, G.D., 1980. An analysis of splash erosion mechanics. In: ASAE 1980 Winter Meeting, Paper No.0-2502, p. 27.
- Poesen, J., Ingelmo Sanchez, F., Mucher, H., 1990. The hydrological response of soil surfaces to rainfall as affected by cover and position of rock fragments in the top layer. *Earth Surf. Proc. Land.* 15, 653–671.
- Regmi, T.P., Thompson, A.L., 2000. Rainfall simulator for laboratory studies. *Appl. Eng. Agric.* 16, 641–652.
- Regüés, D., Gallart, F., 2004. Seasonal patterns of runoff and erosion responses to simulated rainfall in a badland area in Mediterranean mountain conditions (Vallecebre, southeastern Pyrenees). *Earth Surf. Proc. Land.* 29, 755–767.
- Ries, J.B., Seeger, M., Iserloh, T., Wistorf, S., Fister, W., 2009. Calibration of simulated rainfall characteristics for the study of soil erosion on agricultural land. *Soil Till. Res.* 106, 109–116.
- Rose, C.W., 1960. Soil detachment caused by rainfall. *Soil Sci.* 89, 28–35.
- Roth, C.H., Meyer, B., Frede, H.-G., 1985. A portable rainfall simulator to study factors affecting runoff,

infiltration and soil loss. *Catena* 12, 79–85.

Salles, C., Poesen, J., Borselli, L., 1999. Measurement of simulated drop size distribution with an optical spectro pluviometer: sample size considerations. *Earth Surf. Proc. Land.* 24, 545–556.

Schmidt, R.G., 1998. Beobachtung, Messung und Kartierung der Wassererosion. In: Richter, G. (Ed.), *Bodenerosion - Analyse und Bilanz eines Umweltproblems*. Wiss. Buchges., Darmstadt, pp. 110–121.

Scholten, T., Geißler, C., Goc, J., Kühn, P., Wiegand, C., 2011. A new splash cup to measure the kinetic energy of rainfall. *J. Plant Nutr. Soil Sc.* 174 (4), 596–601.

Thies, 2004. Bedienungsanleitung 021340/07/04 des Laser Niederschlags Monitor 5.4110.x0.x00 V1.09.

Torri, D., Regüés, D., Pellegrini, S., Bazzoffi, P., 1999. Within-storm soil surface dynamics and erosive effects of rainstorms. *Catena* 38, 131–150.

van Dijk, A.I.J.M., Bruijnzeel, L.A., Rosewell, C.J., 2002. Rainfall intensity–kinetic energy relationships: a critical literature appraisal. *J. Hydrol.* 261, 1–23.

Wilm, H.G., 1943. The application and measurement of artificial rainfall on types FA and F infiltrometers. *Trans. Am. Geophys. Union* 3, 480–484.

Wischmeier, W.H., Smith, D.D., 1978. Predicting rainfall erosion losses - A guide to conservation planning. In: USDA Agricultural Research Service Handbook 537.

Zhao, Y., Hirschi, M.C., Cooke, R.A., Mitchel, J.K., Ni, B., 1996. Measurement of simulated rainfall characteristics for raindrop erosion studies. ASAE Paper 96-2117, St. Joseph, Mich.

Butzen et al. (2011): Spatial pattern and temporal variability of runoff processes in Mediterranean Mountain environments - a case study of the Central Spanish Pyrenees.

Zeitschrift für Geomorphologie, Vol. 55, Suppl. 3, pp. 025-048, Stuttgart, doi: 10.1127/0372-8854/2011/0055S3-0050.

Spatial pattern and temporal variability of runoff processes in Mediterranean Mountain environments – a case study of the Central Spanish Pyrenees.

¹Verena Butzen, ²Manuel Seeger & ¹Markus Casper

¹Dept. of Physical Geography, FB VI Geography/Geosciences, Trier University (D)

²Dept. of Land Degradation and Development, Wageningen University & Researchcenter (NL)

Abstract

Mediterranean mountain environments like the Central Spanish Pyrenees show a highly variable rainfall-runoff response, mainly explained by the intense intra- and inter-annual variability of precipitation yield. This leads to a highly differentiated moisture status and therefore it is assumed to lead also to highly variable runoff contributing areas.

For the identification of areas with certain dominant runoff processes in an experimental headwater catchment in which agriculture was abandoned several decades ago the concept of the topographical index was extended by means of weighting grids. These weighting rasters were generated using additional information on soils and vegetation. Runoff generating areas were identified widespread in the catchment, with Hortonian overland flow (HOF) dominating the runoff processes on degraded soils, and saturation overland flow (SOF) dominating the footslope areas, where hydromorphic soils were mapped.

Rainfall-runoff experiments were performed to quantify runoff and erosion and to identify seasonal changes using experimental data gained in different seasons of the year. The seasonal changes in runoff response could be localised clearly within the areas of SOF, whereas the other ones showed a similar behaviour. This implied that the procedure of delineation had to be differentiated for dry and moist conditions, and that the SOF areas had to be reclassified as SSF/DP areas for dry conditions. Due to the location of these areas close to the ravine, we could explain the pronounced switching runoff behaviour of the catchment.

GIS techniques combining different levels of topographic, soil and vegetation information showed to be suitable for delineation of areas with different runoff generation processes. The inclusion of seasonally distributed experimental data demonstrated that for dry conditions, slightly different methods have to be applied. Nevertheless, the study showed also the limitations of the combined methods: (I) sub-surface flows and ground water recharge could only be deduced, not demonstrated, (II) finally, there is still a good knowledge of the area needed for an accurate process representation.

Key words: Dominating Runoff Processes (DRP), topographic index, rainfall experiments, Mediterranean mountains.

1 Introduction

Mountainous regions in the Mediterranean in general and the Pyrenees in particular, are marginal areas concerning human settlements and have suffered from a massive decline in population since the beginning of the 20th century. Because of decreasing population density and an aging of the population, a dramatic change in intensity and kind of land-use occurred. This development has led to strong changes in landscape and its functions (GARCÍA-RUIZ et al., 2005; LASANTA-MARTINEZ et al., 2000; VINCENTE SERRANO et al., 2000). The most obvious change is the reduction of cultivated land. The area in agricultural use has been diminished from nearly 30 percent of the whole area in the Central Pyrenees at the beginning of the 20th century to about three percent nowadays (GARCÍA-RUIZ et al., 2005; SEEGER & BEGUERÍA, 2003; SEEGER et al. 2004).

Recent studies concerning the changes in river discharge in the Central Spanish Pyrenees indicate that although precipitation increased or remained at the same level, river discharge decreased significantly. The loss of 30 percent of average annual discharge is primarily traced back to land-use and land-cover changes (BEGUERÍA et al., 2003). This finding has severe consequences for the future development of fresh-water supply for the semi-arid Ebro basin, a region with a rather high population density and widespread irrigation agriculture. GALLART et al. (2002) state that a more profound knowledge of the hydrological functioning of these water supplying areas is necessary in order to assess the impact of further climate and land-cover changes on fresh-water availability.

In the last few decades several methods have been developed in order to assess the hydrological reaction of a certain area within a catchment to intense rainfall events. FLÜGEL (1995) used the concept of hydrological response units (HRUs) for regionalized hydrologic modelling of a meso-scale river basin, whereby the HRUs are delineated using a GIS. Hydrological response units are "distributed, heterogeneously structured entities having a common climate, land use and underlying pedo-topo-geological associations controlling their hydrological dynamics" (FLÜGEL, 1995).

Utilizing a similar concept, SCHERRER & NAEF (2003) and SCHMOCKER-FACKEL et al. (2007) developed a decision scheme for delineating dominant runoff processes (DRP) during heavy rainfall events. This scheme has been developed using the results of rainfall simulation experiments. After SCHERRER & NAEF (2003) the DRP for a certain area is derived mainly from surface cover and soil properties.

According to them, runoff processes can be classified into overland flow processes and subterranean contributions to stream flow. Basically, two different overland flow processes have to be differentiated. On the one hand, Horton or infiltration excess overland flow (HOF), and on the other hand, saturation overland flow (SOF). Subterranean flow processes that occur because of previous rainfall events are subsurface flow (SSF) and deep percolation (DP). SSF, also referred to

as interflow, is a lateral soil water movement, the SSF water can also reach the soil surface again as return flow, but this process was not regarded in greater detail in this study. DP is a vertical flow to the ground water, it only contributes to river runoff after a longer time period as base flow.

CASPER (2002), CASPER et al. (2006) and WALDENMEYER (2002) proposed for the identification of HRUs a system in which a modified topographical index (TI) was combined with soil information. The TI, based on the fundamental work of BEVEN & KIRKBY (1979) was therefore weighted by a factor, resulting from soil depth and general moisture conditions, thus representing the sub-surface flow conditions within a catchment in the northern Black Forest (Germany).

One characteristic of the Mediterranean climate is the pronounced seasonality of precipitations. Regarding large areas, this leads to a clear seasonality of runoff, but in small catchments, this behaviour is not so clear. LLORENS & GALLART (1992) supposed the soil moisture status to be determinant for runoff generation. In climate situations with contrasted seasonality, this leads to a “switching behaviour” (GALLART, 2002) of runoff characteristics. GARCIA-RUIZ et al. (2005) observed in the catchment, which is also subject of the investigations described here, a clear distinction of the rainfall-runoff events into 2 groups. They did not identify a clear seasonal alternation of the groups, but could explain the changes in behaviour by different moisture statuses of the catchment. SEEGER et al. (2004) were also able to detect clear differentiated runoff generation types, which could be explained by the soil moisture status within the catchment and variable contributing areas at each event.

The main question of this study is, how to identify spatially and temporally variable runoff sources within a small headwater catchment. First, GIS techniques are used for the delineation of different runoff process areas. In a second step, the use of rainfall experiments in the field should provide the information about the areas that are responsible for the switching behaviour of the catchment. Finally, we want to focus on the applicability and the limitations of the methods and their combination.

2 Study Area

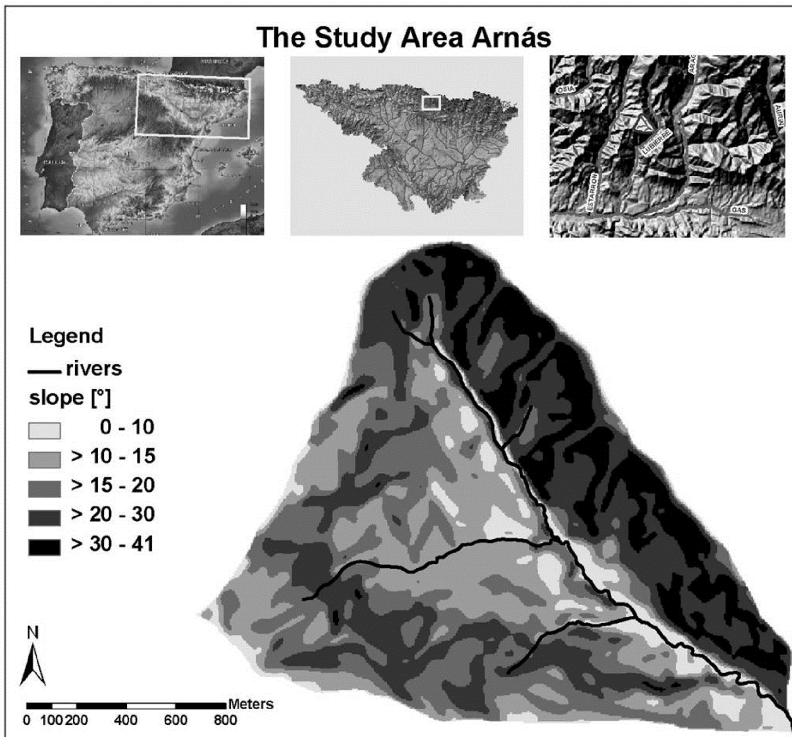


Fig. 1. The study area Arnás.

The study area Arnás is located in the Central Pyrenees in the Province of Aragón in north-eastern Spain (Fig. 1). The catchment covers an area of 2.84 km² and ranges between 905 and 1341 m above sea level (a.s.l.) (LASANTA-MARTÍNEZ et al., 2000). The Arnás valley is situated in the Sierras Interiores of the Aragonese Pyrenees. This is a broad strip of smoothly formed mountains that have developed in the Eocene Flysch (LASANTA-MARTÍNEZ et al., 2000). The sedimentary rocks of the flysch facies in this region are characterized by an alternation of marls and calcareous sandstones sloping to the north (DE LA RIVA, 1997).

The average annual temperature equals 10°C. The mean annual precipitation amount is 1120 mm but precipitation is not equally distributed over all months. A primary minimum in rainfall occurs in summer, as it is typical of a Mediterranean climate, and concerns the months from July to September. A secondary minimum can be determined in March. So the summer months show a deficit in water balance, whereas the other seasons produce a surplus of water. The climate can be characterized as mountainous Mediterranean sub-humid and is called Cfb referring to the Köppen-Geiger classification of climates (GARCÍA-RUIZ et al., 2005; RIES et al., 2000b).

The Arnás brook runs from the northwest to the southeast and separates the valley into the steep southwest-facing and the far gentler northeast-facing slope, therefore the valley shows an asymmetric profile. Because of the exposition as well as the dip direction of the geological strata,

the northeast-facing hillside is rather moist and has numerous wells in contrast to the drier and steeper southwest-facing slope. Concerning evaporation the shady hillside is hydrologically advantaged because of a less intense solar radiation, leading to less water loss by evapo-transpiration (SEEGER, 2001).

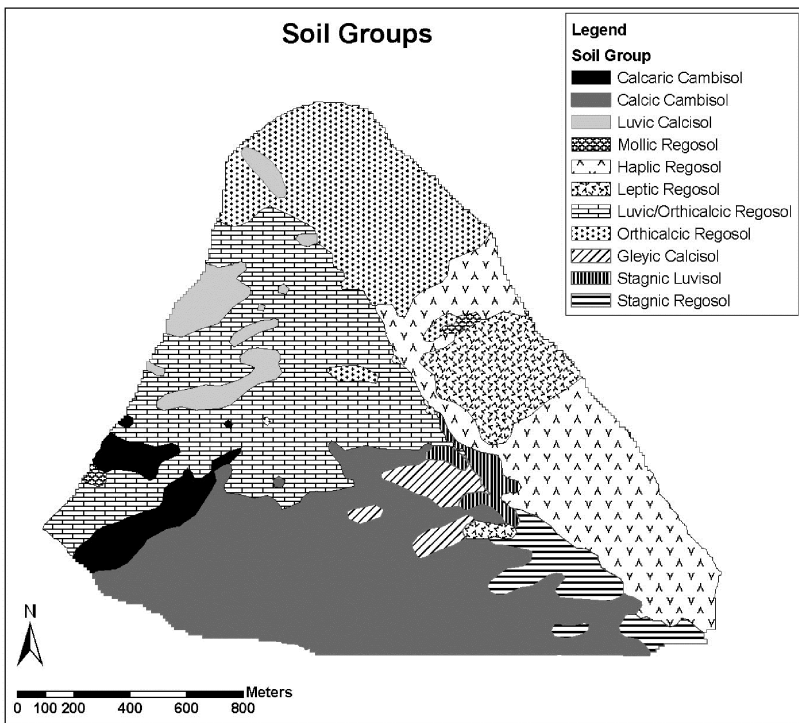


Fig. 2. Soil map.

The pattern of soils (Fig. 2) in the study area shows a clear difference between the south and the north-facing slope, mainly due to slope gradient and former land-use. At the steep south-facing slope almost exclusively shallow Regosols were mapped. Only in the central part of the valley next to the river, on some old lynchets a Stagnic Luvisol has developed, representing the most developed soil in the catchment. At the valley bottom also a Stagnic Regosol was classified. Generally speaking, the gentle north-facing slope shows more profound and developed soils, principally Cambisols. The hillside is covered with Regosols in the upper part of the catchment, and Cambisols at the slopes more downstream (GARCÍA-RUIZ et al., 1994; SEEGER et al., 2005).

The Arnás catchment is part of the Pyrenees that have suffered severe transformations during the last century (LASANTA-MARTINEZ, 1988). The valley was historically used to grow cereals like wheat and barley until about 60 years ago (ARNÁEZ et al., 1999). For that reason the slopes became severely affected by erosion as can be recognized by the residual rock fragment layers that cover large areas of the soil surface. Recently the land is used as pasture for a flock of 300 sheep

almost all over the year. This extensive farming, nevertheless, delays and impedes vegetation succession (RIES et al., 2000b; SEEGER & BEGUERÍA, 2003).

Nowadays, the largest part of the catchment is covered with shrub formations (matorral) of varying density. *Genista scorpius* (a gorse species), *Buxus sempervirens* (box shrub) and *Rosa canina* (briar rose) are the most frequent species on the sunny hillside and the uppermost regions are covered with *Echinospartum horridum* (a cushion shrub species) (SEEGER et al., 2005).

3 Material and Methods

3.1 Determination of Dominant Runoff Processes

The method for the delineation of dominant runoff processes (DRP) is based on the assumption that the hydrological response of a certain area to an intense rainfall event depends on surface characteristics, soil properties (SCHERRER & NAEF, 2003), and topographical situation (BEVEN & KIRKBY, 1979). The delineation of areas dominated by saturated overland flow (SOF), from a digital elevation model (DEM), is achieved using a topographic index (TI) which is based on the TOPMODEL topographic index (TI) after BEVEN & KIRKBY (1979).

The flow routing for the determination of the upslope contributing watershed area is done by means of a multiple flow direction approach. This allows identifying divergent flow in two or more down-slope directions (NETELER & MITASOVA, 2008). For the calculation of topographic indices, the GRASS GIS 6.2 command *r.mapcalc* is used (GRASS DEVELOPMENT TEAM, 2007).

The TI of BEVEN & KIRKBY (1979) is modified by the implication of weighting rasters in order to adapt the TI to the conditions in the study area, using a method developed by WALDENMEYER (2002) and CASPER (2002). The TI map according to BEVEN & KIRKBY (1979) can be regarded in Fig. 3 a). This map shows, that the delineated potentially SOF-dominated areas do not really match to the hydromorphic soils and the mapped wetlands. Accordingly, a weighted TI-map was calculated, by multiplying the local catchment area by a weighting raster derived from the soil map (Fig. 2). The values are given depending on the soils tendency to saturate, which can be deduced from the soil groups. Soils showing hydromorphic features, and thus being saturated during long periods, are given a high value, in this case 1.6. Those soils with typical features of water deficit, namely accumulations of carbonates, get the lowest values, here 0.1. The first weighting raster (w_I) is therefore allocated with values as reflected in Table 1, according to the soils and their distribution in the catchment. The weighting factors can be regarded as calibration factors, the total values are set arbitrarily but matching to the soil map. The relations between the factor values attributed to the different soils are important, the stagnic and gleyic soils get much higher values because they are definitely SOF dominated. The other soils are weighted with much lower values and the soils with

calcic concretions are clearly dominated by vertical water movements and are rather dry, so very low weighting factor values were attributed to these soils (Table 1).

Table 1: Soils with attributed weighting values (w_I)

Soil Group	Weighting Value (w_I)
Stagnic Luvisol	1.6
Stagnic Regosol	1.6
Gleyic Calcisol	1.6
Mollic Regosol	0.9
Leptic & Haplic Regosol	0.5
Luvic/Orthicalcic Regosol	0.2
Calcic/Calcaric Cambisol	0.1
Luvic Cambisol	0.1

Stagnic Luvisols, Stagnic Regosols and Gleyic Calcisols are assigned the highest scores, because at least the top-soils of these soils are often saturated, thus leading to saturation overland flow. The Mollic Regosols are weighted with the value 0.9 due to the coating layer of dead organic material upon the soil surface as well as the high amount of organic carbon in the topsoil, it can be stated that overland flow processes can be expected to occur rather infrequently, but the soils do not dry out as rapidly as the shallow soils without humus layer. The next lower value of 0.5 is allocated to the Leptic and Haplic Regosols because these soils are rather shallow and may become saturated as well, occasionally. The Orthicalcic and Luvic-Orthicalcic Regosols are only weighted with the value 0.2 despite the fact that they are rather shallow as well, because of the concretions of secondary carbonates in their profiles that indicate their liability to desiccation. The soils of greater depth, namely Calcic and Calcaric Cambisols as well as Luvic Calcisols are only weighted with 0.1 due to the fact that a saturation is very unlikely for these rather profound soils with carbonate concretions that indicate predominantly dry soil-moisture conditions.

The weighted TI-map (TI_w) that is used for the delineation of the SOF-areas is calculated using equation 1.

$$TI_w = \ln\left(\frac{w_I * A}{\tan \beta}\right) \quad (1)$$

- TI_w is the weighted topographic index, used to delineate the SOF areas
- w_I being the SOF-weighting factor ranging between 0.1 and 1.6 (Table 1)
- A: local catchment area [m^2]
- β : slope [$^\circ$]

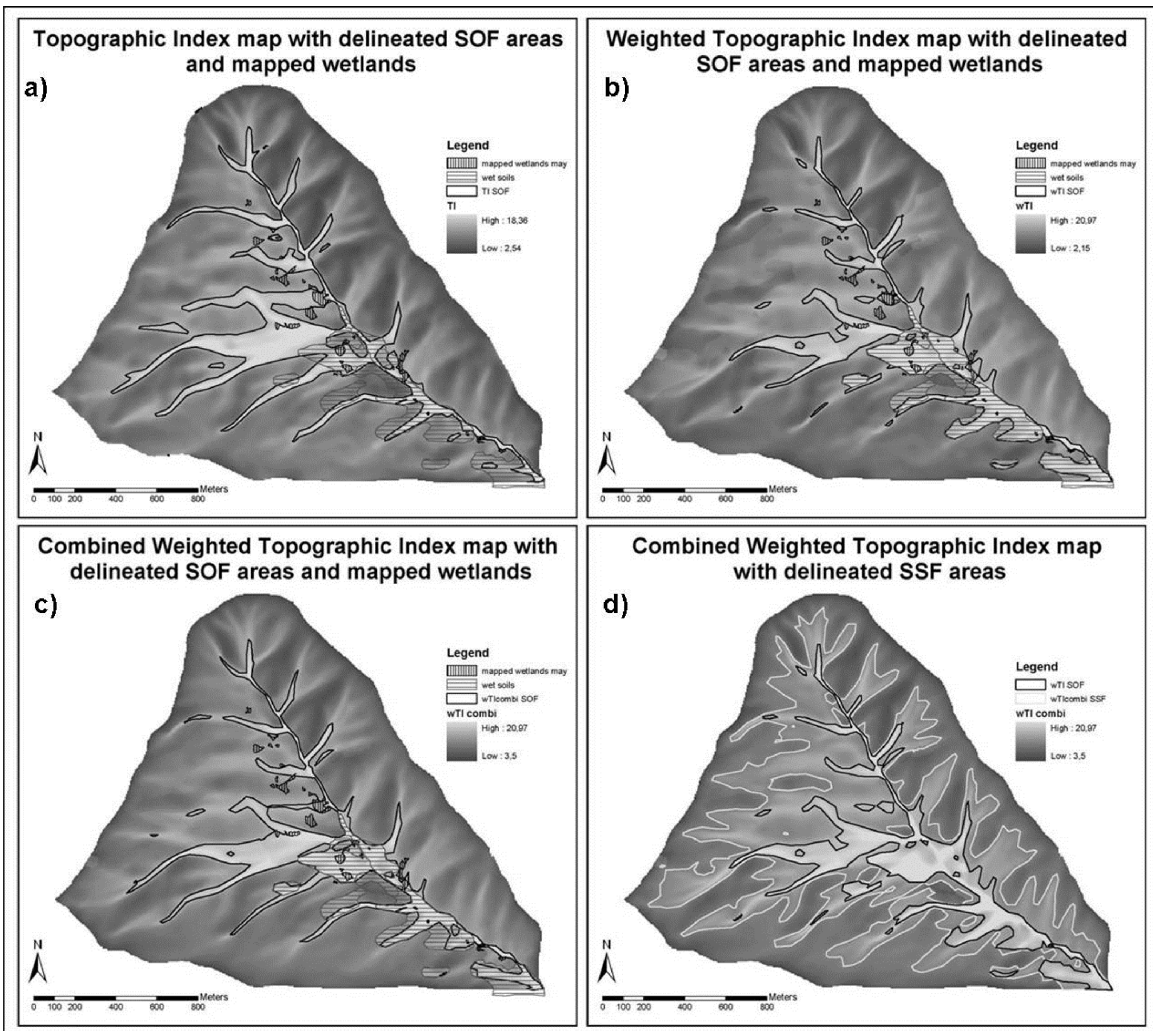


Fig. 3. TI delineation for SOF and SSF.

The resulting TI_w -map includes TI values ranging from 2.15 to 20.97. The threshold value for SOF is determined by means of the ArcGIS 9.1 tool *zonal statistics*. The mean value of the minimum TI-values for mapped wetland areas is delineated resulting in a threshold value of 8.6. The choice of minimum TI values results in a SOF map including most of the mapped wetlands and hydromorphic soil areas, that means that a minimum extend of SOF-area spreading in the wet seasons is covered, so it is very likely that these areas are SOF-dominated. Accordingly, all cells with TI values higher than 8.6 are classified as SOF-dominated areas (Fig. 3 b)). This TI value was determined because the spatial distribution of the resulting SOF areas matches very well to the areas covered by hydromorphic soils in the soil map. The wetland areas were mapped again in May 2010 and also match very well to the hydromorphic soils.

According to CASPER (2002) and WALDENMEYER (2002) it is also possible to assess the occurrence of subsurface flow by means of a further modification of the topographic index. Based

on the assumption that subsurface flow is controlled by slope and the existence of an impermeable soil horizon or bedrock, the shallow soils (Regosols) are supposed to be prone to subsurface flow, due to the low permeability of the bedrock and the steep slopes (see also: Fig. 1 and 2). So an additional SSF-weighting raster (w_2) can be calculated for areas with shallow soils as well as for steep slopes. Accordingly w_2 is calculated according to equation 2 (CASPER, 2002; CASPER et al., 2006; WALDENMEYER, 2002) for the whole catchment area except the stagnic and gleyic soils that are not expected to be prone to SSF, at least not under wet antecedent soil moisture conditions.

$$SSF_{pot} = \sin\beta = w_2 \quad (2)$$

with:

- β : slope [$^{\circ}$]
- $\sin \beta$ describing the lateral component of water fluxes on the slope. The steeper the terrain, the higher the SSF_{pot} -value.

As suggested by WALDENMEYER (2002) and CASPER (2002) both weighting grids can be combined by just summing up the two weighting rasters. Accordingly, the combined TI for the delineation of the SSF areas is then calculated by multiplying the weighting raster for SOF and SSF (w_{sum}) with the local catchment area and calculating the combined TI (TI_{comb}) according to equation 3.

$$TI_{comb} = \ln\left(\frac{(w_1 + w_2) * A}{\tan\beta}\right) \quad (3)$$

- TI_{comb} is the combined weighted topographic index
- w_1 being the SOF-weighting factor ranging between 0 and 1.6 (Table 1)
- w_2 being the SSF-weighting factor ranging between -1 and 1, generated by calculating the sine of slope.
- A : local catchment area [m^2]
- β : slope [$^{\circ}$]

The resulting TI_{comb} raster map shows TI values ranging from 3.5 to 20.97, whereby the highest values are found next to the river. The SOF threshold value was determined in the same way as described above and is 7.14 for the combined TI-map. Comparing the SOF-areas delineated from the wTI-map (Fig. 3 b)) to the SOF-areas delineated from the combined TI-map (Fig. 3 c)), the weighted TI-derived map matches better to the hydromorphic soils and to the mapped wetlands.

The threshold value for the delineation of the SSF-dominated areas was determined with the same method like the SOF-threshold, but for SSF, areas with shallow soils that are not SOF-dominated are used. The resulting SSF-threshold value is 7.14, indicating that all cells with TI-values between 7.14 and 8.6 are classified as SSF-dominated areas (Fig. 3 d)).

The areas dominated by Hortonian overland flow have been delineated from a land cover map. Sparsely shrub-covered areas as well as meadows and pastures that are not covered with stagnic or gleyic soils are classified as potentially HOF generating areas. The highly degraded soils in these areas show residual rock fragment layers on top and have low infiltration capacities (SEEGER et al., 2005). Additionally, the road and pastures are severely affected by HOF due to compaction and consequently limited infiltrability of the topsoil. For this classification according to different criteria, a stepwise classification is needed, so the SOF-dominated areas are given the highest priority followed by the HOF-areas and afterwards SSF and DP.

3.2 Rainfall Simulation Experiments

The rainfall simulation experiments are carried out with a small mobile rainfall simulator based on the one used by CALVO-CASES et al. (1988, 2003), LASANTA et al. (1994) and CERDÀ & GARCÍA-FAYOS (1994-95). The experimental setup can be regarded in Fig. 4. The simulated rainfall has an intensity of around 40 mm h^{-1} and a duration of 30 minutes. The circular bounded plot has an area of 0.28 m^2 (RIES et al., 2000a). Runoff is collected continuously with intervals of 5 minutes duration. The parameters vegetation cover, rock fragment cover, slope, exposition, surface roughness as well as antecedent and subsequent soil moisture are registered as plot characteristics. The simulated rainfall intensity is adjusted before each experiment by means of a calibration plate and after each rainfall simulation the rainfall water amount is tested again.

The resulting runoff water amount is determined gravimetrically and the amount of eroded soil material is ascertained by filtration of the collected runoff water. The runoff coefficient for each rainfall simulation is calculated by dividing the total runoff water amount by the applied rainfall water amount. The suspended sediment concentration is calculated dividing the total suspended sediment load of the rainfall simulation by the total runoff amount.

For a more detailed description of the rainfall simulator and the adaptation in the field please see also RIES et al. (2000a) and RIES et al. (2009).



Fig. 4. Rainfall simulation.

The rainfall simulations were carried out in September 2005 under extremely dry soil moisture conditions and on most of the locations again in March 2007 under rather wet conditions. The collected data of the two field campaigns are analysed separately with methods of descriptive statistics and simple bivariate correlations.

3.3 Modification of the Dominant Runoff Processes Map to suit dry summer conditions

For the generation of the DRP map for dry conditions the same weighted TI raster was used as for the first map, but the order of intersection of the HOF-dominated areas was changed because the most important overland-flow generation process under dry conditions is HOF. For the rest of the year SOF is considered to dominate the runoff behaviour. Under dry conditions no SOF at all can be expected, so the ‘wetland areas’ become SSF or DP dominated, mainly depending on slope, soil depth, and the bedrock if HOF is not the dominating process. Due to the fact that the HOF-areas were delineated from land-cover data whereas the TI was generated using a DEM, the two spatial datasets overlap at certain areas. For the summer map the HOF areas had the highest priority, followed by the other three classes as described above. The next step is a comparison of the generated DRP maps with the results of the rainfall simulations. When necessary and possible, the DRP unit was redefined according to the results of the rainfall simulations. More precisely, for the dry summer conditions the former SOF areas are reclassified to SSF/DP. This reclassification is done due to the results of the rainfall simulations.

4 Results

4.1 Map of Dominant Runoff Processes for moist conditions

The map in Fig. 5 illustrates the spatial pattern of the DRPs for moist soil conditions. The SOF-areas are located in the valley bottoms and are widespread in the rather flat central part of the valley that is characterized by stagnic and gleyic soils.

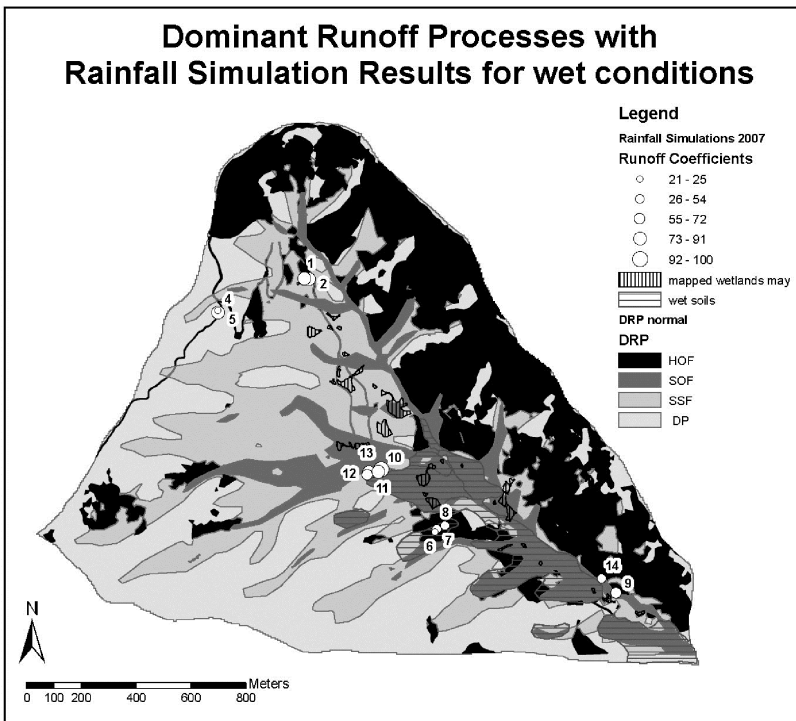


Fig. 5. Dominant runoff processes with rainfall simulation results for wet conditions.

The HOF-areas are represented in the map (Fig. 5) in black colour. HOF-dominated are large areas covered with open shrub vegetation mainly situated at the steep south-facing slope as well as grassland areas that are used as cattle pastures scattered over the catchment. Additionally the roads are designated as HOF-generating areas, visible in the map as linear structures. Altogether 29.1 % of the catchment is classified as HOF-generating (tab. 2).

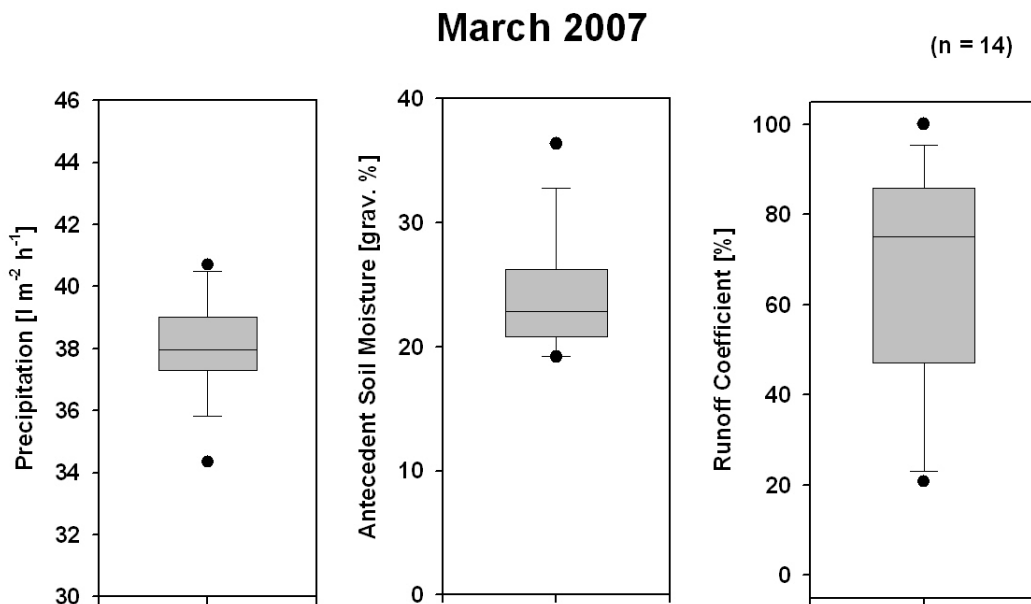
Table 2: Areas in square kilometers and area-percentages of the different DRPs for moist antecedent soil-water conditions (according to the map in Fig. 5)

DRP	Area [km ²]	Area [%]
HOF	0.82	29.1
SOF	0.35	12.4
SSF	0.73	25.9
DP	0.92	32.6

SSF-dominated areas can mainly be found in the upper central part of the catchment and are oriented along the depth contours at the middle and low slope areas (Fig. 5). The remaining parts of the catchment are classified as being dominated by deep percolation (DP), representing 32.6 % of the area. These areas are mainly located at the higher parts of the northeast-facing slope as well as in densely shrub-covered areas on the south-west-facing slope.

4.2 Rainfall Simulation Experiments

Fig. 6 and 7 show the simulated rainfall amount, the antecedent soil moisture percentage, and the runoff coefficients measured in 14 rainfall simulations in March 2007 (Fig. 6) and 27 rainfall simulations carried out in September 2005 (Fig. 7) in the Arnás catchment. Additionally, the complete data of the rainfall simulations are shown in table 3 (simulations of March 2007) and table



4 (simulations of September 2005).

Fig. 6. Simulated rainfall amount in March 2007.

The simulated rainfall amounts of the experiments carried out in March 2007 (Fig. 6, left boxplot) range between 34.34 and 40.71 l m⁻² h⁻¹ with a median of 37.95 m⁻² h⁻¹ and a standard deviation of 1.6 l m⁻² h⁻¹ representing only 4 % of the target value of 40 l m⁻² h⁻¹.

The antecedent soil moisture (Fig. 6, middle box-plot) ranges between 19.2 and 36.4 grav. %, with a median of 22.88 grav. % and a standard deviation of 4.55 grav. %. Altogether the soil moisture can be regarded as very high for most experimental sites, this is reaching mostly values above 80 % of saturation.

The calculated runoff coefficients range between 20.77 and 100 %. The median of runoff coefficients equals 75.11 % and the standard deviation is 24.88 %. The highest runoff coefficients are found in the areas described as HOF and SOF (Fig. 5).

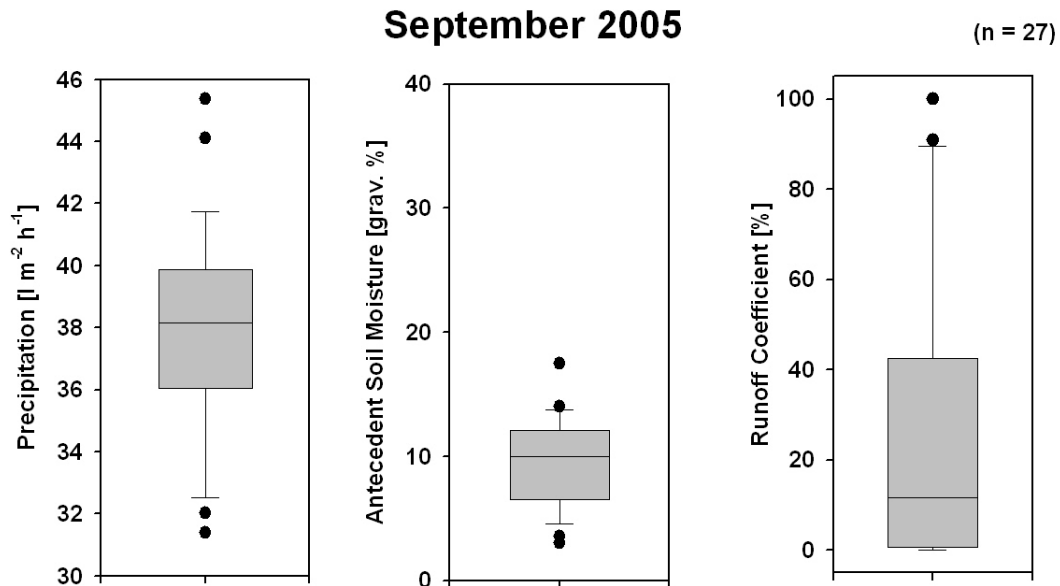


Fig. 7. Simulated rainfall amount in September 2005.

The simulated rainfall amounts in summer 2005 (Fig. 7, left box-plot) range between 31.4 and 45.4 $\text{l m}^{-2} \text{h}^{-1}$ with a median of 38.16 $\text{l m}^{-2} \text{h}^{-1}$ and a standard deviation of 3.2 $\text{l m}^{-2} \text{h}^{-1}$ representing 8 % of the target value of 40 $\text{l m}^{-2} \text{h}^{-1}$.

The antecedent soil moisture (Fig. 7, middle box plot) ranges between 3 and 17.5 grav. % in September, with a median of 9.98 grav. % and a standard deviation of 3.5 grav. %. Altogether the soil moisture can be regarded as very low for most experimental sites. The calculated runoff coefficients in summer (Fig. 7, right box plot) range between 0 and 100 %, thus covering the whole range of possible responses to a simulated rainfall. The median of runoff coefficients is 11.6 % and the standard deviation is consequently high with a value of 30.5 %.

Table 3: Plot characteristics and results of the rainfall simulations conducted in March 2007 in the Arnás catchment.

	Experiment 2007	Simulated rainfall intensity [l m ⁻² h ⁻¹]	Runoff [l m ⁻²]	Runoff coefficient [%]	Start Runoff [Min]	Start Soil Moisture [grav. %]	Vegetation Cover [%]	Stone Cover [%]	Surface Roughness [cm/60cm]	Slope Angle [°]	Soils	Vegetation/Land use
1	37.31	15.83	84.85	00:01:16	36.4	60	5	61	5	Luvic/Orthic alcic Regosol	Pasture Good	
2	37.31	15.79	84.64	00:01:02	25.8	50	30	61.5	10	Luvic/Orthic alcic Regosol	Pasture Good	
3	37.74	16.73	88.65	00:01:39		50	30	61.5	10	Luvic/Orthic alcic Regosol	Pasture Good	
4	37.74	3.92	20.77	00:04:23	21.7	70	0	78.7	21	Luvic Calcisol	Brush Good	
5	38.16	15.00	78.62	00:00:20	22.9	25	30	64.5	20	Luvic Calcisol	Brush Good	
6	40.28	10.85	53.86	00:01:32	26.6	95	5	61.5	9	Gleyic Calcisol	Brush Fair	
7	37.31	8.09	43.35	00:00:54	19.3	20	95	62.9	10	Gleyic Calcisol	Brush Fair	
8	40.71	5.14	25.27	00:01:39	22.5	50	20	62.5	7	Gleyic Calcisol	Brush Fair	
9	40.28	14.42	71.60	00:01:03	27.4	95	5	61	8.5	Haplic Regosol	Pasture Fair	
10	38.59	17.54	90.92	00:01:10	24.2	2	2	65	13	Calcic Cambisol	Brush Fair	
11	34.35	10.93	64.00	00:01:54	19.9	30	15	63.9	14	Calcic Cambisol	Brush Fair	
12	38.59	15.41	79.87	00:01:01	22.1	75	5	63.5	9	Calcic Cambisol	Brush Fair	
13	37.74	19.90	100.00	00:00:14	24.0	50	30	63.5	13	Calcic Cambisol	Brush Fair	
14	38.16	9.24	48.40	00:02:30	19.2	20	75	63	21	Haplic Regosol	Brush Poor	

Table 4: Plot characteristics and results of the rainfall simulations conducted in September 2005 in the Arnás catchment.

	Experiment 2005	Simulated rainfall intensity [l m ⁻² h ⁻¹]	Runoff [l m⁻²]	Runoff coefficient [%]	Start Runoff [Min]	Start Soil Moisture [grav. %]	Vegetation Cover [%]	Stone Cover [%]	Surface Roughness [cm/60cm]	Slope Angle [°]	Soils	Vegetation/Land use
1	32.01	1.86	11.6	00:05:55	11.7	5	7.5	60.6	12	Calcic Cambisol	Brush Fair	
2	44.10	6.92	37.6	00:04:41	5.6	30	10	65.4	12	Calcic Cambisol	Brush Fair	
3	39.86	6.59	33.1	00:04:34	3.6	50	25	62.4	9	Gleyic Calcisol	Farmstead	
4	31.38	0.00	0.0			75	2	60.9	8	Gleyic Calcisol	Wood Good	
5	40.71	0.73	3.6	00:07:44	17.5	45	15	64.3	6	Gleyic Calcisol	Brush Fair	
6	36.04	0.32	1.8	00:13:20	13.5	80	2	62.0	8	Gleyic Calcisol	Brush Fair	
7	38.16	8.12	42.6	00:04:30	10.8	30	30	63.4	16	Leptic Regosol	Brush Fair	
8	36.89	9.03	48.9	00:05:08	6.3	80	5	62.8	9	Stagnic Luvisol	Pasture Fair	
9	36.04	6.61	36.7	00:01:55	3.0	45	10	62.0	8	Haplic Regosol	Brush Good	
10	35.62	0.02	0.1	00:03:31	9.7	95	0	63.2	6	Haplic Regosol	Pasture Fair	
11	39.43	7.96	40.4	00:01:05	7.9	10	70	67.1	13	Haplic Regosol	Brush Good	
12	40.28	2.34	11.6	00:07:41	9.4	95	2	62.5	9	Haplic Regosol	Brush Good	

13	32.65	0.10	0.6	00:02:42	5.6	85	2	62.7	12	Haplic Regosol	Pasture Fair		
14	37.74	3.34	17.7	00:02:27	6.4	5	40	62.8	17	Haplic Regosol	Brush Poor		
15	45.37	20.20	89.1	00:02:08	11.2	25	35	63.5	14	Luvic/Orthica lcic Regosol	Road		
16	39.01	17.73	90.9	00:01:15	12.2	30	0	64.1	8	Luvic/Orthica lcic Regosol	Road		
17	39.43	22.83	100.0	00:02:38		25	45	61.0	9	Luvic/Orthica lcic Regosol	Road		
18	37.31	8.99	48.2	00:03:13	10.3	45	20	62.5	18	Luvic/Orthica lcic Regosol	Brush Good		
19	41.13	0.00	0.0		13.4	0	0	62.8	11.5	Luvic/Orthica lcic Regosol	Brush Good		
20	39.86	0.22	1.1	00:03:11	10.9	0	5	86.9	16	Luvic/Orthica lcic Regosol	Brush Good		
21	39.43	9.41	47.7	00:04:45	7.2	10	10	61.8	8	Luvic Calcisol	Brush Good		
22	37.31	0.74	4.0	00:02:22		55	15	65.1	12	Luvic Calcisol	Brush Good		
23	38.16	1.44	7.5	00:07:53	14.0	85	10	65.4	11	Luvic/Orthica lcic Regosol	Pasture Good		
24	34.77	0.13	0.7	00:05:49	6.6	40	10	62.5	12	Luvic/Orthica lcic Regosol	Brush Good		
25	39.01	0.03	1.6	00:06:10	8.6	80	0	65.6	6	Luvic/Orthica lcic Regosol	Brush Good		
26	39.43	0.00	0.0		10.8	90	0	63.6	2.5	Luvic/Orthica lcic Regosol	Wood Good		
27	38.16	0.00	0.0		12.5	95	0	65.0	5	Luvic/Orthica lcic Regosol	Brush Good		

As the rainfall intensities are determined only at the beginning and the end of the experiment, there is some inaccuracy in the determination of the rainfall applied. As a consequence, extreme runoff of 100 % can be measured, when the amount of water oscillated during the experiment.

4.3 Map of Dominant Runoff Processes for dry conditions

Under dry antecedent soil moisture conditions in the summer months especially the just described SOF-areas show a different hydrological reaction. Due to the different processes a second map for dry antecedent soil moisture conditions is displayed in Fig. 8.

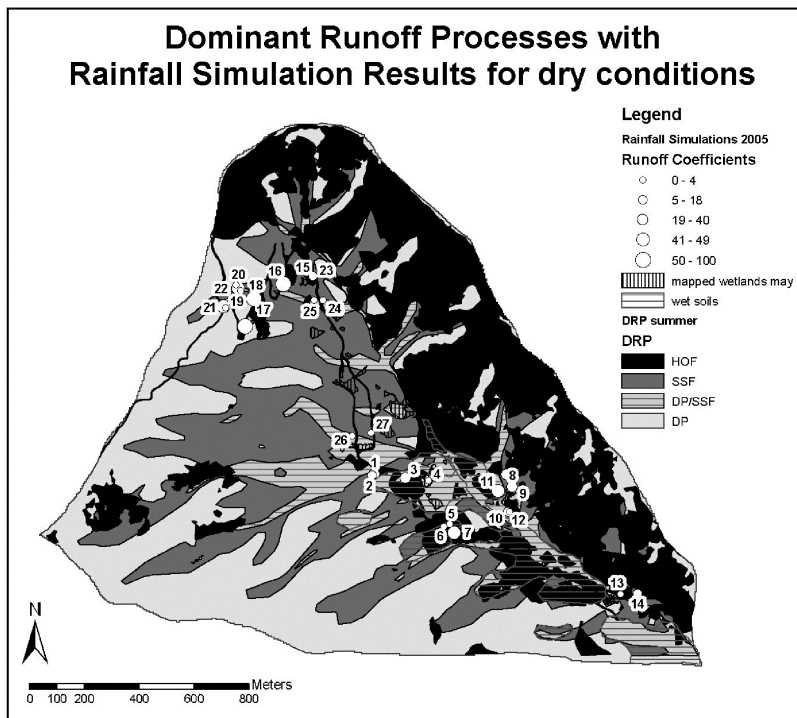


Fig. 8. Dominant runoff processes with rainfall simulation results for dry conditions.

In the summer map no SOF areas are classified at all. The bed of the main river can dry out partially, thus showing a decreasing ground water table in the long dry periods. Instead, the former SOF-areas are dominated by deep percolation or by subsurface flow mainly, but some sparsely vegetation covered areas are also classified as HOF-dominated. Accordingly, the area-percentage dominated by HOF has increased from 29.1 % in (Fig. 5) to 33 % in the map for dry conditions (Table 5). The DP/SSF-dominated areas represent 8.5 % of the whole catchment area. These are the main differences compared to the map for moist conditions.

Additionally, the DRP-map for dry conditions in Fig. 8 shows the rather heterogeneous results of the rainfall simulations in September 2005. The runoff coefficients ranged between 0 and almost 100 %. Most of the experimental results match more or less to the DRP map.

Table 5: Areas in square meters and area-percentages of the different DRPs for dry antecedent soil moisture conditions (according to the map in Fig. 8)

DRP	Area [km ²]	Area [%]
HOF	0.93	33.0
DP/SSF	0.24	8.5
SSF	0.73	25.9
DP	0.92	32.6

4.3 Comparison of the Results of the Rainfall Experiments with the GIS Results

The results of the rainfall experiments accomplished in March 2007 match relatively well to the DRP map for moist conditions, displayed in Fig. 5. In the experiments located in the central part of the catchment, saturation of the soils was reached during each of the experiments. All these simulations are located in the area that was classified as SOF-dominated area. The soil moisture conditions in March 2007 can be described as very wet, so even a larger area was saturated than the DRP map indicates. This is not surprising considering the fact that the soils were almost saturated everywhere in the catchment due to snowmelt. One of the rare experimental runs of March 2007 in which saturation was not quite reached is the rainfall simulation located in the convex part of the southwest-facing slope resulting in a runoff coefficient of 48 percent. In the DRP-map this area is classified as HOF dominated like the experimental results also show. The rather low RC value of 21 percent in one of the experiments in the upper part of the valley can be explained by the fact that an *Echinospartum horridum* shrub covered the plot surface and so infiltration rate was enhanced along the roots.

The rainfall simulations accomplished in September 2005 show rather inhomogeneous results concerning the measured runoff coefficients. The rainfall simulations on dry conditions show, that the SOF areas produce considerably lower runoff than under wet conditions (Fig. 9, SOF 2005 and SOF 2007, respectively). Especially on dry conditions the variability in experimentally generated runoff is extremely high, thus showing the spatial heterogeneity of the soils.

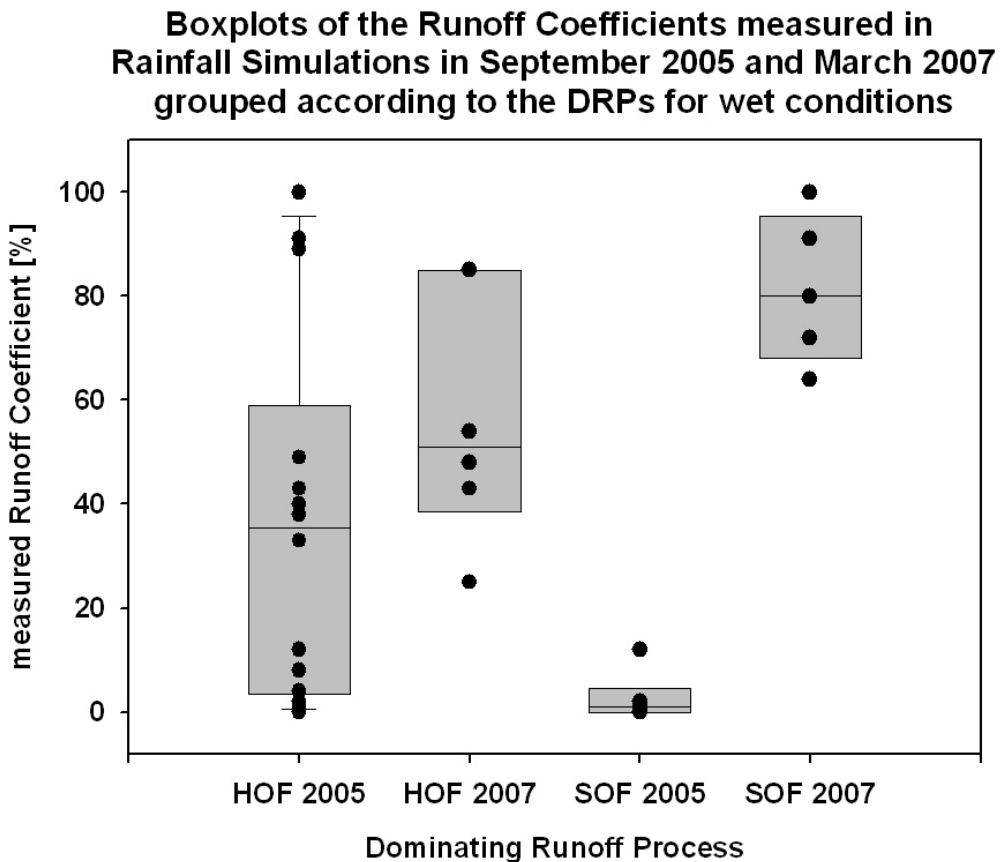


Fig. 9. Boxplots of the runoff coefficients measured in rainfall simulations in September 2005 and March 2007 grouped according to the DRPs for wet conditions.

According to these experimental results, the SOF areas have to be redefined for dry catchment and soil conditions. In this case, they react as slow SSF or even DP areas, as they tend to absorb the water arriving by rainfall or SSF. This lead to the reclassification as shown in the DRP map for dry soil conditions (Fig. 8).

5 Discussion

The catchment is characterised by large areas generating Hortonian overland flow (HOF). In addition, large areas close to the creek are identified to contribute runoff by saturation overland flow (SOF). This accords with the analysis of runoff data (GARCÍA-RUIZ et al., 2005, SEEGER et al., 2004) indicating a very rapid and intense response of the catchment, especially under wet conditions. In both publications there is reported a considerable difference in catchment response between dry and moist soil moisture conditions. GARCÍA-RUIZ et al. (2005) were able to group the rainfall-runoff events into two groups, which were depending on catchment moisture status. SEEGER et al. (2004) identified three different runoff types, and two of them were depending on

the soil moisture status. The authors postulated, after interpretation of hydrographs and sedigraphs, the presence of large areas contributing with rapid Hortonian response to runoff, whereas additional runoff sources were only switched on with high moisture status, and for this indicated partially saturated conditions. The rainfall experiments carried out under two different catchment moisture conditions show the same behaviour. The areas with strongly degraded soils, and thus also very low infiltration rates (SEEEGER et al., 2002; SEEEGER & RIES, 2008) showed a similar runoff generation pattern under moist and dry conditions and thus have to be assigned for this as HOF. In contrast to this, also areas could be identified where rainfall simulations under moist conditions delivered high runoff coefficients according to the expectations, but under dry conditions no runoff is generated. These experiments were concentrated in the areas where hydromorphic soils and wetlands have been mapped, matching with this the observations of GALLART et al. (1994) and GALLART et al. (2002), which explain the “switching behaviour” of forested Mediterranean catchments by the highly oscillating moisture within the wetlands, which are mainly found on old lynchets. GALLART et al. (2002) also stress out the important interaction between sub surface flow and the wetland recharge, which is also reflected clearly in the position of SSF and SOF within the Arnás catchment. The first ones are wrapped around the latter ones.

The definition of SSF areas or its differentiation towards DP is a critical issue regarding the methodologies applied. The rainfall simulations are not able to reproduce subsurface processes, and there are no flumes installed within the catchment. So, only the available soil information is used to deduce areas with dominant sub surface flow, disregarding the lithological variability of the Flysch. As a consequence, the definition of SSF and DP areas have to be evaluated as weak, but indicating clearly areas with a retarded contribution to the catchments runoff. Regarding the results of the Arnás catchment, the stepwise introduction of additional information to the TI (BEVEN & KIRKBY, 1979) as a basis for the DRP map helps to mitigate the emphasis on the lower slopes concerning their disposition to saturation (CASPER et al. 2006). Especially the incorporation of soil maps and vegetation patterns leads to a coherent distribution of runoff process units in the catchment, and confirms GÜNTNER et al. (2004), who found best results when incorporating soil and climate information to topographic indices for the identification of wetlands in the Black Forest Mountains. CEBALLOS & SCHNABEL (1998) also used the TOPMODEL topographic index to delineate saturation areas in a Mediterranean catchment and compared the results, as well as the results of aerial photograph interpretation, to field observations. They state that the topographic index brought more realistic findings at least if subsurface flow is also taken into account. The introduction of a weighting raster (CASPER, 2002, WALDENMEYER, 2002), including additional knowledge about the catchments characteristics, leads to very satisfactorily results in the Mediterranean mountain environment of Arnás.

But therefore the values of weighting raster w_I have to be chosen carefully, which is one of the critical points of the methodology. A coarse sorting of the different soil types can be achieved according to the soils characteristics, but the fine tuning is an iterative process, which needs good knowledge about the studied area, and thus is a severe constraint to the generalised application of the methodology.

Additional process understanding was gained by the introduction of the rainfall experiments. On one hand, they confirmed the widespread appearance of HOF areas on the steep south facing slope, as there was a similar amount of runoff generated under dry and moist conditions. On the other hand, with the rainfall experiments we could identify the areas responsible for the switching behaviour of the catchment, as reported by GALLART et al. (2002) and explicitly for this small headwater catchment by GARCÍA-RUIZ et al. (2005). But there remains still the identification of the areas with dominant SSF as a major problem. With this kind of experimental setup it is not possible to reflect other processes than infiltration of incipient surface runoff (SEEGER 2007), so the definition of SSF areas is still subject to deduction. LLORENS & GALLART (1992) and GALLART et al. (2002) reported about the importance of sub-surface flow processes for the control of soil moisture on certain morphological units of the analysed catchments, and according to this, SSF has been defined here to be up-slope of the SOF areas, and thus contributing to their saturation. Another constraint is the differentiation between SSF and deep percolation (DP), which cannot be made, either. Due to the steep slopes, it is assumed that at least a large part of the water in the soils is transported as a shallow sub-surface flow.

6 Conclusions

Concerning Mediterranean mountain environments, a great variety of runoff generation processes can be identified. Besides the dominance of Hortonian processes, which is found primarily on degraded soils, the experimental results indicate a strongly switching behaviour of runoff producing areas between recharge of the soil and runoff generation.

We can conclude that Mediterranean mountain catchments show highly variable source areas of runoff. The investigated case shows that in Mediterranean mountain environments there are large areas showing a switching hydrological reaction from rapid and high overland flow generation on moist conditions and recharge when the catchment is dry.

The identification of dominant runoff processes by means of the development of a weighted topographical index seems to be a suitable tool for the spatially distributed definition of runoff source areas. Especially the introduction of qualitative soil information as soil maps helps to enhance the results substantially. Nevertheless, experimental data are indispensable to understand

the real process dominance under highly changing conditions. As an additional constraint, the definition of areas with dominating sub-surface runoff processes remains a challenge.

Acknowledgements

We would like to acknowledge the anonymous reviewers for their valuable and critical comments. They helped us to improve the manuscript considerably. Many thanks also to all the students of Trier University who made the field work possible.

References

- Arnáez, J.; Martí-Bono, C.; Beguería, S.; Lorente, A.; Errea, M.P. & García-Ruiz, J.M. (1999): Factores en la generación de crecidas en una cuenca de campos abandonados, Pirineo Central Español. Cuadernos de Investigación Geográfica, 25, pp. 7–24.
- Beguería, S.; López Moreno, J.I.; Lorente, A.; Seeger, M. & García-Ruiz, J.M. (2003): Assessing the Effect of Climate Oscillations and Land-use Changes on Stream flow in the Central Spanish Pyrenees. Ambio, 32, Nr. 4, pp. 283–286.
- Beven, K.J. & Kirkby, M.J. (1979): A physically based variable contributing area model of basin hydrology. Hydrol. Science Bull. 24, Nr. 1, pp. 43–69.
- Calvo-Cases, A.; Boix-Fayos, C. & Imeson, A.C. (2003): Runoff generation, sediment movement and soil water behaviour on calcareous (limestone) slopes of some Mediterranean environments in southeast Spain. Geomorphology, 50, pp. 269–291.
- Calvo-Cases, A.; Gisbert, J.; Palau, E. & Romero, M. (1988): Un simulador de lluvia portátil de facil construcción. In Sala, M./Gallart, F., editors: Métodos y técnicas para la medición en el campo de procesos geomorfológicos. Logroño: Sociedad Española de Geomorfología, pp. 6–15.
- Casper, M. (2002): Die Identifikation hydrologischer Prozesse im Einzugsgebiet des Dürreychbaches (Nordschwarzwald). Ph.D thesis, Fakultät für Bauingenieur- und Vermessungswesen der Universität Fridericiana Karlsruhe (TH), Karlsruhe, p. 184+30.
- Casper, M.; Waldenmeyer, G. & Herbst, M. (2006): Modelling moisture patterns and runoff in a Black Forest sandstone catchment: Incorporating expert knowledge into the Topographical Index concept. Z. Geomorphol. Suppl.-Vol. 142, pp. 307–317.
- Ceballos, A. & Schnabel, S. (1998): Hydrological behaviour of a small catchment in the dehesa landuse system (Extremadura, SW Spain). Journal of Hydrology, 210, pp. 146–160.
- Cerdà, A. & García-Fayos, P. (1994-95): Relaciones entre las pérdidas de agua y semillas en zonas acarcavadas. Influencia de la pendiente. Cuadernos I. Geográfica, 20-21, pp. 47–63.
- De la Riva, J. (1997): Chap. II. Factores físicos de los Montes Jacetanos. In Serie Investigación. Volume 10, Los Montes de la Jacetania. Caracterización física y explotación forestal. Zaragoza: Consejo de Protección de la Naturaleza, pp. 105-160.

- Flügel, W.-A. (1995): Delineating hydrological response units by geographical information system analyses for regional hydrological modelling using PRMS/MMS in the drainage basin of the river Bröl, Germany. *Hydrological Processes* 9, pp. 423-436.
- Gallart, F.; Llorens, P. & Latron, J. (1994): Studying the role of old agricultural terraces on runoff generation in a small Mediterranean mountainous basin. *J. Hydrol.* 159, pp. 291–303.
- Gallart, F.; Llorens, P.; Latron, J. & Regués, D. (2002): Hydrological processes and their seasonal controls in a small Mediterranean mountain catchment in the Pyrenees. *Hydrol. Earth Syst. Sci.* 6, Nr. 3, pp. 527–537 hURL: <http://www.hydrol-earth-syst-sci.net/6/527/2002/hess-6-527-2002.pdf>.
- García-Ruiz, J.M.; Lasanta, T.; Ruiz-Flano, P.; Martí, C.; Ortigosa, L. & González, C. (1994): Soil erosion and desertification as a consequence of farmland abandonment in mountain areas. *Desertification Control Bulletin*, 25, pp. 27–33, United Nations Environment Programme.
- García-Ruiz, J.M.; Arnáez, J.; Beguería, S.; Seeger, M.; Martí-Bono, C.; Regués, D.; Lana-Renault, N. & White, S. (2005): Runoff generation in an intensively disturbed, abandoned farmland catchment, Central Spanish Pyrenees. *Catena*, 59, pp. 79–92.
- GRASS Development Team (2007): Geographic Resources Analysis Support System (GRASS GIS) Software. Trento, Italy: ITC, 2007 hURL: <http://grass.itc.it/>, Downloaded on 1 December 2007.
- Güntner, A.; Seibert, J. & Uhlenbrook, S. (2004): Modeling spatial patterns of saturated areas: An evaluation of different terrain indices. *Water Resour. Res.* 40, p.W05114.
- Lasanta Martínez, T. (1988): The process of desertion of cultivated areas in the Central Spanish Pyrenees. *Pirineos*, 132, pp. 15–36.
- Lasanta, T.; Pérez Rontomé, M.C. & García-Ruiz, J.M. (1994): Efectos hidromorfológicos de diferentes alternativas de retirada de tierras en ambientes semiáridos de la depresión del Ebro. In García-Ruiz, J.M./Lasanta, T., editors: *Efectos geomorfológicos del abandono de tierras*. Zaragoza: Sociedad Española de Geomorfología, pp. 69–82.
- Lasanta Martínez, T.; Vicente Serrano, S.M. & Cuadrat Prats, J.M. (2000): Marginación productiva y recuperación de la cubierta vegetal en el Pirineo: un caso de estudio en el Valle de Bórau. *Boletín de la A.G.E.* 29, pp. 5–28.
- Llorens, P. & Gallart, F. (1992): Small BasinResponse in a Mediterranean Mountainous Abandoned Farming Area: Research Design and Preliminary Results. *Catena*, 19, pp. 309–320.
- Neteler, M. & Mitasova, H. (2008): OPEN SOURCE GIS. A GRASS GISS Approach. 3rd edition. Springer Science+Business Media, LCC, p. 406.
- Ries, J.B.; Langer, M. & Rehberg, C. (2000a): Experimental investigations on water and wind erosion on abandoned fields and arable land in the central Ebro Basin. *Z. Geomorphol. Suppl.-Bd.* 121, pp. 91–108.
- Ries, J.B.; Marzolff, I. & Seeger, M. (2000b): Der Beweidungseinfluss auf Vegetationsbedeckung und Bodenerosion in der Flysch-Zone der spanischen Pyrenäen. In Freiburger Geographische Hefte. Freiburg i. Br.: Institut für Physische Geographie, Albert-Ludwigs-Universität Freiburg i. Br., pp. 167–194.

Ries, J., M. Seeger, T. Iserloh, S. Wistorf, und W. Fister (2009), Calibration of simulated rainfall characteristics for the study of soil erosion on agricultural land, *Soil and Tillage Research*, 106(1), 109–116, DOI: 10.1016/j.still.2009.07.005.

Scherrer, S. & Naef, F. (2003): A decision scheme to indicate dominant hydrological flow processes on temperate grassland. *Hydrol. Process.* 17, pp. 391–401.

Schmocke-Fackel, P.; Naef, F. & Scherrer, S. (2007): Identifying runoff processes on the plot and catchment scale. *Hydrology and Earth System Sciences*, 11, Nr. 2, pp. 891–906 hURL: <http://www.hydrol-earth-syst-sci.net/11/891/2007/hess-11-891-2007.pdf>.

Seeger, M. (2001): Boden und Bodenwasserhaushalt als Indikatoren der Landdegradierung auf extensivierten Nutzflächen in Aragón / Spanien. Ph.D thesis, Institut für Physische Geographie, Albert-Ludwigs-Universität Freiburg i. Br., Freiburg i. Br., p. 184+30.

Seeger, M. (2007): Uncertainty of factors determining runoff and erosion processes as quantified by rainfall simulations. *Catena*, 71, 56-67.

Seeger, M. & Ries, J. B. (2008): Soil degradation and soil surface process intensities on abandoned fields in Mediterranean mountain environments. *Land Degrad. Develop.* 19, pp. 1-14.

Seeger, M.; Ries, J.B. & Sauer, T. (2002): Hydraulic conditions of soils on abandoned fields of the Aragonese Pyrenees (Spain). In Rubio, J. L./Morgan, R. P. C./ Asins, S./Andreu, V., editors: Proceedings of the third International Congress Man and Soil at the Third Millennium. Logroño: Geoforma Ediciones, pp. 493–505.

Seeger, M. & Beguería, S. (2003): Das hydrologische Verhalten zweier kleiner Einzugsgebiete mit unterschiedlicher Nutzungsgeschichte und -intensität in den aragonesischen Pyrenäen. - La respuesta hidrológica en dos cuencas experimentales con diferentes usos del suelo en el Pirineo Aragonés. In: Landnutzungswandel und Landdegradation in Spanien - El cambio en el uso del suelo y la degradación del territorio en España. Zaragoza, Frankfurt: Universidad de Zaragoza, Johann Wolfgang Goethe Universität Frankfurt am Main, pp. 203–221.

Seeger, M.; Errea, M.P.; Beguería, S.; Arnáez, J.; Martí, C. & García-Ruiz, J.M. (2004): Catchment soil moisture and rainfall characteristics as determinant factors for discharge/suspended sediment hysteretic loops in a small headwater catchment in the Spanish Pyrenees. *J. Hydrol.* 288, pp. 299–311.

Seeger, M.; Errea-Abad, M.P. & Lana-Renault, N. (2005): Spatial distribution of soils and their properties as indicators of degradation/regredation processes in a highly disturbed Mediterranean mountain catchment. *Journal of Mediterranean Ecology*, 6, Nr. 1, pp. 53–59 URL: <http://www.jmecology.com/%5Cpdf%5C2005%5C53-59%20SEEEGER.pdf>.

Vincente Serrano, S.; Lasanta Martinez, T. & Cuadrat Prats, J. (2000): Transformaciones en el paisaje del Pirineo como consecuencia del abandono de las actividades económicas tradicionales. *Pirineos*, 2000, 155, 111-133.

Waldenmeyer, G. (2002): Abflussbildung und Regionalisierung in einem forstlich genutzten Einzugsgebiet (Dürreychtal, Nordschwarzwald). Ph.D thesis, Institut für Geographie und Geoökologie der Universität Karlsruhe (TH), Karlsruhe, p. 195.

Butzen et al. (2014): Quantification of Hortonian overland flow generation and soil erosion in a Central European Low Mountain range using rainfall experiments. Catena, Vol. 113, pp. 202-212.

Quantification of Hortonian overland flow generation and soil erosion in a Central European Low Mountain range using rainfall experiments

V. Butzen^a, M. Seeger^a, S. Wirtz^a, M. Huemann^b, C. Mueller^c, M. Casper^a, and J. B. Ries^a

^aDep. of Physical Geography, Trier University, Behringstraße, 54296 Trier, Germany

^bDep. of Soil Sciences, Trier University, Behringstraße, 54296 Trier, Germany

^cDep. of Geography, Koblenz-Landau University, Universitätsstraße 1, 56070 Koblenz, Germany

Corresponding Author:

Verena Butzen

Trier University

Behringstraße

54296 Trier, Germany

Tel.: +49-651-201-4522

Fax.: +49-651-201-3976

e-Mail: butzen@uni-trier.de

Abstract

In the framework of the EU-INTERREG-IVb-project ForeStClim (Transnational Forestry Management Strategies in Response to Regional Climate Change Impacts) a combination of experimental methods has been applied for the investigation of the spatial and temporal variance and intensity of overland flow generation and soil erosion processes.

In the presented study, the influences of land-use type and land-management practices on overland flow generation and soil erosion are investigated for three low mountain range catchments in Luxembourg and in Rhineland-Palatinate, Germany. The key questions of the study can be summarized as follows: Can Hortonian overland flow generation be observed on all land-use types in the investigated areas in the Central European low mountain range? How can the contribution of forested areas to the flood and erosion dynamics be evaluated under humid climate conditions in Central Europe and what are the most important factors of influence? The Results of the presented study show that forest areas can also be sources for overland flow and sediment, particularly artificial linear structures like unpaved roads and harvester tracks, where runoff coefficients between 41.2 and 97.1 %, and erosion values between 2.6 and 122.5 g m⁻² were determined using rainfall experiments. Another important factor is soil water repellency, this factor can pre-eminently be observed under rather dry soil moisture conditions in summer and can have severe influence on overland flow generation

particularly in forested areas. The results of the rainfall experiments in coniferous forests show runoff coefficients ranging from 0 to 86.9 %, here the high values can all be traced back to water repellency influence, as the field observations suggest.

In the context of flood generation, it is becoming more and more important to improve knowledge on overland flow generation and soil erosion processes occurring in forested catchments, particularly considering the expected climate change.

Keywords

forest; management practice; overland flow generation; soil erosion; water repellency

1 Introduction

The most important factors controlling overland flow generation and soil erosion in a Central European low mountain range can be divided into two separate categories: Soil surface characteristics such as land-use, vegetation/litter cover, and water repellency effects on the one hand (Bens et al., 2007; Buczko et al., 2007, Doerr et al., 2009a; Greiffenhagen et al., 2006; Hartmann et al., 2009; Neris et al., 2012), and: Soil specific parameters such as antecedent soil moisture and compaction by heavy machinery on the other (Robichaud et al., 2010; Roth, 1996; Wagenbrenner et al., 2010). A surface cover by vegetation or litter generally reduces splash erosion because some parts of the soil surface are protected from direct drop impact (Morgan, 1986). On permanently vegetation covered land, like grassland and forests, one of the most important variables influencing overland flow generation and thus soil erosion processes is the occurrence or absence of water repellency (Buczko et al., 2002; Doerr et al., 2009b, 2000; Orfánus et al., 2008; Wahl et al., 2005, 2003; Wessolek et al., 2008). According to Doerr et al. (2000) the substances that lead to soil hydrophobicity can be provided by plant material in different decomposition states or by fungi or micro-organisms in the organic layers or the mineral soil (Atanassova and Doerr, 2010; Morley et al., 2005). Another important factor influencing water repellency is the soil moisture. Doerr et al. (2000) state that a hydrophobic soil becomes hydrophilic again, if a certain critical water content is exceeded. A second factor that can be responsible for severe runoff generation and soil erosion under forest is the compaction of the soil matrix by heavy machinery like harvesters (Horn et al., 2007; Robichaud et al., 2010; Wagenbrenner et al., 2010).

Soil erosion by water mainly consists of the processes of overland flow generation, detachment, transport and deposition (Roth, 1996). Soil detachment is initiated by the impact of rain drops (splash-effect) and by overland flow itself. The splash-effect is controlled by the kinetic energy of the raindrops and by the condition of the soil surface; it provides for the allocation of small soil particles that can be transported by arising overland flow (Kretzschmar, 1992; Morgan, 1986; Roth, 1996). Transport rates achieved by superficially flowing water usually exceed the total erosive effort of the splash-effect by far (Roth, 1996).

In the following, these research questions are going to be answered:

1. Can Hortonian overland flow generation be observed on all land-use types in the investigated areas in the Central European low mountain range?
2. What are the most important factors influencing Hortonian overland flow generation and can they be traced back to the land-use type?
3. Does this lead to soil erosion processes and under which conditions?

Therefore, the main objective of this study is the quantification of overland flow generation and soil erosion processes using field rainfall simulation experiments in combination with a mapping of linear structures such as roads and tracks. The rainfall simulations enable an objective comparison of the overland flow generation of areas under different land-use in response to exactly the same rainfall input. That has not been possible using long term plots and natural rainfall. Furthermore, there is still a lack of studies with plots or experiments in Central European forest areas, thus the presented study can provide a profound data basis helping to fill this gap.

Climate Change makes it even more important to find answers to the above questions. The frequency of heavy summer rainstorm events is expected to increase and large winter rain periods are to become more frequent (Solomon et al., 2007). Additionally, the occurrence of dry periods in late spring and summer is to become more likely (Solomon et al., 2007). Such a development might lead to an increased influence of water repellency effects, particularly in Central European forests. Another important point is, that forest management changes the soil and the flow paths; firstly due to flow concentration on roads and tracks, and secondly due to compaction (Horn et al., 2007).

In 2010, altogether 30.1 % of the total area in Germany and even 42 % of the total area in Rhineland-Palatinate are under forestal use (German Federal Office of Statistics, 2012). This

high percentage underlines the importance of the forests possible contribution to flood and erosion prevention. As part of the EU-INTERREG IVB project ForeStClim (Transnational Forestry Management Strategies in Response to Regional Climate Change Impacts) the overland flow generation and soil erosion processes are investigated in three small catchments in Luxemburg and Rhineland-Palatinate, Germany. The study areas are partially under forestry use and partially under agricultural and grassland use, so the influence of different land-use types can be tested.

This study is focused on the overland flow processes in heavy rainstorm events. The subterranean contributions to stream flow are not investigated.

2 Study Areas

The study areas are situated in South-West Germany and in Luxemburg (Fig. 1). The three study areas were chosen, because they represent typical areas in the studied region. The Holzbach catchment for example is typical for the large forest areas in the Hunsrück (Hochwald), covered with spruce and beech forests mainly (Gallus et al., 2007). The Frankelbach is typical for the land-use in many small catchments in the Pfälzer-Bergland-region, with agricultural use at the plain highlands, forest at the steep valley sides and grassland use in the valley bottom (Johst, 2010). The Huewelerbach catchment with mainly beech-forest is typical for the forested areas in the Eich-Marmer Gutland (Luxembourg) (Gerrits et al., 2007; Juilleret et al., 2012; Pfister et al., 2005).

The main characteristics of the study sites together with the total number of rainfall simulations are given in Table 1. It also depicts the number of rainfall simulations without overland flow generation.

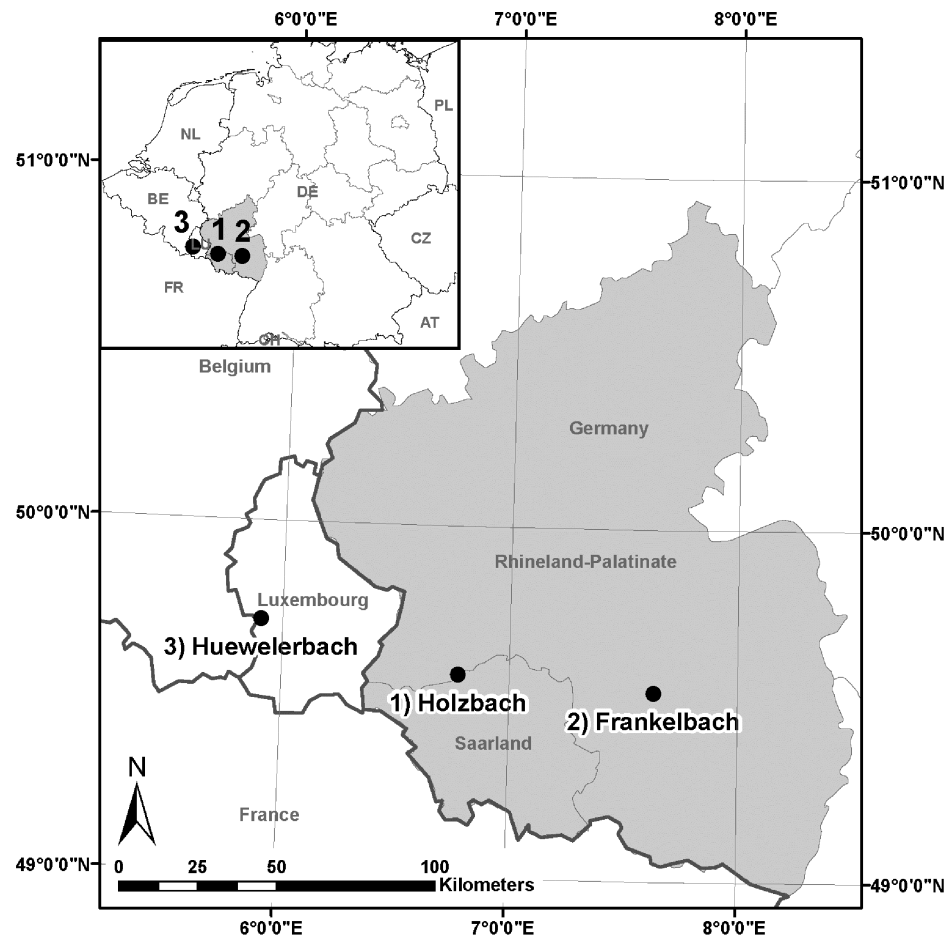


Figure 1: Map of the location of the study areas. (1) Holzbach, 2) Frankelbach, 3) Huewelerbach)

Table 1: Main characteristics and number of rainfall simulations for each study area

	Holzbach^a	Frankelbach^b	Huewelerbach^c
Geographic coordinates	N49° 34' 31.`` E6° 46' 27.984``	N49° 32' 4.56`` E7° 38' 0.024``	N49° 43' 0.12`` E5° 54' 13.968``
Landscape	Schwarzwälder Hochwald (RLP, Germany)	Pfälzer Bergland (RLP, Germany)	Eisch-Mamer Gutland (Luxembourg)
Geology	Devonian Quarzite	Permian Sand- and Siltstones	Lias Sandstones, Keuper clays
Soils	Cambisol, Podsol, stagnic Cambisol	Cambisol, Colluvic Regosol, Regosol	Cambisol, Podsol, Colluvic Regosol, Gleysol
Precipitation [mm y⁻¹]	1160	800	740
Mean annual temperature [°C]	8.7	9.0	9.0
Area [km²]	2.2	5.0	2.7
Land-use			
deciduous forest [%]	39.3	43.0	77.8
coniferous forest [%]	54.2	9.8	16.0
afforestation [%]	6.3	2.4	-
grassland [%]	0.2	23.0	6.0
agriculture [%]	-	19.0	-
settlement area [%]	-	2.8	0.2
Road net density [m ha⁻¹]	97.97	77.1	116.5
Harvester track density [m ha⁻¹]	189	-	0
Rainfall Simulations (No.)	17	24	32
Rainfall Simulations without OF	4	1	10
Rainfall Simulations without OF after 30 min	6	1	10

^aGallus et al., 2007; German Meteorological Service, 2005^bJohst, 2010^cGerrits et al., 2007; Juilleret et al., 2012; Pfister et al., 2005

(RLP: Rhineland-Palatinate, OF: overland flow)

3 Material and Methods

3.1 Field Mapping and GIS Methods

For the mapping, a printed mapping basis consisting of topographical maps and high resolution aerial photographs is used and the roads and tracks were recorded on this foundation. In all of the three study areas the forestry and agricultural roads were mapped, because some differences in the road network had been recorded during the field work in comparison to the topographical maps and older GIS data. In all study areas erosion rills were mapped according to the DVWK field mapping guide (DVWK — Deutscher Verband für Wasserwirtschaft und Kulturbau e. V., 1996). The harvester tracks were only mapped in a part of the Holzbach study area. Here, this type of linear structures is very dense and therefore important for the runoff and erosion dynamics. In the Huewelerbach catchment, almost no harvester tracks could be recognized visually and in the Frankelbach area the tracks were not mapped.

For the preparation of the study area maps (Figs. 3-5) the field maps were digitized using the GIS-software ArcGIS 9.3 (Esri Inc., 2008) with which all other GIS-analyses were carried out as well. The density of linear structures for each study area was calculated by division of the line length of the road net by the total catchment area. For the Holzbach the density of harvester tracks for the mapped area was calculated in the same way.

3.2 Water drop penetration time (WDPT) test for water repellency

For the determination of mineral soil water repellency in the field, the water drop penetration time (WDPT) test was used according to Doerr (1998). The differentiation between humus layers and mineral soil was determined according to the German soil mapping guide (Ad-hoc-ARBEITSGRUPPE BODEN, 1996). After removing the humus layers, three drops of water were placed on the surface of the mineral soil and the time needed for infiltration was recorded. The test was only carried out for up to 300 s. If the drop was still present afterwards, 300 s were recorded as WDPT. The drops were formed using a glass-pipette of a standard amber glass bottle. The water amount for each drop was about 50-60 µL. For the evaluation of the results of the WDPT tests, the classification scheme of Doerr et al. (2006) was used in a slightly modified version: Classes 6 and 7 were aggregated into one class, because the measurements of WDPT in the field were stopped after 300 seconds. The modified class 6, with more than 300 s WDPT is evaluated as 'severe' water repellency. The classification scheme is shown in table 2.

Table 2: Classification scheme for WDPT tests with classes, as well as corresponding time classes and evaluation of the intensity of water repellency

WDPT class	WDPT intervals [sec]	evaluation of repellency
0	≤ 5	Non repellent
1	6-10	slight
2	11-30	slight
3	31-60	slight
4	61-180	moderate
5	181-300	moderate
6	> 300	severe

(Table modified after Doerr et al. 2006)

3.3 Rainfall simulation experiments

The rainfall simulator used for the rainfall simulation experiments is a small and mobile device improved by Iserloh et al. (2012) and Iserloh et al. (2010) based on the device used by Cerdà et al. (1997) and Ries et al. (2000). The experimental setup is shown in Fig. 2. The rainfall intensity simulated was about 40 mm h^{-1} . The duration of each experiment was 30 min on the harvester tracks and forest roads, but 60 min for most of the other experiments. Only the first 30 min of each experiment were used in the statistical analyses. The circular bounded plot has an area of 0.28 m^2 (Ries et al., 2000). The runoff plots were installed by driving the bounding metal ring about 10-15 cm into the forest soil using a rubber-headed mallet. In order to prevent soil disturbance the ring was hammered into the soil very slowly and 2 people were standing on the ring to reduce vibrations, in this way the rim effect could be reduced to a minimum. Runoff was collected continuously in intervals of 5 minutes length. The following plot characteristics were recorded: (1) vegetation cover, (2) slope, (3) exposition, (4) surface roughness, and (5) water repellency. The vegetation/litter cover percentage of the direct soil surface was estimated in the field and checked again using perpendicular plot photographs. The slope of the plot surface in flow direction was measured using a clinometer (Suunto). The surface roughness is measured using a small steering chain that is placed on the soil surface following the micro relief in flow direction from the highest point of the plot to the outlet (diameter). The length of the chain needed for the ‘micro relief diameter’ is divided by the ring diameter and the resulting ratio is used as a measure for surface roughness.

The rainfall intensity was adjusted prior to each rainfall simulation experiment, and it was measured again after each experiment. The amount of runoff was measured gravimetrically. The amount of eroded soil material was determined by filtration of the collected runoff water. After each rainfall experiment the test plot was dug up in order to determine the depth of the infiltration front (Butzen et al., 2011).

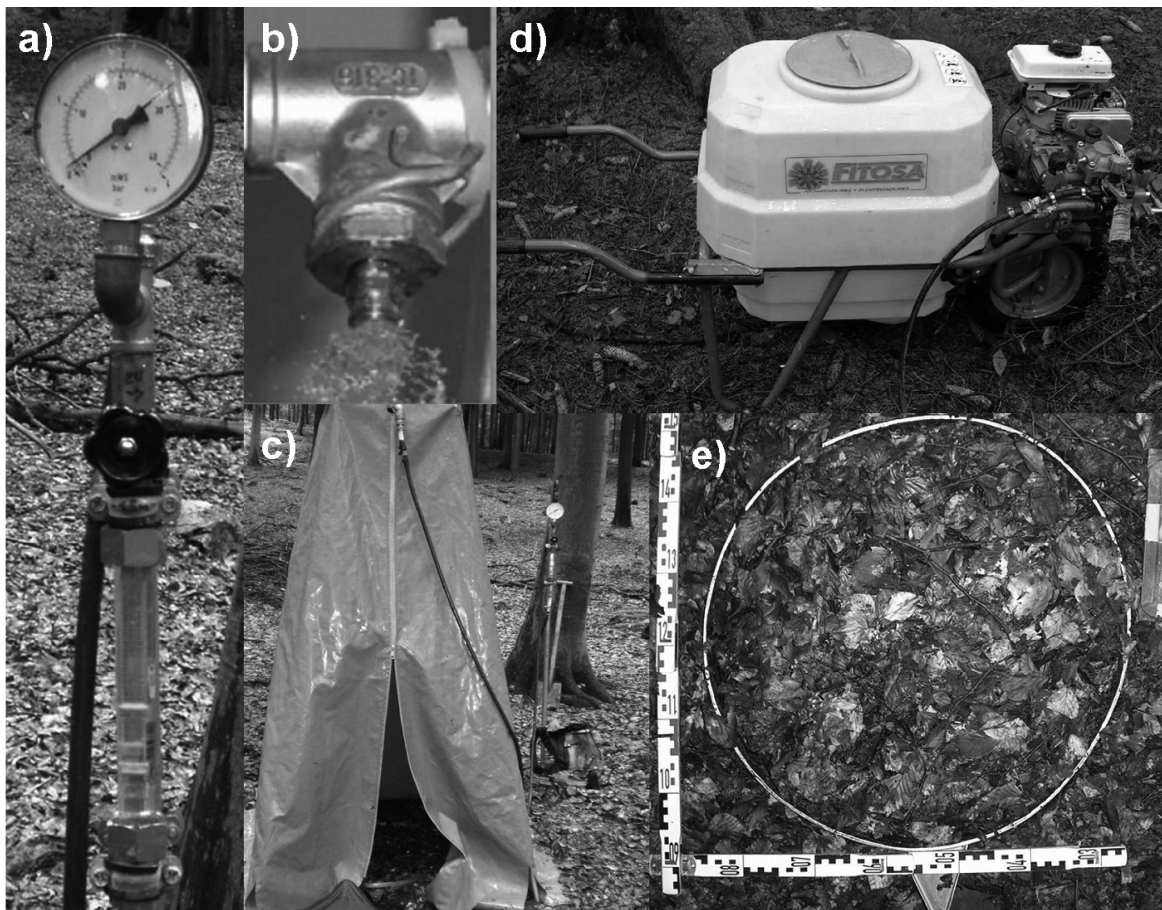


Figure 2: Main parts of the portable rainfall simulator.

- a) Flow meter for adjustment of discharge
- b) Full cone nozzle (Lechler 460.608)
- c) Aluminum linkage (height: 2 m), rubber tarpaulin
- d) Motor driven pump with 100 l water tank
- e) Test plot bounded by a steel ring, diameter: 60 cm, plot area: 0.283 m²

Two different nozzles were used for the experiments. A hollow cone nozzle (Hardi Syntal 1553-89 10) was used in the experiments in the Frankelbach study area and during the first field trip

in the Huewelerbach area. In all other experiments a full cone nozzle (Lechler 460.608) was used due to better spraying characteristics. The water flow rate is regulated by means of a flow meter (KSK-1200HIG100) (Fister et al., 2011; Iserloh et al., 2012, 2010). For a more detailed description of the rainfall simulator and the adaptation in the field please refer to Ries et al. (2009, 2000) and Fister et al. (2011).

In Ries et al. (2009) and Iserloh et al. (2010) a laser distrometer was used for the measurement of drop size distribution and fall velocities of the simulated rainfall for the two nozzle setups that were used here. Concerning the kinetic energy and momentum, the two nozzles are very similar to each other. For further information on the characteristics of the nozzles, please refer to Fister et al. (2011), Iserloh et al. (2012), Iserloh et al. (2010), and Ries et al. (2009). Accordingly, the experimental results gained with the two nozzle setups are quite comparable and thus the data were analyzed together.

Dunkerley (2008) states that simulated rainfall intensity and kinetic energy of rainfall simulation experiments should be comparable to the properties of natural rainfall events in the respective study area. The used rainfall intensity of 40 mm h^{-1} can be regarded as a realistic intensity for a heavy rainfall event in our study areas. For the Holzbach study area, the German Meteorological Service (Deutscher Wetterdienst - Abteilung Hydrometeorologie) states a return period of 1 year for a rainfall intensity of 40 mm h^{-1} with a duration of 15 minutes, and a return period of 5 years for the same intensity with a duration of 30 minutes for the meteorological station in Weiskirchen (German Meteorological Service, 2005) at the lower course of the Holzbach river. Therefore, the simulated rainfall intensity is regarded as a realistic extreme rainfall event for the investigated area concerning the rainfall intensity. The rainfall is simulated in a constant way and not with the intense fluctuations in rainfall intensity that are typical for natural rainfall. Only with a constant rainfall intensity a high reproducibility of the experiments can be ensured and the results can be compared for different plots and study areas. (Iserloh et al., 2013; Ries et al., 2013)

3.3.1 Sites of the rainfall experiments

The sites for the rainfall experiments were chosen in the field due to site characteristics like land-use, vegetation cover of the plot and slope. Each rainfall experiment is representative for a larger area within the specific study area or, in case of the Harvester tracks, the rainfall

experiment is representative for a specific treatment. In order to obtain reliable results, at least two rainfall experiments were carried out on similar surfaces next to each other.

3.4 Statistical methods

The plot characteristics as well as the experimental results of the rainfall experiments are described with commonly used methods of descriptive statistics using the explorative data analysis tools of the SPSS 17.0 software (SPSS Inc., 2008). None of the statistically analysed data sets on rainfall simulations and water repellency is normally distributed, accordingly only non-parametric tests can be used for statistical analysis. In a first step, Median and Huber-M-estimator are calculated as well as the standard deviation and minimum and maximum values. Secondly, boxplots of the data, grouped by land-use are created in order to simplify data interpretation. In a third step the differences between the data in the different boxes (groups) are tested using the Kruskal-Wallis test for several independent samples, in order to find out whether the groups are significantly different from each other. If this test is significant, the groups are tested in pairs using the Mann-Whitney-test and the Kolmogorov-Smirnov-test in order to find out which of the groups are significantly different from each other and which are not. The results of these tests enable a statistically secured interpretation of the boxplots. (Field, 2009; SPSS Inc., 2008; Untersteiner, 2007)

The Spearman-Rho rank correlation coefficient is used for the computation of bivariate correlations. The correlation matrix using the Spearman-Rho correlation coefficient includes the plot characteristics vegetation cover, slope and water repellency as well as the output variables runoff amount, runoff coefficient, suspended sediment load and suspended sediment concentration. The correlations are calculated for all experiments and additionally for the different land-use types (coniferous forest, deciduous forest, afforestation, agricultural field, grassland, and harvester track/road) separately. In the statistical analysis of the rainfall simulation data only the first 30 minutes of each experiment are considered because otherwise not all experiments could have been included. (Field, 2009; SPSS Inc., 2008; Untersteiner, 2007)

4 Results

4.1 Field mappings of linear structures and GIS Analyses

The maps in Figs. 3-5 show the results of the mappings of linear structures that were carried out in all study areas.

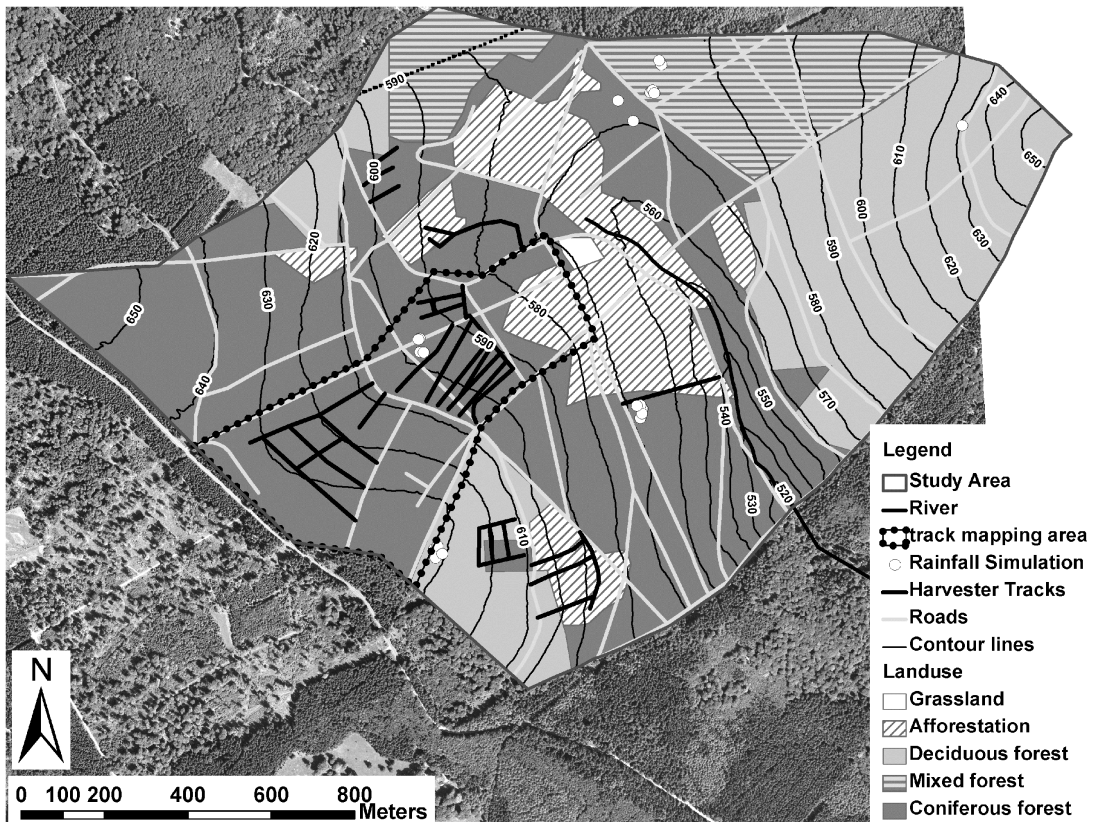


Fig. 3: Map of the study area Holzbach with the mapping of linear structures and the sites of the rainfall simulations.

The map in Fig. 3 shows the roads and harvester tracks that were mapped in the Holzbach area. The density of the unpaved forestry roads in Holzbach is 97.97 m ha^{-1} (see table 1), and additionally 91.3 m ha^{-1} of harvester tracks were mapped for the smaller mapping area marked by the dotted line. Thus the total density of linear structures in the Holzbach area is 189 m ha^{-1} , at least in the small harvester track mapping area, which is really a very high value compared to the other study areas presented here.

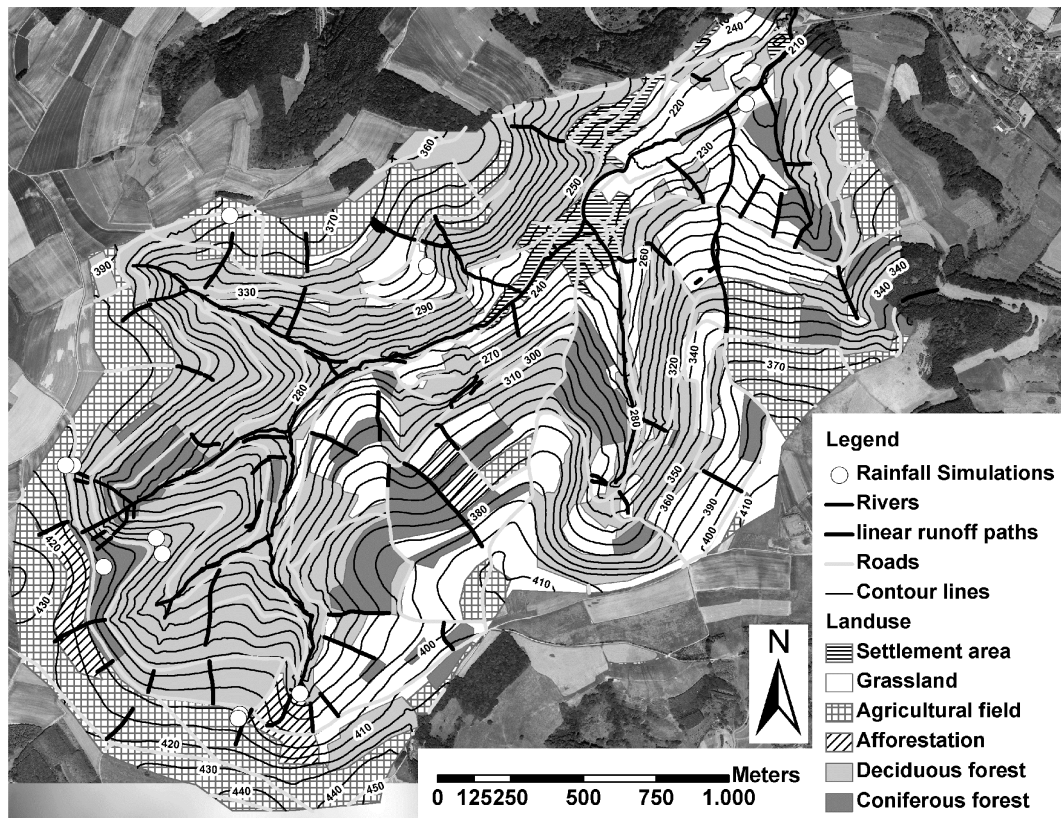


Fig. 4: Map of the study area Frankelbach with the mapping of linear structures and the sites of the rainfall simulations.

The results of the mapping of linear structures in the Frankelbach study area can be regarded in Fig. 4, but here only roads and some linear flow paths between the roads were included into the mapping. The density of the forestry road net amounts to 77.1 m ha^{-1} (see table 1), this value is a bit lower than in the other study areas.

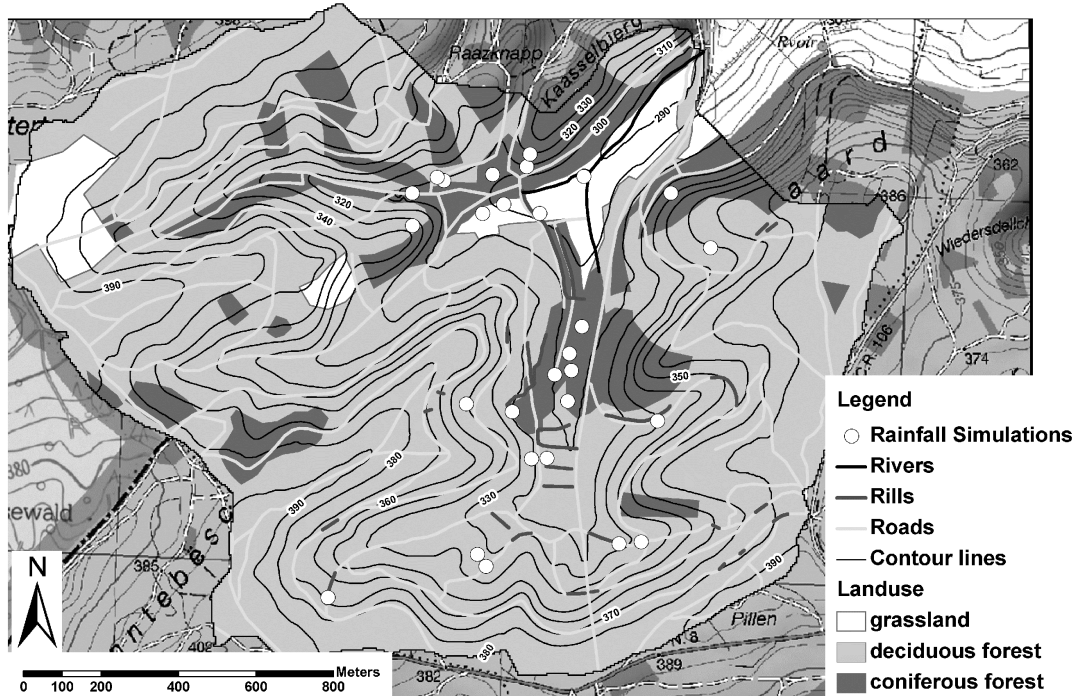


Fig. 5: Map of the study area Huewelerbach with the mapping of linear structures and the sites of the rainfall simulations.

The results of the mapping of linear structures for the Huewelerbach catchment can be regarded in Fig. 5. In this study area the roads and additionally some erosion rills, partially on the unpaved forestry roads, were mapped. The density of the road net for the Huewelerbach area is a bit higher than in the other areas with 116.5 m ha^{-1} (see table 1). Harvester tracks could not be observed visually as linear structures in the study area Huewelerbach.

4.2 Results of the Rainfall Simulation Experiments

The sites of the rainfall simulation experiments are shown in Figs. 3-5. The measuring points are marked by the white dots in the maps.

4.2.1 Descriptive statistics of the rainfall simulation experiments

Table 3 shows the main data of the descriptive statistics of all rainfall simulations, including the plot characteristics vegetation cover, slope and water repellency as well as the results regarding runoff and sediment yield.

Table 3: Descriptive statistics of all rainfall simulations

Variable	N	Huber M-estimator ^a	Median	Min.	Max.	Standard dev.
Veg. cover [%]	73	94	95	0	100	41.4
Slope [°]	72	7.6	7.5	2	27	6.2
Water rep. [sec]	33		1	0	300	74.3
Rainfall [L m^{-2}]	73	39.4	39.9	32.4	52.6	2.5
Runoff start [sec]	58	216	191	19	3000	552
Overland flow [L m^{-2}]	56	3.4	2.9	0	19.5	6.2
Sediment yield [g m^{-2}]	56	1.8	1.4	0	122.5	28.5
Sed. conc. [g L^{-1}]	56	0.9	0.8	0	24.7	3.8
RC [%]	73	6.9	5.2	0	97.1	30.0

(a: weighting constant: 1.339)

The rainfall simulations were carried out on plots with slopes between 2° and 27°. The cover percentage with litter and vegetation of the rainfall simulation test plots range between 0 and 100 % with a median of 95 % and a high standard deviation of 41.4 %. Most of the plots were completely covered by a litter layer of several centimeters thickness, except for most of the harvester tracks and forest roads. The water repellency was recorded at 33 sites and the values range between 0 and 300 s with a median value of 1 s and a standard deviation of 74.3 s.

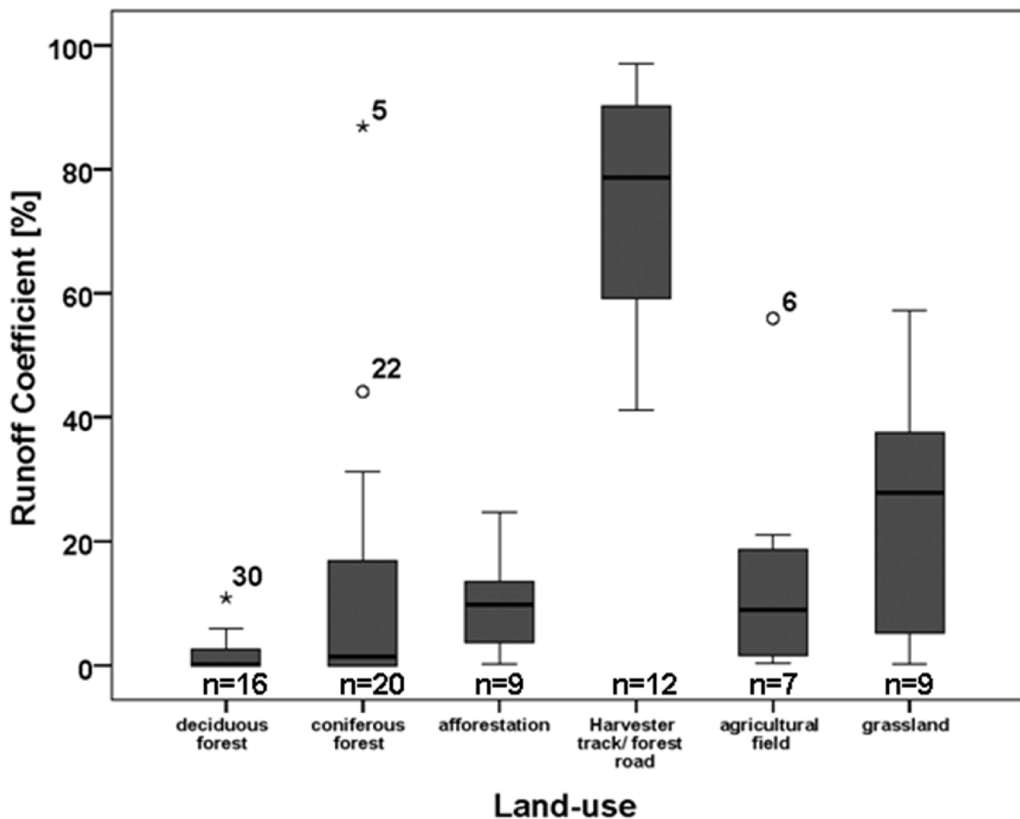


Fig. 6: Boxplots of the runoff coefficients of all 73 rainfall experiments grouped by land-use.

The boxplots of the runoff coefficients are grouped by the land-use (Fig. 6). The significance of the differences in the runoff coefficients between the land-use groups can be regarded in the table 4. According to the Mann-Whitney test (MW), the deciduous forest runoff coefficients differ significantly from all other groups except the coniferous forest. The coniferous forest sites differ significantly from grassland and tracks (MW) and from the afforestation sites (Kolmogorov-Smirnov: KS). The runoff coefficients measured on afforestation sites differ significantly from deciduous forest, coniferous forest and all land-use groups differ significantly from the tracks.

The deciduous forest sites showed very low runoff coefficients regarding the low median value of only 0.2 % and the coniferous forests also show rather low values with a median runoff coefficient of only 1.3 %. Nevertheless, there are also very high values of up to 86.9 % if water repellency comes into play. The median runoff coefficient of the afforestation sites is higher

with 9.8 % but here the highest value is only 24.7 %. The highest runoff coefficients were measured on the harvester tracks and forest roads, with a median runoff coefficient of 78.6 %. These values are much higher than the runoff coefficients measured on agricultural fields and grassland with medians of 8.9 % and 27.8 % respectively. The high overland flow rates on harvester tracks can be explained by the compaction of the topsoil due to the use of heavy machinery in forest management.

Table 4: Significance of group differences for the runoff coefficients according to Mann-Whitney (MW) and Kolmogorov-Smirnov (KS) tests

Significance of Mann-Whitney test					
	DF	CF	AFF	AGR	GRASS
CF	0.324				
AFF	0.000*	0.099			
AGR	0.007*	0.190	1.000		
GRASS	0.000*	0.018*	0.297	0.408	
TRACKS	0.000*	0.000*	0.000*	0.000*	0.000*

Significance of Kolmogorov-Smirnov test					
	DF	CF	AFF	AGR	GRASS
CF	0.229				
AFF	0.001*	0.015*			
AGR	0.059	0.183	0.714		
GRASS	0.003*	0.068	0.126	0.430	
TRACKS	0.000*	0.000*	0.000*	0.001*	0.001*

*groups are significantly different ($p < 0.05$)

(DF: deciduous forest, CF: coniferous forest, AFF: afforestation, AGR: agricultural field, GRASS: grassland, TRACKS: harvester tracks and unpaved forest roads).

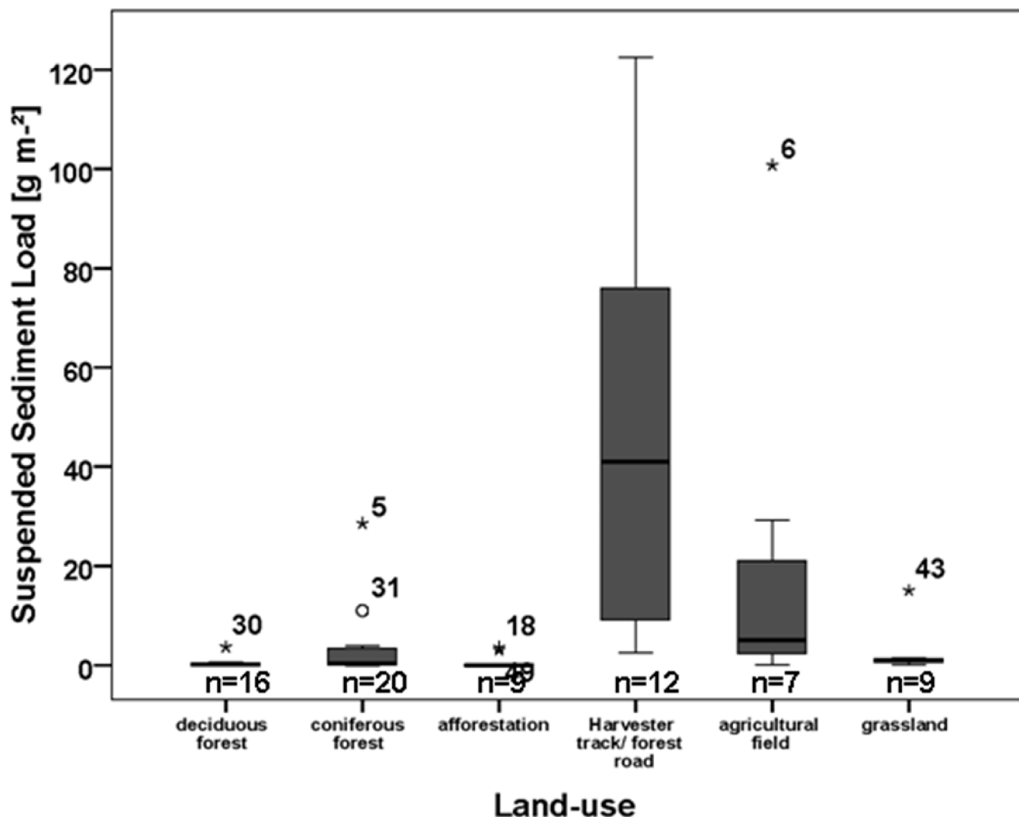


Fig. 7: Boxplots of the suspended sediment loads of all 73 rainfall experiments grouped by land-use.

The boxplots of suspended sediment yields of all rainfall simulation experiments grouped by land-use are shown in Fig. 7. The significance of the differences in suspended sediment yield between the land-use groups can be regarded in the table 5. The deciduous forest runoff suspended sediment loads differ significantly from the agricultural fields and from the tracks. The coniferous forest sites differ significantly from afforestation and tracks. The suspended sediment loads measured on afforestation sites differ significantly from all land-use groups except deciduous forest.

The suspended sediment loads on coniferous forest sites are rather low with a median value of only 0.4 g m^{-2} , despite the considerably high runoff coefficients. The deciduous forests and the grassland also showed almost no erosion regarding median values of 0.3 and 0.9 g m^{-2} respectively. At the afforestation sites also almost no erosion was measured.

The highest values for suspended sediment yield were measured on the harvester tracks and forest roads with sediment yields ranging between 2.6 and 122.5 g m⁻² and a very high median value of 41.1 g m⁻² which is two orders of magnitude higher than the erosion values on the forest and grassland sites. These values are even higher than the values measured on agricultural fields with almost bare soil, where the median suspended sediment yield was only 5.0 g m⁻². Regarding the high density of compacted and unpaved linear structures (see table 1), the spatial relevance of the results gained by means of the rainfall simulations that were carried out on harvester tracks and roads becomes obvious. This emphasizes the importance of the influence of the linear structures on sediment mobilization and transport in the study areas.

Table 5: Significance of group differences for the suspended sediment loads according to Mann-Whitney (MW) and Kolmogorov-Smirnov (KS) tests

b) Significance of Mann-Whitney test					
	DF	CF	AFF	AGR	GRASS
CF	0.543				
AFF	0.167	0.034*			
AGR	0.012*	0.085	0.004*		
GRASS	0.062	0.725	0.026*	0.042*	
TRACKS	0.000*	0.000*	0.000*	0.068	0.000*

*groups are significantly different ($p < 0.05$)					
Significance of Kolmogorov-Smirnov test					
	DF	CF	AFF	AGR	GRASS
CF	0.550				
AFF	0.116	0.050			
AGR	0.024*	0.383	0.008*		
GRASS	0.097	0.490	0.006*	0.015*	
TRACKS	0.000*	0.002*	0.000*	0.126	0.000*

*groups are significantly different ($p < 0.05$)					
--	--	--	--	--	--

(DF: deciduous forest, CF: coniferous forest, AFF: afforestation, AGR: agricultural field, GRASS: grassland, TRACKS: harvester tracks and unpaved forest roads).

4.2.2 Correlations of the rainfall simulation experiments

A correlation matrix including plot characteristics and experimental results for all 73 rainfall simulation experiments is given in table 6. We see a significant correlation between the vegetation cover and the overland flow values. The correlation between vegetation cover and

soil erosion is even higher. The negative correlation value indicates that a lower vegetation cover leads to higher overland flow values. The negative correlation between vegetation cover and runoff coefficient is higher with -0.447 and this correlation is even significant at the 0.01-level.

The correlation coefficients between vegetation cover percentage and the soil erosion measures 'suspended sediment load' and 'suspended sediment concentration' are in the same order of magnitude: The coefficients are -0.423 and -0.440 respectively. Both correlations are significant at the 0.01-level. The water repellency does only show a significant correlation with slope, but not to any other variable as long as all experiments are analyzed together.

Table 6: Correlation Matrix with Spearman-Rho Correlation Coefficients for all 73 Rainfall Simulations

	VC [%]	S. [°]	WR [sec]	OF [$L m^{-2}$]	SSL [$g m^{-2}$]	SSC [$g L^{-1}$]
VC [%]	1					
S. [°]	0.120	1				
WR [sec]	0.138	-0.385*	1			
OF [$L m^{-2}$]	-0.304*	-0.108	-0.159	1		
SSL [$g m^{-2}$]	-0.423**	-0.087	0.028	0.754**	1	
SSC [$g L^{-1}$]	-0.440**	-0.002	0.031	0.251	0.788**	1
RC [%]	-0.447**	-0.075	0.145	0.996**	0.754**	0.250

** Correlation is significant at the 0.01-level.

* Correlation is significant at the 0.05-level.

(VC: vegetation cover, S: slope, WR: water repellency, P: rainfall intensity, Start R.: start time of runoff, OF: overland flow, SSL: suspended sediment load, SSC: suspended sediment concentration, RC: runoff coefficient)

The correlation matrices for all rainfall simulations are grouped according to the six distinguished land-use classes (Table 7). On coniferous forest sites 20 rainfall simulations were carried out and a Spearman-Rho correlation coefficient of -0.584 with significance at the 0.01-level is determined between vegetation cover and runoff coefficient. This negative correlation coefficient indicates that a higher cover percentage leads to lower runoff coefficients. For 12 of the 20 coniferous forest sites a second significant correlation exists between water repellency and the runoff coefficients with a Spearman-Rho correlation coefficient of 0.887, significant at the 0.01- level. For the other 8 rainfall simulation experiments under coniferous forest no WDPT-tests were accomplished. The 16 experiments on deciduous forest sites show a

significant correlation between the slope and suspended sediment concentration with a Spearman-Rho correlation coefficient of 0.724 significant at the 0.05-level. For the nine rainfall simulations on afforestation sites none of the investigated variables vegetation or litter cover, slope and water repellency, shows a significant correlation to the resulting variables. Also no significant and interpretable correlations can be determined for the experiments on agricultural fields, grassland, and on harvester tracks and forest roads.

Table 7: Correlation Matrix with Spearman-Rho Correlation Coefficients for the Rainfall Simulations grouped by the six land-use classes

	VC [%]	S. [°]	WR [sec]	OF [L m^{-2}]	SSL [g m^{-2}]	SSC [g L^{-1}]
Afforestation (n=9)						
S. [°]	0.429	1				
WR [sec]						
OF [L m^{-2}]	-0.378	0.391		1		
SSL [g m^{-2}]	0.107	0.645		0.287	1	
SSC [g L^{-1}]	0.207	0.506		0.018	0.846**	1
RC [%]	-0.279	0.453		0.983**	0.287	0.018
Agricultural field (n=7)						
S. [°]	-0.411	1				
WR [sec]						
OF [L m^{-2}]	-0.257	-0.546		1		
SSL [g m^{-2}]	-0.404	-0.346		0.929**	1	
SSC [g L^{-1}]	-0.587	0.327		0.071	0.393	1
RC [%]	-0.257	-0.546		1.000**	0.929**	0.071
Coniferous forest (n=20)						
S. [°]	-0.194	1				
WR [sec]		-0.536	1			
OF [L m^{-2}]	-0.387	0.037	0.866	1		
SSL [g m^{-2}]	-0.094	-0.082	0.866	0.891**	1	
SSC [g L^{-1}]	0.297	-0.164	0.866	0.682*	0.873**	1
RC [%]	-0.584**	0.010	0.887**	0.991**	0.882**	0.673*
Deciduous forest (n=16)						
S. [°]	-0.099	1				
WR [sec]						
OF [L m^{-2}]	0.294	-0.024		1		
SSL [g m^{-2}]	-0.452	0.469		0.289	1	
SSC [g L^{-1}]	-0.540	0.724*		-0.084	0.739*	1
RC [%]	-0.053	-0.240		0.976**	0.229	-0.108
Grassland (n=9)						
S. [°]	0.935**	1				
WR [sec]						
OF [L m^{-2}]	-0.246	-0.218		1		

SSL [g m⁻²]	0.000	0.075		0.683*	1	
SSC [g L⁻¹]	0.097	0.243		-0.650	-0.050	1
RC [%]	-0.228	-0.201		0.967**	0.733*	-0.550
Track/road (n=12)						
S. [°]	0.606*	1				
WR [sec]	0.415	-0.618	1			
OF [L m⁻²]	0.057	0.297	-0.577	1		
SSL [g m⁻²]	-0.487	-0.302	-0.412	0.343	1	
SSC [g L⁻¹]	-0.458	-0.316	-0.247	0.112	0.965**	1
RC [%]	0.014	0.380	-0.577	0.986**	0.294	0.063

** Correlation is significant at the 0.01 level.

* Correlation is significant at the 0.05 level.

(VC: vegetation cover, S: slope, WR: water repellency, P: rainfall intensity, Start R.: start time of runoff, OF: overland flow, SSL: suspended sediment load, SSC: suspended sediment concentration, RC: runoff coefficient)

5 Discussion

Water repellency of the soil surface and the soil matrix is one of the most important factors influencing overland flow generation and thereby heightening the probability of soil erosion activity in forested areas. During the field work in Frankelbach and especially Holzbach, water repellency of the humus layers and the upper centimeters of the mineral soil were observed using the WDPT-test in the field. It is important to note that the soils were only water repellent under rather dry soil moisture conditions. These field observations correspond to the results of Zehe and Sivapalan (2009), and Zehe et al. (2007) who state that water repellency can be regarded as a threshold process, that can occur if the soil moisture drops below a specific value, which relates to the presence of certain organic compounds (Shakesby et al., 2003; Zavala et al., 2010; Zehe et al., 2007). Doerr et al. (2000) state that a hydrophobic soil becomes hydrophilic again, if a certain, critical water content is exceeded. In this context it can be clearly stated for the Holzbach study area that no hydrophobic reaction was observed under wet conditions in spring time. However, under dry conditions, the coniferous forest sites in particular showed severely hydrophobic properties.

A highly significant correlation was detected between the WDPT (water repellency measure) and the runoff coefficient of the rainfall simulation. This was proven for 12 of the coniferous forest sites. For these 12 rainfall simulations on coniferous forest sites, mainly under spruce and Douglas fir, the intensity of water repellency explains more than 80 % of the variance in measured runoff coefficients (coefficient of determination R²). In addition, the highly

significant Spearman-Rho correlation coefficient of 0.887 confirms these findings. Doerr et al. (2006) state that under dry soil moisture conditions the occurrence of water repellency is typical for land-uses with permanent vegetation cover such as grassland and forests. This is even true in humid climates. For the coniferous forest sites presented in this study, water repellency was observed under, rather dry soil moisture conditions, but not for deciduous forest sites, nor the grassland.

Gerrits et al. (2007) state that forest floor interception is a generally disregarded process that is important for overland flow generation and evaporation processes in forests. They applied a new measurement technique for forest floor interception in the Huewelerbach catchment in Luxembourg. The importance of the organic layers above the mineral soil for interception of rainfall water is supported by the experimental results presented here. In many experiments the water did not reach the mineral soil. This was particularly true for the water repellent sites and under rather dry antecedent soil moisture conditions. In these cases, the water infiltrates into the uppermost humus layers (Ol and partially Of) and the ‘overland flow’ is observed mainly above the Of and Oh layers (mapped according to Ad-hoc-ARBEITSGRUPPE BODEN, 1996). These results are also confirmed by plot-scale sprinkling experiments accomplished by the Soil Science Dept. in the Frankelbach catchment (Hümann et al. 2011).

Generally, the data on surface processes in forest areas is not very extensive, because only few plot measurements and experimental results are published. Auerswald et al. (2009) combined the data of many soil erosion studies in order to delineate rates of sheet and rill erosion for Germany. In the 27 studies evaluated, with altogether 1076 plot years and 96 erosion plots, only three of the plots were under forest. On these three forest plots, soil erosion rates between 0.01 and $0.3 \text{ g m}^{-2} \text{ y}^{-1}$ were determined in altogether in only 13.4 plot years. These very low erosion rates are in the same range as the results of the rainfall simulations presented here. We found a median erosion rate of 0.4 g m^{-2} on undisturbed forest sites. Of course these are only the results of single experiments of 30 minutes duration, and thus difficult to compare to long-term plot measurements. Considering the fact, that the highest percentage of total erosion is delivered by only a few heavy rainfall events (Auerswald et al., 2009; Deumlich et al., 2006), such a comparison seems quite reasonable. In contrast to the low erosion rates in the rather undisturbed forested areas, the rainfall simulations presented in this study show very high erosion rates on the harvester tracks and forest roads.

Unsealed linear structures like harvester tracks and roads play a key role in overland flow generation and sediment delivery in forested areas. This statement is generally accepted (Arnáez et al., 2004; Eastaugh et al., 2008; Heede and King, 1990; MacDonald and Coe, 2008; MacDonald et al., 2001; Ramos-Scharrón and MacDonald, 2007; Robichaud et al., 2010, 1993; Wagenbrenner et al., 2010). Eastaugh et al. (2008) also recognized that forest roads are the main source of sediments to rivers in forested areas and developed a connectivity index for roads to the river network. Croke and Hairsine (2006) present a review on the influences of timber harvesting methods on sediment and overland flow delivery in managed forests, and they present ‘best management practices’ which are suitable to prevent the transportation of sediments to the channel.

Robichaud et al. (1993) carried out rainfall simulation experiments on forest roads and wheel ruts in US forests and they also found much higher sediment yields and overland flow intensities than on undisturbed forest sites, depending on the traffic frequency. Arnáez et al. (2004) carried out rainfall simulation experiments on unpaved forest roads in Spain, and he also underlined the importance of roads, cut-slopes and side-cast fills as sediment sources in forests. The cut-slopes delivered the highest sediment yield with 161 g m^{-2} in a rainfall simulation with an intensity of 75 mm h^{-1} for 30 minutes duration. The rainfall simulation experiments presented here reach sediment yields of 122 g m^{-2} in 30 min with a rainfall intensity of 40 mm h^{-1} and thus, they are in the same range.

Besides the harvester tracks and forestry roads, afforestation sites are potentially affected by overland-flow generation and soil erosion processes. At an afforestation site, the soils may still behave like an agricultural field or a grassland site for a period of several years or even decades (Hümann et al., 2011). This largely depends on the vegetation cover percentage. In the study presented here, nine afforestation sites of different age have been investigated. The runoff coefficients ranged between less than 1 % and 25 %. All sites showed overland flow generation. In most of the experiments minor erosion rates were measured, except for two sites, one in the Frankelbach and one in the Huewelerbach study area, with sediment yields of 3.1 g m^{-2} and 3.6 g m^{-2} respectively. These results show that the afforestation sites are at least prone to overland flow generation and can produce significant sediment yields. Therefore afforestation sites can be regarded as potential sediment sources. Accordingly, the areas planned for afforestation should be treated before the actual afforestation e.g. by deep loosening. This has an additional

positive effect regarding forest growth and adapting the forest to regional climate change impacts since less climate induced stress situations occur (Hümann et al., 2010).

Field rainfall simulation experiments are a widely used method in soil erosion research, especially in semi-arid and arid environments (Arnáez et al., 2007, 2004; Bowyer-Bower and Burt, 1989; Butzen et al., 2011; Cerdà et al., 1997, Iserloh et al., 2013; Ries et al., 2000, 2009). At first sight, the application of rainfall simulations underneath the forest canopy under humid climate conditions is questionable. Nevertheless, rainfall simulation is the only method enabling a direct comparison of the experimental results for a single study area. They also allow a comparison of different study areas, whereas plot measurements under natural rainfall are characterized by different rainfall conditions for each site, especially in forested areas. The rainfall simulations enable the application of the 'same' rainfall to each test site, with a very high reproducibility of both spatial distribution and drop size distribution of the rainfall (Ries et al., 2009).

Gerrits et al. (2010) measured an average canopy interception of 18 % in the leaf-on period and of 5 % in the leaf-off period for beech stands in the Huewelerbach in Luxembourg. This equals an interception of between 2 and 7.2 mm for our simulated rainfall intensity of 40 mm h^{-1} . Holko et al. (2009) measured a canopy interception of only 0.8-0.9 mm per day for a spruce forest site in Slovakia. Even assuming a maximum canopy interception in the range of 8 to 10 mm, most of the water of a heavy rainfall event reaches the forest floor. The application of rainfall simulations below the forest canopy is therefore still appropriate.

6 Conclusions

We found a clear dependency of overland flow generation and soil erosion on the land-use type. High overland flow and soil erosion rates were measured on agricultural fields, on harvester tracks, and on unpaved roads. Considerable overland flow rates were determined on grassland, on afforestation sites, and in coniferous forests with organic layers under dry, water repellent conditions.

Artificial linear structures like harvester tracks and unpaved roads are the main sediment sources in our study areas, at least concerning areas under forest. Thus, the future land-management should focus on a reduction of harvester tracks, wherever this is possible. One solution is the increased use of soil-protecting logging methods such as winch traction.

The afforestation sites showed considerable overland flow generation but only low soil erosion rates. Hence, the soils of the tested afforestation sites still react like agricultural fields with rather high Hortonian overland flow rates, but show low soil erosion values due to surface cover.

Water repellency effects are an important factor influencing the hydrological response of coniferous forest sites to heavy rainfall events on dry soil. This was proven in the Holzbach and the Frankelbach study areas. Further work is necessary to improve knowledge on the conditions of the appearance of water repellency and on the effects on Hortonian overland flow generation. The analysis of our rainfall experiments leads to the conclusion that Central European forest areas in general, rarely contribute to overland flow generation and soil erosion process activity. Contrasting to that, the occurrence of water repellency and artificial linear structures like harvester tracks and forest roads lead to considerable overland flow generation and also to soil erosion in the forests. Due to the climate change, dry periods in late spring and summer will become more frequent and this can lead to an increased probability of water repellency effects in Central European forests.

Acknowledgements

This study has received European Regional Development Funding through the INTERREG IVB NWE project ForeStClim, and the INTERREG IIIB NWE-project WaReLa.

References

- Ad-hoc-ARBEITSGRUPPE BODEN, 1996. Bodenkundliche Kartieranleitung, 4. verbesserte und erweiterte Auflage., Finnern H., Grottenthaler W., Kühn D., Pälchen W., Schraps W.-G., Sponagel H. (Eds.), Bundesanstalt für Geowissenschaften und Rohstoffe und Geologische Landesämter, Hannover.
- Arnáez, J., Larrea, V., Ortigosa, L., 2004. Surface runoff and soil erosion on unpaved forest roads from rainfall simulation tests in northeastern Spain. *Catena*, 57(1), 1–14, doi:10.1016/j.catena.2003.09.002.
- Arnaez, J., Lasanta, T., Ruiz-Flaño, P., Ortigosa, L., 2007. Factors affecting runoff and erosion under simulated rainfall in Mediterranean vineyards. *Soil and Tillage Research*, 93(2), 324–334, doi:10.1016/j.still.2006.05.013.
- Atanassova, I., Doerr, S., 2010. Organic compounds of different extractability in total solvent extracts from soils of contrasting water repellency. *European Journal of Soil Science*, 61(2), 298–313.
- Auerswald, K., Fiener, P., Dikau, R., 2009. Rates of sheet and rill erosion in Germany -- A meta-analysis. *Geomorphology*, 111(3-4), 182–193, doi:10.1016/j.geomorph.2009.04.018.

- Bens, O., Wahl, N. A., Fischer, H., Hüttl, R. F., 2007. Water infiltration and hydraulic conductivity in sandy cambisols: impacts of forest transformation on soil hydrological properties. *European Journal of Forest Research*, 126(1), 101–109, doi:10.1007/s10342-006-0133-7.
- Bowyer-Bower, T. A. S., Burt, T. P., 1989. Rainfall simulators for investigating soil response to rainfall. *Soil Technology*, 2(1), 1–16, doi:10.1016/S0933-3630(89)80002-9.
- Buczko, U., Bens, O., Fischer, H., Hüttl, R., 2002. Water repellency in sandy luvisols under different forest transformation stages in northeast Germany. *Geoderma*, 109(1–2), 1–18, doi:10.1016/S0016-7061(02)00137-4.
- Buczko, U., Bens, O., Hüttl, R. F., 2007. Changes in soil water repellency in a pine–beech forest transformation chronosequence: Influence of antecedent rainfall and air temperatures. *Ecological Engineering*, 31(3), 154–164, doi:10.1016/j.ecoleng.2007.03.006.
- Butzen, V., Seeger, M., Casper, M., 2011. Spatial pattern and temporal variability of runoff processes in Mediterranean Mountain environments - A case study of the Central Spanish Pyrenees. *Zeitschrift für Geomorphologie*, 55(Suppl. 3), 25–48.
- Cerdà, A., Ibáñez, S., Calvo, A., 1997. Design and operation of a small and portable rainfall simulator for rugged terrain. *Soil Technology*, 11(2), 163–170, doi:10.1016/S0933-3630(96)00135-3.
- Croke, J. C., Hairsine, P. B., 2006. Sediment delivery in managed forests: a review. *Environmental Reviews*, 14(1), 59–87, doi:10.1139/a05-016.
- Deumlich, D., Funk, R., Frielinghaus, M., Schmidt, W.-A., Nitzsche, O., 2006. Basics of effective erosion control in German agriculture. *Journal of Plant Nutrition and Soil Science*, 169(3), 370–381, doi:10.1002/jpln.200621983.
- Doerr, S. H., 1998. On standardizing the ‘Water Drop Penetration Time’ and the ‘Molarity of an Ethanol Droplet’ techniques to classify soil hydrophobicity: A case study using medium textured soils. *Earth Surface Processes and Landforms*, 23(7), 663–668, doi:10.1002/(SICI)1096-9837(199807)23:7<663::AID-ESP909>3.0.CO;2-6.
- Doerr, S. H., Shakesby, R. A., Dekker, L. W., Ritsema, C. J., 2006. Occurrence, prediction and hydrological effects of water repellency amongst major soil and land-use types in a humid temperate climate. *European Journal of Soil Science*, 57(5), 741–754, doi:10.1111/j.1365-2389.2006.00818.x.
- Doerr, S. H., Shakesby, R. A., MacDonald, L. H., 2009a. Soil Water Repellency: A Key Factor in Post-Fire Erosion., in: Cerdà A., Robichaud P. (Eds.), *Fire Effects on Soils and Restoration Strategies*. Science Publishers Inc., Enfield, New Hampshire, USA, S. 197–224.
- Doerr, S. H., Shakesby, R. A., Walsh, R. P. D., 2000. Soil water repellency: its causes, characteristics and hydro-geomorphological significance. *Earth-Science Reviews*, 51(1–4), 33–65, doi:10.1016/S0012-8252(00)00011-8.
- Doerr, S. H., Woods, S. W., Martin, D. A., Casimiro, M., 2009b. „Natural background“ soil water repellency in conifer forests of the north-western USA: Its prediction and relationship to wildfire occurrence. *Journal of Hydrology*, 371(1–4), 12–21, doi:10.1016/j.jhydrol.2009.03.011.
- Dunkerley, D., 2008. Rain event properties in nature and in rainfall simulation experiments: a comparative review with recommendations for increasingly systematic study and reporting. *Hydrological Processes*, 22(22), 4415–4435, doi:10.1002/hyp.7045.

- DVWK – Deutscher Verband für Wasserwirtschaft und Kulturbau e. V., 1996. Bodenerosion durch Wasser – Kartieranleitung zur Erfassung aktueller Erosionsformen. Merkblätter zur Wasserwirtschaft, 239, Bonn.
- Eastaugh, C. S., Rustomji, P. K., Hairsine, P. B., 2008. Quantifying the altered hydrologic connectivity of forest roads resulting from decommissioning and relocation. *Hydrological Processes*, 22(14), 2438–2448, doi:10.1002/hyp.6836.
- ESRI, 2008. ESRI ArcMap 9.3, Esri Deutschland GmbH. [online] Available from: <http://esri-germany.de/products/arcgis/about/whats-coming.html>
- Field, A., 2009. Discovering Statistics Using SPSS, 3rd Edition., SAGE Publications Ltd., London.
- Fister, W., Iserloh, T., Ries, J. B., Schmidt, R.-G., 2011. Comparison of rainfall characteristics of a small portable rainfall simulator and a combined portable wind and rainfall simulator. *Zeitschrift für Geomorphologie*, 55, 109–126, doi:10.1127/0372-8854/2011/0055S3-0054.
- Gallus, M., Ley, M., Schubert, D., Schüler, G., Segatz, E., Werner, W., 2007. Renaturierung von Hangbrüchen im Hunsrück zur Glättung von Abflussspitzen, in: Schüler G., Gellweiler I., Seeling S. (Eds.), Dezentraler Wasserrückhalt in der Landschaft durch vorbeugende Maßnahmen der Waldwirtschaft, der Landwirtschaft und im Siedlungswesen. Trippstadt, S. 21–30.
- German Federal Office of Statistics (Statistisches Bundesamt) (Eds.), 2012. Statistisches Jahrbuch - Statistisches Jahrbuch 2012 - Statistisches Bundesamt (Destatis). Available from: <https://www.destatis.de/DE/Publikationen/StatistischesJahrbuch/StatistischesJahrbuch2012.html> (Zugegriffen 10 Dezember 2012).
- German Meteorological Service, 2005. *KOSTRA-DWD-2000 - Starkniederschlagshöhen für Deutschland*. Tech. rep., DWD (Deutscher Wetterdienst), Offenbach.
- Gerrits, A. M. J., Pfister, L., Savenije, H. H. G., 2010. Spatial and temporal variability of canopy and forest floor interception in a beech forest. *Hydrological Processes*, 24(21), 3011–3025, doi:10.1002/hyp.7712.
- Gerrits, A. M. J., Savenije, H. H. G., Hoffmann, L., Pfister, L., 2007. New technique to measure forest floor interception – an application in a beech forest in Luxembourg. *Hydrol. Earth Syst. Sci.*, 11(2), 695–701.
- Greiffenhagen, A., Wessolek, G., Facklam, M., Renger, M., Stoffregen, H., 2006. Hydraulic functions and water repellency of forest floor horizons on sandy soils. *Geoderma*, 132(1–2), 182–195, doi:10.1016/j.geoderma.2005.05.006.
- Hartmann, P., Fleige, H., Horn, R., 2009. Physical properties of forest soils along a fly-ash deposition gradient in Northeast Germany. *Geoderma*, 150(1–2), 188–195, doi:10.1016/j.geoderma.2009.02.005.
- Heede, B.-H., King, R.-M., 1990. State-of-the-art timber harvest in an Arizona mixed conifer forest has minimal effect on overland flow and erosion / L'exploitation rationnelle du bois d'oeuvre dans une forêt mixte de conifères a un effet minimal sur l'écoulement de surface et l'érosion. *Hydrological Sciences Journal*, 35(6), 623, doi:10.1080/02626669009492468.
- Holko, L., Škvarenina, J., Kostka, Z., Frič, M., Staroň, J., 2009. Impact of spruce forest on rainfall interception and seasonal snow cover evolution in the Western Tatra Mountains, Slovakia. *Biologia*, 64(3), 594–599, doi:10.2478/s11756-009-0087-6.
- Horn, R., Vossbrink, J., Peth, S., Becker, S., 2007. Impact of modern forest vehicles on soil physical properties. *Forest Ecology and Management*, 248(1–2), 56–63, doi:10.1016/j.foreco.2007.02.037.

- Hümann, M., Schneider, R., Schüler, G., 2010. Auswirkungen von Tieflockerung auf erstaufgeforsteten Flächen. AFZ-DerWald 5, 8–12.
- Hümann, M., Schüler, G., Müller, C., Schneider, R., Johst, M., Caspari, T., 2011. Identification of runoff processes - Impact of different forest types and soil properties on soil-water interrelations and floods. *J. Hydrol.* 409, 637–649, doi:10.1016/j.jhydrol.2011.08.067.
- Iserloh, T., Fister, W., Ries, J.B., Seeger, M., 2010. Design and calibration of the small portable rainfall simulator of Trier University. *Geophysical Research Abstracts* 12, [EGU2010-2769](#).
- Iserloh, T., Fister, W., Seeger, M., Willger, H., Ries, J. B., 2012. A small portable rainfall simulator for reproducible experiments on soil erosion. *Soil and Tillage Research*, 124(0), 131–137, doi:10.1016/j.still.2012.05.016.
- Iserloh, T., Ries, J.B., Cerdà, A., Echeverría, M.T., Fister, W., Geißler, C., Kuhn, N.J., León, F.J., Peters, P., Schindewolf, M., Schmidt, J., Scholten, T., Seeger, M., 2013. Comparative measurements with seven rainfall simulators on uniform bare fallow land. *Zeitschrift für Geomorphologie, Supplementary Issues* 57, 11–26, doi:10.1127/0372-8854/2012/S-00085.
- Johst, M., 2010. Experimentelle und modellgestützte Untersuchungen zur Hochwasserentstehung im Nordpfälzer Bergland unter Verwendung eines neuartigen Spatial-TDR-Bodenfeuchtemessgeräts. Dissertation, Universität Trier, Trier, <http://ubt.opus.hbz-nrw.de/volltexte/2011/651/>.
- Juilleret, J., Iffly, J.F., Hoffmann, L., Hissler, C., 2012. The potential of soil survey as a tool for surface geological mapping: a case study in a hydrological experimental catchment (Huewelerbach, Grand-Duchy of Luxembourg). *Geologica Belgica* 15(1-2), 36–41, <http://popups.ulg.ac.be/Geol/document.php?id=3496>.
- Kretzschmar, R., 1992. Handbuch des Bodenschutzes. Bodenökologie und -belastung - Vorbeugende und abwehrende Schutzmaßnahmen, in: Blume H.-P. (Ed.), ecomed, Landsberg/Lech, S. 182–200, 2. Auflage.
- MacDonald, L.H., Coe, D.B.R., 2008. Road Sediment Production and Delivery: Processes and Management, Proceedings of the First World Landslide Forum, International Consortium on Landslides, Tokyo, Japan, S. 385–388. [online] Available from: <http://ucanr.org/sites/forestry/files/138028.pdf> (Zugegriffen 23 April 2013)
- MacDonald, L.H., Sampson, R.W., Anderson, D.M., 2001. Runoff and road erosion at the plot and road segment scales, St John, US Virgin Islands. *Earth Surface Processes and Landforms*, 26(3), 251–272, doi:10.1002/1096-9837(200103)26:3<251::AID-ESP173>3.0.CO;2-X.
- Morgan, R.P., 1986. Soil Erosion and Conservation. Rev. and enl. ed. of Soil erosion, publ. 1979., Davidson D.A. (Ed.), Longman, Harlow.
- Morley, C. P., Mainwaring, K. A., Doerr, S. H., Douglas, P., Llewellyn, C. T., Dekker, L. W., 2005. Organic compounds at different depths in a sandy soil and their role in water repellency. *Australian Journal of Soil Research*, 43(3), 239–249, doi:10.1071/SR04094.
- Neris, J., Tejedor, M., Rodríguez, M., Fuentes, J., Jiménez, C., 2012. Effect of forest floor characteristics on water repellency, infiltration, runoff and soil loss in Andisols of Tenerife (Canary Islands, Spain). *Catena*, doi:10.1016/j.catena.2012.04.011. [online] Available from: <http://www.sciencedirect.com/science/article/pii/S0341816212000951> (Zugegriffen 21 November 2012)
- Orfánus, T., Bedrna, Z., Lichner, L., Hallett, P. D., Knava, K., Sebín, M., 2008. Spatial variability of water repellency in pine forest soil. *Soil and Water Research*, (3), 123–129.

- Pfister, L., Wagner, C., Vansuyepene, E., Drogue, G., Hoffmann, L. (Eds.), 2005. *Atlas climatique du Grand-Duché de Luxembourg*. Johnen-Druck GmbH & Co, Bernkastel-Kues.
- Ramos-Scharrón, C. E., MacDonald, L. H., 2007. Runoff and suspended sediment yields from an unpaved road segment, St John, US Virgin Islands. *Hydrological Processes*, 21(1), 35–50, doi:10.1002/hyp.6175.
- Ries, J.B., Iserloh, T., Seeger, M., Gabriels, D., 2013. Rainfall simulations constraints, needs and challenges for a future use in soil erosion research. *Zeitschrift für Geomorphologie, Supplementary Issues*, 57(1), 1–10, doi:10.1127/0372-8854/2013/S-00130.
- Ries, J.B., Langer, M., Rehberg, C., 2000. Experimental investigations on water and wind erosion on abandoned fields and arable land in the central Ebro Basin. *Z. Geomorphol., Suppl.-Bd. 121*, 91–108.
- Ries, J.B., Seeger, M., Iserloh, T., Wistorf, S., Fister, W., 2009. Calibration of simulated rainfall characteristics for the study of soil erosion on agricultural land. *Soil and Tillage Research*, 106(1), 109–116, doi:10.1016/j.still.2009.07.005.
- Robichaud, P.R., Foltz, R.B., Luce, C.H., 1993. Development of an on site sediment prediction model for forest roads and timber harvest areas. *Sediment Problems: Strategies for Monitoring, Prediction and Control*, S. 135–140.
- Robichaud, P.R., Wagenbrenner, J.W., Brown, R.E., 2010. Rill erosion in natural and disturbed forests: 1. Measurements. *Water Resources Research*, 46(10), 14, doi:10.1029/2009WR008314.
- Roth, C.H., 1996. Physikalische Ursachen der Wassererosion., in: Blume H.P., Frede G.H., Fischer W., Felix-Henningsen P., Horn R., Stahr K. (Eds.), *Handbuch der Bodenkunde*, Ecomed, Taunusstein, S. 1–34.
- Shakesby, R.A., Chafer, C.J., Doerr, S.H., Blake, W.H., Wallbrink, P., Humphreys, G.S., Harrington, B.A., 2003. Fire Severity, Water Repellency Characteristics and Hydrogeomorphological Changes Following the Christmas 2001 Sydney Forest Fires. *Australian Geographer*, 34(2), 147, doi:10.1080/00049180301736.
- Solomon, S., Qin, D., Manning, M., Chen, Z., Marquis, M., Averyt, K.B., Tignor, M., Miller, H. L. (Eds.), 2007. *Climate Change 2007: The Physical Science Basis - Contribution of Working Group I to the Fourth Assessment Report of the Intergovernmental Panel on Climate Change*. Cambridge University Press, Cambridge, UK and New York, USA. [online] Available from: http://www.ipcc.ch/publications_and_data/publications_ipcc_fourth_assessment_report_wg1_report_the_physical_science_basis.htm
- SPSS Inc., 2008. *SPSS Statistics Base 17.0 User's Guide*, SPSS Inc., Chicago, IL. [online] Available from: <http://www.hks.harvard.edu/fs/pnorris/Classes/A%20SPSS%20Manuals/SPSS%20Statistics%20Base%20User%27s%20Guide%2017.0.pdf> (Zugegriffen 13 November 2012)
- Untersteiner, H., 2007. *Statistik - Datenauswertung mit Excel und SPSS*, 2. Auflage., facultas.wuv, Wien. [online] Available from: <http://www.utb-shop.de/autoren/untersteiner-hubert/statistik-datenauswertung-mit-excel-und-spss.html> (Zugegriffen 13 November 2012)
- Wagenbrenner, J.W., Robichaud, P.R., Elliot, W.J., 2010. Rill erosion in natural and disturbed forests: 2. Modeling Approaches. *Water Resources Research*, 46(10), 14, doi:10.1029/2009WR008315.

- Wahl, N., Bens, O., Schäfer, B., Hüttl, R., 2003. Impact of changes in land-use management on soil hydraulic properties: hydraulic conductivity, water repellency and water retention. *Physics and Chemistry of the Earth, Parts A/B/C*, 28(33-36), 1377–1387.
- Wahl, N.A., Wöllecke, B., Bens, O., Hüttl, R.F., 2005. Can forest transformation help reducing floods in forested watersheds? Certain aspects on soil hydraulics and organic matter properties. *Physics and Chemistry of the Earth, Parts A/B/C*, 30(8–10), 611–621, doi:10.1016/j.pce.2005.07.013.
- Wessolek, G., Schwärzel, K., Greiffenhagen, A., Stoffregen, H., 2008. Percolation characteristics of a water-repellent sandy forest soil. *European Journal of Soil Science*, 59(1), 14–23, doi:10.1111/j.1365-2389.2007.00980.x.
- Zavala, L.M., Granged, A.J.P., Jordán, A., Bárcenas-Moreno, G., 2010. Effect of burning temperature on water repellency and aggregate stability in forest soils under laboratory conditions. *Geoderma*, 158(3-4), 366–374, doi:10.1016/j.geoderma.2010.06.004.
- Zehe, E., Elsenbeer, H., Lindenmaier, F., Schulz, K., Blöschl, G., 2007. Patterns of predictability in hydrological threshold systems. *Water Resources Research*, 43(7), doi:10.1029/2006WR005589. [online] Available from: <http://europa.agu.org.ezproxy.library.wur.nl/?view=article&uri=/journals/wr/wr0707/2006WR005589/2006WR005589.xml&t=wr,2007,zehe> (Zugegriffen 12 Mai 2011)
- Zehe, E., Sivapalan, M., 2009. Threshold behaviour in hydrological systems as (human) geo-ecosystems: manifestations, controls, implications. *Hydrol. Earth Syst. Sci.*, 13(7), 1273–1297.

Butzen et al. (re-submitted in March 2015):
Water repellency under coniferous and
deciduous forest - Experimental assessment and
impact on overland flow. Catena

Water repellency under coniferous and deciduous forest – Experimental assessment and impact on overland flow

Verena Butzen^a, Manuel Seeger^a, Amaia Marruedo^b, Lianne de Jonge^b, René Wengel^a, Johannes B. Ries^a & Markus C. Casper^a

^aDept. of Physical Geography, FB VI Geography/Geosciences, Trier University (D)

^bDept. of Soil Physics and Land Management, Wageningen University & Research Center (NL)

Corresponding Author:

Verena Butzen

Universität Trier

Behringstraße

54296 Trier, Germany

Tel.: +49-651-201-4522

Fax.: +49-651-201-3976

e-Mail: verena.butzen@gmx.de

Abstract

Particularly concerning the current climate change, a deeper understanding of the runoff generation processes in Central European forests is necessary. Soil water repellency (SWR) can severely influence overland flow generation in forested areas. In this study the differences between coniferous and deciduous forest concerning SWR and overland flow generation were investigated in a small catchment in the Hunsrück low mountain range, Rhineland-Palatinate, Germany.

A combination of experimental methods was applied to investigate both, occurrence and persistence of SWR and also its influence on overland flow generation. The field water drop penetration time (WDPT) test results ranged from wettable ($WDPT < 5$ s) up to more than 900 seconds persistence of water repellency in both forest types. The median WDPT was 30 seconds for the coniferous forest and 1 second for the deciduous forest sites. On the deciduous forest soils, only the O_H-horizon showed considerable water repellency. The runoff coefficients of the rainfall experiments ranged from 0 % to 63 %, thus the lowest measured infiltration rate of the rainfall experiments was only 11.58 mm h^{-1} . The highest runoff coefficients were measured on water repellent ($WDPT > 300$ s) coniferous forest sites. The overland flow starts significantly earlier with water repellent soil conditions. The median runoff rate for the wettable forest soils is 2.7 %, whereas the water repellent sites show a median runoff coefficient of 11.4 %.

According to the results presented here, the occurrence of SWR can lead to considerable overland flow generation under forest.

Keywords:

Soil water repellency; WDPT; overland flow; forest

1 Introduction

Temperate humid forests are often regarded as water retention areas rather than sources for overland flow (Hümann et al., 2011; Wahren et al., 2012). Compacted areas like harvester tracks or forest roads are an exception, here very high overland flow rates can be measured (Arnáez et al., 2004; Butzen et al., 2014; Eastaugh et al., 2008; Robichaud et al., 2010; Wagenbrenner et al., 2010). Nevertheless, there is another important factor influencing overland flow generation processes in forests: the occurrence of soil water repellency (SWR) (Bens et al., 2007; Buczko et al., 2007; Doerr et al., 2000; Hartmann et al., 2009; Lichner et al. 2013; Neris et al., 2012; Wahl et al., 2005; Wessolek et al., 2008). All these studies are located in Central Europe and emphasize that SWR is an important factor influencing the infiltration process even under a humid temperate climate.

According to Wessolek (2008) the processes of water repellency in the different organic layers of forest soils has not been investigated properly yet because most of the studies were focussed on the influence of fire (Arcenegui et al., 2007; Bodí et al., 2012; Cerdà and Doerr, 2008; Shakesby, 2011; Zavala et al., 2009) or on the water repellency of mineral soil horizons (Doerr et al., 2006; Woche et al., 2005). In the context of water repellency occurring after forest fires in the Mediterranean, there are some experimental field studies showing that SWR can intensify overland flow generation (Cerdà and Doerr, 2008; Imeson et al., 1992; León et al., 2013; Malvar et al., 2013). The influence of SWR on overland flow generation was investigated for example by Gomi et al. (2008) and Miyata et al. (2009) on test plots under Cypress forest in Japan. Overland flow was measured on all plots even for storms of lower intensity (<10mm total precipitation) (Gomi et al., 2008). Nevertheless, there is still a lack of experimental data and studies on the quantification of the impact of water repellency on overland flow generation for Central Europe. The presented paper offers experimental data from field rainfall simulations in order to close this gap.

According to Doerr et al. (2000) a surface shows hydrophobic behavior, if the surface tension of a water droplet (cohesion) is higher than the adhesive forces of the surface. Organic polymers or waxes can have lower forces of attraction. This leads to hydrophobic properties of a surface. The hydrophobic substances can be provided by living or dead plant material in different decomposition states or by fungi or micro-organisms in organic layers and mineral soil (Chau et al., 2012; Doerr et al., 2000; Morley et al., 2005; Atanassova and Doerr,

2010, 2011). Water repellency can also be a consequence of forest fires (Arcenegui et al., 2007; Bodí et al., 2012; Cerdà et al., 2008; Robichaud and Hungerford, 2000; Rodríguez-Alleres et al., 2012; Shakesby et al., 2003; Zavala et al., 2009, 2010; Zehe et al., 2007).

Another important factor influencing SWR is soil moisture. Soil water repellency typically shows temporal variations, which are strongly related to the seasons (Buczko et al., 2007). During dry periods in the summer months, the soils are most frequently affected by SWR influence (De Jonge, 1999; Orfánus, 2014; Zehe, 2007). Doerr et al. (2000) state that a hydrophobic soil becomes hydrophilic again, if a critical water content is exceeded. According to Dekker and Ritsema (1994) and Zehe and Sivapalan (2009) SWR can be regarded as a threshold process, that can occur if the soil moisture drops below a certain value and if certain organic compounds are present (Atanassova and Doerr, 2010; Morley et al., 2005; Neris et al., 2012). In the last 20 years, important advances in the field of water repellency research were achieved, particularly concerning the mechanisms that control occurrence and severity of water repellency effects (Doerr et al., 2000, 2009). In the last decade several studies on soil hydrophobicity in European temperate forests have been published (Bens et al., 2007; Buczko et al., 2005, 2006; Doerr et al., 2006; Greiffenhagen et al., 2006; Orfánus et al., 2014; Wahl et al., 2003). The investigated sites were situated in Southern UK (Doerr et al., 2006), South-western Slovakia (Orfánus et al., 2008, 2014), Eastern Germany (Wessolek et al., 2008) and North-eastern Germany (Bens et al., 2007; Buczko et al., 2005, 2007; Hartmann et al., 2009; Wahl et al., 2003). In the course of Climate Change, we expect that dry periods in late spring and summer will become more frequent, this could lead to an increased influence of water repellency effects also in Central European forests (IPCC 2007, 2013) particularly in conjunction with heavy summer rainstorm events. In 2010, 30.1 % of the total area in Germany and even 42 % of the total area in Rhineland-Palatinate was forested (German Federal Office of Statistics, 2012). Regarding this high proportion of forests, the importance of the forests as possible sources for overland flow becomes clear. Forests have a protective function, they can diminish flood peaks because the forest soils can absorb much of water and release the infiltrated water with a long delay (Hausler and Scherer-Lorenzen, 2001). Spatial and temporal distribution of overland flow generation and were investigated in a small catchment. The study area Holzbach is situated in the Hunsrück low mountain range, Rhineland-Palatinate, Germany.

The presented work aims at answering the following research questions: i: to what extent is water repellency present in the study area (Central European temperate forest)?; ii: are there differences between coniferous and deciduous forests?; iii: Which humus and mineral soil

horizons are the most water repellent ones?; and iv: how does water repellency influence overland flow generation in forests? v: does soil moisture influence water repellency?

2 Study Area

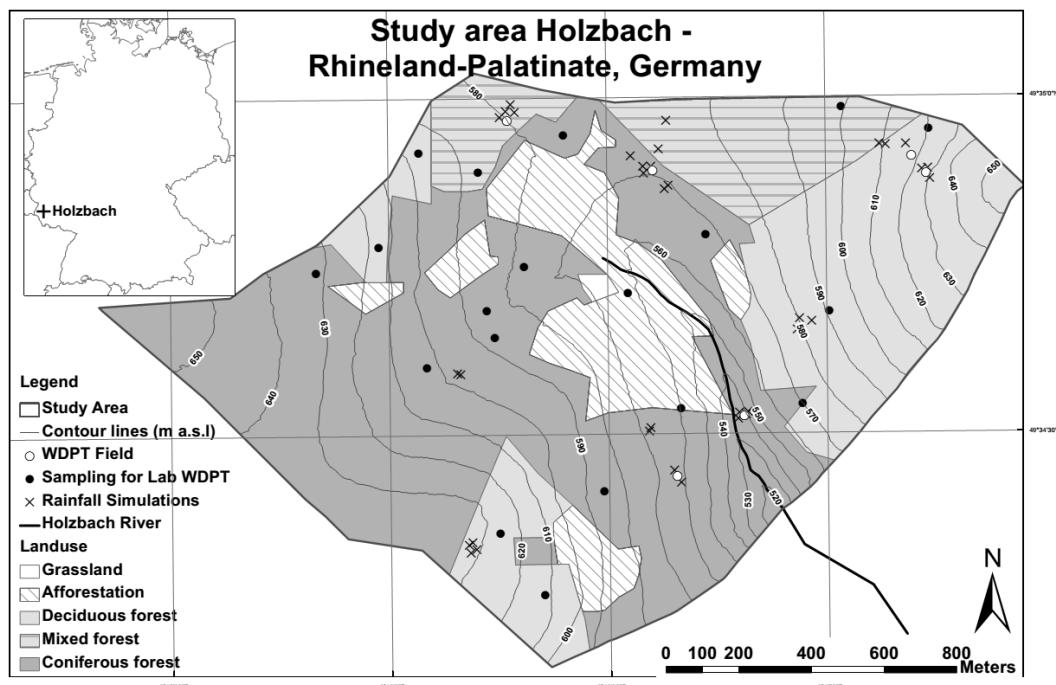


Fig. 1: Map of the study area Holzbach with the locations of WDPT-field-sampling sites (white dots), the sample sites for the laboratory measurements of WDPT (black dots), and the sites of the rainfall experiments (black crosses).

The study area Holzbach (Fig. 1) covers an area of 2.3 km² and is situated in the Hunsrück low mountain range in Germany. At the climate station "Weiskirchen/Saar" (N 49° 33' 02" E 6° 49' 03") situated at the gauge of the Holzbach River, the mean annual rainfall amount is about 1186 mm, and the mean temperature is 9.4 °C (German Meteorological Service, 2012: climate data from the 1st of January 1982 to the 31st of December 2011). The Holzbach area belongs to the south-western part of the Rhenish Slate Mountains. The bedrock is a quartzite belonging to the lower Devonian and the soils are mainly acidic Cambisols, Podzols and stagnic Cambisols with soil textures ranging from sand to sandy loam (Ad-hoc-Arbeitsgruppe Boden, 1996). The study area is almost completely covered by forest, 25.4 % of the area is deciduous forest (mainly *Fagus sylvatica*), 50.2 % is coniferous forest (mainly *Picea abies*), 10.5 % is mixed forest (e.g. *Picea abies* and *Fagus sylvatica*), 13.7 % is a 10-15-year-old afforestation area and 0.2 % is covered by grassland.

Within the study area, drained wetland was equipped with small dams to cut the artificial runoff paths in order to rewet peat areas. These land-management measures were carried out in the course of the EU-INTERREG IIIB NWE Project WaReLa (Water Retention by Land-Use) in order to enhance water retention (Gallus et al., 2007, Segatz et al., 2009).

3 Material and Methods

3.1 Sampling strategy

Table 1: Field sampling dates and number of field and lab samples for rainfall experiments and WDPT-tests

Field Trip	Field sampling dates	Rainfall Exp. Coniferous Forest	Rainfall Exp. Deciduous Forest	WDPT Coniferous Forest	WDPT Deciduous Forest
1	10.08.-15.08.2009	7	6	7	6
2	28.06.-30.06.2010	-	-	1475 (Lab)	841 (Lab)
3	12.07.-23.08.2011	14	8	273	170

The data presented in this paper were gathered in the study area Holzbach between 2009 and 2011. Table 1 gives an overview of the field sampling dates and the number of samples. In the 2009 campaign, field rainfall simulation experiments and WDPT measurements were carried out. In summer 2010, samples of the humus and top soil horizons were collected at 19 sites spread all over the study area. The sample sites were chosen with the intention to be representative for a typical land-use in the study area, this is mainly spruce forest and beech forest. These two forest types are compared concerning the persistence of water repellency (WDPT-tests) and overland flow generation (rainfall experiments).

A third field campaign was accomplished in summer 2011 with further WDPT measurements and rainfall experiments with the focus on the investigation of the differences between forest types and on the temporal changes in water repellency in the summer months.

3.2 Characterization of the topsoil

The topsoil was characterized according to the soil mapping guide published by the German Federal Institute for Geosciences and Natural Resources (Ad-Hoc-Arbeitsgruppe Boden, 2005). According to this soil mapping guide, the humus horizons (L, Of, Oh) were distinguished as well as the uppermost mineral soil horizon (Ah). The volumetric moisture

content (VMC) of the soil samples was measured in the lab by weighing the field moist 100 cm³ soil cylinders and subtracting the dry weight.

3.3 Water repellency assessment

In this study, the water drop penetration time (WDPT) measurement method was used in the field and in the laboratory, for the determination of the occurrence and persistence of water repellency (Doerr, 1998; Doerr et al., 2000; Zehe et al., 2007; Zehe and Sivapalan, 2009). The different WDPT-sampling settings are described in the following sections.

3.3.1 Field measurements of water repellency by water drop penetration time (WDPT)

The water drop penetration time (WDPT) was measured according to Doerr (1998, 2006). The soil surface was prepared by carefully exposing small spots of the different humus horizons (L, Of, Oh) and the uppermost mineral soil horizon (Ah). Three drops of water (vol. 50-60 µL) were placed on the surface of the Ah, L, Of, and Oh horizons by means of a glass-pipette. For the field WDPT measurements the infiltration time of each drop was recorded for up to 900 seconds and the drop tests were performed on all four horizons of the topsoil (L, Of, Oh, Ah) separately. At seven different sites in the Holzbach area, altogether 38 WDPT measurements were carried out next to the rainfall experiments between July and August 2011. For each of the 38 tests, three drops were placed on each of the humus horizons (L, Of, Oh and Ah). So, altogether 456 measurements of WDPT were performed at the seven sites (rainfall experiments). For measurements carried out at the sites of rainfall experiments (summers 2009 and 2011), the WDPT was only timed for up to 300 seconds and considered only for the mineral soil (Ah). If the drop was still present afterwards, 300 seconds were recorded as the WDPT.

3.3.2 Laboratory measurement of WDPT

A series of laboratory WDPT measurements were carried out on undisturbed soil samples from the Holzbach study area. The soil samples were taken on the 28th-30th of June 2010 at 19 different sites in the study area, at each site three parallel samples were taken for comparison. Each approx. 10 x 10 x 10 cm soil block was carefully taken with a folding spade, and divided into the upper and the lower part of approx. 5 cm thickness. Usually the upper part includes L, Of, and partially Oh, and the lower part consisted of Oh and Ah horizons. The rather undisturbed soil samples were placed in rectangular aluminium cups of

about 10 x 12 cm size and 4 cm height. For each tested sample the respective classified mineral soil or organic horizon was recorded.

The lab-WDPT measurements were carried out in an acclimatized laboratory with a constant air temperature of 20°C, here the samples were also stored covered with aluminium foil. The soil moisture was determined gravimetrically directly before each WDPT test. In this way a drying time series of the WDPT was generated in relation to the declining soil moisture. Altogether 731 WDPT measurements were executed in the lab. In the lab WDPT tests the water drops (vol. 50-60 µL) were also formed using a glass-pipette of a standard amber glass bottle and then placed on the surface of the soil/humus samples. The lab-tests were carried on for up to 5 hours, if the drops were still present afterwards, a WDPT of 5 hours (18000s) was recorded. The soil samples were dried out starting at field soil moisture, the WDPT was measured repeatedly every two or three days for a period up to 16 days until no changes in soil moisture content were recorded anymore.

3.4 Assessment of runoff generation

To assess runoff generation processes at the plot scale, rainfall simulations were conducted (see also Butzen et al. (2014, 2011)). The used small rainfall simulator (Fig. 2) was described in detail by Ries et al. (2000) and Iserloh et al. (2010, 2012). A rainfall intensity of 40 mm h⁻¹ was applied for 60 minutes on a circular bounded plot of 0.28 m² (Ries et al., 2000). Runoff was collected with plastic bottles, filled continuously in intervals of 5 minutes length. Vegetation cover, slope and water repellency of the plot area were noted before each experiment. An inclinometer (Suunto PM5) was used for the measurement of slope in flow direction. The antecedent soil moisture and the amount of runoff were measured gravimetrically.

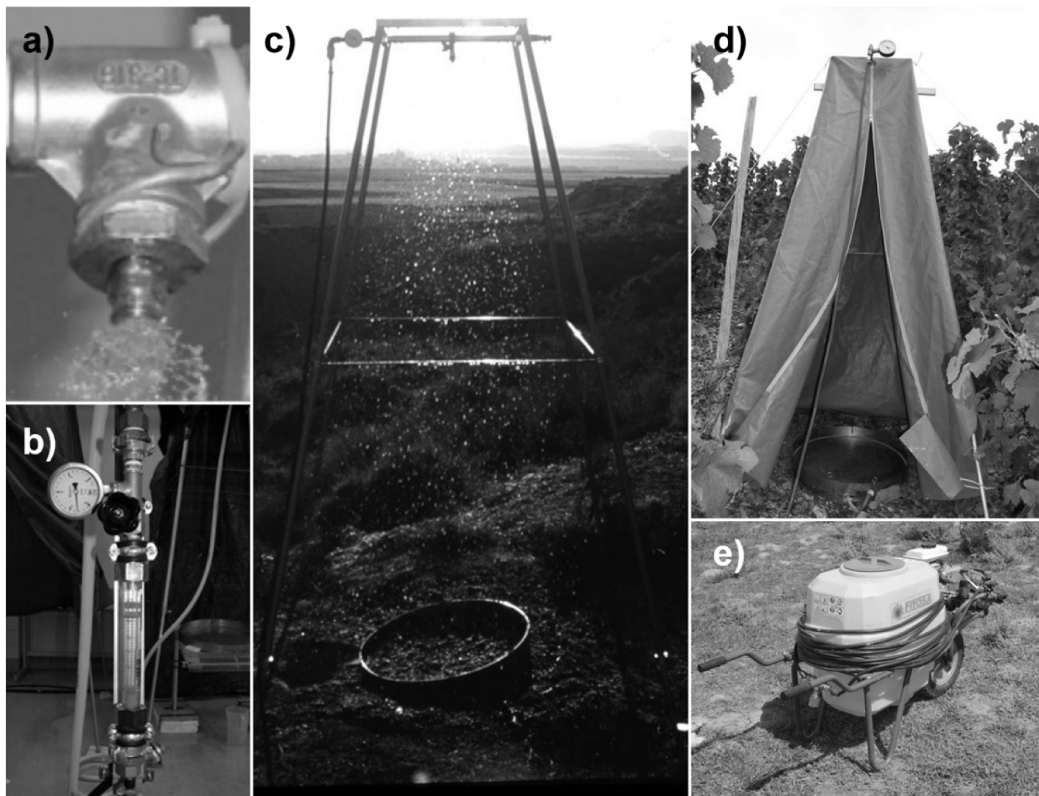


Fig. 2: Small portable rainfall simulator.

- a) Full cone nozzle (Lechler 460.608)
- b) Flow meter for adjustment of discharge
- c) Aluminum linkage (height: 2 m) with test plot bounded by a steel ring, diameter: 60 cm
- d) Frame covered by rubber tarpaulin
- e) Motor driven pump with 100 l water tank

For the rainfall simulation experiments a full cone nozzle (Lechler 460.608) was used and fixed in a height of 2 m above the plot. For a more detailed description of the rainfall simulator and the adaptation in the field please refer to Ries et al. (2000, 2009) and Fister et al. (2011).

The sites of the rainfall simulation experiments were located both, under deciduous forest (mainly beech) and under coniferous forest (mainly spruce) in order to enable a comparison of the influence of water repellency on overland flow generation in the two different forest types. The rainfall experiments on ‘mixed forest’ were carried out on plot sites with either spruce or beech trees around, so they could explicitly be allocated to one of the two forest types. The sites are marked by black crosses (Fig. 1).

4 Results

4.1 Water repellency field measurements at Holzbach

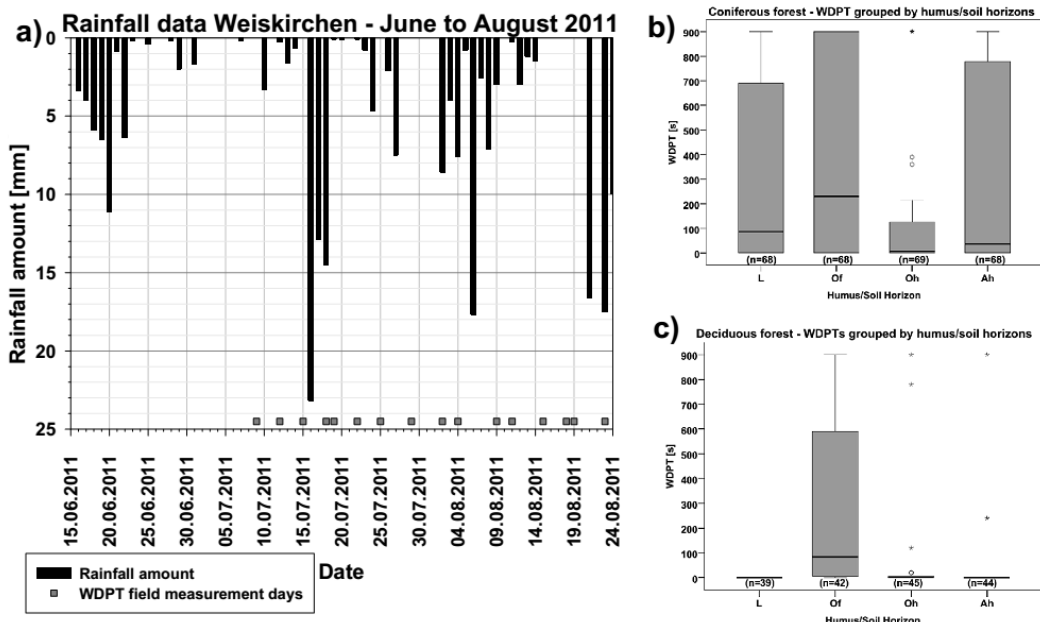


Fig. 3a: Rainfall Data for the climate station Weiskirchen for the sampling period of the field WDPT-tests in July and August 2011. The measuring days are marked by the grey squares. Fig. 3b and c: Boxplots of the WDPT-field-measurements grouped by the humus/soil horizons for b) the coniferous, and c) the deciduous forest sites. Under each box-plot the number of measurements is given (e.g. n=68).

During the WDPT field measurement period, different soil moisture states were in place, as the rainfall time series suggests (Fig. 3a). The measurement days of the field WDPT measurements are marked by the grey squares. The data set of the WDPT-field measurements was split into two groups, the coniferous forest data and the deciduous forest data. The WDPT under deciduous forest was generally much lower than under coniferous forest (Tab. 2). Within deciduous forest most of the data only ranged between 0 and 20 s WDPT, whereas under coniferous forest, often the maximum value of 900 s was reached.

Table 2: Descriptive statistics of the WDPT field measurements WDPT grouped by forest type

	WDPT- coniferous forest [s]	WDPT- deciduous forest [s]
Mean	290	92
Median	30	1
Std. Dev.	383	242
Std. Err.	23	18
Size	274	171
Total	79325	15809
Minimum	0	0
Maximum	900	900

In order to detect possible differences between the humus horizons, the WDPT-values measured at the coniferous forest sites were grouped by horizons (Fig. 3b). For the Of-horizon, the widest range of values (0-900 s) and the highest median (230 s) were measured, followed by the L-horizon with a median of 87 s (both moderate water repellency according to Doerr et al. (2006)). The median WDPT-values of Oh and Ah (mineral soil) were equally low with 8 s and 10 s, respectively. This was evaluated as slight water repellency.

The WDPT- values measured at the deciduous forest test sites showed the Of-horizon being again by far the most intensely water repellent horizon (Fig. 3c), but a median of 84.5 s (moderate water repellency) is still much lower than the one measured on the Of-horizon at the coniferous forest sites (230 s). For deciduous forest, no water repellency could be detected in the L-layer. The median WDPT for the Oh layer was 2 s and for the mineral soil Ah the median WDPT is 0 s. Both were classified as wettable.

Altogether, the presented data (Fig. 3b) and Fig. 3c)) clearly showed higher WDPT values under coniferous forest than under deciduous forest for all horizon groups. The Of-horizon generally exhibited the highest WDPT in both, the coniferous and the deciduous forest sites.

Table 3: Spearmans-Rho Correlation Coefficients for the WDPT-field time series data

Korrelationen Spearman-Rho n=114		WDPT L	WDPT Of	WDPT Oh	WDPT Ah	VMC humus	VMC mineral	Rainfall 1d	Rainfall 3d	Rainfall 7d
WDPT L	1.000									
WDPT Of	.238*	1.000								
WDPT Oh	.506**	.244*	1.000							
WDPT Ah	.457**	.433**	.510**	1.000						
VMC humus	-.267**	-.431**	-.459**	-.481**	1.000					
VMC mineral	-.238*	-.245*	-.264**	-.516**	.596**	1.000				
Rainfall 24h	-.421**	-.200*	-.494**	-.172	.077	-.253**	1.000			
Rainfall 3d	-.358**	-.301**	-.572**	-.285**	.234*	.061	.838**	1.000		
Rainfall 7d	-.473**	-.405**	-.571**	-.360**	.290**	.297**	.579**	.759**	1.000	

(WDPT: water drop penetration time [seconds], L: uppermost humus horizon, Of: second humus horizon, Oh: third (lowest) humus horizon, VMC humus: volumetric moisture content of the humus horizons [part], VMC mineral: volumetric moisture content of the upper mineral soil horizon [part], rainfall 1d, 3d, 7d: rainfall sum of 1 day, 3 days, 7 days before the soil sampling [mm])

The complete set of the WDPT-field measurements (n=114) showed significant correlations of WDPT (all horizons) with the volumetric moisture contents of both, humus and mineral soil (see table 3). In addition to the volumetric moisture content, also the antecedent rainfall 24 hours, 3 and 7 days before the measuring day was tested for correlation with WDPT. The Spearman's-Rho correlation coefficients indicated that the antecedent rainfall of 3 and 7 days before measurement showed a high correlation with WDPT for all soil/humus horizons. Hence, the rainfall in the preceding days clearly determined the severity of water repellency. In some cases the Spearman's-Rho correlation coefficients between antecedent rainfall and WDPT were even higher than for the volumetric moisture contents of mineral soil and humus, particular for the L and Oh horizons (see Tab. 3).

Table 4: Spearmans-Rho Correlation Coefficients divided into Coniferous and Deciduous forest sites - WDPT-field time series data

Coniferous forest		Korrelationen Spearmans-Rho n=69								
		WDPT L	WDPT Of	WDPT Oh	WDPT Ah	VMC humus	VMC mineral	Rainfall 1d	Rainfall 3d	Rainfall 7d
WDPTL		1.000								
WDPTOf		.306*	1.000							
WDPTOh		.546**	.360**	1.000						
WDPTAh		.279*	.531**	.466**	1.000					
VMChumus		-.212	-.425**	-.535**	-.368**	1.000				
VMCmineral		.028	-.285*	-.057	-.428**	.545**	1.000			
Rainfall24h		-.576**	-.120	-.555**	-.131	-.028	-.326**	1.000		
Rainfall3d		-.603**	-.243*	-.617**	-.314**	.207	-.003	.897**	1.000	
Rainfall7d		-.553**	-.387**	-.670**	-.379**	.271*	.186	.678**	.886**	1.000
Deciduous Forest		Korrelationen Spearmans-Rho n=45								
WDPTOf		1.000								
WDPTOh		-.164	1.000							
WDPTAh		.351*	.452**	1.000						
VMChumus		-.636**	-.047	-.484**	1.000					
VMCmineral		-.081	-.464**	-.282	.445**	1.000				
Rainfall24h		-.409**	-.349*	-.508**	.211	-.203	1.000			
Rainfall3d		-.387*	-.496**	-.569**	.225	.151	.726**	1.000		
Rainfall7d		-.430**	-.286	-.273	.131	.354*	.427**	.511**	1.000	

(WDPT: water drop penetration time [seconds], L: uppermost humus horizon, Of: second humus horizon, Oh: third (lowest) humus horizon, VMC humus: volumetric moisture content of the humus horizons [part], VMC mineral: volumetric moisture content of the upper mineral soil horizon [part], rainfall 1d, 3d, 7d: rainfall sum of 1 day, 3 days, 7 days before the soil sampling [mm])

The WDPT-field measurements under coniferous forest (Tab. 4: top) showed significant correlations of volumetric moisture contents of the humus layers (VMChumus) with the WDPT measured on the Of-, Oh-, and Ah-horizons. The WDPT of the L-horizon showed high correlations with the antecedent rainfall sums of the last 24 h, 3 days, and 7 days before the measurement day. For the Oh-horizon, the WDPT-results showed a high correlation with all rainfall indices. The WDPT of the Of-horizon correlated with the 3-days and the 7-days rainfall sums (see Tab. 4).

The WDPT-field measurements under deciduous forest (Tab. 4: bottom) correlated significantly with the volumetric moisture contents of the humus layers (VMChumus) for the Of-, and Ah-horizons. The WDPT measured on the Of-horizon showed high correlations with all three antecedent rainfall sums. For the Oh-horizon, the WDPT showed a significant correlation with the 24 hours and the 3 days rainfall sum. The negative correlations between antecedent rainfall and WDPT in the humus horizons means that low rainfall amounts during

24 h, 3 days, and 7 days before WDPT-measurement lead to significantly higher WDPT values within the humus horizons.

Accordingly, the results of the measured field-WDPT showed high correlations with the volumetric moisture contents of soil and humus and to the pre-test rainfall amounts. Particularly regarding the WDPT measured in the L- and Oh-horizons, the pre-test rainfall amounts showed higher correlations than the moisture contents of humus and mineral soil (see Tab. 3).

4.2 Laboratory measurements of WDPT on soil samples from Holzbach

In June 2010 the soil samples for the laboratory WDPT measurements were collected under dry soil moisture conditions, since the last 18 days before the field sampling only showed 3 mm antecedent rainfall. The humus and soil samples from the beech and spruce forests were tested under field-moist conditions (see also tab. 5).

Table 5: Laboratory measurements of WDPT on field-moist samples grouped by forest type - descriptive statistics

	WDPT- Coniferous forest [s]	WDPT-Deciduous forest [s]
Mean	2311.6	998.9
Median	260	479.5
Std. Dev.	5494.8	1405.2
Size	53	42
Minimum	0	1
Maximum	18010	6849

Field sampling was carried out between June the 28th and June the 30th in 2010.
(WDPT: water drop penetration time)

The descriptive statistics of the WDPT-test results on the field-moist soil samples in the laboratory showed a wide range in WDPT values (tab. 5) for both coniferous and deciduous forest sites. The WDPT-data set was grouped by the two studied forest types. The initial lab measurements represented the WDPT at field soil moisture, whereas the last WDPT measurements represented the WDPT of completely dry soils. The initial lab measurements of summer 2010 (field soil moisture) showed much higher WDPT as the field WDPT measurements of summer 2011, because in summer 2010 the soil moisture was much lower and there was no rain in the 20 days before the field sampling.

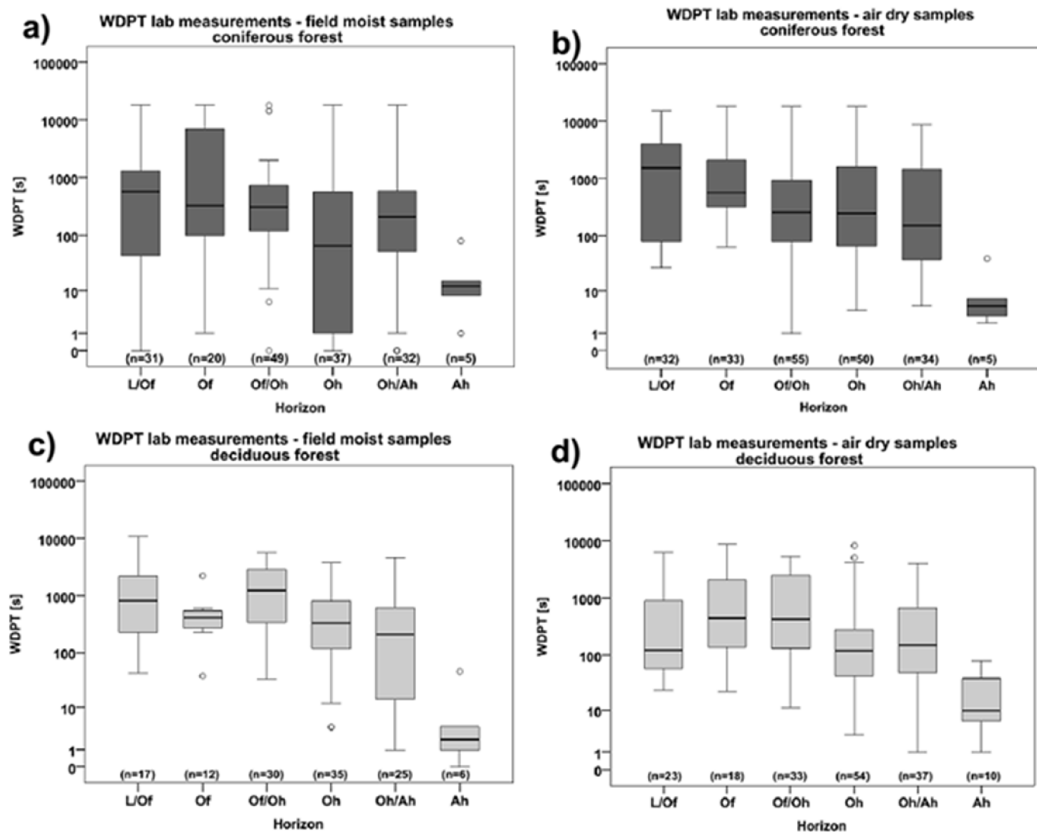


Fig. 4a) and c): Boxplots of the first laboratory WDPT-measurements grouped by the humus/soil horizons (from top to bottom) for a) the coniferous forest sites, and c) the deciduous forest sites. Fig. 4b) and d): Boxplots of the last laboratory WDPT-measurements grouped by the humus/soil horizons (from top to bottom) b) for the coniferous forest sites, and d) for the deciduous forest sites. Under each box-plot the number of measurements is given (e.g. n=31). (WDPT: water drop penetration time [seconds], L: uppermost humus horizon, Of: second humus horizon, Oh: third (lowest) humus horizon, Ah: uppermost mineral soil horizon).

Figure 4 shows box-plots of the WDPT of the initial and the last lab measurement grouped by the sampled humus and soil horizons. The data set was also split into coniferous forest (4a and 4b) and deciduous forest sites (4c and 4d). The field moist soil samples from the coniferous forest sites (fig. 4a) showed a very wide range of values from 0 s to 18,000 s (5h) WDPT for all horizons, except for the Ah-horizon.

The field moist deciduous forest samples (Fig. 4c) showed a slightly different behaviour: here no horizon showed the highest value of 5h WDPT. The highest WDPT of 10,800 s (3h) was reached in the uppermost horizons which includes L/Of-horizon material. In general, a decrease of the WDPT minimum, maximum and median values with increasing horizon-depth could be observed for the deciduous forest data.

The Boxplots in figure 4b) and 4d) show the results of the WDPT lab-measurement on dry soil for the coniferous forest sites (fig. 4b) and for the deciduous forest sites (fig. 4d).

The results of the coniferous forest sites showed a clear decrease of the median WDPT-values with increasing soil-depth. The maximum WDPT of the upper four horizon groups from L/Of to Oh all reach the highest measured value of 18,000 s WDPT. The two lowest horizon-groups showed WDPT of less than 10,000 s (Oh/Ah) and less than 100 s (Ah).

The WDPT for deciduous forest were generally lower than for the coniferous forest. The maximum value for deciduous forest is 8,706 s WDPT. The minimum and maximum WDPT decreased with horizon-depth, but the highest median WDPT-values were measured in the Of- and Of/Oh-horizon-groups.

The lab data on WDPT showed a very high spatial variability. The soil samples were collected at 19 sites, and on each site, three parallel samples were taken close by. Even the variability of WDPT measured on a single site was very high. We found a high variability from almost no water repellency for wet samples to extremely high WDPT-values for dryer samples.

The results of the laboratory WDPT measurements showed a high influence of the tested humus/soil horizon on the measured WDPT. The samples including parts of the Of-horizon showed by far the highest WDPT, whereas the lower horizons show considerably lower WDPT-values.

4.3 Rainfall Simulation Experiments

In this study altogether 35 rainfall experiments are analysed, 13 of the rainfall experiments were already published in Butzen et al. (2014).

Table 6: Antecedent volumetric moisture content of the rainfall experiments - descriptive statistics

	wettable	water repellent
	VMC [part.]	VMC [part.]
	WDPT [s]	WDPT [s]
Mean	0.252	0.175
Median	0.240	0.165
Std. Dev.	0.077	0.090
Size	12	6
Minimum	0.140	0.080
Maximum	0.400	0.340
Mean	0.7	277.5
Median	0	300
Std. Dev.	1.5	63.6
Size	22	8
Min	0	120
Max	5	300

Field sampling was carried out between July the 9th and August the 23rd in 2011. According to the Mann-Whitney test, the VMC values of the water repellent sites differ significantly from the VMC values measured on the wettable sites.

(VMC: volumetric moisture content, wettable: values of VMC for non-water repellent sites, water repellent: values of VMC for water repellent sites (WDPT > 5s))

Table 6 indicates clearly, that the volumetric moisture content (VMC) at the water repellent sites is lower than at the wettable sites, the difference between the two groups of data is also significant according to the results of the Mann-Whitney test (level of significance always: 0.05). According to table 6, the WDPT values with water repellency ('WR true') ranged from 120 s to 300 s with a mean value of 277 s, whereas the WDPT of the wettable sites ('WR false') ranged between 0 s and 5 s with a mean value of 0.7 s. At the water repellent sites the runoff of the rainfall experiment already started between 85 s and 466 s after the beginning of the experiment, with a median of 230 s. On the wettable sites, the runoff started much later, between 140 s and 3000 s after the beginning, with a median starting time of 843 s.

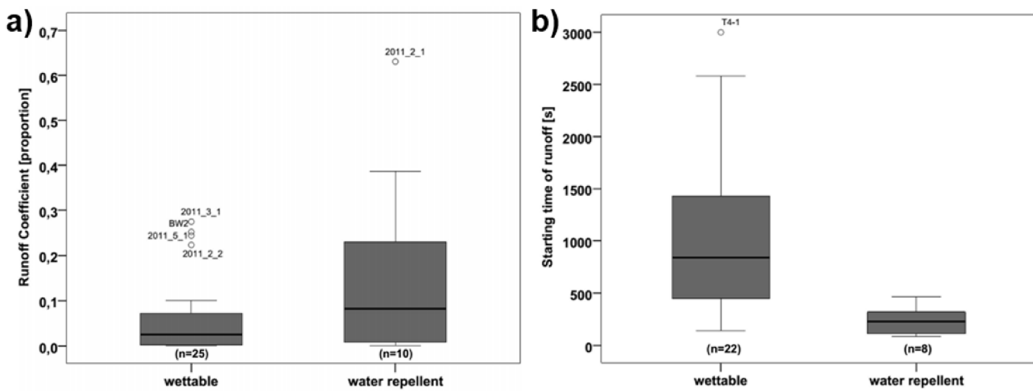


Fig. 5: Boxplots of a) the runoff coefficients (RC), and b) the starting time of overland flow, the rainfall experiments are grouped into wettable and water repellent soil conditions.

Fig. 5 a shows that the measured runoff coefficients of the rainfall simulations were higher under water repellent conditions than under wettable conditions. Nevertheless, according to the Mann-Whitney test, the two groups of runoff coefficient data did not differ significantly from each other.

During the rainfall experiments, the overland flow started much earlier with water repellency influence (true) (median: 230 s) than without water repellency (median: 842 s). Under water repellent conditions, the runoff started after 466 s at the latest, for the wettable sites it could take up to 3000 s (see fig. 5 b). For the starting time of runoff, the Mann-Whitney tests shows, that the groups with wettable soils and the water repellent soils differed significantly from each other.

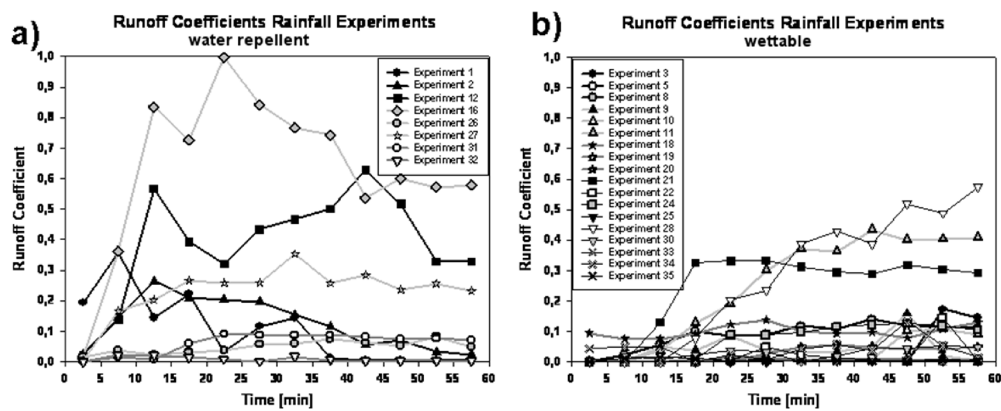


Fig. 6: Development of the runoff coefficients for a) water repellent and b) wettable conditions during the rainfall experiments.

Figure 6 a) shows the development of the runoff coefficients during the rainfall simulations on sites with soil water repellency (SWR). Very high runoff coefficients of up to 97 % (in a five minutes interval) were measured under water repellent conditions. Only three of the eight experiments with SWR stayed below an RC of 10 % and were thus comparable to the experiments without SWR. All rainfall simulations with runoff coefficients higher than 15 % also showed a decrease in runoff coefficients after 10 to 45 minutes, probably due to decreasing water repellency.

In figure 6 b) the courses of the rainfall experiments with wettable soils are shown. Only three of the 18 experiments showed runoff coefficients of larger than 15-20 % after 20 minutes. Usually the runoff coefficients stayed below 15 % without SWR.

The runoff coefficients measured in the rainfall simulation ranged between 0 % and 63.1 % with a median value of 2.8 % for all rainfall simulations. The experiments with wettable soils ranged between 0 % and 27.5 % with a median runoff coefficient of 2.3 %. The experiments with water repellent soils ranged between 0 % and 63.1 % with a median of 11.4 %. Nevertheless, the runoff coefficients of the two groups WR-true and WR-false did not differ significantly according to the Mann-Whitney test (level of significance: 0.05). In contrast to that, the starting time of the runoff of the two groups differed with a very high significance.

5 Discussion

5.1 Influence of VMC, forest type and topsoil horizons on WDPT

During the field work, water repellency of the humus layers and the upper centimetres of the mineral soil were measured. It is important to note that the soils were only water repellent when the soils were not wet. These field measurements correspond to the results of Zehe et al. (2007) as well as Zehe and Sivapalan (2009) who state that water repellency can be regarded as a threshold process, that can occur if the soil moisture drops below a specific value, which relates to the presence of certain organic compounds (Shakesby et al., 2003; Zavala et al., 2010; Zehe et al., 2007). The antecedent volumetric soil moisture content data presented in table 6 show that water repellency can occur in the field under a wide range of soil moisture values, here an antecedent volumetric moisture content of 0.34 is the highest value for a soil with water repellent behaviour. This 0.34 VMC value is a bit higher, but still in the same range as the results of Doerr et al. (2006), who state a threshold value of about 0.28 VMC, above which no water repellency was observed in their study areas in the UK. Additionally, the data in tables 3 and 4 shows significant correlations of volumetric moisture

content (VMC) and antecedent rainfall on SWR. This was also stated by Martínez-Murillo et al. (2013) for study areas in southern Spain. On the other hand, non-water-repellent soils show antecedent VMC starting already at 0.14 (table 4). Accordingly, it is difficult to determine a specific soil moisture threshold value under which the soil definitely reacts water repellent.

Doerr et al. (2006) also found that the studied coniferous forest sites (in Southern GB) were moderately to extremely water repellent, whereas most of the broadleaved forest sites were wettable or slightly water repellent. Only one deciduous forest site was evaluated as extremely water repellent. Woche et al. (2006) studied water repellency in 14 study areas in Germany, here also the coniferous and mixed forest sites often reached higher WDPT values (up to >3600s) than the deciduous forest sites. Our results confirm these findings of Doerr et al. (2006) and Woche et al. (2006).

In literature by now, the water repellency within the humus horizons under forest is usually not investigated, most studies only present data on water repellency in the mineral soil. Woche et al. (2005) and Wahl et al. (2003) for example studied water repellency in different depths within the mineral soil, the water repellency for the different humus horizons under forest were not distinguished here. Hence, the data of the presented study can help to fill this gap.

Buczko et al. (2005) used fixed sampling depths (e.g. the upper 5 cm include the main part of the humus layer) and did not distinguish single humus horizons. According to Buczko et al. (2005) the uppermost samples generally showed by far the highest WDPT. Our results show that the highest WDPT in forest soils could be measured in the humus horizons and here mainly in the Of-horizon. Greiffenhagen et al., (2006) analysed laboratory WDPT-data on samples from 11 sandy pine forest stands with different pf-values. They also distinguished WDPT for Of- and Oh-horizons. Most of our data were measured in the field, so the results cannot be compared directly. Nevertheless, for wet conditions Greiffenhagen et al. (2006) state very low WDPT of only a few seconds, and for very dry conditions, WDPT values of up to 6h were measured. Greiffenhagen et al. (2006) and Wessolek et al. (2008) also carried out studies on the influence of different soil and humus horizons on the WDPT in forests, but the focus was more on the influence of the soil moisture on WDPT and not the differences between the humus horizons.

5.2 Influence of WDPT on overland flow generation

Water repellency has a significant influence on overland flow generation. At least for our study area, this could clearly be demonstrated by means of the rainfall experiments. Gerrits et al. (2007) state that forest floor interception is a generally disregarded process that is important for overland flow generation and evaporation processes in forests. They applied a new measurement technique for forest floor interception in the Huewelerbach catchment in Luxembourg. The importance of the organic layers above the mineral soil for the interception of rainfall water can be supported by the experimental results presented here. In many rainfall experiments the water did not reach the mineral soil. This was particularly true for the water repellent sites and under rather dry antecedent soil moisture conditions. In these cases, the water infiltrates into the uppermost humus layers (L and partially Of) and the 'overland flow' was observed mainly above the Of and Oh layers (mapped according to Ad-hoc-ARBEITSGRUPPE BODEN, 1996). These results were also confirmed by rainfall experiments accomplished on 30 m² plots in the Frankelbach catchment near Kaiserslautern, Germany (Hümann et al. 2011). Martínez-Murillo and Ruiz-Sinoga (2010) carried out small-plot (0.24 m²) rainfall experiments on litter covered and bare soil in a study area in southern Spain. They also found a clear correlation of litter cover with high WDPT values and thus with high overland flow rates.

At first sight, the application of rainfall simulations underneath the forest canopy under humid climate conditions is questionable. Nevertheless, rainfall simulation is the only method enabling a direct comparison of the experimental results for a whole study area. Gerrits et al. (2010) measured an average canopy interception of 18 % in the leaf-on period and of 5 % in the leaf-off period for beech stands in Luxembourg. This equals an interception of between 2 and 7.2 mm for our simulated rainfall intensity of 40 mm h⁻¹. Holko et al. (2009) measured a canopy interception of only 0.8-0.9 mm per day for a spruce forest site in Slovakia. Even assuming a maximum canopy interception in the range of 8 to 10 mm, most of the water of a heavy rainfall event reaches the forest floor. The application of rainfall simulations below the forest canopy is therefore still appropriate.

In this study, the rainfall simulations were used for the determination of overland flow generation in a forest catchment in Western Germany in order to determine the influence of soil water repellency on the surface processes. In the context of water repellency, only few studies used rainfall simulation experiments before, and these studies were mainly focussed on water repellency as a consequence of forest fires (Shakesby et al., 2003; Shakesby, 2011; Arcenegui et al., 2007; Doerr et al., 2009; Zavala et al., 2010).

Doerr et al. (2000) state that a hydrophobic soil becomes hydrophilic again, if a certain, critical water content is exceeded. In this context, it can be clearly stated for the Holzbach study area, that no hydrophobic reaction was observed under wet conditions in spring, in the first weeks after snowmelt. However, under dry conditions, the coniferous forest sites in particular showed severely hydrophobic properties, but also the deciduous forest sites reacted water repellent, at least the O_H-horizons. The persistence of water repellency shows no clear correlation to the volumetric moisture content of the tested soil; this statement matches the results of Doerr et al. (2006). Nevertheless, in late spring and summer, our data-set clearly shows significant negative correlations of the WDPT with the antecedent rainfall amounts in the last one, three, and seven days before the WDPT field measurements (Tables 3 and 4).

The WDPT-data shows a very high spatial variance, even with only a few centimetres in between two drop tests, extremely different WDPT-values can be measured. The rainfall simulations are also carried out on a small area of only 0.283 m², but this area is much larger than the area of a WDPT measurement (drop-size). Thus, the rainfall simulations average the spatial variability of water repellency to a certain extent, because of the larger measurement area. If two rainfall experiments are carried out next to each other, the result is usually quite similar.

6 Conclusions

This study clearly confirms that water repellency occurs in Central European forests. Water repellency is primarily restricted to the humus layers and almost no water repellency was measured in the mineral soil (Ah). Also water content and decomposition state of the O-horizons have an important influence on the intensity of water repellency. The O_H-horizon can clearly be considered the most hydrophobic horizon in the studied soils. Furthermore, coniferous forest soils are much more intensely threatened by water repellency than deciduous forest soils. Under deciduous forest the O_H-horizon is almost the only part of the soil that shows water repellency at all. Further studies on the differences in water repellency of different soil horizons are necessary in the future.

Considerable overland flow rates were determined on many forest sites with organic layers under dry, water repellent conditions. Particularly on coniferous forest sites, water repellency effects are an important factor triggering overland flow generation. In the context of water repellency, further work is necessary to improve process knowledge.

Due to climate change, dry periods in late spring and summer are expected to become more frequent and this can lead to an increased probability of water repellency effects in Central European forests.

Acknowledgements

This study has received European Regional Development Funding through the INTERREG IVB NWE project ForeStClim.

References

- Ad-hoc-ARBEITSGRUPPE BODEN, A., 2005. Bodenkundliche Kartieranleitung (Sponagel, H., Grottenthaler, W., Hartmann, K.-J., Hartwich, R., Janetzko, P., Joisten, H., Kühn, D., Sabel, K.-J., and Traidl, R. (Eds.)). 5th ed. Bundesanstalt für Geowissenschaften und Rohstoffe und Geologische Landesämter.
- Arcenegui, V., Mataix-Solera, J., Guerrero, C., Zornoza, R., Mayoral, A.M., and Morales, J., 2007. Factors controlling the water repellency induced by fire in calcareous Mediterranean forest soils. *European Journal of Soil Science* 58, 1254–1259, doi:10.1111/j.1365-2389.2007.00917.x.
- Arnáez, J., Larrea, V., and Ortigosa, L., 2004. Surface runoff and soil erosion on unpaved forest roads from rainfall simulation tests in northeastern Spain. *CATENA* 57, 1–14, doi:10.1016/j.catena.2003.09.002.
- Atanassova, I., and Doerr, S., 2010. Organic compounds of different extractability in total solvent extracts from soils of contrasting water repellency. *European Journal of Soil Science* 61, 298–313, doi: 10.1111/j.1365-2389.2009.01224.x.
- Atanassova, I., and Doerr, S.H., 2011. Changes in soil organic compound composition associated with heat-induced increases in soil water repellency. *European Journal of Soil Science* 62, 516–532, doi:10.1111/j.1365-2389.2011.01350.x.
- Bens, O., Wahl, N.A., Fischer, H., and Hüttl, R.F., 2007. Water infiltration and hydraulic conductivity in sandy cambisols: impacts of forest transformation on soil hydrological properties. *European Journal of Forest Research* 126, 101–109, doi:10.1007/s10342-006-0133-7.
- Bodí, M.B., Doerr, S.H., Cerdà, A., and Mataix-Solera, J., 2012. Hydrological effects of a layer of vegetation ash on underlying wettable and water repellent soil. *Geoderma* 191, 14–23, doi:10.1016/j.geoderma.2012.01.006.
- Buczko, U., Bens, O., and Hüttl, R.F., 2005. Variability of soil water repellency in sandy forest soils with different stand structure under Scots pine (*Pinus sylvestris*) and beech (*Fagus sylvatica*). *Geoderma* 126, 317–336, doi:10.1016/j.geoderma.2004.10.003.
- Buczko, U., Bens, O., and Hüttl, R.F., 2006. Water infiltration and hydrophobicity in forest soils of a pine–beech transformation chronosequence. *Journal of Hydrology* 331, 383–395, doi:10.1016/j.jhydrol.2006.05.023.
- Buczko, U., Bens, O., and Hüttl, R.F., 2007. Changes in soil water repellency in a pine–beech forest transformation chronosequence: Influence of antecedent rainfall and air temperatures. *Ecological Engineering* 31, 154–164, doi:10.1016/j.ecoleng.2007.03.006.
- Butzen, V., Seeger, M., and Casper, M., 2011. Spatial pattern and temporal variability of runoff processes in Mediterranean Mountain environments - A case study of the Central Spanish Pyrenees. *Zeitschrift für Geomorphologie* 55, 25–48, doi:10.1127/0372-8854/2011/0055S3-0050.

- Butzen, V., Seeger, M., Wirtz, S., Huemann, M., Mueller, C., Casper, M., Ries, J.B., 2014. Quantification of Hortonian overland flow generation and soil erosion in a Central European low mountain range using rainfall experiments. *CATENA* 113, 202–212, doi:10.1016/j.catena.2013.07.008.
- Cerdà, A., and Doerr, S.H., 2008. The effect of ash and needle cover on surface runoff and erosion in the immediate post-fire period. *CATENA* 74, 256–263. doi:10.1016/j.catena.2008.03.010.
- Chau, H.W., Goh, Y.K., Vujošanović, V., and Si, B.C., 2012. Wetting properties of fungi mycelium alter soil infiltration and soil water repellency in a γ -sterilized wettable and repellent soil. *Fungal Biology*, doi:10.1016/j.funbio.2012.10.004.
- De Jonge, L.W., Jacobsen, O.H., Moldrup, P., 1999. Soil Water Repellency: Effects of Water Content, Temperature, and Particle Size. *Soil Science Society of America Journal* 63, 437. doi:10.2136/sssaj1999.03615995006300030003x.
- Dekker, L.W., Ritsema, C.J., 1994. How water moves in a water repellent sandy soil: 1. Potential and actual water repellency. *Water Resour. Res.* 30, 2507–2517. doi:10.1029/94WR00749.
- Doerr, S.H., 1998. On standardizing the “Water Drop Penetration Time” and the “Molarity of an Ethanol Droplet” techniques to classify soil hydrophobicity: A case study using medium textured soils. *Earth Surface Processes and Landforms* 23, 663–668, doi:10.1002/(SICI)1096-9837(199807)23:7<663::AID-ESP909>3.0.CO;2-6.
- Doerr, S.H., Shakesby, R.A., Dekker, L.W., and Ritsema, C.J., 2006. Occurrence, prediction and hydrological effects of water repellency amongst major soil and land-use types in a humid temperate climate. *European Journal of Soil Science* 57, 741–754, doi:10.1111/j.1365-2389.2006.00818.x.
- Doerr, S.H., Shakesby, R.A., and MacDonald, L.H., 2009. Soil Water Repellency: A Key Factor in Post-Fire Erosion. p. 197–224. In Cerdà, A., Robichaud, P. (eds.), *Fire Effects on Soils and Restoration Strategies*. Science Publishers Inc., Enfield, New Hampshire, USA.
- Doerr, S.H., Shakesby, R.A., and Walsh, R.P.D., 2000. Soil water repellency: its causes, characteristics and hydro-geomorphological significance. *Earth-Science Reviews* 51, 33–65, 10.1016/S0012-8252(00)00011-8.
- Eastaugh, C.S., Rustomji, P.K., and Hairsine, P.B., 2008. Quantifying the altered hydrologic connectivity of forest roads resulting from decommissioning and relocation. *Hydrological Processes* 22, 2438–2448, doi:10.1002/hyp.6836.
- Fister, W., Iserloh, T., Ries, J.B., and Schmidt, R.-G., 2011. Comparison of rainfall characteristics of a small portable rainfall simulator and a combined portable wind and rainfall simulator. *Zeitschrift für Geomorphologie* 55, 109–126, doi:10.1127/0372-8854/2011/0055S3-0054.
- Gallus, M., Ley, M., Schubert, D., Schüler, G., Segatz, E., and Werner, W., 2007. Renaturierung von Hangbrüchern im Hunsrück zur Glättung von Abflussspitzen. p. 21–30. In Schüler, G., Gellweiler, I., Seeling, S. (eds.), *Dezentraler Wasserrückhalt in der Landschaft durch vorbeugende Maßnahmen der Waldwirtschaft, der Landwirtschaft und im Siedlungswesen. Mitteilungen aus der Forschungsanstalt für Waldökologie und Forstwirtschaft (FAWF) Rheinland-Pfalz*. Trippstadt.
- German Federal Office of Statistics (Statistisches Bundesamt) (Hrsg.), 2012. *Statistisches Jahrbuch - Statistisches Jahrbuch 2012 - Statistisches Bundesamt (Destatis)*. [online] Available from: <https://www.destatis.de/DE/Publikationen/StatistischesJahrbuch/StatistischesJahrbuch2012.html> (Zugegriffen 10 Dezember 2012)
- German Meteorological Service (Deutscher Wetterdienst), 2012. Climate station "Weiskirchen/Saar", climate data (daily measures) from 01.01.1982-31.12.2011, data sheet called up at 25.06.2012.

- Gerrits, A.M.J., Savenije, H.H.G., Hoffmann, L., and Pfister, L., 2007. New technique to measure forest floor interception – an application in a beech forest in Luxembourg. *Hydrol. Earth Syst. Sci.* 11, 695–701.
- Gerrits, A.M.J., Pfister, L., Savenije, H.H.G., 2010. Spatial and temporal variability of canopy and forest floor interception in a beech forest. *Hydrological Processes* 24, 3011–3025.
- Gomi, T., Sidle, R.C., Ueno, M., Miyata, S., Kosugi, K., 2008. Characteristics of overland flow generation on steep forested hillslopes of central Japan. *Journal of Hydrology* 361, 275–290. doi:10.1016/j.jhydrol.2008.07.045
- Greiffenhagen, A., Wessolek, G., Facklam, M., Renger, M., and Stoffregen, H., 2006. Hydraulic functions and water repellency of forest floor horizons on sandy soils. *Geoderma* 132, 182–195, doi:10.1016/j.geoderma.2005.05.006.
- Hartmann, P., Fleige, H., and Horn, R., 2009. Physical properties of forest soils along a fly-ash deposition gradient in Northeast Germany. *Geoderma* 150, 188–195, doi:10.1016/j.geoderma.2009.02.005.
- Hausler, A., and Scherer-Lorenzen, M., 2001. Sustainable Forest Management in Germany: The Ecosystem Approach of the Biodiversity Convention reconsidered. (G. F. A. f. N. Conservation. Bundesamt für Naturschutz, Ed.). Bonn, Germany.
- Holko, L., Škvarenina, J., Kostka, Z., Frič, M., and Staroň, J., 2009. Impact of spruce forest on rainfall interception and seasonal snow cover evolution in the Western Tatra Mountains, Slovakia. *Biologia* 64, 594–599.
- Hümann, M., Schüller, G., Müller, C., Schneider, R., Johst, M. and Caspari, T., 2011. Identification of runoff processes - Impact of different forest types and soil properties on soil-water interrelations and floods. *J. Hydrol.* 409, 637–649, doi:10.1016/j.jhydrol.2011.08.067.
- Imeson, A.C., Verstraten, J.M., van Mulligen, E.J., Sevink, J., 1992. The effects of fire and water repellency on infiltration and runoff under Mediterranean type forest. *CATENA* 19, 345–361.
- IPCC (Intergovernmental Panel on Climate Change), 2007. Climate Change 2007: The Physical Science Basis - Contribution of Working Group I to the Fourth Assessment Report of the Intergovernmental Panel on Climate Change. Cambridge University Press, Cambridge, UK and New York, USA.
- IPCC (Intergovernmental Panel on Climate Change), 2013. Climate Change 2013: The Physical Science Basis - Contribution of Working Group I to the Fifth Assessment Report of the Intergovernmental Panel on Climate Change. Cambridge University Press, Cambridge, UK and New York, USA.
- Iserloh, T., Fister, W., Ries, J.B. and Seeger, M., 2010. Design and calibration of the small portable rainfall simulator of Trier University, *Geophysical Research Abstracts* 12, EGU2010–2769.
- Iserloh, T., Fister, W., Seeger, M., Willger, H., and Ries, J.B., 2012. A small portable rainfall simulator for reproducible experiments on soil erosion. *Soil and Tillage Research* 124, 131–137, doi: 10.1016/j.still.2012.05.016.
- León, J., Bodí, M.B., Cerdà, A., Badía, D., 2013. The contrasted response of ash to wetting: The effects of ash type, thickness and rainfall events. *Geoderma* 209–210, 143–152.
- Lichner, L., Capuliak, J., Zhukova, N., Holko, L., Czachor, H., Kollár, J., 2013. Pines influence hydrophysical parameters and water flow in a sandy soil. *Biologia* 68, 1104–1108. doi:10.2478/s11756-013-0254-7.
- Malvar, M.C., Martins, M.A.S., Nunes, J.P., Robichaud, P.R., Keizer, J.J., 2013. Assessing the role of pre-fire ground preparation operations and soil water repellency in post-fire runoff and inter-rill erosion by repeated rainfall simulation experiments in Portuguese eucalypt plantations. *CATENA* 108, 69–83.

- Martínez-Murillo, J.F., Gabarrón-Galeote, M.A., Ruiz-Sinoga, J.D., 2013. Soil water repellency in Mediterranean rangelands under contrasted climatic, slope and patch conditions in southern Spain. CATENA 110, 196 – 206.
- Martínez-Murillo, J.F., Ruiz-Sinoga, J.D., 2010. Water repellency as run-off and soil detachment controlling factor in a dry-Mediterranean hillslope (South of Spain). Hydrological Processes 24, 2137–2142.
- Miyata, S., Kosugi, K., Gomi, T., Mizuyama, T., 2009. Effects of forest floor coverage on overland flow and soil erosion on hillslopes in Japanese cypress plantation forests. Water Resour. Res. 45, W06402. doi:10.1029/2008WR007270.
- Morley, C.P., Mainwaring, K.A., Doerr, S.H., Douglas, P., Llewellyn, C.T., and Dekker, L.W., 2005. Organic compounds at different depths in a sandy soil and their role in water repellency. Australian Journal of Soil Research 43, 239–249, doi:10.1071/SR04094.
- Neris, J., Tejedor, M., Rodríguez, M., Fuentes, J., and Jiménez, C., 2012. Effect of forest floor characteristics on water repellency, infiltration, runoff and soil loss in Andisols of Tenerife (Canary Islands, Spain). CATENA Available at <http://www.sciencedirect.com/science/article/pii/S0341816212000951> (verified 21 November 2012).
- Orfánus, T., Bedrna, Z., Lichner, L., Hallett, P.D., Knava, K., and Sebín, M., 2008. Spatial variability of water repellency in pine forest soil. Soil and Water Research, 123–129.
- Orfánus, T., Dlapa, P., Fodor, N., Rajkai, K., Sándor, R., Nováková, K., 2014. How severe and subcritical water repellency determines the seasonal infiltration in natural and cultivated sandy soils. Soil and Tillage Research 135, 49–59. doi:10.1016/j.still.2013.09.005.
- Ries, J.B., Langer, M., and Rehberg, C., 2000. Experimental investigations on water and wind erosion on abandoned fields and arable land in the central Ebro Basin. Z. Geomorphol. Suppl.-Bd. 121, 91–108.
- Ries, J.B., Seeger, M., Iserloh, T., Wistorf, S., and Fister, W., 2009. Calibration of simulated rainfall characteristics for the study of soil erosion on agricultural land. Soil and Tillage Research 106, 109–116, doi:10.1016/j.still.2009.07.005.
- Robichaud, P., and Hungerford, R., 2000. Water repellency by laboratory burning of four northern Rocky Mountain forest soils. Journal of Hydrology 231–232, 207–219, doi:10.1016/S0022-1694(00)00195-5.
- Robichaud, P.R., Wagenbrenner, J.W., and Brown, R.E., 2010. Rill erosion in natural and disturbed forests: 1. Measurements. Water Resour. Res. 46, 14, doi:10.1029/2009WR008314.
- Rodríguez-Alleres, M., Varela, M.E., and Benito, E., 2012. Natural severity of water repellency in pine forest soils from NW Spain and influence of wildfire severity on its persistence. Geoderma 191, 125–131, doi:10.1016/j.geoderma.2012.02.006.
- Segatz, E., Gellweiler, I., Gallus, M., and Schüler, G., 2009. Holzbach. p. 101–136. In Seeling, S., Gellweiler, I., Hill, J., Schüler, G. (eds.), Wege zum dezentralen Hochwasserschutz. Trierer Geographische Studien. Trier.
- Shakesby, R.A., 2011. Post-wildfire soil erosion in the Mediterranean: Review and future research directions. Earth-Science Reviews 105, 71–100, doi:10.1016/j.earscirev.2011.01.001.
- Shakesby, R.A., Chafer, C.J., Doerr, S.H., Blake, W.H., Wallbrink, P., Humphreys, G.S., and Harrington, B.A., 2003. Fire Severity, Water Repellency Characteristics and Hydrogeomorphological Changes Following the Christmas 2001 Sydney Forest Fires. Australian Geographer 34, 147, doi:10.1080/00049180301736.
- Wagenbrenner, J.W., Robichaud, P.R., and Elliot, W.J., 2010. Rill erosion in natural and disturbed forests: 2. Modeling Approaches. Water Resour. Res. 46, 14, doi:10.1029/2009WR008315.

- Wahl, N., Bens, O., Schäfer, B., and Hüttl, R., 2003. Impact of changes in land-use management on soil hydraulic properties: hydraulic conductivity, water repellency and water retention. *Physics and Chemistry of the Earth, Parts A/B/C* 28, 1377–1387.
- Wahl, N.A., Wöllecke, B., Bens, O., and Hüttl, R.F., 2005. Can forest transformation help reducing floods in forested watersheds? Certain aspects on soil hydraulics and organic matter properties. *Physics and Chemistry of the Earth, Parts A/B/C* 30, 611–621, doi:10.1016/j.pce.2005.07.013.
- Wahren, A., Schwärzel, K., Feger, K.-H., 2012. Potentials and limitations of natural flood retention by forested land in headwater catchments: evidence from experimental and model studies. *Journal of Flood Risk Management* 5, 321–335.
- Wessolek, G., Schwärzel, K., Greiffenhagen, A., and Stoffregen, H., 2008. Percolation characteristics of a water-repellent sandy forest soil. *European Journal of Soil Science* 59, 14–23, doi:10.1111/j.1365-2389.2007.00980.x.
- Woche, S.K., Goebel, M. -O., Kirkham, M.B., Horton, R., Van der Ploeg, R.R., and Bachmann, J., 2005. Contact angle of soils as affected by depth, texture, and land management. *European Journal of Soil Science* 56, 239–251, doi:10.1111/j.1365-2389.2004.00664.x.
- Zavala, L.M., González, F.A., and Jordán, A., 2009. Fire-induced soil water repellency under different vegetation types along the Atlantic dune coast-line in SW Spain. *CATENA* 79, 153–162, doi:10.1016/j.catena.2009.07.002.
- Zavala, L.M., Granged, A.J.P., Jordán, A., and Bárcenas-Moreno, G., 2010. Effect of burning temperature on water repellency and aggregate stability in forest soils under laboratory conditions. *Geoderma* 158, 366–374, doi:10.1016/j.geoderma.2010.06.004.
- Zehe, E., Elsenbeer, H., Lindenmaier, F., Schulz, K., and Blöschl, G., 2007. Patterns of predictability in hydrological threshold systems. *Water Resour. Res.*, 43, 7, doi:10.1029/2006WR005589.
- Zehe, E., and Sivapalan, M., 2009. Threshold behaviour in hydrological systems as (human) geo-ecosystems: manifestations, controls, implications. *Hydrol. Earth Syst. Sci.* 13, 1273–1297.

Wirtz et al. (2012): Soil erosion on abandoned land in Andalusia - a comparison of interrill- and rill erosion rates. ISRN Soil Science, doi: 10.5402/2012/730870.

Research Article

Soil Erosion on Abandoned Land in Andalusia: A Comparison of Interrill- and Rill Erosion Rates

S. Wirtz,¹ T. Iserloh,¹ G. Rock,² R. Hansen,¹ M. Marzen,¹ M. Seeger,¹ S. Betz,¹
A. Remke,¹ R. Wengel,¹ V. Butzen,¹ and J. B. Ries¹

¹Department of Physical Geography, Trier University, Behringstraße, 54286 Trier, Germany

²Department of Remote Sensing, Trier University, Behringstraße, 54286 Trier, Germany

Correspondence should be addressed to S. Wirtz, wirtz@uni-trier.de

Received 13 July 2012; Accepted 30 August 2012

Academic Editors: J. Albergel, L. D. Chen, and Z. L. He

Copyright © 2012 S. Wirtz et al. This is an open access article distributed under the Creative Commons Attribution License, which permits unrestricted use, distribution, and reproduction in any medium, provided the original work is properly cited.

The present paper is based on several field investigations (monitoring soil and rill erosion by aerial photography, rainfall simulations with portable rainfall simulators, and manmade rill flooding) in southern Spain. Experiments lead now to a closer understanding of the dynamics and power of different soil erosion processes in a gully catchment area. The test site Freila (Andalusia, Spain) covers an area of 10.01 ha with a rill density of 169 m ha^{-1} , corresponding to a total rill length of 1694 m. Assuming an average rill width of 0.15 m, the total rill surface can be calculated at 250 m^2 (0.025 ha). Given that, the surface covered by rills makes up only 0.25% of the total test site. Since the rill network drains 1.98 ha, 20% of the total runoff comes from rills. The rills' sediment erosion was measured and the total soil loss was then calculated for detachment rates between 1685 g m^{-2} and 3018 g m^{-2} . The interrill areas (99.75% of the test site) show values between 29 and 143 g m^{-2} . This suggests an important role of rill erosion concerning runoff and soil detachment.

1. Introduction

Soil erosion by water involves different physical processes at variable spatial and temporal scales. The two main processes are interrill- and rill erosion by runoff water; the mechanisms of these two processes are completely different. The soil detachment in interrill erosion is induced and enhanced by splash and shallow overland flow [1]. In addition, it is influenced by the intrinsic characteristics of the soils [2–4] and rainfall intensity [5, 6]. In contrast, rill erosion is caused by a concentrated overland flow [6–8]. This is considered to be the most important process of sediment erosion and soil loss [9, 10]. As a result, the new rills can become persistent and form gullies, potentially constraining further land use [11–14]. Especially on fallow and shrub land, rills can develop without being disturbed by land management measures like ploughing. Since huge areas in the Mediterranean are covered by fallow and shrub land [15], rill erosion can be assumed to be a major process of soil erosion in the Mediterranean.

The outstanding importance of linear erosion for all intents and purposes (geomorphology, hydrology and economy) can be explained by the amount of kinetic energy of water, running as a concentrated runoff in channels. When concentrated, water reaches its maximum impact concerning erosion and transport [16]. The percentage of interrill, rill, and gully erosion on the total soil loss in a catchment area is difficult to determine, and results of many research groups differ considerably in comparing the effectiveness of the different soil erosion processes.

Results concerning the proportion of gully erosion on total soil erosion vary between 10% and more than 90% [17]. Gullies need high-intensity rainfall events to be activated. Most thunderstorms do not activate the gully in a catchment, but are able to generate or reactivate smaller forms, the rills. Faust and Schmidt [18] considered the geomorphologic importance of gullies as quite low, corresponding to the rare activity of the gullies. They state an activity frequency of one single event in 20 years, compared with an assumed activity of the rills of about four times per year. On that

account, the rills deliver smaller sediment quantities, but this can occur several times within one year. Meyer et al. [19] suggested a triplication of erosion rates due to rill development. Cornfields in Bedfordshire (UK) lost as much as 9 to 21 times more sediment by rill erosion, compared with erosion only affected by interrill erosion [20]. Cerdan et al. [9] reported the soil loss by rill erosion in Normandy during only a few heavy rainfall events to be up to 90% of the total soil loss.

During the last decades, several approaches have been developed to describe and predict soil detachment and sediment transport in rills in a reliable way [7, 21, 22]. In contrast, the factors influencing the development and the behaviour of rills have not been comprehensively assessed yet. The relationships between factors influencing these processes remain unclear as well. Knapen et al. [8] attribute this to the lack of comparable data that could be used for a meta-analysis on rill erosion. Furthermore, there is still little known about the function of rills in specific environments.

In this paper, the results of a set of experimental methods are used to draw conclusions from the differences between interrill- and rill erosion dynamics on a gully catchment in Andalusia (Spain). Three main questions were to be answered.

- (1) Which proportion of the test site area is drained by rill networks?
- (2) Which runoff intensities appear in the rills, which on the interrill areas?
- (3) How effective is the rill erosion compared to the interrill erosion in the catchment?

2. Material and Methods

2.1. Study Area. The study area Freila is situated in the Hoya de Baza sedimentary basin (see Figure 1) in Andalusia (southeast Spain). The bedrock mostly consists of Pliocene sedimentary rocks, that is, marls and fine grained sandstones. At the surface the marls and sandstones are weathered to calcareous loamy to sandy lithosols. The semiarid climate is characterised by a mean annual temperature of about 14.2°C. The annual precipitation is down to only 368 mm, with a high interannual variability. The vegetation is dominated by low shrub land of *Thymus vulgaris* and *Stipa tenacissima* grassland. The land use on the southern lakeside of the Negratin reservoir is dominated by abandoned cereal fields, which are extensively grazed by flocks of sheep. Agricultural land use comprises mainly cereal dry farming [23]. At the top of the catchment, a gully has developed.

2.2. Methods. During the field work, we combined the experimental methods rill experiment and rainfall simulation with field mapping. As a geodetic control of the maps we used large scale aerial photographs, taken with our own equipment.

2.2.1. Rill Experiment. During the rill experiments, water was pumped into an existing erosion rill using a motor-driven pump. For low flow experiments (LFEs) we used a constant discharge at the inlet of 9 L min^{-1} for 8 minutes. The total amount of water was 72 L. In the high flow experiments (HFEs) we used a pump with a capacity between 250 and 330 L min^{-1} . During 3 to 4 minutes we reached a water discharge of about 1000 L. The mobilisation of sediments due to turbulences of water at the inlet of the measuring channel was suppressed by a special inlet construction.

Each rill experiment consisted of two runs. In the first run the rill was tested under field (dry) conditions and in the second run, about 15 min later, the same rill was tested under wet conditions. The flow velocity within the rill was measured by recording the travel times of the waterfront and of two applied colour tracers. In the LFEs, the colour tracers were used after the flow stabilisation (3 and 6 minutes) and in the HFEs after 1 and 2 minutes. Accordingly, three velocity curves were recorded and changes in flow dynamics can be detected. The used colour tracers were the food colourings E 124 (red) and E 13 (blue).

The rill's slope was measured using a spring bow of 1 m range with a digital spirit level. It has to be considered that slope measuring provided only average slopes for each meter of the rill length, so steps or knickpoints in the rill were not captured. However, the position of each step or knick-point and also the heights were separately recorded.

At each of the three measuring points (MP) along the rill, four water samples were taken: the first directly when the waterfront has reached the sampling point, the second 30 sec later, the third after 90 sec, and the fourth 150 sec after the arrival of the waterfront. The sediment concentration of each sample was determined by filtration in the laboratory [24, 25].

At each MP, the rill cross-section was measured by means of a yardstick (LFEs) or a laser rangefinder (HFEs). The distance between ground level and sensor, respectively, and rill bottom was measured in 0.02 m steps. This method allowed an accurate calculation of the rill's cross section area and also an estimation of the rills' volume at the MP.

The water height was measured simultaneously with the time of sampling by means of a yardstick in the LFEs or continuously by ultrasonic sensors (HFEs) at each measuring point.

2.2.2. Rainfall Simulations. The test plot was circular, with a diameter of 60 cm and an area of 0.28 m^2 . It was delimited by a steel ring of 7 cm height, which was introduced into the soil for at least 3 cm. The outlet was V-shaped and was placed at the deepest point of the plot at surface level. The commercial full cone nozzle (Lechler 460.608) was fed with a pressure of about 40 kPa (0.4 bars) at a height of 2 m. The water flow was regulated by a flow meter (Type KSK-1200HIG100) positioned on a separate pole in 1.5 m height. The resulting rainfall intensity was maintained throughout the experiments at around 40 mm h^{-1} , which is considered to be mean thunderstorm rainfall intensity with a return period

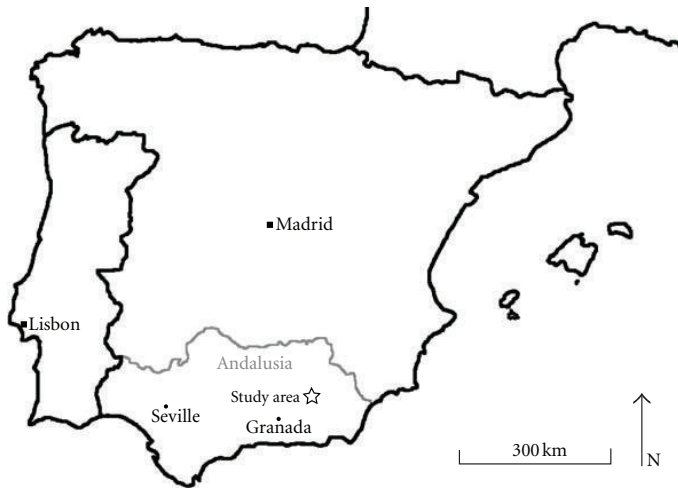


FIGURE 1: Test site in Andalusia (UTM: 509864 E-4154369 N).

TABLE 1: Setup parameters of the tested rills.

Experiment	Rill	Inflow intensity (L min ⁻¹)	Inflow duration (min)	Catchment area (m ²)	Tested rill length (m)	Estimated rill width (m)	Rill area (m ²)
RE1_2008	1	9	8	415	15	0.4	6
RE2_2008	2	9	8	203	21	0.4	8.4
RE3_2008	3	9	8	579	15	0.5	7.5
RE4_2009	1	250	4	415	16	0.4	6.4
RE5_2009	4	250	4	187	17	0.4	6.8
RE6_2009	5	330	3	1641	21	2.1	44.1
RE7_2009	1	250	4	415	16	0.4	6.4

of about 2 years [26]. The complete runoff was collected and runoff and soil detachment was determined gravimetrically. [23, 27–30]. The standard deviation of the rainfall intensity is < 5% [28].

Plot surface parameters were rock fragment cover, separated in embedded and overlying, vegetation cover, bare soil area, separated in crusted and uncrusted, and finally the slope of the plot. These parameters were optically estimated in the field and validated again with the help of digital photographs taken from every plot and preferably taken at an angle of 90° to the plot surface. The slope was measured by a clinometer.

For comparing the variability of the different parameters, we calculated the average of the relative measurement errors (RME) following the DIN 1319-1 [31]. This error is defined as

$$f = \frac{|x_a - x_r|}{x_r} * 100, \quad (1)$$

where x_a are the measured values and x_r are “correct” values; we used the mean of the measured values as x_r . This value describes the deviation of each single experiment from the mean of all experiments.

2.2.3. Small Format Aerial Photography (SFAP). The photos were taken using three different camera carriers depending on the wind conditions, requested flight level (photographed area) and available manpower: a hot air blimp, a kite, or an unmanned aerial vehicle (UAV). A detailed description of the camera carriers and aerial photography in general is to be found in Aber et al. [32]; the hot air blimp is also described in Ries and Marzolff [33].

The first used camera was a Canon 350D with a Canon EF-S 20 mm objective, the maximum solution of the photos is 8 MP, and the resulting stereoscopic images show a ground resolution between 0.5 and 11 cm, depending on the flying height.

The second used camera was a Nikon Coolpix S6000 digital compact camera with a maximum solution of 14.48 MP. The zoom objective has an aperture angle dynamic between 28 and 144 mm and a light intensity between 2.8 and 5.6.

Aerial photographs were used during field work as a basis for the mapping and the classification in “vegetation areas” and “no vegetation areas.”

2.2.4. Field Mapping and GIS Analysis. The field mapping based on the self-made aerial photographs should deliver

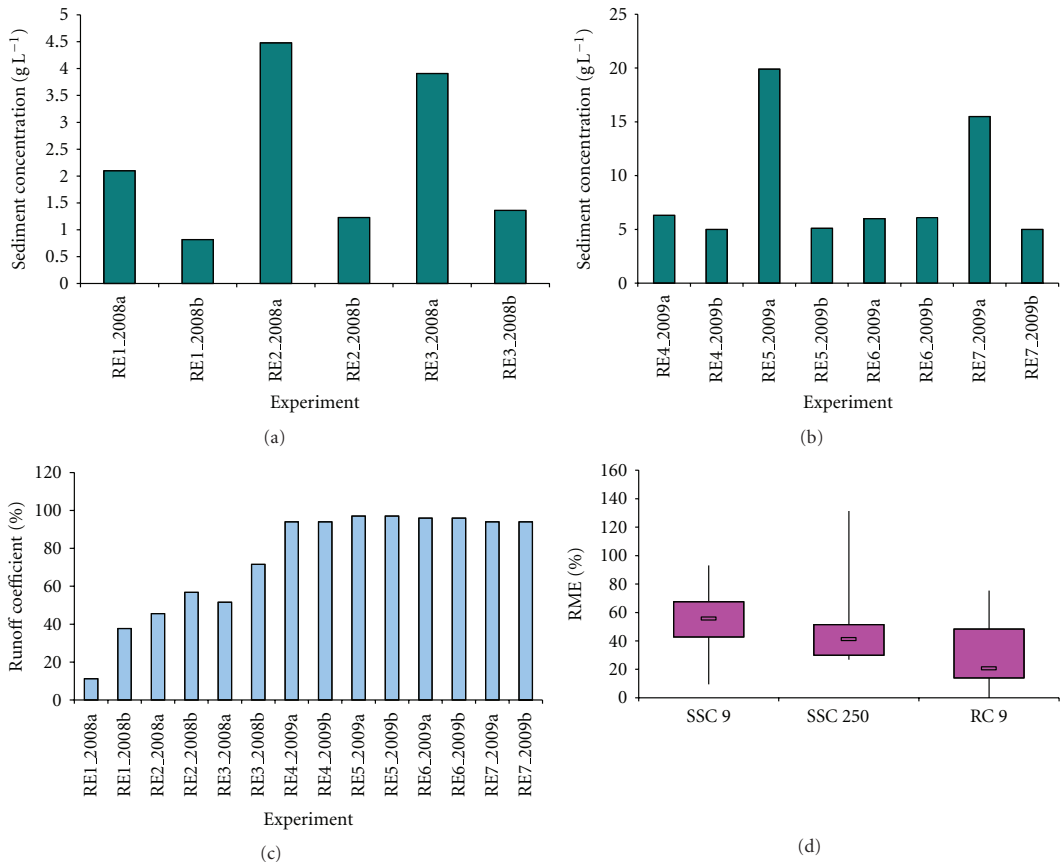


FIGURE 2: Results of the rill experiments: sediment concentrations of the 6 runs of the 3 rill experiments with an inflow intensity of 9 L min^{-1} (a), sediment concentrations of the 8 runs of the 4 rill experiments with an inflow intensity higher than 250 L min^{-1} (b), runoff coefficients of all rill experiments (c), relative measurements errors of the sediment concentrations (separated in experiments with an inflow intensity of 9 L min^{-1} and an inflow intensity higher than 250 L min^{-1}), and the runoff coefficients (d).

information about the spatial distribution of linear erosion forms, the catchment areas of these forms, and a total rill length on the test site. With this information, different parameters can be calculated.

The total rill area is calculated as follows:

$$A_R = W_R * L_R, \quad (2)$$

where A_R is the total rill area [m^2], W_R is the estimated average rill width [m], and L_R is the total rill length in the test site [m].

The rill density is calculated using the following equation:

$$D_R = \frac{L_R}{A_T}, \quad (3)$$

where D_R is the rill density [m ha^{-1}], L_R is the total rill length in the test site [m], and A_T is the test site area [ha].

The rill drainage index is calculated as follows:

$$I_R = \frac{C_R}{A_T}, \quad (4)$$

where I_R is the rill drainage index [ha ha^{-1}], C_R is the total area of all rill catchments [ha], and A_T is the test site area [ha].

2.2.5. Classification of the Aerial Photographs. In order to obtain spatial information about the different land cover types and distribution, a classification of digital UAV imagery has been performed. First, an unsupervised classification was done for identifying the classes that can be statistically distinguished. As a result, only three classes could be distinguished, that is, “vegetation,” “no vegetation/soil,” and “shadow.” A drawback of classifying UAV imagery was the fact that for such a large area, multiple flights were needed to cover the whole site. This led to a change of the illumination conditions

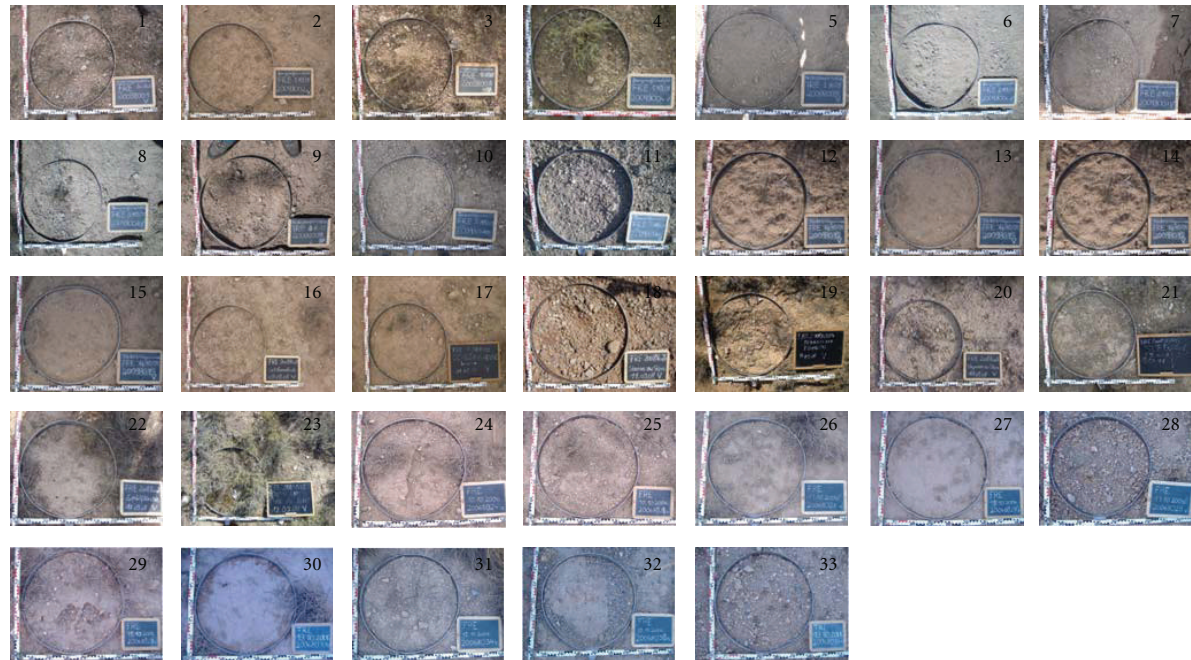


FIGURE 3: Surfaces of the used rainfall simulation plots.

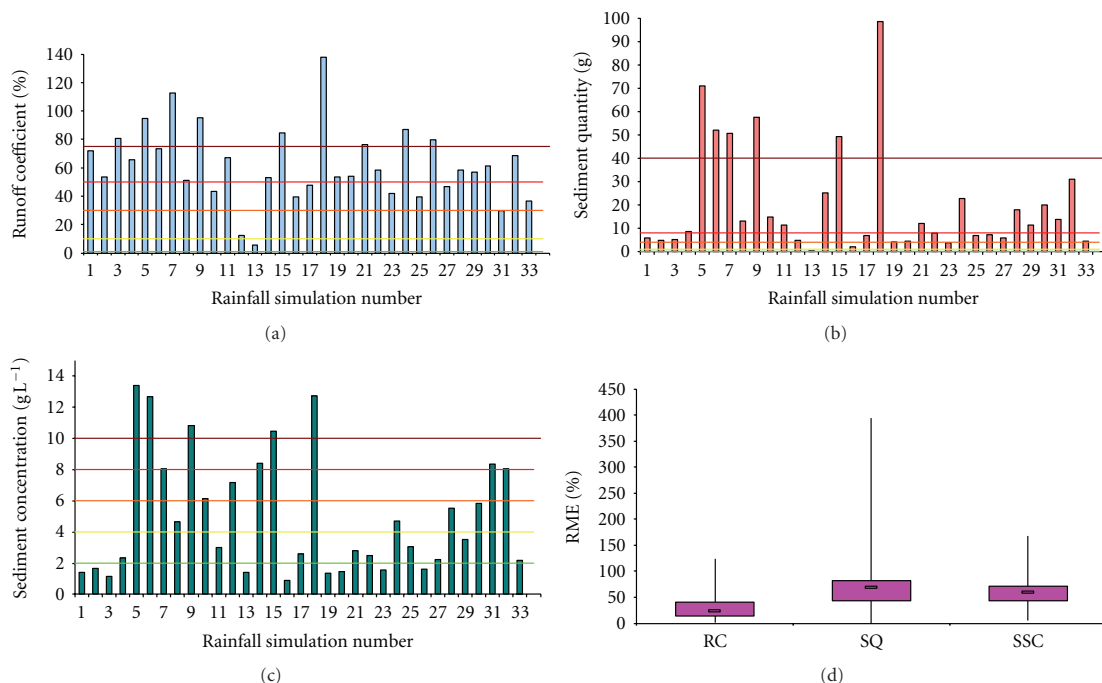


FIGURE 4: Results of the rainfall simulations: runoff coefficients (a), sediment quantities (b), and sediment concentrations (c). The limits between extremely high, very high, high, middle, low, and very low are marked. (d) Relative Measuring errors of the runoff coefficients (RC), the sediment quantities (SQ), and the sediment concentrations (SSC) of the rainfall simulations.

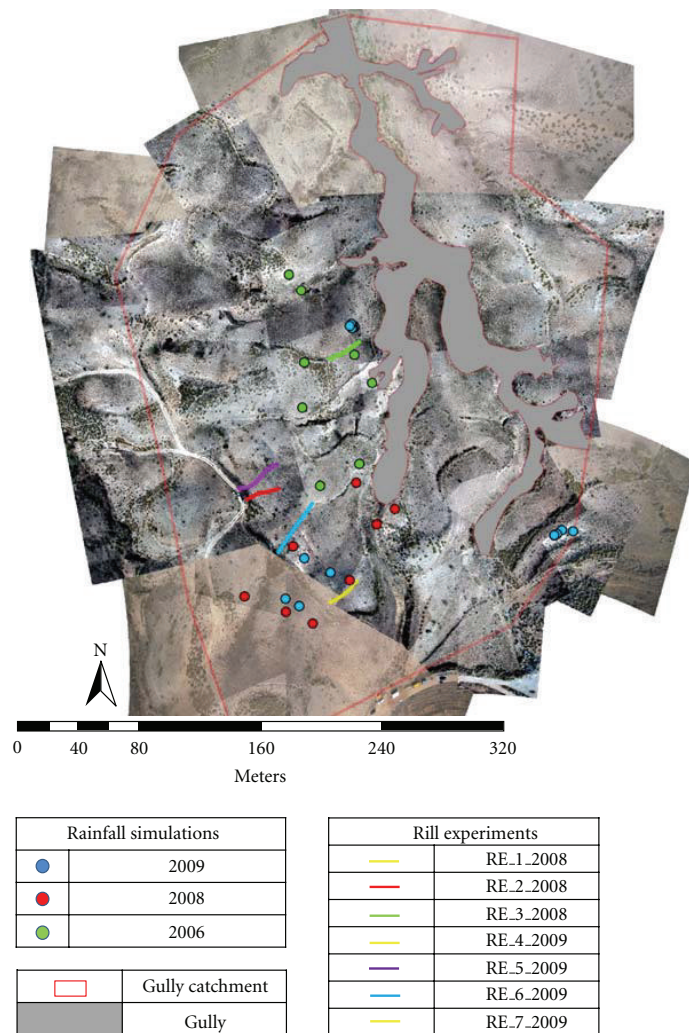


FIGURE 5: Positions of the rainfall simulations and the rill experiments.

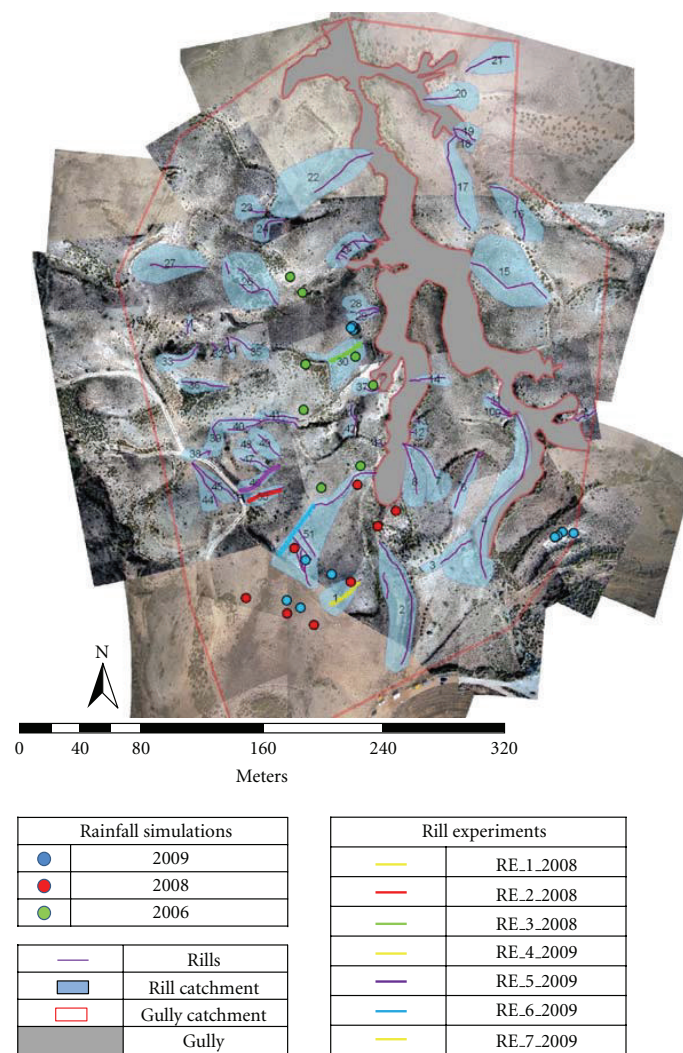
for the different flights' images. Considering these facts, every tile of the mosaic needed to be classified individually. Using manually digitised training areas, the maximum likelihood classifier was chosen. After classification of every single tile, a mosaic was calculated.

3. Results and Interpretation

3.1. Rill Experiments. The rill experiments were accomplished in five different rills; one rill was tested three times, once in a LFE and two times in a HFE. The catchment areas of the tested rills were between 190 and 1600 m²; the tested rill parts showed lengths between 15 and 21 m and widths between 0.4 and 2.1 m, resulting in rill areas between 6 and 44 m². These values are summarised in Table 1.

Figure 2 shows the results of the rill experiments. The sediment concentrations in the rill experiments with an

inflow intensity of 9 L min⁻¹ showed a data range between 0.8 (RE1_2008b) and 4.5 g L⁻¹ (RE2_2008a); the average sediment concentration was 2.3 g L⁻¹. The rill experiments with an inflow intensity higher than 250 L min⁻¹ showed sediment concentrations between 5 (RE4_2009b, RE5_2009b and RE7_2009b) and 20 g L⁻¹ (RE5_2009a); the average sediment concentration in these experiments was 8.6 g L⁻¹, that means about 3.5 times higher than in the experiments with an inflow intensity of 9 L min⁻¹. The runoff coefficients RCs showed a data range between 11 and around 95%. In the experiments with an inflow quantity of 1000 L per run, nearly the complete water amount reached the end of the tested rill part. Using the RC and the flow length of the LFEs, we could calculate an average infiltration rate in L m⁻¹. This value was used to calculate the RC of the HFEs. The percentages of infiltrated water in the HFEs were between 3% and 6% so we used RCs between 94% and



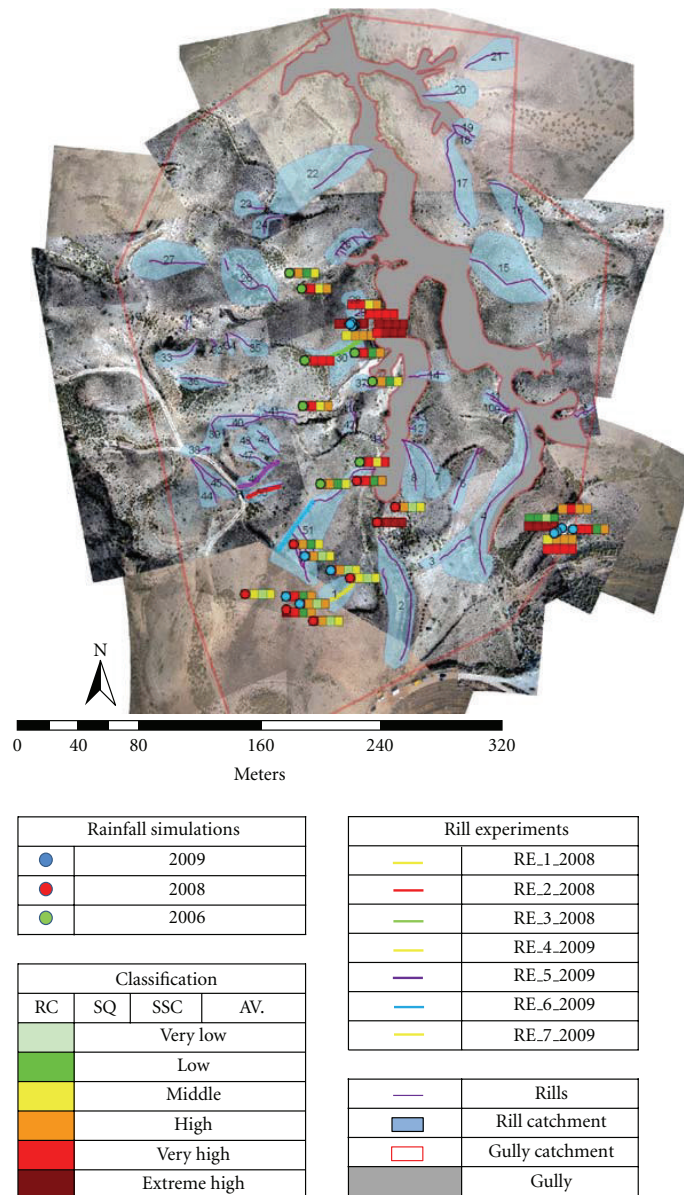


FIGURE 7: Additionally, classification of runoff coefficient, sediment quantity, sediment concentration, and average assessment of the rainfall simulations.

The runoff coefficients, the amounts of eroded material, and the sediment concentration of the experiments were classified in 6 classes from very low (class 0) to extreme high (class 5) as shown in Table 4. Each class was symbolised by a box in a certain colour in Figure 7. The first box represented the runoff coefficient, the second the sediment quantity, and the third the sediment concentration. In the fourth box, the average class value from these three parameters was calculated. These values describe the hazard class of the tested plot against the called parameters. The class limits for runoff

coefficient and sediment quantity were defined on the basis of the experience from about 400 rainfall simulations of the working group in semi-arid landscapes in North Africa and Spain during the past 16 years (e.g., [23, 27, 34]). For the definition of the sediment concentration class limits, we did not divide the sediment quantity and the runoff quantity, we defined other limits. The reason for this decision was, that in the other case, that nearly all rainfall simulations would show “very high” or even “extreme high” sediment concentrations even in cases of low sediment quantities (and low runoff

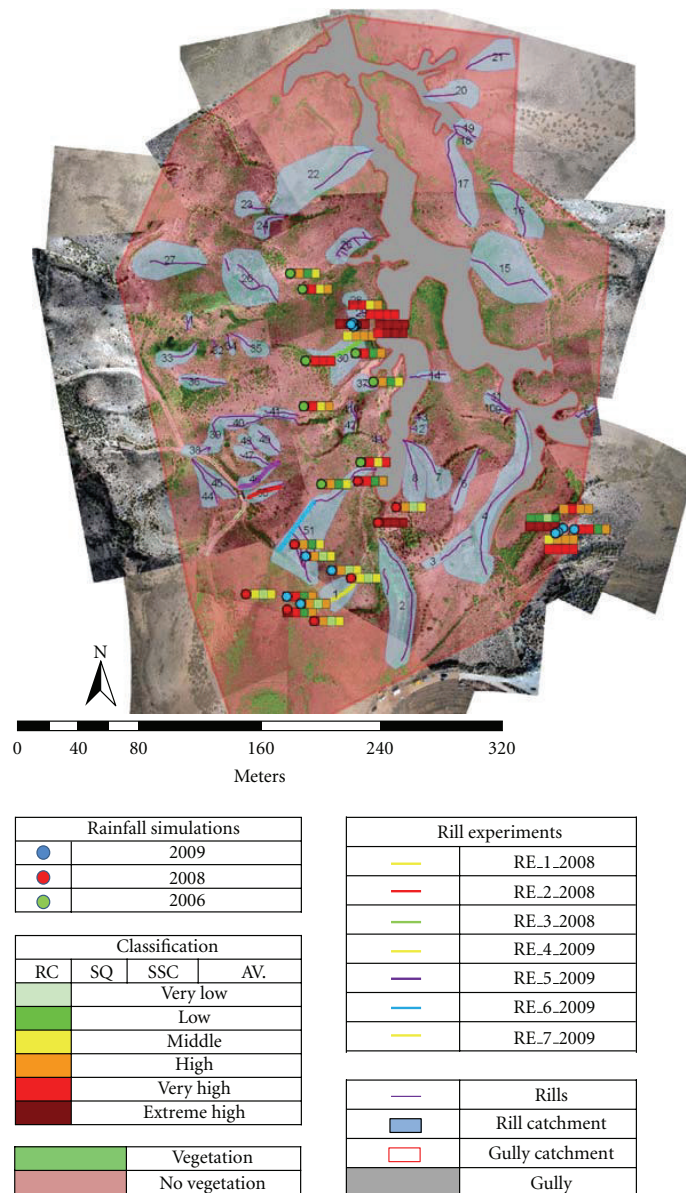


FIGURE 8: Additionally, soil surface coverage.

values). So we defined the limits “independent” of runoff coefficient and sediment quantity.

Regarding runoff coefficients (Figure 4(a)), a wide range from 5.6% to 100% could be observed. In the two cases the maximum RC of 100% was exceeded with values of 112.6% and 138% due to seepage of water from outside the plot ring. We still did not omit them because 91% of the rainfall simulation experiments showed high (21%), very high (42%), or extreme high (27%) runoff coefficients. Only 9% showed middle (6%) or low (3%) values and no RC was very low.

Also 91% of the sediment quantity values were high (33%), very high (39%), or extreme high (18%) and also only 9% showed middle (6%) or low (3%) values (Figure 4(b)). The range of sediment quantity was between 0.4 g and 98.5 g.

Sediment concentrations of the rainfall simulation experiments ranged between 0.9 g L^{-1} and 13.4 g L^{-1} (Figure 4(c)). 33% of these values were high (9%), very high (9%), and extreme (15%). 67% were middle (12%), low (27%), and very low (27%).

Most of the RMEs were between 13.5 (25% quartile) and 40.7% (75% quartile) for the runoff coefficients, between

TABLE 2: Sediment concentrations and runoff coefficients of the rill experiments.

Experiment	Rill	Sediment concentration (g L ⁻¹)	Runoff coefficient (%)
RE1_2008a	1	2.10	11.27
RE1_2008b		0.82	37.75
RE2_2008a	2	4.48	45.61
RE2_2008b		1.23	56.78
RE3_2008a	3	3.91	51.56
RE3_2008b		1.36	71.54
RE4_2009a	1	6.30	94.00
RE4_2009b		5.00	94.00
RE5_2009a	4	19.90	97.00
RE5_2009b		5.10	97.00
RE6_2009a	5	6.00	96.00
RE6_2009b		6.10	96.00
RE7_2009a	1	15.50	94.00
RE7_2009b		5.00	94.00

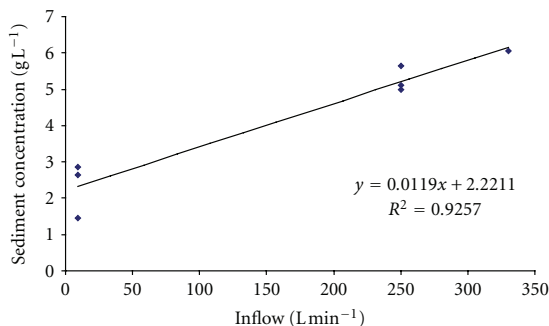


FIGURE 9: Relationship between the inflow intensity and the sediment concentration in the rill experiments.

43.4 and 81.8% for the sediment quantities, and between 43.4 and 71.8 for the sediment concentrations. The sediment quantity showed the highest maximum RME (394.7%) and the highest median RME (70.4%). The runoff values generally showed lower RME values than the erosion parameters, suggesting that the single values showed lower differences from an average value.

Regarding runoff coefficient classes, sediment quantity classes and sediment concentration classes that separated following the 3 groups (1) with mechanical treatment, (2) without mechanical treatment, and (3) high vegetation cover, a clear statement could be made: plots with a vegetation cover of maximal about 1/3 (highest value in these groups: 36%) and without mechanical treatment showed average class values of 3.9 (very high) for runoff coefficient, 3.6 (very high) for sediment quantity, and 1.5 (low-middle) for sediment concentration (Table 5). Although absolute values

TABLE 3: Plot parameters and results of the 33 rainfall simulations: RFC_e: rock fragment cover embedded, VC: vegetation cover, BS_c: bare soil crusted, RFC_o: rock fragment cover overlying, BS_u: bare soil uncrusted, RC: runoff coefficient, SQ: sediment quantity, SSC: sediment concentration.

Id	RFC _e (%)	VC (%)	BS _c (%)	RFC _o (%)	BS _u (%)	Slope (°)	RC (%)	SQ (g)	SSC (g L ⁻¹)
01	85	14	0	1	0	9	72.0	5.8	1.4
02	1	1	98	0	0	11	53.3	4.9	1.7
03	63	36	0	1	0	15	80.6	5.1	1.1
04	6	35	58	1	0	13	65.9	8.7	2.4
05	1	0	0	11	88	5	94.6	70.8	13.4
06	1	0	0	13	86	5	73.5	52.2	12.7
07	1	0	0	40	59	5	112.6	50.6	8.0
08	25	6	68	1	0	9	51.0	13.2	4.6
09	25	18	56	1	0	11	95.2	57.6	10.8
10	91	0	8	1	0	15	43.2	14.9	6.2
11	99	0	0	1	0	15	66.9	11.3	3.0
12	1	3	0	4	92	15	12.2	4.9	7.2
13	1	2	0	11	86	15	5.6	0.4	1.4
14	1	3	0	4	92	15	53.1	25.0	8.4
15	1	2	0	11	86	15	84.4	49.4	10.4
16	18	0	81	1	0	12	39.5	1.9	0.9
17	9	4	86	1	0	10	47.7	6.9	2.6
18	96	0	3	1	0	16	138.0	98.5	12.7
19	27	15	57	1	0	13	53.4	4.1	1.4
20	60	1	38	1	0	11	54.1	4.5	1.5
21	25	10	64	1	0	16	76.3	12.0	2.8
22	1	17	82	0	0	6	58.2	8.1	2.5
23	1	99	0	0	0	11	42.0	3.6	1.5
24	22	17	60	1	0	6	86.8	22.9	4.7
25	77	16	6	1	0	9	39.5	6.7	3.0
26	1	19	80	0	0	4	79.8	7.2	1.6
27	1	10	89	0	0	1.8	46.6	5.9	2.3
28	96	2	1	1	0	19	58.2	17.9	5.5
29	20	8	71	1	0	12.3	57.0	11.2	3.5
30	0	6	94	0	0	2	61.3	20.0	5.8
31	85	2	12	1	0	8	29.6	13.9	8.3
32	52	0	47	1	0	7.5	68.4	30.9	8.1
33	97	0	2	1	0	17	36.6	4.4	2.2

showed differences, we found this an appropriate method for classification of subareas. The mechanical-treated plots representing goat trails also showed "very high" runoff coefficient and sediment quantity values (3.7 and 4.0). The sediment concentration showed in contrast to the other group also the class "very high" (3.7). That means that we defined for the test site area without vegetation and without goat trampling a very high RC (50.1–75% runoff under a rainfall event of 40 mm h⁻¹ for 30 minutes), a very high detachment rate (8.1–40 g per 0.28 m², that means 29–143 g m⁻² under the simulated rainfall event), and a middle sediment concentration (4.1–6 g L⁻¹). The only

TABLE 4: Classification of the rainfall simulations regarding runoff coefficient (RC), sediment quantity (SQ), and sediment concentration (SSC).

Value	RC (%)	SQ (g)	SSC (g L^{-1})	Colour
Extreme high	5	>75	>40	>10
Very high	4	50.1–75	8.1–40	8.1–10
High	3	30.1–50	4.1–8	6.1–8
Middle	2	10.1–30	1.1–4	4.1–6
Low	1	1–10	0.1–1	2–4
Very low	0	<1	<0.1	<2

Regarding Figures 7 and 8: First (left) box: RC class value; second box: SQ class value; third box: SSC class value; fourth (right) box: average class value.

rainfall simulation (Id 23) with high vegetation cover (99%) showed lower class values, the RC was still “high” (30–50%), the sediment loss could be classified as “middle” (4–14 g m^{-2}), and the sediment concentration as “very low” (<2 g L^{-1}).

3.3. Mapping, GIS Analyses and Aerial Photography. Figure 5 shows the positions of the 5 tested rills and the positions of 33 rainfall simulations. The different colours represent the year of accomplishment. Additionally, the outlines of the test site are marked. Figure 6 includes the mapped rills and their catchment areas; in Figure 7 the classification of the rainfall simulations is added. The classification system is presented in Table 4. In Figure 8, the soil coverage, divided in “vegetation” and “no vegetation,” is presented additionally.

Table 6 lists the calculated test site parameters. The total rill length in the study area (10.01 ha) was 1694 m. These rills drained an area of 1.98 ha, which was about 20% of the whole test area. The measured rills had an average width of 0.15 m (based on field mapping and SFAP), so there was an estimated rill area of about 0.025 ha (0.25% of the study area). Accordingly, we could calculate the total interrill area at about 9.99 ha (99.75% of the study area). The rill density was 169 m ha^{-1} . In the study area, a total trail length of about 365 m was mapped; the average width of these trails was about 1 m. That means that an area of 365 m^2 was covered with uncrusted soil and/or overlying rock fragments what makes up for only 0.5% of the nonvegetated area.

4. Combination of the Results and Discussion

To compare both, the results of the rill experiments and the rainfall simulations, we wanted to calculate the inflow intensity which would reach the rill under a real rainfall event of 40 mm h^{-1} , an event simulated in our rainfall experiments. From the inflow intensity we could estimate the average sediment concentration following Figure 9. In this figure, we ignored two peaks: In RE5_2009a was a technical problem in sampling and in RE7_2009a 600 goats were crossing the rill before the measurement, so the quantity of lost material was too high. We therefore assumed in both cases the same sediment concentration as measured in run b of the experiment.

The relationship between runoff and the sediment concentration gave a high significance R^2 in our experiments but

the database is still too small for general statements of these correlations. So in this study we used the relationship only for this test site and only for an approximate estimation of the sediment concentration, caused by runoff of a 40 mm h^{-1} rainfall event. The relationship between runoff and sediment yield is to be found in several studies. Parsons et al. [35], for example, measured runoff and eroded material from 8 runoff plots during 10 natural storm events and described a clear correlation between runoff coefficient and the sediment yield.

A critical point in upscaling the results from rainfall simulator area to catchment area scale was the well-known scale problem [36]. The plot size used in the rainfall simulations (0.28 m^2) is too small for rill initiation. On the other hand, only much longer plot or slope lengths can cause rill development and, in consequence, initiate soil loss processes and runoff change. An important condition for the initiation of soil erosion in general is exceeding a certain threshold determined by soil parameters, such as soil shear strength or critical shear stress, via hydraulic parameters (shear stress, unit length shear force, and stream power). Those values are used to calculate transport and detachment capacities. Soil erosion can occur as long as the transport or detachment rate does not exceed the transport or detachment capacity. Exceeding this threshold will cause sedimentation of the excess material (e.g., [37]). Different research groups defined different thresholds that separate the interrill erosion from the initiation of rill erosion. Emmett [38] found that flowing water on entirely flat surfaces runs partially in preferred runoff paths with higher flow velocity, runoff depth, and consequently with different erosional behaviour. Other research groups stated 2–3° [39, 40] or 3–7° [41] as critical slope for rill initiation. When we assume a critical slope of 3°, only two (6%) of our rainfall plots showed lower values; 8 plots (24%) showed slope values lower than 7°. That denotes that upscaling the results from the rainfall simulation plots to a greater area will underestimate the real erosion and runoff values. Another critical value for rill initiation is a Froude number between 2.4 and 3 [39] or $1 + 0.0035 * D$, where D is the median of grain size in μm [42]. Giménez and Govers [43] and Giménez [44] assume that there is a threshold Froude number. In laboratory experiments, they found that the flow velocity in natural (rough) rills was independent of the slope angle because of a feedback between rill bed morphology and flow parameters. The frequency of macroroughness (steps, pools) increased

TABLE 5: Class values separated following “crusted soil,” “rock fragment cover embedded,” and “rock fragment cover overlying.”

Rainfall Sim. Id	RC class	SQ class	SSC class	Average class
Group 1: with mechanical treatment				
5	5	5	5	5
6	4	5	5	5
7	5	5	3	4
12	2	3	4	3
13	1	1	0	1
14	4	4	4	4
15	5	5	5	5
Average group 1	3.7	4.0	3.7	3.9
Group 2: without mechanical treatment				
1	4	3	0	2
2	4	3	0	2
3	5	3	0	3
4	4	4	1	3
8	4	4	2	3
9	5	5	5	5
10	3	4	3	3
11	4	4	1	3
18	5	5	5	5
16	3	2	0	2
17	3	3	1	2
19	4	3	0	2
20	4	3	0	2
21	5	4	1	3
22	4	4	1	3
24	5	4	2	4
25	3	3	1	2
26	5	3	0	3
27	3	3	1	2
28	4	4	2	3
29	4	4	1	3
30	4	4	2	3
31	2	4	4	3
32	4	4	4	4
33	3	3	1	2
Average group 2	3.9	3.6	1.5	2.9
Special group: vegetation cover				
23	3	2	0	2

with slope and, as a consequence, an increase of the flow velocity was prevented. With increasing slope, the water accelerated until a Froude number between 1.3 and 1.7 was reached. At this point, an “hydraulic jump” occurred and a plungepool could develop [44, 45]. The Froude number of the runoff on our rainfall simulation plots was clearly below 1, so the mentioned critical values were not reached. In contrast to the cited research groups, Torri et al. [46] and Merz and Bryan [47] stated that the Froude number was not applicable to discriminate between rill and interrill flow because runoff in rills was not implicit supercritical.

TABLE 6: Different test site parameters.

Parameter	Value
Total rill length L_R (m)	1694
Area of the test site A_T (ha)	10.01
Catchment area of all rills C_R (ha)	1.98
Estimated average rill width W_R (m)	0.15
Total rill area A_R (ha)	0.025
Interrill area A_I (ha)	9.99
Rill amount on total test site (%)	0.25
Interrill amount on total test site (%)	99.75
Rill density D_R (m ha^{-1})	169
Rill drainage index I_R (%)	20
Trail length (m)	365
Trail area (m^2)	365

A third possible factor influencing the rill initiation is the runoff intensity. Loch and Donnellan [48] observed rill development on clay soils with a slope angle of 2.3° , where the runoff reached an intensity of 0.3 to 0.6 L sec^{-1} . Moss et al. [49] determined a value of 0.6 L sec^{-1} on noncohesive quartz sand with a slope of 0.2 - 0.3° . Loch and Thomas [50] found much higher values: they determined minimum runoff intensities of more than 3 L sec^{-1} . In our rainfall experiments, 100% runoff was $5.6 \text{ L 30 min}^{-1}$, that means an average value of 0.003 L sec^{-1} . In consequence to the reported critical runoff intensities of the research groups, none of our rainfall simulation plots was able to develop any rills. Merz [16] doubts the importance about the runoff as a significant value for rill initiation. In his studies, the runoff was measured at the lowermost part of a test plot. These values could not describe a reliable average of the hydraulic situation since the runoff was not constant over the whole plot. Merz [16] assumed that different critical runoff values in both studies are based on variations in cohesive forces of the substratum and other soil physical parameters. Therefore, the critical runoff should not be used as a confirmed parameter for rill development.

More detailed results of soil and water movement under defined conditions are listed below in Table 7. The conditions for the precipitation were 40 mm h^{-1} rainfall event within 30 min. The field mapping provided size and position of catchments areas. The classification of the surface in “vegetation” and “no vegetation” was done by aerial images. We assumed that the complete runoff from “no vegetation” areas can reach the rills. Rainfall experiments of Cerdà [51] in southeast Spain on *Stipa tenacissima* areas showed that surface runoff and erosion were negligible in the tussock and quite high in bare areas. So we could calculate the rainfall quantity that reaches to uncovered surface areas of the rill catchments by multiplying the “no-vegetation” area in each catchment with 20 (40 mm h^{-1} but duration just 30 min). The rainfall simulations were accomplished on areas with very low vegetation cover and the classification of the rainfall experiments showed a “very high” (class 4) runoff coefficient between 50% and 75%, independent of the soil surface cover (crusted, overlying, or embedded rock fragments). Because

TABLE 7: Runoff and erosion parameters of the rill catchments. The presented values based on the class limits.

Id.	Rill catchment				Rill			Erosion rate (g m ⁻²)
	Area (m ²)	Vegetation area (m ²)	No vegetation area (m ²)	Runoff quantity (L)	Rill length (m)	Runoff intensity (L min ⁻¹)	SSC (g L ⁻¹)	
1	415	89	326	3256–4884	26	106–161	3–4	34–61
2	1346	477	869	8695–13042	106	281–426	6–7	54–107
3	87	3	84	843–1264	26	26–40	3–3	23–38
4	1852	382	1470	14696–22044	121	480–725	8–11	78–160
5	59	23	36	365–547	16	11–17	2–2	21–34
6	280	17	263	2633–3950	51	84–127	3–4	31–54
7	466	63	403	4033–6049	32	132–199	4–5	37–68
8	448	64	384	3839–5759	35	125–189	4–4	36–66
9	41	11	30	299–449	10	9–14	2–2	21–34
10	61	19	42	424–636	16	13–20	2–2	21–35
11	66	25	41	407–610	19	12–19	2–2	21–34
12	66	17	49	489–733	4	16–24	2–3	24–37
13	43	32	11	110–166	5	3–5	2–2	20–32
14	133	21	112	1121–1682	24	35–54	3–3	25–41
15	1616	393	1223	12235–18352	60	403–607	7–9	69–140
16	622	231	391	3913–5870	49	126–192	4–5	36–66
17	692	41	651	6513–9770	67	212–320	5–6	46–89
18	81	30	51	513–770	18	16–24	2–3	22–35
19	155	17	138	1379–2068	17	45–68	3–3	27–44
20	443	11	432	4323–6484	21	142–214	4–5	39–71
21	491	0	491	4909–7363	31	161–243	4–5	41–76
22	1658	253	1405	14053–21079	48	464–699	8–11	77–157
23	255	33	222	2222–3333	12	73–110	3–4	30–52
24	177	31	146	1460–2189	22	47–71	3–3	27–45
25	408	63	345	3454–5182	58	110–168	4–4	34–62
26	1120	345	775	7752–11629	62	253–382	5–7	51–100
27	916	232	684	6844–10267	38	225–339	5–6	48–93
28	183	57	126	1265–1897	15	41–62	3–3	26–44
29	109	28	81	811–1216	17	26–39	3–3	24–39
30	579	92	487	4870–7305	26	160–241	4–5	41–76
31	49	16	33	334–500	8	10–16	2–2	22–35
32	37	10	27	268–402	6	8–13	2–2	22–34
33	250	90	160	1598–2397	20	52–78	3–3	27–46
34	46	10	36	364–545	10	11–17	2–2	22–35
35	195	67	128	1285–1927	19	41–63	3–3	26–43
36	237	93	144	1444–2166	30	46–70	3–3	26–44
37	151	15	136	1363–2045	11	45–67	3–3	27–45
38	117	18	99	986–1479	8	32–49	3–3	26–41
39	365	96	269	2689–4034	73	84–128	3–4	30–54
40	128	30	98	978–1466	24	31–47	3–3	24–40
41	132	26	106	1058–1587	34	32–50	3–3	24–40
42	68	10	58	579–869	12	18–28	2–3	23–37
43	15	4	11	109–164	6	3–5	2–2	19–31
44	224	42	182	1824–2736	34	58–88	3–3	28–48
45	259	80	179	1791–2686	38	57–86	3–3	27–47
46	188	42	146	1456–2183	33	46–70	3–3	26–44
47	171	26	145	1447–2171	21	46–71	3–3	27–45
48	79	14	65	649–973	9	21–32	2–3	24–38

TABLE 7: Continued.

Id.	Rill catchment			Rill				
	Area (m ²)	Vegetation area (m ²)	No vegetation area (m ²)	Runoff quantity (L)	Rill length (m)	Runoff intensity (L min ⁻¹)	SSC (g L ⁻¹)	Erosion rate (g m ⁻²)
49	297	44	253	2534–3801	21	83–125	3–4	31–55
50	203	35	168	1675–2513	26	54–82	3–3	27–47
51	1641	306	1335	13352–20028	187	429–652	7–10	71–146
410	30	4	26	257–386	12	8–12	2–2	20–33

TABLE 8: Comparison of rill and interrill areas. The erosion values are only valid for the rill areas, not for the rill catchment areas (specific explanation in the text).

	Rills/rill catchments	Interrill area without gully
Area complete (m ²)	254/19750	100079
Area, vegetation (m ²)	X/4174	21912
Area, no vegetation (m ²)	X/15576	78167
Erosion rate (g m ⁻²)	1685–3018/X	29–143
Erosion quantity (kg)	425–762/X	2267–11178
Runoff intensity (m ³ s ⁻¹)	0.08–0.13/X	0.43–0.65
Runoff intensity per m ² (cm s ⁻¹)	0.03–0.05/X	0.0006–0.0008

of the range in the runoff classification, we also got a range in the runoff and erosion parameters in Table 7. We could calculate the runoff quantity and the runoff intensity. Based on the runoff values of our rill experiments, we assumed that there was an average infiltration rate of 2.5 L m⁻¹ in the rill so we could calculate the water quantity and the runoff intensity which was able to cause erosion. Figure 7 shows the correlation between the runoff intensity and the sediment concentration calculated from the results of the rill experiments. Using the currently known runoff intensity in the rill and the equation in Figure 7, we could calculate the sediment concentrations in the rills. Runoff quantity, rill lengths, and the average rill widths were known, so we could calculate the absolute erosion quantity and the erosion rate per unit area.

It has to be considered that the rill catchments were only used to calculate the runoff for the rills, erosion only taking place directly in the rills. That means that the rill catchments were on the “rill site” regarding the runoff but on the “interrill site” concerning the erosion parameters. Table 8 summarises the results of Table 7: the complete interrill areas without gully covered 100079 m²; 19750 m² of which were catchments for rills which covered 254 m² resulting from the total rill length and an average rill width. 21912 m² were covered with vegetation; 78167 m² showed bare soil. The erosion rates in the rills reached values between 1685 and 3018 g m⁻² (under a 40 mm h⁻¹ rainfall event of 30 min), whereas the soil loss in the interrill areas was only between 29 and 143 g m⁻² (20–60 times less). This relationship is confirmed by Morgan [52], who stated that rill sediment transport exceeded interrill transport by a factor of 40 on an 11° slope. Due to the much larger area of the interrill areas,

the total soil loss quantity was about 5 to 15 times higher than in the rills. The runoff intensity of the water from the interrill area was about 5 times higher than the runoff intensity of the rill flow. Regarding the runoff intensity per square meter, the rills’ value exceeded the interrills’ value by the factor 50.

One ignored point in our study is the gully in the test site. This is acceptable in so far as the gully is not active. An active gully would certainly raise the runoff and erosion values on the gully bottom.

We probably underestimated the rill erosion values: during a real rainfall event, the water would fill the rill from upstream and from both sides, whereas in the experiments, the water entered the rill at a single point. The measured sediment concentrations in the rills (maximum 19.9 g L⁻¹ in RE5_2009a) showed relatively low values. In the surrounding area of the presented test site, we still measured much higher sediment concentrations of up to 438 g L⁻¹ that caused by an inflow intensity of only 9 L min⁻¹ [25]. This means that the rill effectiveness could be even higher than the presented results implicate. Unfortunately, we do not (yet) have enough data of the surrounding test sites for a comparison of the different areas.

5. Conclusions

The aim of this study was to compare the effectiveness of rill and interrill areas concerning soil erosion on one abandoned land site in Andalusia. The results are only valid for the tested area; they cannot easily be adapted to other areas or used as general statement about the relation between rill and interrill erosion. We combined the results of rill experiments, rainfall simulations, field mapping, and small scale aerial photographs to get an idea about the dimension of the soil loss caused by rill and interrill flow. In our test site, the rills reached much higher erosion rates than the interrill erosion (20–60 times higher). Because of the much larger interrill area, the absolute erosion values of the interrill areas were 5–15 times higher than these of the rill area. The rills in our study area drained 19800 m² of the 100079 m² study area; this means that 0.25% of the study area were responsible for 20% of the area providing runoff. The results clearly proved the importance of the rills as sediment provider as well as runoff accumulator. The possible influence of the gully in our study area was ignored in this study, so we cannot state the possibly erosion-activating effect of our applied rainfall intensity of 40 mm h⁻¹. We know about the problems and the limitations of upscaling experimental field assessments but as

we only presented ranges or class limits, we assume that the results remain in realistic dimensions.

Acknowledgments

The research was supported by the “Internationales Graduiertenzentrum” of Trier University, by the Deutsche Forschungsgemeinschaft (DFG) Project nos. Ri 835/2 and Ri-835/6-1, and by the “Freundeskreis Trierer Universität e.V.” Additionally, we thank all participants of the field trips to Andalusia in September 2006, September 2008, and September 2009 who supported the accomplishment of the experiments. Special thanks go to Dr. A. Keller for the support in data analysis. Finally, the authors would like to thank the reviewers for their remarks.

References

- [1] L. Beuselinck, G. Govers, P. B. Hairsine, G. C. Sander, and M. Breynaert, “The influence of rainfall on sediment transport by overland flow over areas of net deposition,” *Journal of Hydrology*, vol. 257, no. 1–4, pp. 145–163, 2002.
- [2] N. J. Kuhn and R. B. Bryan, “Drying, soil surface condition and interrill erosion on two Ontario soils,” *Catena*, vol. 57, no. 2, pp. 113–133, 2004.
- [3] N. J. Kuhn, R. B. Bryan, and J. Navar, “Seal formation and interrill erosion on a smectite-rich Kastanozem from NE Mexico,” *Catena*, vol. 52, no. 2, pp. 149–169, 2003.
- [4] Y. Le Bissonnais, O. Cerdan, V. Lecomte, H. Benkhadra, V. Souchère, and P. Martin, “Variability of soil surface characteristics influencing runoff and interrill erosion,” *Catena*, vol. 62, no. 2–3, pp. 111–124, 2005.
- [5] I. Brodie and C. Rosewell, “Theoretical relationships between rainfall intensity and kinetic energy variants associated with stormwater particle washoff,” *Journal of Hydrology*, vol. 340, no. 1–2, pp. 40–47, 2007.
- [6] R. B. Bryan, “Soil erodibility and processes of water erosion on hillslope,” *Geomorphology*, vol. 32, no. 3–4, pp. 385–415, 2000.
- [7] G. Govers, R. Giménez, and K. Van Oost, “Rill erosion: exploring the relationship between experiments, modelling and field observations,” *Earth-Science Reviews*, vol. 84, no. 3–4, pp. 87–102, 2007.
- [8] A. Knapen, J. Poesen, G. Govers, G. Gyssels, and J. Nachtergael, “Resistance of soils to concentrated flow erosion: a review,” *Earth-Science Reviews*, vol. 80, no. 1–2, pp. 75–109, 2007.
- [9] O. Cerdan, Y. Le Bissonnais, A. Couturier, H. Bourennane, and V. Souchère, “Rill erosion on cultivated hillslopes during two extreme rainfall events in Normandy, France,” *Soil and Tillage Research*, vol. 67, no. 1, pp. 99–108, 2002.
- [10] J. Poesen, “Transport of rock fragments by rill flow—a field study,” in *Rill Erosion—Process and Significance*, R. B. Bryan, Ed., vol. 8 of *Catena*, pp. 35–54, Cremlingen, Germany, 1987.
- [11] D. J. Oostwoud Wijdenes, J. Poesen, L. Vandekerckhove, and M. Ghesquiere, “Spatial distribution of gully head activity and sediment supply along an ephemeral channel in a Mediterranean environment,” *Catena*, vol. 39, no. 3, pp. 147–167, 2000.
- [12] L. Vandekerckhove, J. Poesen, D. O. Wijdenes, and T. De Figueiredo, “Topographical thresholds for ephemeral gully initiation in intensively cultivated areas of the Mediterranean,” *Catena*, vol. 33, no. 3–4, pp. 271–292, 1998.
- [13] D. E. Woodward, “Method to predict cropland ephemeral gully erosion,” *Catena*, vol. 37, no. 3–4, pp. 393–399, 1999.
- [14] G. R. Hancock, D. Crawter, S. G. Fityus, J. Chandler, and T. Wells, “The measurement and modelling of rill erosion at angle of repose slopes in mine spoil,” *Earth Surface Processes and Landforms*, vol. 33, no. 7, pp. 1006–1020, 2008.
- [15] Ries and J. B. ;, “Landnutzungswandel und Landdegradation in Spanien—Eine Einführung,” in *Landnutzungswandel Und Landdegradation in Spanien*, I. Marzolff, J. B. Ries, J. De La Riva, and M. Seeger, Eds., pp. 11–29, 2003.
- [16] W. Merz, “Experimentelle Untersuchungen zur Rillenerosion auf landwirtschaftlich genutzten Böden in Kanada und der Volksrepublik China,” Freiburger Geographische Hefte, Heft 40, Selbstverlag des Institutes für Physische Geographie der Albert-Ludwig-Universität Freiburg i.Br., Freiburg, Germany, 1993.
- [17] J. Poesen, C. Valentin, J. Nachtergael, and G. Verstraeten, “Gully erosion and environmental change: importance and research needs,” *Catena*, vol. 50, no. 2–4, pp. 91–133, 2003.
- [18] D. Faust and M. Schmidt, “Soil erosion processes and sediment fluxes in a Mediterranean Marl landscape, campiña de Cádiz, SW Spain,” *Zeitschrift Für Geomorphologie*, vol. 53, no. 2, pp. 247–265, 2009.
- [19] L. D. Meyer, G. R. Forster, and M. J. M. Römkens, “Source of soil eroded by water from upland slopes,” in *Proceedings of the 1972 Sediment Yield Workshop*, pp. 177–189, US Department of Agriculture, National Sedimentation Laboratory, Oxford, Miss, USA, 1975.
- [20] R. P. C. Morgan, L. Martin, and C. A. Noble, “Soil erosion in the United Kingdom: a case study from Mid-Bedfordshire, England,” Occasional Paper 14, 1987.
- [21] R. Giménez and G. Govers, “Flow detachment by concentrated flow on smooth and irregular beds,” *Soil Science Society of America Journal*, vol. 66, no. 5, pp. 1475–1483, 2002.
- [22] R. Hessel and V. Jetten, “Suitability of transport equations in modelling soil erosion for a small Loess Plateau catchment,” *Engineering Geology*, vol. 91, no. 1, pp. 56–71, 2007.
- [23] M. Seeger, “Uncertainty of factors determining runoff and erosion processes as quantified by rainfall simulations,” *Catena*, vol. 71, no. 1, pp. 56–67, 2007.
- [24] S. Wirtz, M. Seeger, and J. B. Ries, “The rill experiment as a method to approach a quantification of rill erosion process activity,” *Zeitschrift Für Geomorphologie*, vol. 54, no. 1, pp. 47–64, 2010.
- [25] S. Wirtz, M. Seeger, and J. B. Ries, “Field experiments for understanding and quantification of rill erosion processes,” *Catena*, vol. 91, pp. 21–34, 2012.
- [26] Ministerio de Fomento, Secretaría de Estado de Infraestructuras y Transportes, and Dirección General de Carreteras, *Máximas Iluvias Diarias En La España Peninsular*, 1999.
- [27] J. B. Ries, M. Langer, and C. Rehberg, “Experimental investigations on water and wind erosion on abandoned fields and arable land in the central Ebro basin, Aragon/Spain,” *Zeitschrift Für Geomorphologie*, vol. 121, pp. 91–108, 2000.
- [28] T. Iserloh, W. Fister, M. Seeger, H. Willger, and J. B. Ries, “A small portable rainfall simulator for reproducible experiments on soil erosion,” *Soil and Tillage Research*, vol. 124, pp. 131–137, 2012.
- [29] J. B. Ries, M. Seeger, T. Iserloh, S. Wistorf, and W. Fister, “Calibration of simulated rainfall characteristics for the study of soil erosion on agricultural land,” *Soil and Tillage Research*, vol. 106, no. 1, pp. 109–116, 2009.

- [30] W. Fister, T. Iserloh, J. B. Ries, and R. G. Schmidt, "Comparison of rainfall characteristics of a small portable rainfall simulator and a combined portable wind and rainfall simulator," *Zeitschrift Für Geomorphologie*, vol. 55, no. 3, pp. 109–126, 2011.
- [31] DIN 1319-1, *Grundlagen Der Messtechnik—Teil 1: Grundbegriffe*, Deutsches Institut für Normung e.V., 1995.
- [32] J. S. Aber, I. Marzolff, and J. B. Ries, *Small-Format Aerial Photography: Principles, Techniques and Geoscience Applications*, Elsevier, Amsterdam, The Netherlands, 2010.
- [33] J. B. Ries and I. Marzolff, "Identification of sediment sources by large-scale aerial photography taken from a monitoring blimp," *Physics and Chemistry of the Earth*, vol. 22, no. 3-4, pp. 295–302, 1997.
- [34] J. B. Ries, "Methodologies for soil erosion and land degradation assessment in mediterranean-type ecosystems," *Land Degradation & Development*, vol. 21, no. 2, pp. 171–187, 2010.
- [35] A. J. Parsons, R. E. Brazier, J. Wainwright, and D. M. Powell, "Scale relationships in hillslope runoff and erosion," *Earth Surface Processes and Landforms*, vol. 31, no. 11, pp. 1384–1393, 2006.
- [36] E. Amore, C. Modica, M. A. Nearing, and V. C. Santoro, "Scale effect in USLE and WEPP application for soil erosion computation from three Sicilian basins," *Journal of Hydrology*, vol. 293, no. 1–4, pp. 100–114, 2004.
- [37] U. Scherer, *Prozessbasierte Modellierung der Bodenerosion in einer Lösslandschaft [Ph.D. thesis]*, Fakultät für Bauingenieur-, Geo- und Umweltwissenschaften, Universität Fridericiana zu Karlsruhe (TH), Karlsruhe, Germany, 2008.
- [38] W. W. Emmett, "The hydraulics of overland flow on hillslopes," US Geological Survey Professional Paper 662-A, United States Government Printing Office, Washington, DC, USA, 1970.
- [39] J. Savat and J. De Ploey, "Sheetwash and rill development by surface flow," in *Badland Geomorphology and Piping*, Geo Books, Norwich, UK, 1982.
- [40] G. Govers, "Spatial and temporal variability in rill development processes at the Huldenberg experimental site," in *Rill Erosion*, vol. 8 of *Catena*, pp. 17–34, Catena, Braunschweig, Germany, 1987.
- [41] R. Evans, "Water erosion in British farmers' fields—some causes, impacts, predictions," *Progress in Physical Geography*, vol. 14, no. 2, pp. 199–219, 1990.
- [42] W. Boon and J. Savat ;, "A Nomogram for the Prediction of Rill Erosion," in *Soil Conservation: Problems and Prospects*, pp. 303–319, John Wiley & Sons, Cranfield, UK, 1981.
- [43] R. Giménez and G. Govers, "Interaction between bed roughness and flow hydraulics in eroding rills," *Water Resources Research*, vol. 37, no. 3, pp. 791–799, 2001.
- [44] R. Giménez, *The interaction between rill hydraulics, rill geometry, and sediment detachment: an experimental approach [Proefschrift ingedien tot het behalen van de graad van Doctor in de Wetenschappen]*, Katholieke Universiteit Leuven, Faculteit Wetenschappen, Department Geografie-Geologie, 2003.
- [45] R. Giménez, O. Planchon, N. Silvera, and G. Govers, "Longitudinal velocity patterns and bed morphology interaction in a rill," *Earth Surface Processes and Landforms*, vol. 29, no. 1, pp. 105–114, 2004.
- [46] D. Torri, M. Sfalanga, and G. Chisci, "Threshold conditions for incipient rilling," in *Rill Erosion*, vol. 8 of *Catena*, pp. 97–105, Catena, Braunschweig, Germany, 1987.
- [47] W. Merz and R. B. Bryan, "Critical conditions for rill initiation on sandy loam Brunisols: laboratory and field experiments in southern Ontario, Canada," *Geoderma*, vol. 57, no. 4, pp. 357–385, 1993.
- [48] R. J. Loch and T. E. Donnellan, "Field rainfall simulator studies on two clay soils of the Darling Downs, Queensland. I. The effects of plot length and tillage orientation on erosion processes and runoff and erosion rates," *Australian Journal of Soil Research*, vol. 21, no. 1, pp. 33–46, 1983.
- [49] A. J. Moss, P. Green, and J. Hutka, "Small channels: their experimental formation, nature, and significance," *Earth Surface Processes & Landforms*, vol. 7, no. 5, pp. 401–415, 1982.
- [50] R. J. Loch and E. C. Thomas, "Resistance to rill erosion: observations on the efficiency of rill erosion on a tilled clay soil under simulated rain and run-on water," in *Rill Erosion—Processes and Significance*, vol. 8 of *Catena*, pp. 71–83, Catena, Braunschweig, Germany, 1987.
- [51] A. Cerdà, "The effect of patchy distribution of *Stipa tenacissima* L. on runoff and erosion," *Journal of Arid Environments*, vol. 36, no. 1, pp. 37–51, 1997.
- [52] R. P. C. Morgan, "Soil erosion in the United Kingdom: field studies in the Silsoe area, 1973–75," Occasional Paper 4, National College of Agricultural Engineering, 1977.

9

Synthese

Im Folgenden wird zunächst eine Zusammenschau der in dieser Arbeit bereits vorgestellten Ergebnisse erstellt (Kapitel 9). Aus dem so entstehenden Gesamtbild werden weitere, übergeordnete Zusammenhänge erschlossen, die für die Gesamtaussage der Arbeit eine weiterführende Bedeutung haben. Gegenstand der hier vorgestellten Untersuchungen sind zeitliche und räumliche Variabilität von Oberflächenabfluss- und Bodenerosionsprozessen, die in fünf Testgebieten in Deutschland, Luxemburg und Spanien untersucht worden sind. Aufgrund der Lage der Untersuchungsgebiete in unterschiedlichen Klimazonen sind jeweils andere Einflussfaktoren und teilweise sogar andere Prozesse entscheidend für die Reaktion der Testflächen auf den gleichen Niederschlagsimpuls. Die Prozessdynamik kann je nach Jahreszeit und Vorfeuchte „umschalten“.

9.1 Methodische Aspekte

Der Artikel ISERLOH u.a. (2013) (Kapitel 4) zeigt, dass es mittels einer einheitlichen Messung der Niederschlagscharakteristika unterschiedlicher Beregnungsanlagen möglich ist, die Ergebnisse dieser Anlagen miteinander zu vergleichen und in Beziehung zu setzen. Die vorgestellten Methoden (*Thies Laser Precipitation Monitor* - LPM, flächendeckende Niederschlagssammler, Niederschlagsmengen-Kalibrierplatte) und der einheitliche, systematische Ablauf des Messkonzeptes, stellen eine überzeugende Antwort auf Forschungsfrage 1 dar (siehe Kapitel 1.1: Wie kann man die Ergebnisse unterschiedlicher Beregnungsanlagen vergleichbar machen?).

Eine vergleichende Untersuchung von Oberflächenabflussbildung und Bodenerosion auf der Fläche ist nur mittels reproduzierbarer experimenteller Geländemessmethoden möglich, wie etwa den hier angewendeten

Niederschlagssimulationen. So bewirkt der aufgebrachte Starkregen mit einer Intensität von 40 mm h^{-1} auf einer verschlämmten Brachfläche in Andalusien Abflussbeiwerte von bis zu 100 %, bei Sedimentkonzentrationen von bis zu 13.4 g l^{-1} (WIRTZ u. a. (2012a), Kapitel 8). In Deutschland lag der höchste mit dieser Untersuchung auf unbedeckten Ackerflächen gemessene Abflussbeiwert bei 55.9 %, mit einer Sedimentkonzentration von 8.25 g l^{-1} (BUTZEN u. a. (2014), Kapitel 6). Vor allem sind die Niederschlagssimulationen aber auch unersättlich, um die Abflussreaktion derselben Fläche bei unterschiedlichen Systemzuständen mit dem gleichen Niederschlagsimpuls untersuchen zu können.

In einigen Fällen war es nur durch die Anwendung der experimentellen Methoden im Gelände und die dabei gemachten Beobachtungen möglich, die wesentlichen Einflussfaktoren auf die Oberflächenabflussbildung zu identifizieren. Die Hydrophobizität der Humusaufslagen unter trockenen Ausgangsbedingungen an vielen Waldstandorten beispielsweise wurde erst im Laufe der ersten Berechnungen entdeckt, weil dort deutliche Oberflächenabflüsse gemessen wurden, die zunächst nicht erklärt werden konnten. Erst die Ergebnisse der WDPT-Tests zeigen, dass die Humusauflage und die obersten Zentimeter des Ah-Horizontes hydrophob reagieren und dadurch die Infiltrationsrate verringern (BUTZEN u. a. (2014), Kapitel 6).

Ein weiteres Beispiel für eine Verbesserung der Prozesskenntnis durch die Anwendung der experimentellen Geländemethoden wird in BUTZEN u. a. (2011) (Kapitel 5) vorgestellt. Hier wurden einige Standorte des Untersuchungsgebietes in den spanischen Pyrenäen sowohl im Sommer als auch im Frühjahr mit der Kleinberechnungsanlage berechnet. Der Vergleich der Ergebnisse zeigt, dass ein im Zentrum des Tals gelegenes Feuchtgebiet im Sommer komplett austrocknet und dadurch von einem sonst SOF-dominierten Gebiet zu einem durch Tiefensickerung (DP) dominierten Gebiet wechselt. Die Abgrenzung dieser Fläche wurde durch eine Kombination aus Geländekartierung (Boden, Geomorphologie) und GIS-basierter Auswertung von digitalem Geländemodell und Luftbildern erreicht. Die Beispiele zeigen, dass die experimentellen Geländemessungen eine Verbesserung der Prozesskenntnis für das jeweilige Untersuchungsgebiet erreichen und in Kombination mit Geländekartierungen und GIS-Auswertungen zumindest eine qualitative Übertragung der punktuellen Messergebnisse auf die Fläche ermöglichen.

9.2 Prozessdifferenzierung

Von den sechs eingangs formulierten Forschungsfragen (Kapitel 1.1) beschäftigen sich die Fragen 2-6 mit den Oberflächenabfluss- und Bodenerosionsprozessen, sowie mit den wesentlichen Einflussfaktoren, von denen die Prozesse gesteuert werden. Diese Oberflächenprozesse und deren Einflussfaktoren sind im Rahmen dieser Arbeit in den Testgebieten untersucht worden.

Forschungsfrage 2 (Welches sind die wichtigsten Faktoren, die Oberflächenabflussbildung und Bodenerosion beeinflussen?) wird in den Artikeln BUTZEN u. a. (2011), BUTZEN u. a. (2014), BUTZEN u. a. (subm) und WIRTZ u. a. (2012a) (Kapitel 5-8) jeweils für das entsprechende Untersuchungsgebiet beantwortet. Die Antwort auf diese Frage ist je nach Klima und Landnutzung sehr unterschiedlich, dies wird in den folgenden Abschnitten thematisiert.

Die Frage nach dem Einfluss der Bodenfeuchte auf die untersuchten Oberflächenprozesse (Forschungsfrage 3) wird in BUTZEN u. a. (2011) (Kapitel 5) für das Untersuchungsgebiet Arnas in den zentralen Spanischen Pyrenäen beantwortet. Unter subhumidem Mittelmeerklima (Cfb nach Köppen-Geiger) (RIES u. a. 2000; SEEGER 2001; GARCÍA-RUIZ u. a. 2005) findet hier auf größeren Flächen ein Umschalten des dominierenden Abflussprozesses statt. Bei nassen Bedingungen im Frühjahr herrscht dort starker Sättigungsoberflächenabfluss (Saturation overland flow: SOF) vor, wohingegen unter eher trockenen Bedingungen ein „Umschalten“ hin zu Tiefensickerung (Deep Percolation: DP) stattfindet. Die Anwendung der Berechnungen in unterschiedlichen Jahreszeiten ermöglichte hierbei die Erfassung des jahreszeitlich bedingten Umschaltens der dominierenden Abflussprozesse.

Wesentlich deutlicher werden die klimatisch bedingten Unterschiede aber bei anderen Landnutzungsformen, wie etwa den Waldflächen. Waldböden mit Humusauflagen von mehreren Zentimetern Mächtigkeit wurden in der Form nur in Deutschland und Luxemburg gefunden und beprobt (BUTZEN u. a. (2014) und BUTZEN u. a. (subm), Kapitel 6 und 7), nicht jedoch in Spanien.

Die Humusauflage hat auf die Oberflächenabflussbildung und damit auch auf die Bodenerosion einen wesentlichen, steuernden Einfluss. Zum einen sorgt die Humusauflage für einen effizienten Schutz des Mineralbodens vor Bodenerosion, zum anderen steuert sie die Infiltrationsrate durch ein Umschalten zwischen Hydrophobizität und Hydrophilizität (Forschungsfrage 4: Wie beeinflusst die Hydrophobizität die Oberflächenabflussbildung unter Wald?). Hierbei spielt vor allem der von Pilzhypen durchzogene Of-Horizont eine entscheidende Rolle. In

den Sommermonaten weist die Streuauflage, und hier vor allem der Of-Horizont, bei trockenen Bedingungen häufig hydrophobe Eigenschaften auf. Dadurch dringt ein großer Teil des Niederschlagswassers gar nicht bis zum Mineralboden durch, sondern wird in der Streuschicht gehalten oder fließt innerhalb der Streuschicht quasi oberflächlich ab.

Die Humusauflage schützt den Waldboden sehr effektiv vor Bodenerosion durch einschlagende Regentropfen (*Splash*), sowie vor Erosion durch flächenhaften Oberflächenabfluss. Dennoch kann es im Wald, in Folge von extrem starken Niederschlagsereignissen, sogar zu starken Erosionserscheinungen wie Rinnenerosion und Gullyerosion kommen. Dies wurde beispielsweise im Untersuchungsgebiet Frankelbach von JOHST (2011) beobachtet und festgehalten (siehe Abbildung 9.1). Es handelte sich hier um ein einziges Starkregenereignis, bei dem es zu starker Oberflächenabflussbildung kam.



Abb. 9.1: Foto: Grabenerosion am Oberlauf des Frankelbachs, verursacht durch Starkregen im Mai 2002, (aufgenommen am 15. April 2005). (Quelle: JOHST (2011), Seite: 32, Abb. 3.4)

Neben diesen Extremereignissen kann auch die Bewirtschaftung des Waldes durch den Menschen zu einer Zerstörung der Streuschicht führen (Forschungsfrage 5: Wie beeinflussen Landnutzung und -bedeckung die Oberflächenabflussbildung und die Bodenerosion?). Der Einsatz von großen Harvesternten zur Baumernte kann

zum Beispiel zu tiefen Fahrspuren im Waldboden führen, die stark verdichtet sind, und die Oberfläche des Mineralbodens freilegen. Hier entsteht sehr leicht Oberflächenabfluss und linienhafte Erosion in den Fahrspuren. Vor allem im Testgebiet Holzbach wurde dies festgestellt (BUTZEN u. a. (2014), Kapitel 6).

Die Frage, wie effizient die Rinnenerosion im Vergleich zu flächenhafter Erosion ist (Forschungsfrage 6), wird im Artikel WIRTZ u. a. (2012a) (Kapitel 8) für das Testgebiet in Andalusien beantwortet. Im Testgebiet Freila, im südspanischen Andalusien, wurden neben den Berechnungen im Gelände noch weitere Untersuchungsmethoden angewendet. Mit Hilfe der Rinnenspülversuche ist es möglich, die Effizienz der Rinnenerosion zu messen und zu vergleichen. In diesem Zusammenhang ist es besonders interessant, die Abtragsraten der Rinnenerosion mit den Abtragsraten der flächenhaften Erosion zu vergleichen, die wir mit den Berechnungen messen. Die experimentellen Messungen in Verbindung mit einem digitalen Geländemodell ermöglichen zusätzlich die Berechnung der Rinneneinzugsgebiete. Durch die Kombination der Berechnungsergebnisse mit Kartierungen von Geomorphodynamik und Landnutzung können den Rinneneinzugsgebieten Oberflächenabflusskoeffizienten und dazu passende Bodenabtragsraten zugeordnet werden. Allerdings gelten diese Raten nur für die gemessene Niederschlagsintensität. Außerdem können die so berechneten Abfluss- und Erosionswerte der Rinneneinzugsgebiete bestenfalls die Größenordnung der ablaufenden Prozessdynamik angeben. Es kann keinesfalls davon ausgegangen werden, dass diese Werte tatsächlich genau so für das gesamte Rinneneinzugsgebiet, oder sogar für noch größere Flächen, gelten.

Generell gilt, dass die experimentell gemessenen Ergebnisse zu Oberflächenabflussbildung und Bodenerosion so nur für die beprobten Flächen gültig sind und nicht ohne Weiteres auf größere Flächen übertragen werden können. Dies ist nur (zumindest qualitativ) mit sehr guter Geländekenntnis und nach einer detaillierten geomorphologischen Kartierung mit Hilfe der Ausweisung von (hydrologischen und/oder prozessgeomorphologischen) Landschaftseinheiten möglich (siehe Kapitel 5 und 8).

Die Untersuchungen und Ergebnisse aus den einzelnen Testgebieten zeigen, dass die experimentellen Messungen der in den jeweiligen Testgebieten wichtigen Kenngrößen (Oberflächenabfluss, flächenhafte Erosion, Rinnenerosion, Hydrophobizität, etc.), in Kombination mit Kartierungen und Luftbildauswertung, weiterführende Aussagen zur aktuellen Prozessdynamik erlauben. Die Kartierungen ermöglichen zumindest eine qualitative Übertragung der punktuellen

Messungen auf die jeweilige Fläche. Es wird allerdings durch die hier vorgestellten Methodenkombinationen und Ergebnisse auch deutlich, dass eine Anpassung des Messkonzeptes an die Gegebenheiten des jeweiligen Testgebietes absolut unerlässlich ist, um sinnvolle Aussagen zur rezenten Prozessdynamik treffen zu können.

10

Schlussfolgerungen und Ausblick

Im Ausblick (Kapitel 10) werden nochmal kurz die wesentlichen Schlussfolgerungen, die sich aus dieser Arbeit ergeben, dargestellt. Außerdem werden kritische Punkte im hier untersuchten Forschungsfeld genannt an denen zukünftige Forschung ansetzen kann und sollte.

Die im Rahmen dieser Arbeit vorgestellten Ergebnisse zeigen, dass experimentelle Geländemessmethoden (Beregnungen, Rinnenerosionsversuche, usw.) sehr gut geeignet sind, um die jeweils untersuchten Oberflächenprozesse zu erfassen und zu quantifizieren. Die angewendeten Niederschlagssimulationen ermöglichen es, Oberflächenabflussbildung und flächenhafte Bodenerosion durch Wasser auf unterschiedlichen Flächen zu messen und die Ergebnisse zu vergleichen. Nur so ist es möglich, die Abflussreaktion derselben Fläche bei unterschiedlichen Systemzuständen mit demselben Niederschlag zu untersuchen. In Zukunft sollten auch Beregnungen mit verschiedenen Niederschlagsintensitäten durchgeführt werden, um zum Beispiel auch die Reaktion der Fläche auf einen noch stärkeren Niederschlag als $40 \text{ mm } h^{-1}$ zu erfassen. Ebenso könnten auch die Rinnenerosionsversuche mit mehreren verschiedenen Intensitäten durchgeführt werden, um Unterschiede in der Erosionsleistung der Rinnen feststellen zu können.

Insgesamt konnte durch die Anwendung der experimentellen Geländemessmethoden in der Regel eine Verbesserung der Prozesskenntnis für das jeweilige Untersuchungsgebiet erreicht werden, die so mit nicht experimentellen Methoden nicht möglich gewesen wäre. Die Kombination der experimentellen Messungen mit Geländekartierungen und GIS-Auswertungen ermöglichen zumindest eine qualitative Übertragung der punktuellen Messergebnisse auf die Fläche. Die Identifikation dominierender Abflussprozesse mittels eines gewichteten topographischen Indexes ist in diesem Zusammenhang eine geeignete Methode zur Untersuchung der räumlichen Verteilung von SOF-generierenden Flächen (SOF:

saturation overland flow). Die sichere Ausweisung von SSF-dominierten (SSF: *subsurface flow*) Flächen stellt allerdings nach wie vor eine große Herausforderung dar, auch weil es hier noch an geeigneten Geländemethoden mangelt, um die notwendige Datengrundlage zu schaffen.

Flächenhaftes Auftreten und Intensität von hydrophoben Eigenschaften der Böden ist vor allem für die Mitteleuropäischen Wälder noch unzureichend erforscht. Hier sind weitere Forschungsarbeiten nötig, vor allem um die Auswirkungen der Hydrophobizität auf die Oberflächenabflussbildung zu untersuchen. Auch die Unterschiede der Persistenz der Hydrophobizität in den verschiedenen Humushorizonten sollte Gegenstand zukünftiger Forschung sein. In Zukunft sollte auch die Hydrophobizität Eingang in die Modellierung der Oberflächenabflussbildung finden, vor allem um zu verhindern, dass die Oberflächenabflussbildung unter Wald in den trockenen Sommermonaten unterschätzt wird.

Eine weitere Eigenschaft der Humusaufgabe ist der effektive Schutz des Waldbodens vor Bodenerosion. Durch den Einsatz von großen Walderntemaschinen (*Harvestern*) kann diese Schutzschicht allerdings zerstört werden. In den Fahrspuren der *Harvester* entstehen, durch Verdichtung und Freilegen des Mineralbodens, meist Oberflächenabfluss und linienhafte Erosion in den vorgezeichneten linearen Strukturen. Für die Zukunft wäre eine Reduzierung dieser Fahrspuren wünschenswert. Dies könnte durch eine vermehrte Anwendung bodenschonender Forstmethoden erreicht werden, z. B. durch Waldernte mit Seilwinden.

Die im Rahmen dieser Arbeit verwendeten Rinnenerosionsversuche ermöglichen es, die Effizienz natürlicher Erosionsrinnen zu messen und zu vergleichen. Durch die Verwendung von beiden Methoden, Berechnung und Rinnenerosionsversuch, können die im Rinneneinzugsgebiet gemessenen Abtragsraten und -mengen mit den Abtragswerten der Erosionsrinne selbst verglichen werden. Die so gemessenen Raten gelten allerdings nur für die bei den Berechnungen verwendete Niederschlagsintensität. Außerdem können die so berechneten Abfluss- und Erosionswerte der Rinneneinzugsgebiete bestenfalls die Größenordnung der ablaufenden Prozessdynamik angeben.

Insgesamt zeigen die hier vorgestellten Ergebnisse aus den einzelnen Testgebieten, dass die Ergebnisse der experimentellen Messungen in Kombination mit Kartierung (aktuelle Geomorphodynamik) und Luftbildauswertung, weiterführende Aussagen zur aktuellen Prozessdynamik erlauben. Allerdings

ist eine Anpassung des Messkonzeptes an die Gegebenheiten des jeweiligen Untersuchungsbereiches absolut unerlässlich, um die wichtigsten Einflussfaktoren und Prozesse zu erfassen und sinnvolle Aussagen zur rezenten Prozessdynamik treffen zu können.

Literaturverzeichnis

Arcenegui u. a. 2007

ARCENEGUI, V. ; MATAIX-SOLERA, J. ; GUERRERO, C. ; ZORNOZA, R. ; MAYORAL, A. M. ; MORALES, J.: Factors controlling the water repellency induced by fire in calcareous Mediterranean forest soils. In: *European Journal of Soil Science* 58 (2007), Nr. 6, 1254–1259. <http://dx.doi.org/10.1111/j.1365-2389.2007.00917.x>. – DOI 10.1111/j.1365-2389.2007.00917.x. – ISSN 1365–2389

Atanassova u. Doerr 2010

ATANASSOVA, I. ; DOERR, S.: Organic compounds of different extractability in total solvent extracts from soils of contrasting water repellency. In: *European Journal of Soil Science* 61 (2010), Nr. 2, 298–313. <http://dx.doi.org/10.1111/j.1365-2389.2009.01224.x>. – ISSN 1365–2389

Atanassova u. Doerr 2011

ATANASSOVA, I. ; DOERR, S. H.: Changes in soil organic compound composition associated with heat-induced increases in soil water repellency. In: *European Journal of Soil Science* 62 (2011), Nr. 4, 516–532. <http://dx.doi.org/10.1111/j.1365-2389.2011.01350.x>. – DOI 10.1111/j.1365-2389.2011.01350.x. – ISSN 1365–2389

Bens u. a. 2007

BENS, Oliver ; WAHL, Niels A. ; FISCHER, Holger ; HÜTTL, Reinhard F.: Water infiltration and hydraulic conductivity in sandy cambisols: impacts of forest transformation on soil hydrological properties. In: *European Journal of Forest Research* 126 (2007), Nr. 1, 101–109. <http://dx.doi.org/10.1007/s10342-006-0133-7>. – DOI 10.1007/s10342-006-0133-7. – ISSN 1612–4669, 1612–4677

Beven 2004

BEVEN, Keith: Robert E. Horton's perceptual model of infiltration processes. In: *Hydrological Processes* 18 (2004), Nr. 17, 3447–3460. <http://dx.doi.org/10.1002/hyp.5740>. – DOI 10.1002/hyp.5740. – ISSN 1099–1085

Bodí u. a. 2012

BODÍ, Merche B. ; DOERR, Stefan H. ; CERDÀ, Artemi ; MATAIX-SOLERA, Jorge: Hydrological effects of a layer of vegetation ash on underlying wettable and water repellent soil. In: *Geoderma* 191 (2012), Dezember,

14–23. <http://dx.doi.org/10.1016/j.geoderma.2012.01.006>. – DOI 10.1016/j.geoderma.2012.01.006. – ISSN 0016–7061

Brevik 2013

BREVIK, Eric C.: The Potential Impact of Climate Change on Soil Properties and Processes and Corresponding Influence on Food Security. In: *Agriculture* 3 (2013), Juli, Nr. 3, 398–417. <http://dx.doi.org/10.3390/agriculture3030398>. – DOI 10.3390/agriculture3030398

Brodie u. Rosewell 2007

BRODIE, Ian ; ROSEWELL, Colin: Theoretical relationships between rainfall intensity and kinetic energy variants associated with stormwater particle washoff. In: *Journal of Hydrology* 340 (2007), Juni, Nr. 1–2, 40–47. <http://dx.doi.org/10.1016/j.jhydrol.2007.03.019>. – DOI 10.1016/j.jhydrol.2007.03.019. – ISSN 0022–1694

Bryan 2000

BRYAN, Rorke B.: Soil erodibility and processes of water erosion on hillslope. In: *Geomorphology* 32 (2000), März, Nr. 3–4, 385–415. [http://dx.doi.org/10.1016/S0169-555X\(99\)00105-1](http://dx.doi.org/10.1016/S0169-555X(99)00105-1). – DOI 10.1016/S0169-555X(99)00105-1. – ISSN 0169–555X

Buczko u. a. 2002

BUCZKO, U ; BENS, O ; FISCHER, H ; HÜTTL, R.F: Water repellency in sandy luvisols under different forest transformation stages in northeast Germany. In: *Geoderma* 109 (2002), September, Nr. 1–2, 1–18. [http://dx.doi.org/10.1016/S0016-7061\(02\)00137-4](http://dx.doi.org/10.1016/S0016-7061(02)00137-4). – DOI 10.1016/S0016–7061(02)00137–4. – ISSN 0016–7061

Buczko u. a. 2005

BUCZKO, U. ; BENS, O. ; HÜTTL, R.F.: Variability of soil water repellency in sandy forest soils with different stand structure under Scots pine (*Pinus sylvestris*) and beech (*Fagus sylvatica*). In: *Geoderma* 126 (2005), Juni, Nr. 3–4, 317–336. <http://dx.doi.org/10.1016/j.geoderma.2004.10.003>. – DOI 10.1016/j.geoderma.2004.10.003. – ISSN 0016–7061

Buczko u. a. 2006

BUCZKO, U. ; BENS, O. ; HÜTTL, R.F.: Water infiltration and hydrophobicity in forest soils of a pine–beech transformation chronosequence. In: *Journal of Hydrology* 331 (2006), Dezember, Nr. 3–4, 383–395. <http://dx.doi.org/10.1016/j.jhydrol.2006.05.023>. – DOI 10.1016/j.jhydrol.2006.05.023. – ISSN 0022–1694

Buczko u. a. 2007

BUCZKO, U. ; BENS, O. ; HÜTTL, R.F.: Changes in soil water repellency in a pine–beech forest transformation chronosequence: Influence of antecedent rainfall and air temperatures. In: *Ecological Engineering* 31 (2007), November, Nr. 3, 154–164. <http://dx.doi.org/10.1016/j.ecoleng.2007.03.006>. – DOI 10.1016/j.ecoleng.2007.03.006. – ISSN 0925–8574

Busche u. a. 2005

BUSCHE, D. (Hrsg.) ; KEMPF, J. (Hrsg.) ; STENGEL, I. (Hrsg.):

Landschaftsformen der Erde - Bildatlas der Geomorphologie. Darmstadt : Wissenschaftliche Buchgesellschaft, 2005. – ISBN 3-89678-552-4

Butzen u. a. 2011

BUTZEN, V. ; SEEGER, M. ; CASPER, M.: Spatial pattern and temporal variability of runoff processes in Mediterranean Mountain environments - A case study of the Central Spanish Pyrenees. In: *Zeitschrift für Geomorphologie* 55 (2011), April, Nr. Suppl. 3, S. 25–48. <http://dx.doi.org/10.1127/0372-8854/2011/0055S3-0050>. – DOI 10.1127/0372-8854/2011/0055S3-0050

Butzen u. a. subm

BUTZEN, V. ; SEEGER, M. ; MARRUEDO, A. ; JONGE, L. d. ; WENGEL, R. ; RIES, J. B. ; CASPER, M. C.: Water repellency under coniferous and deciduous forest - Experimental assessment of temporal variability and impact on surface runoff. In: *CATENA* (submitted)

Butzen u. a. 2014

BUTZEN, V. ; SEEGER, M. ; WIRTZ, S. ; HUEMANN, M. ; MUELLER, C. ; CASPER, M. ; RIES, J.B.: Quantification of Hortonian overland flow generation and soil erosion in a Central European low mountain range using rainfall experiments. In: *CATENA* 113 (2014), Februar, 202–212. <http://dx.doi.org/10.1016/j.catena.2013.07.008>. – DOI 10.1016/j.catena.2013.07.008. – ISSN 0341-8162

Cerdà u. Doerr 2008

CERDÀ, Artemi ; DOERR, Stefan H.: The effect of ash and needle cover on surface runoff and erosion in the immediate post-fire period. In: *CATENA* 74 (2008), August, Nr. 3, 256–263. <http://dx.doi.org/10.1016/j.catena.2008.03.010>. – DOI 10.1016/j.catena.2008.03.010. – ISSN 0341-8162

Chau u. a. 2012

CHAU, Henry W. ; GOH, Yit K. ; VUJANOVIC, Vladimir ; SI, Bing C.: Wetting properties of fungi mycelium alter soil infiltration and soil water repellency in a γ -sterilized wettable and repellent soil. In: *Fungal Biology* 116 (2012), Dezember, Nr. 12, 1212–1218. <http://dx.doi.org/10.1016/j.funbio.2012.10.004>. – DOI 10.1016/j.funbio.2012.10.004. – ISSN 1878-6146

Doerr u. Shakesby 2012

DOERR, S. H. ; SHAKESBY, R. A.: Chapter 19: Soil Water Repellency. In: HUANG, P. M. (Hrsg.) ; LI, Yuncong (Hrsg.) ; SUMNER, M. E. (Hrsg.): *Handbook of soil sciences - Volume II: Resource Management and Environmental Impacts* Bd. 2. 2. Boca Raton, Fla.; London : CRC ; Taylor & Francis [distributor], 2012. – ISBN 9781439803059 1439803056 9781439803073 1439803072 9781439803035 143980303X, S. 19–1 – 19–11

Doerr u. a. 2006

DOERR, S. H. ; SHAKESBY, R. A. ; DEKKER, L. W. ; RITSEMA, C. J.: Occurrence, prediction and hydrological effects of water repellency amongst major soil and land-use types in a humid temperate climate. In: *European Journal of Soil Science* 57 (2006), Oktober, Nr. 5,

741–754. <http://dx.doi.org/10.1111/j.1365-2389.2006.00818.x>. – DOI 10.1111/j.1365-2389.2006.00818.x. – ISSN 1365–2389

Doerr u. a. 2000

DOERR, S. H. ; SHAKESBY, R. A. ; WALSH, R. P. D.: Soil water repellency: its causes, characteristics and hydro-geomorphological significance. In: *Earth-Science Reviews* 51 (2000), August, Nr. 1-4, 33–65. [http://dx.doi.org/10.1016/S0012-8252\(00\)00011-8](http://dx.doi.org/10.1016/S0012-8252(00)00011-8). – DOI 10.1016/S0012-8252(00)00011-8. – ISSN 0012–8252

Doerr u. a. 2009

DOERR, S.H. ; SHAKESBY, R.A. ; MACDONALD, L.H.: Soil Water Repellency: A Key Factor in Post-Fire Erosion. In: CERDA, A. (Hrsg.) ; ROBICHAUD, P. (Hrsg.): *Fire Effects on Soils and Restoration Strategies*. Enfield, New Hampshire, USA : Science Publishers Inc., 2009. – ISBN 978–1–57808–526–2, S. 197–224

García-Ruiz u. a. 2005

GARCÍA-RUIZ, J. M. ; ARNÁEZ, J. ; BEGUERÍA, S. ; SEEGER, M. ; MARTÍ-BONO, C. ; REGUÉS, D. ; LANA-RENAULT, N. ; WHITE, S.: Runoff generation in an intensively disturbed, abandoned farmland catchment, Central Spanish Pyrenees. In: *CATENA* 59 (2005), Januar, Nr. 1, 79–92. <http://dx.doi.org/10.1016/j.catena.2004.05.006>. – DOI 10.1016/j.catena.2004.05.006. – ISSN 0341–8162

García-Ruiz 2010

GARCÍA-RUIZ, José M.: The effects of land uses on soil erosion in Spain: A review. In: *CATENA* 81 (2010), April, Nr. 1, 1–11. <http://dx.doi.org/doi:DOI:10.1016/j.catena.2010.01.001>. – DOI doi: DOI: 10.1016/j.catena.2010.01.001. – ISSN 0341–8162

Govers u. a. 2007

GOVERS, Gerard ; GIMÉNEZ, Rafael ; VAN OOST, Kristof: Rill erosion: Exploring the relationship between experiments, modelling and field observations. In: *Earth-Science Reviews* 84 (2007), Oktober, Nr. 3–4, 87–102. <http://dx.doi.org/10.1016/j.earscirev.2007.06.001>. – DOI 10.1016/j.earscirev.2007.06.001. – ISSN 0012–8252

Greiffenhagen u. a. 2006

GREIFFENHAGEN, A. ; WESSOLEK, G. ; FACKLAM, M. ; RENGER, M. ; STOFFREGEN, H.: Hydraulic functions and water repellency of forest floor horizons on sandy soils. In: *Geoderma* 132 (2006), Mai, Nr. 1–2, 182–195. <http://dx.doi.org/10.1016/j.geoderma.2005.05.006>. – DOI 10.1016/j.geoderma.2005.05.006. – ISSN 0016–7061

Grünewald u. Merz 2011

GRÜNEWALD, U. ; MERZ, B.: Kapitel 1: Einführung. In: MERZ, B. (Hrsg.) ; BITTNER, R. (Hrsg.) ; GRÜNEWALD, U. (Hrsg.) ; PIROTH, K. (Hrsg.): *Management von Hochwasserrisiken*. Stuttgart : Schweizerbart'sche Verlagsbuchhandlung, 2011. – ISBN 978–3–510–65268–6, S. 1–13

Hartmann u. a. 2009

HARTMANN, Peter ; FLEIGE, Heiner ; HORN, Rainer: Physical properties

of forest soils along a fly-ash deposition gradient in Northeast Germany. In: *Geoderma* 150 (2009), April, Nr. 1–2, 188–195. <http://dx.doi.org/10.1016/j.geoderma.2009.02.005>. – DOI 10.1016/j.geoderma.2009.02.005. – ISSN 0016–7061

Huang u. a. 2012

HUANG, P. M. (Hrsg.) ; LI, Yuncong (Hrsg.) ; SUMNER, M. E. (Hrsg.): *Handbook of soil sciences - Volume II: Resource Management and Environmental Impacts*. Bd. 2. 2. Boca Raton, Fla.; London : CRC ; Taylor & Francis [distributor], 2012. – ISBN 9781439803059 1439803056 9781439803073 1439803072 9781439803035 143980303X

Hümann u. a. 2011

HÜMANN, Marco ; SCHÜLER, Gebhard ; MÜLLER, Christoph ; SCHNEIDER, Raimund ; JOHST, Margret ; CASPARI, Thomas: Identification of runoff processes – The impact of different forest types and soil properties on runoff formation and floods. In: *Journal of Hydrology* 409 (2011), November, Nr. 3–4, 637–649. <http://dx.doi.org/10.1016/j.jhydrol.2011.08.067>. – DOI 10.1016/j.jhydrol.2011.08.067. – ISSN 0022–1694

IPCC 2007

IPCC ; SOLOMON, S. (Hrsg.) ; QIN, D. (Hrsg.) ; MANNING, M. (Hrsg.) ; CHEN, Z. (Hrsg.) ; MARQUIS, M. (Hrsg.) ; AVERYT, K. B. (Hrsg.) ; TIGNOR, M. (Hrsg.) ; MILLER, H. L. (Hrsg.): *Climate Change 2007: The Physical Science Basis - Contribution of Working Group I to the Fourth Assessment Report of the Intergovernmental Panel on Climate Change*. Cambridge, UK and New York, USA : Cambridge University Press, 2007 http://www.ipcc.ch/publications_and_data/publications_ipcc_fourth_assessment_report_wg1_report_the_physical_science_basis.htm

IPCC 2013

IPCC ; STOCKER, T. F. (Hrsg.) ; QIN, D. (Hrsg.) ; PLATTNER, G.-K. (Hrsg.) ; TIGNOR, M. (Hrsg.) ; ALLEN, S. K. (Hrsg.) ; BOSCHUNG, J. (Hrsg.) ; NAUELS, A. (Hrsg.) ; XIA, Y. (Hrsg.) ; BEX, V. (Hrsg.) ; MIDGLEY, P. M. (Hrsg.): *Climate Change 2013: The Physical Science Basis - Contribution of Working Group I to the Fifth Assessment Report of the Intergovernmental Panel on Climate Change*. Cambridge, UK and New York, USA : Cambridge University Press, 2013 http://www.climatechange2013.org/images/report/WG1AR5_ALL_FINAL.pdf

Iserloh u. a. 2012

ISERLOH, T. ; FISTER, W. ; MARZEN, M. ; SEEGER, M. ; KUHN, N.J. ; RIES, J.B.: The role of wind-driven rain for soil erosion an experimental approach. In: *Zeitschrift für Geomorphologie, Supplementary Issues* 57 (2012), Nr. 1, S. 193–201. <http://dx.doi.org/10.1127/0372-8854/2012/S-00118>. – DOI 10.1127/0372-8854/2012/S-00118

Iserloh u. a. 2013

ISERLOH, T. ; RIES, J.B. ; ARNÁEZ, J. ; BOIX-FAYOS, C. ; BUTZEN, V. ; CERDÀ, A. ; ECHEVERRÍA, M.T. ; FERNÁNDEZ-GÁLVEZ, J. ; FISTER, W. ; GEISSLER, C. ; GÓMEZ, J.A. ; GÓMEZ-MACPHERSON, H. ; KUHN, N.J. ;

LÁZARO, R. ; LEÓN, F.J. ; MARTÍNEZ-MENA, M. ; MARTÍNEZ-MURILLO, J.F. ; MARZEN, M. ; MINGORANCE, M.D. ; ORTIGOSA, L. ; PETERS, P. ; REGUÉS, D. ; RUIZ-SINOGA, J.D. ; SCHOLTEN, T. ; SEEGER, M. ; SOLÉ-BENET, A. ; WENGEL, R. ; WIRTZ, S.: European small portable rainfall simulators: A comparison of rainfall characteristics. In: *CATENA* 110 (2013), November, 100–112. <http://dx.doi.org/10.1016/j.catena.2013.05.013>. – DOI 10.1016/j.catena.2013.05.013. – ISSN 0341–8162

Johst 2011

JOHST, Margret: *Experimentelle und modellgestützte Untersuchungen zur Hochwasserentstehung im Nordpfälzer Bergland unter Verwendung eines neuartigen Spatial-TDR-Bodenfeuchtemessgeräts*. Trier, Universität Trier, Diss., 2011

Kajiura u. a. 2012

KAJIURA, Masako ; ETORI, Yoshie ; TANGE, Takeshi: Water condition control of in situ soil water repellency: an observational study from a hillslope in a Japanese humid-temperate forest. In: *Hydrological Processes* 26 (2012), Nr. 20, 3070–3078. <http://dx.doi.org/10.1002/hyp.8310>. – DOI 10.1002/hyp.8310. – ISSN 1099–1085

Kidron 2014

KIDRON, Giora J.: The role of crust thickness in runoff generation from microbiotic crusts. In: *Hydrological Processes* (2014), August. <http://dx.doi.org/10.1002/hyp.10243>. – DOI 10.1002/hyp.10243. – ISSN 1099–1085

Kretzschmar 1992

KRETZSCHMAR, R.: Bodenökologie und -belastung - Vorbeugende und abwehrende Schutzmaßnahmen. In: BLUME, H. P. (Hrsg.): *Handbuch des Bodenschutzes*. 2. Landsberg/Lech : ecomed, 1992, S. 182–200

Kron 2013

KRON, W.: Kapitel 10: Versicherung von Hochwasserschäden. In: PATT, H. (Hrsg.) ; JÜPNER, R. (Hrsg.): *Hochwasser-Handbuch - Auswirkungen und Schutz*. 2. Berlin, Heidelberg : Springer-Verlag, 2013. – ISBN 978-3-642-28190-7, S. 553–607

Kuhn u. Bryan 2004

KUHN, Nikolaus J. ; BRYAN, Rorke B.: Drying, soil surface condition and interrill erosion on two Ontario soils. In: *CATENA* 57 (2004), Juli, Nr. 2, 113–133. <http://dx.doi.org/10.1016/j.catena.2003.11.001>. – DOI 10.1016/j.catena.2003.11.001. – ISSN 0341–8162

Le Bissonnais u. a. 2005

LE BISSONNAIS, Y. ; CERDAN, O. ; LECOMTE, V. ; BENKHADRA, H. ; SOUCHÈRE, V. ; MARTIN, P.: Variability of soil surface characteristics influencing runoff and interrill erosion. In: *CATENA* 62 (2005), August, Nr. 2-3, 111–124. <http://dx.doi.org/10.1016/j.catena.2005.05.001>. – DOI 10.1016/j.catena.2005.05.001. – ISSN 0341–8162

Li u. a. 2014

LI, Xiang ; NIU, Jianzhi ; XIE, Baoyuan: The Effect of Leaf Litter Cover on Surface Runoff and Soil Erosion in Northern China. In: *PLoS ONE* 9

(2014), September, Nr. 9, e107789. <http://dx.doi.org/10.1371/journal.pone.0107789>. – DOI 10.1371/journal.pone.0107789

Maetens u. a. 2012

MAETENS, W. ; VANMAERCKE, M. ; POESEN, J. ; JANKAUSKAS, B. ; JANKAUSKIENE, G. ; IONITA, I.: Effects of land use on annual runoff and soil loss in Europe and the Mediterranean A meta-analysis of plot data. In: *Progress in Physical Geography* 36 (2012), Oktober, Nr. 5, 599–653. <http://dx.doi.org/10.1177/0309133312451303>. – DOI 10.1177/0309133312451303. – ISSN 0309-1333, 1477-0296

Marzolff u. a. 2003

MARZOLFF, I. (Hrsg.) ; RIES, J. B. (Hrsg.) ; RIVA, J. De l. (Hrsg.) ; SEEGER, M. (Hrsg.): *Landnutzungswandel und Landdegradation in Spanien. - Cambios de uso del suelo y degradación del territorio en España*. Zaragoza, Frankfurt : Universidad de Zaragoza, Johann Wolfgang Goethe Universität Frankfurt am Main, 2003

Merz 2006

MERZ, B.: *Hochwasserrisiken - Grenzen und Möglichkeiten der Risikoabschätzung*. Stuttgart : Schweizerbart'sche Verlagsbuchhandlung, 2006. – ISBN 3-510-65220-7

Morgan 2005

MORGAN, R. P. C.: *Soil Erosion and Conservation*. 3. Malden (MA, USA) : Blackwell Science Ltd., 2005. – ISBN 9781405144674

Morgan 1986

MORGAN, R. . ; DAVIDSON, D. A. (Hrsg.): *Soil Erosion and Conservation*. Rev. and enl. ed. of Soil erosion, publ. 1979. Harlow : Longman, 1986

Morley u. a. 2005

MORLEY, C. P. ; MAINWARING, K.A. ; DOERR, S. H. ; DOUGLAS, P. ; LLEWELLYN, C.T. ; DEKKER, L. W.: Organic compounds at different depths in a sandy soil and their role in water repellency. In: *Australian Journal of Soil Research* 43 (2005), Nr. 3, S. 239–249. <http://dx.doi.org/10.1071/SR04094>. – DOI 10.1071/SR04094

Mullan 2013

MULLAN, Donal: Soil erosion under the impacts of future climate change: Assessing the statistical significance of future changes and the potential on-site and off-site problems. In: *CATENA* 109 (2013), 234–246. <http://dx.doi.org/10.1016/j.catena.2013.03.007>. – DOI 10.1016/j.catena.2013.03.007. – ISSN 0341-8162

Müller 2010

MÜLLER, C.: *Hochwasserschutz in der Landwirtschaft - Validierung und Modellierung ausgewählter Maßnahmen..* Bd. 15. Trier : Trierer Bodenkundliche Schriften, 2010. – ISBN 978-3-9813264-4-4

Müller u. Bistry 2008

MÜLLER, M. ; BISTRY, T.: Überschwemmungen in Mitteleuropa: Ursachen, Auswirkungen und Perspektiven. In: *promet* 34 (2008), Nr. 1-2, 21-32. <http://www.dwd.de/bvbw/generator/DWDWWW/Content/0effentlichkeit/>

PB/PBFB/Periodika/Promet/PDF/promet_34_1-2,templateId=raw,
property=publicationFile.pdf/promet_34_1-2.pdf

Neris u. a. 2012

NERIS, J. ; JIMÉNEZ, C. ; FUENTES, J. ; MORILLAS, G. ; TEJEDOR, M.: Vegetation and land-use effects on soil properties and water infiltration of Andisols in Tenerife (Canary Islands, Spain). In: *CATENA* 98 (2012), November, 55–62. <http://dx.doi.org/10.1016/j.catena.2012.06.006>. – DOI 10.1016/j.catena.2012.06.006. – ISSN 0341–8162

Neris u. a. 2013

NERIS, J. ; TEJEDOR, M. ; RODRÍGUEZ, M. ; FUENTES, J. ; JIMÉNEZ, C.: Effect of forest floor characteristics on water repellency, infiltration, runoff and soil loss in Andisols of Tenerife (Canary Islands, Spain). In: *CATENA* 108 (2013), September, 50–57. <http://dx.doi.org/10.1016/j.catena.2012.04.011>. – DOI 10.1016/j.catena.2012.04.011. – ISSN 0341–8162

Orfánus u. a. 2008

ORFÁNUS, T. ; BEDRNA, Z. ; LICHNER, L. ; HALLETT, P. D. ; KNAVA, K. ; SEBÍN, M.: Spatial variability of water repellency in pine forest soil. In: *Soil and Water Research* (2008), Nr. 3, S. 123–129

Parker 1987

PARKER, S. D.: *Encyclopedia of Science and Technology*. New York : McGraw-Hill, 1987

Pimentel 2006

PIMENTEL, David: Soil Erosion: A Food and Environmental Threat. In: *Environment, Development and Sustainability* 8 (2006), Februar, Nr. 1, 119–137. <http://dx.doi.org/10.1007/s10668-005-1262-8>. – DOI 10.1007/s10668-005-1262-8. – ISSN 1387–585X, 1573–2975

Pimentel u. Burgess 2013

PIMENTEL, David ; BURGESS, Michael: Soil Erosion Threatens Food Production. In: *Agriculture* 3 (2013), August, Nr. 3, 443–463. <http://dx.doi.org/10.3390/agriculture3030443>. – DOI 10.3390/agriculture3030443

Ravi u. a. 2009

RAVI, Sujith ; D'ODORICO, Paolo ; ZOBECK, Ted M. ; OVER, Thomas M.: The effect of fire-induced soil hydrophobicity on wind erosion in a semiarid grassland: Experimental observations and theoretical framework. In: *Geomorphology* 105 (2009), April, Nr. 1-2, 80–86. <http://dx.doi.org/10.1016/j.geomorph.2007.12.010>. – DOI 10.1016/j.geomorph.2007.12.010. – ISSN 0169–555X

Richter 1998

RICHTER, G. (Hrsg.): *Bodenerosion: Analyse und Bilanz eines Umweltproblems*. Darmstadt : Wissenschaftliche Buchgesellschaft, 1998. – ISBN 3–534–12574–6

Ries 2012

RIES, J. B.: Bodenerosion. In: GEBHARDT, H. (Hrsg.) ; GLASER, R. (Hrsg.) ; RADTKE, U. (Hrsg.) ; REUBER, P. (Hrsg.): *Geographie - Physische*

Geographie und Humangeographie. 2. Heidelberg : Spektrum, 2012. – ISBN 978-3-8274-2816-5, S. 506–515

Ries u. a. 2000

RIES, J. B. ; LANGER, M. ; REHBERG, C.: Experimental investigations on water and wind erosion on abandoned fields and arable land in the central Ebro Basin. In: *Z. Geomorphol.* Suppl.-Bd. 121 (2000), Mai, S. 91–108

Ries 2000

RIES, Johannes B.: Mikro- und Nanorelief an Barranco-Wänden - Untersuchungen zur Verteilung und Genese von Kleinformen in Gullies im Ebrobecken/Spanien. In: *Zeitschrift für Geomorphologie* Suppl. 123 (2000), Dezember, S. 25–41

Rodríguez-Alleres u. a. 2012

RODRÍGUEZ-ALLERES, M. ; VARELA, M.E. ; BENITO, E.: Natural severity of water repellency in pine forest soils from NW Spain and influence of wildfire severity on its persistence. In: *Geoderma* 191 (2012), Dezember, 125-131. <http://dx.doi.org/10.1016/j.geoderma.2012.02.006>. – DOI 10.1016/j.geoderma.2012.02.006. – ISSN 0016–7061

Roth 1996

ROTH, C. H.: Physikalische Ursachen der Wassererosion. In: BLUME, H. P. (Hrsg.) ; FREDE, G. H. (Hrsg.) ; FISCHER, W. (Hrsg.) ; FELIX-HENNINGSEN, P. (Hrsg.) ; HORN, R. (Hrsg.) ; STAHR, K. (Hrsg.): *Handbuch der Bodenkunde*. Taunusstein : Ecomed, 1996, S. 1–34

Scherrer u. Naef 2003

SCHERRER, Simon ; NAEF, Felix: A decision scheme to indicate dominant hydrological flow processes on temperate grassland. In: *Hydrological Processes* 17 (2003), Nr. 2, 391–401. <http://dx.doi.org/10.1002/hyp.1131>. – DOI 10.1002/hyp.1131

Schmocke-Fackel u. a. 2007

SCHMOCKER-FACKEL, P. ; NAEF, F. ; SCHERRER, S.: Identifying runoff processes on the plot and catchment scale. In: *Hydrol. Earth Syst. Sci.* 11 (2007), Februar, Nr. 2, 891–906. <http://www.hydrol-earth-syst-sci.net/11/891/2007/>. – ISSN 1027–5606

Seeger 2001

SEEGER, M.: *Boden und Bodenwasserhaushalt als Indikatoren der Landdegradierung auf extensivierten Nutzflächen in Aragón / Spanien.*, Institut für Physische Geographie, Albert-Ludwigs-Universität Freiburg i. Br., Diss., 2001

Shakesby u. a. 2003

SHAKESBY, R. A. ; CHAFER, C. J. ; DOERR, S. H. ; BLAKE, W. H. ; WALLBRINK, P. ; HUMPHREYS, G. S. ; HARRINGTON, B. A.: Fire Severity, Water Repellency Characteristics and Hydrogeomorphological Changes Following the Christmas 2001 Sydney Forest Fires. In: *Australian Geographer* 34 (2003), Nr. 2, 147. <http://dx.doi.org/10.1080/00049180301736>. – DOI 10.1080/00049180301736. – ISSN 0004–9182

Shakesby 2011

SHAKESBY, R.A.: Post-wildfire soil erosion in the Mediterranean: Review and future research directions. In: *Earth-Science Reviews* 105 (2011), April, Nr. 3–4, 71–100. <http://dx.doi.org/10.1016/j.earscirev.2011.01.001>. – DOI 10.1016/j.earscirev.2011.01.001. – ISSN 0012–8252

Simonit u. Perrings 2011

SIMONIT, Silvio ; PERRINGS, Charles: Sustainability and the value of the ‘regulating’ services: Wetlands and water quality in Lake Victoria. In: *Ecological Economics* 70 (2011), April, Nr. 6, 1189–1199. <http://dx.doi.org/10.1016/j.ecolecon.2011.01.017>. – DOI 10.1016/j.ecolecon.2011.01.017. – ISSN 0921–8009

Symader 2004

SYMADER, W.: *Was passiert, wenn der Regen fällt? - Eine Einführung in die Hydrologie*. Stuttgart : Ulmer, 2004

Tschapek 1984

TSCHAPEK, M.: Criteria for determining the hydrophilicity-hydrophobicity of soils. In: *Zeitschrift für Pflanzenernährung und Bodenkunde* 147 (1984), S. 137–149

Wahl u. a. 2003

WAHL, N.A. ; BENS, O. ; SCHÄFER, B. ; HÜTTL, R.F.: Impact of changes in land-use management on soil hydraulic properties: hydraulic conductivity, water repellency and water retention. In: *Physics and Chemistry of the Earth, Parts A/B/C* 28 (2003), Nr. 33-36, 1377–1387. http://www.sciencedirect.com/science?_ob=GatewayURL&_origin=ScienceSearch&_method=citationSearch&_pikey=S1474706503002328&_version=1&_returnURL=http%3A%2F%2Fwww.scirus.com%2Fsrsapp%2F&md5=b44e5275f81cf4301089a96036d2c5d1

Wahl u. a. 2005

WAHL, N.A. ; WÖLLECKE, B. ; BENS, O. ; HÜTTL, R.F.: Can forest transformation help reducing floods in forested watersheds? Certain aspects on soil hydraulics and organic matter properties. In: *Physics and Chemistry of the Earth, Parts A/B/C* 30 (2005), Nr. 8–10, 611–621. <http://dx.doi.org/10.1016/j.pce.2005.07.013>. – DOI 10.1016/j.pce.2005.07.013. – ISSN 1474–7065

Wessolek u. a. 2008

WESSOLEK, G. ; SCHWÄRZEL, K. ; GREIFFENHAGEN, A. ; STOFFREGEN, H.: Percolation characteristics of a water-repellent sandy forest soil. In: *European Journal of Soil Science* 59 (2008), Februar, Nr. 1, 14–23. <http://dx.doi.org/10.1111/j.1365-2389.2007.00980.x>. – DOI 10.1111/j.1365-2389.2007.00980.x. – ISSN 1365–2389

Wirtz u. a. 2012a

WIRTZ, S. ; ISERLOH, T. ; ROCK, G. ; HANSEN, R. ; MARZEN, M. ; SEEGER, M. ; BETZ, S. ; REMKE, A. ; WENGEL, R. ; BUTZEN, V. ; RIES, J. B.: Soil Erosion on Abandoned Land in Andalusia: A Comparison of Interrill- and Rill

- Erosion Rates. In: *ISRN Soil Science* 2012 (2012), 1–16. <http://dx.doi.org/10.5402/2012/730870>. – DOI 10.5402/2012/730870. – ISSN 2090–875X
- Wirtz u. a. 2010**
- WIRTZ, S. ; SEEGER, M. ; RIES, J. B.: The rill experiment as a method to approach a quantification of rill erosion process activity. In: *Zeitschrift für Geomorphologie* 54 (2010), März, 47–64. <http://dx.doi.org/10.1127/0372-8854/2010/0054-0004>. – DOI 10.1127/0372-8854/2010/0054-0004. – ISSN 03728854
- Wirtz u. a. 2012b**
- WIRTZ, S. ; SEEGER, M. ; RIES, J.B.: Field experiments for understanding and quantification of rill erosion processes. In: *CATENA* 91 (2012), April, 21–34. <http://dx.doi.org/10.1016/j.catena.2010.12.002>. – DOI 10.1016/j.catena.2010.12.002. – ISSN 0341–8162
- Witter u. a. 1991**
- WITTER, J.V. ; JUNGERIUS, P.D. ; HARKEL, M.J. ten: Modelling water erosion and the impact of water repellency. In: *CATENA* 18 (1991), April, Nr. 2, 115–124. [http://dx.doi.org/10.1016/0341-8162\(91\)90011-L](http://dx.doi.org/10.1016/0341-8162(91)90011-L). – DOI 10.1016/0341-8162(91)90011-L. – ISSN 0341–8162
- Yoo u. a. 2014**
- YOO, James ; SIMONIT, Silvio ; CONNORS, John P. ; KINZIG, Ann P. ; PERRINGS, Charles: The valuation of off-site ecosystem service flows: Deforestation, erosion and the amenity value of lakes in Prescott, Arizona. In: *Ecological Economics* 97 (2014), Januar, 74–83. <http://dx.doi.org/10.1016/j.ecolecon.2013.11.001>. – DOI 10.1016/j.ecolecon.2013.11.001. – ISSN 0921–8009
- Zavala u. a. 2009**
- ZAVALA, Lorena M. ; GONZÁLEZ, Félix A. ; JORDÁN, Antonio: Fire-induced soil water repellency under different vegetation types along the Atlantic dune coast-line in SW Spain. In: *CATENA* 79 (2009), November, Nr. 2, 153–162. <http://dx.doi.org/10.1016/j.catena.2009.07.002>. – DOI 10.1016/j.catena.2009.07.002. – ISSN 0341–8162
- Zehe u. a. 2007**
- ZEHE, E. ; ELSENBEER, H. ; LINDENMAIER, F. ; SCHULZ, K. ; BLÖSCHL, G.: Patterns of predictability in hydrological threshold systems. In: *Water Resources Research* 43 (2007), Juli, Nr. 7. <http://dx.doi.org/10.1029/2006WR005589>. – DOI 10.1029/2006WR005589. – ISSN 0043–1397
- Zehe u. Sivapalan 2009**
- ZEHE, E. ; SIVAPALAN, M.: Threshold behaviour in hydrological systems as (human) geo-ecosystems: manifestations, controls, implications. In: *Hydrol. Earth Syst. Sci.* 13 (2009), Juli, Nr. 7, 1273–1297. <http://www.hydrol-earth-syst-sci.net/13/1273/2009/>. – ISSN 1027–5606
- Zepp 2011**
- ZEPP, Harald: *Geomorphologie: Eine Einführung*. 5. Paderborn (D) : Ferdinand Schöningh, 2011 (Grundriß Allgemeine Geographie). – ISBN 9783825235932

Zisman 1964

ZISMAN, W. A.: Relation of equilibrium contact angle to liquid and solid constitution. In: FOWKES, F. M. (Hrsg.): *Contact Angle, Wettability, and Adhesion*. Bd. 43. Amer Chemical Society, 1964. – ISBN 9780841200449, Kapitel 1, S. 1–51

Zucco u. a. 2014

ZUCCO, G. ; BROCCA, L. ; MORAMARCO, T. ; MORBIDELLI, R.: Influence of land use on soil moisture spatial-temporal variability and monitoring. In: *Journal of Hydrology* 516 (2014), August, 193–199. <http://dx.doi.org/10.1016/j.jhydrol.2014.01.043>. – DOI 10.1016/j.jhydrol.2014.01.043. – ISSN 0022–1694

Lebenslauf

Lebenslauf

Verena Butzen

Adresse	Engelstraße: 5 54292 Trier
Geboren	am 03.12.1979 in Wittlich

Beruflicher Werdegang

12/2012 – 02/2015	Fertigstellung der Dissertationsschrift im EU-INTERREG IVb-Projekt ForeStClim
02/2009 - 11/2012	wissenschaftliche Mitarbeiterin der Physischen Geographie an der Uni Trier im EU-INTERREG IVb-Projekt ForeStClim
04/2008 - 02/2009	Nebenberufliche Tätigkeit im Bereich Individuelle Schwerstbehindertenbetreuung (ISB) beim Club Aktiv e.V. Trier
11/2008 - 02/2010	wissenschaftliche Hilfskraft mit Abschluss in der Physischen Geographie an der Universität Trier
04/2008 - 08/2008	Lehrauftrag (Physische Geographie, Universität Trier) Planung und Mitbetreuung einer Süddeutschland/Alpen-Exkursion
04/2006 - 04/2008	Wissenschaftliche Hilfskraft ohne Abschluss in der Physischen Geographie an der Universität Trier

Akademische Ausbildung

04/2008 - heute	Promotion im Fach Physische Geographie Universität Trier. Dissertation im Themenbereich Messung und Modellierung von Oberflächenabflussprozessen und Bodenerosion
4/2004-3/2008	Studium Angewandte Physische Geographie Universität Trier Nebenfächer: Hydrologie und Anglistik => Abschluss: Diplom <u>Diplomarbeit:</u> <i>"Spatial Pattern of Runoff and Erosion Processes - Experimental Measurement and GIS-Modeling for a Small Catchment in the Central Spanish Pyrenees."</i>
10/1999-3/2004	Studium Lehramt Gymnasium an der Universität Trier Fächer: Geographie und Anglistik => Studiengangwechsel

Schulbildung

1990 - 1999	Gymnasium Traben-Trarbach => Abschluss: Abitur
-------------	---